Exploring the potential for recombinant protein production in microalgae

A thesis submitted to

University College London

For the degree of

Doctor of Philosophy

In Biochemical Engineering By

Stephanie Constanze Braun Galleani

2014

Department of Biochemical Engineering

University College London

DECLARATION

"I, Stephanie Constanze Braun Galleani, confirm that the work presented in this thesis is my own. Where information has been derived from other sources, I confirm that this has been indicated in the thesis"

ACKNOWLEDGEMENTS

Firstly, I would like to thank my sponsor Becas Chile, from Ministerio de Educación, Gobierno de Chile, because without their trust in my capabilities and financial support this PhD would have never happened.

I would like to express my earnest gratitude to my supervisors, Dr Saul Purton and Dr Frank Baganz, for giving me the opportunity to work with them and to start my research career in such an intellectually stimulating environment. I would like to thank you for your guidance, support, understanding and freedom to carry out my work. This experience has been a constant learning process which has contributed immensely to my development as a researcher and I have gained countless skills that will surely allow me to go further in my academic career.

Also, I would like to thank Dr Joanna Sacharz, from Professor Conrad Mullineaux group at QMUL, for her generous help and advice with confocal microscopy, and Dr Amandine Marechal from UCL for her help in protein structure design.

I have had the privilege to meet and share this journey with truly great people that have been not only lab mates but friends. I would like to thank the Purton's bunch for being such a great lab atmosphere, and special mention goes to Dr Tommaso Barbi for making me realise that there are never enough negative/positive controls for an experiment. Additionally, I would like to thank our lab manager Thushi for her constant dedication to keep everything up and running.

And life is nothing without friends to share it with, so I would like to thank life itself for putting amazing people on my path. Special thanks go to Pacha, Johannes, Scott, Tom, Lamya and Max for reading my thesis and making really valuable comments and suggestions. And a big hug goes to my life-long friends Anrru, Coty, Feña and Vitto for being always there and for making these thousands of kilometres of distance unnoticeable.

And finally, this thesis is dedicated to the most important people in my life, my family, my mom, dad and sister, who have always supported me with words, company and above all, unconditional love. This achievement is because of you, Vanina and Jorge.

ABSTRACT

Microalgae are considered as attractive platforms for the synthesis of high-value heterologous proteins due to their many beneficial attributes including ease of cultivation, lack of pathogenic agents, and low-cost downstream processing. However, recombinant protein levels are low compared to microbial platforms and commercial production is not a reality yet. Promising research using the model microalga *Chlamydomonas reinhardtii* has highlighted this potential, particularly for transgene expression in the chloroplast.

The objective of this research was to study different strategies for expression in the *C. reinhardtii* chloroplast aimed at increasing growth rate and recombinant protein production, by means of cell engineering and bioprocess optimisation. Two main approaches were considered for this purpose. Firstly, the insertion of the light-harvesting protein proteorhodopsin (PR) into the cell membrane, that has been reported to increase growth rate and culture lifespan in bacterial systems. This has resulted in PR accumulation to low yet detectable levels providing a moderate increase (12 %) of specific cell growth. Noteworthy, this is the first demonstration of an integral membrane recombinant protein expressed in the chloroplast.

The second approach was to express a gene for a novel fluorescent protein (VFP) under the control of different regulatory elements. Detectable VFP levels were produced, with increased protein levels when using the *psaA* promoter/5'UTR element, and with co-expression of a gene for the Spy chaperone. These strains were used to study the effect of temperature, media and light intensity on recombinant protein production and cell growth. Protein levels and fluorescence allowed determining improved cultivation conditions as 30 °C under mixotrophic mode, and these conditions were tested for the accumulation of a therapeutic protein (Cpl-1 endolysin). In conclusion, protein productivity was observed to be protein-specific and improved conditions that increase protein levels for one protein cannot necessarily be extrapolated to the accumulation of a different protein.

ABBREVIATIONS AND NOMENCLATURE

ΔpsbH	*psbH*-deficient strain
ΔrbcL	*rcbL*-deficient strain
A_{520}	absorbance at 520 nm
A_{680}	absorbance at 680 nm
A_{740}	absorbance at 740 nm
aadA	aminoglycoside 3' adenyl transferase
Amp	ampicillin
ATP	adenosine triphosphate
bp	base pairs
dNTP	nucleotides mix
DsRed	*Discosoma sp.* red fluorescent protein
ECL	enhanced chemiluminescence
EGFP	enhanced green fluorescent protein
FP	fluorescent protein
GFP	green fluorescent protein
HA	hemagglutinin
HSM	high salt minimal medium
Kb	kilo bases
kDa	kilo Dalton
LHCs	light-capture complexes
LS	large subunit of the RuBisCo enzyme
mM	millimolar
mRNA	messenger RNA
NADPH	nicotinamide adenine dinucleotide phosphate
OD_{750}	optical density at 750 nm
PCR	polymerase chain reaction
PFD	photon flux density

PR	proteorhodopsin
PSI	photosystem I
PSII	photosystem II
RuBisCo	ribulose-1,5-bisphosphate carboxylase/oxygenase
SDS	sodium dodecyl sulphate
Sp	spectinomycin
SS	small subunit of the RuBisCo enzyme
St	streptomycin
TAP	tris-acetate-phosphate medium
TP	tris-acetate-phosphate medium without acetate or tris-minimal
tRNA	transfer RNA
TSP	total soluble protein
UTR	untranslated region
VFP	vivid verde fluorescent protein
μ	specific growth rate
μmol m^{-2} s^{-1}	light intensity unit that refers to μmol of photons per unit of area and time

STRAIN NOMENCLATURE

Bst-same	*Chlamydomonas reinhardtii* ΔpsbH recipient strain
BST-VFP	Bst-same transformed with the pASapI.VFP plasmid
CC-2653	*Chlamydomonas reinhardtii* ΔrbcL recipient strain
CC-2803	*Chlamydomonas reinhardtii* ΔrbcL recipient strain
CC-F	CC-2653 transformed with the P266-rbcL-VFP plasmid
H1	TN72 transformed with the empty pSRSapI expression vector
TN72	*Chlamydomonas reinhardtii* ΔpsbH recipient strain (cell wall-less)
TN72-Cpl1	TN72 expressing the Cpl-1 endolysin
TN72-PR	TN72 transformed with the pASapI.PR plasmid
TN72-PRΔpsbC	TN72-PR, with disrupted *psbC* gene
TN72-PRΔpsbK	TN72-PR, with disrupted *psbK* gene
TN72-VFPpA (pA)	TN72 transformed with the pASapI.VFP plasmid
TN72-VFPpAX	TN72 transformed with the pASapI.VFP.noHA plasmid
TN72-VFPpS (pS)	TN72 transformed with the pSRSapI.VFP plasmid
TN72-VFPSpy (Spy)	TN72 transformed with the pASapI.VFP.Spy plasmid
TNE	TN72 transformed with the empty pASapI expression vector
TNEΔpsbC	TNE with disrupted *psbC* gene
TNEΔpsbK	TNE with disrupted *psbK* gene

PLASMID NOMENCLATURE

P-266	plasmid containing the native *rbcL* gene from *C. reinhardtii*
P266-rbcL-VFP	plasmid containing the fusion construct rbcL-VFP
pASapI	expression vector containing the C*. reinhardtii atpA* promoter/ 5'UTR and the C*. reinhardtii rbcL* 3' UTR
pASapI.PR	pASapI containing the *proteorhodopsin* gene
pASapI.VFP	pASapI containing the *vfp* gene
pASapI.VFP.noHA	pASapI containing the *vfp* gene without the HA tag sequence
pASapI.VFP.Spy	pASapI containing the *vfp* gene and the *Spy* chaperone gene
pJET.psbC	pJET vector containing the *psbC* gene from *C. reinhardtii*
psbC.KO	plasmid for *psbC* knockout, containing the aadA-disrupted *psbC* gene
psbK.KO	plasmid for *psbK* knockout, containing the aadA-disrupted *psbK* gene
pSRSapI	expression vector containing the C*. reinhardtii psaA* promoter/5'UTR and the C*. reinhardtii rbcL* 3' UTR
pSRSapI.VFP	pSRSapI containing the *vfp* gene
pUC.atpX.AAD	plasmid containing the aadA cassette

TABLE OF CONTENTS

LIST OF FIGURES

LIST OF TABLES

CHAPTER 1

INTRODUCTION

1 INTRODUCTION

Traditionally, the production of recombinant proteins has been carried out using bacterial and yeast fermentation systems, or mammalian cell cultures. Fermentation-based systems are generally low-cost, robust and flexible, with well-established procedures for the expression of heterologous genes in order to produce mostly small non-glycosylated proteins. However, these microbial systems have some significant disadvantages, such as being unable to perform appropriate post-translational modifications, which are crucial for the biological functionality of most eukaryotic proteins, with a tendency to produce the proteins as insoluble aggregates. Additionally, bacterial cells naturally produce endotoxins, which can lead to purification obstacles and potential adverse effects for the final users. As a consequence, several restrictions are faced when considering these systems for the production of bio-products for human application. On the other hand, mammalian cell cultures, although effective in producing properly folded active proteins, are expensive and pose several drawbacks as well, such as the use of complex media, high sensitivity to shear stress, accumulation of toxic metabolites, possible pathogenic contamination and relatively low productivity (Rasala and Mayfield, 2011; Walker et al., 2005). In addition to these platforms, baculovirus-infected insect cells have generated promising results in terms of recombinant protein expression; however, the development of this system is still in progress.

Transgenic plants have gained significant attention in the last few years as a potential host for recombinant proteins due to the high level of protein expression achieved and the low cost of cultivation (Ma et al., 2003; Xu et al., 2012). Nevertheless, critical issues arise from the lack of transgene containment and possible allergic reactions to plant antigens. Microalgae, the subject of the research presented in this thesis, have the same photosynthetic mechanism as higher plants. However, the energy from photosynthesis is directed to cellular growth and reproduction rather than maintaining differentiated structures such as woody stems, and thus the level of protein could reach up to 30-50 % of dry weight biomass. Potentially, microalgae offer all the benefits of higher plants coupled with the high productivity associated with microbial fermentations. Moreover, microalgae can be grown in suspension with nutrients at or near optimal conditions (Maliga and Bock, 2011; Walker et al., 2005; Wijffels et al., 2013).

1.1 Microalgae

The term microalgae describes a very diverse group of prokaryotic (cyanobacteria) and eukaryotic organisms which are unicellular or filamentous microbial species capable of performing photosynthesis; therefore, they are primary producers and basic components of the food chain. Some microalgae can grow in mixotrophic conditions, using an organic carbon source in addition to CO_2, or even in heterotrophic mode (Leite et al., 2013). This versatility makes them suitable to inhabit various different environments, from hyper-saline to freshwater environments to relatively dry ones, such as soil and rocks. Figure 1.1 shows different microalgae used in research, such as *Chlamydomonas reinhardtii* and *Volvox carteri*, and in commercial applications, notoriously *Dunaliella salina* for the production of β-carotene, *Haematococcus pluvialis* for the production of astaxanthin, and *Arthrospira platensis* (also known as Spirulina) which is commonly used as a food supplement (Borowitzka, 2013).

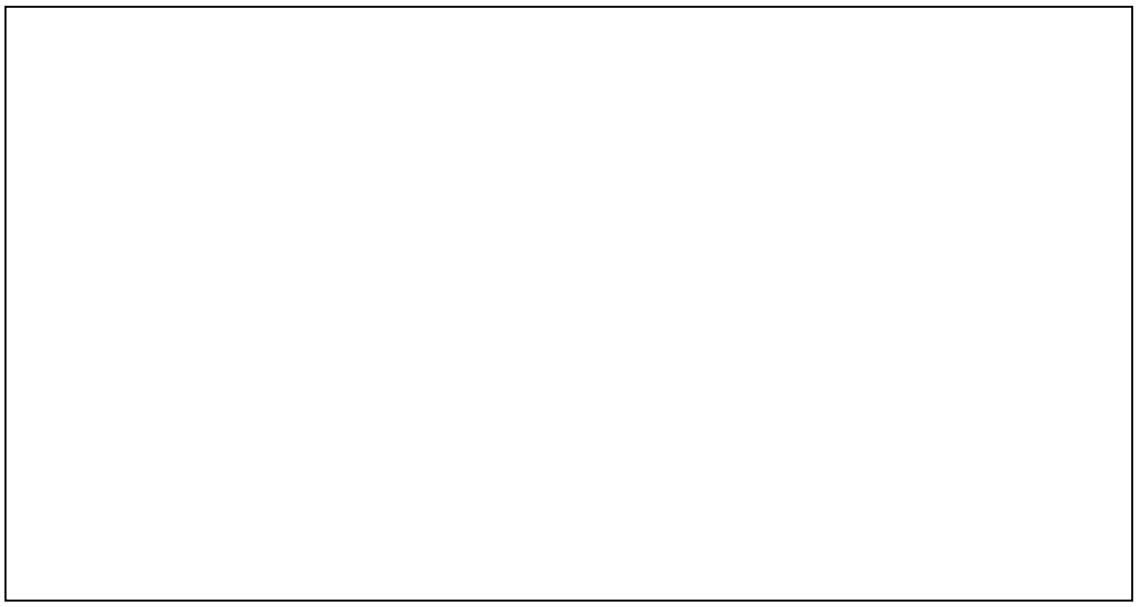

Figure 1.1 Different microalgae that are widely used in research and for commercial purposes: *Chlorella vulgaris* for production of biolipids, *Dunaliella salina* for the production of β-carotene, *Chlamydomonas reinhardtii* and *Volvox carteri*, widely used in research as a model organism, *Haematococcus pluvialis* for the production of astaxanthin, and *Arthrospira platensis* (also known as Spirulina) used as a food supplement (photographs taken from www.sbs.utexas.edu/utex).

These organisms are considered a major natural source of high-value compounds such as carotenoids, long-chain polyunsaturated fatty acids and phycocolloids (Spolaore et al., 2006). In the last decade, there has been considerable interest in new biotechnological applications of microalgae, including the generation of renewable fuels (biodiesel), treatment of wastewater and control of water pollution, atmosphere regeneration in

biospheres, production of high-value products such as bioplastics, nutraceuticals and therapeutics, mitigation of greenhouse gases, production of hydrogen and, more recently, bioremediation or as a biosensor of environmental toxins such as heavy metals (Leite et al., 2013; Spolaore et al., 2006; Walker et al., 2005). This diversity in applications illustrates the potential of these diverse organisms to carry out a variety of functions in different environments and conditions.

A number of species of microalgae are categorised as **G**enerally **R**ecognised **A**s **S**afe (GRAS status) for human consumption since they do not suffer from issues of bacterial endotoxin, prion or viral contamination (Franklin & Mayfield 2004). This aspect is a major concern in other expression systems currently used for recombinant protein production, and a great advantage in microalgae due to the potential of using these organisms with reduced purification requirements for direct oral administration.

1.1.1 Green microalgae

Green microalgae are a subgroup of microalgae that comprise thousands of species that share the presence of both chlorophyll *a* and *b* in double-membrane bound plastids (chloroplasts) and have the ability to store its reserves in the form of starch (amylose or amylopectin) (Lewis and McCourt, 2004).

They also share the common feature of containing a mixture of light-harvesting complex proteins (LHC) especially adapted to their own environment's light exposure. These antenna complexes are divided into two distinctive protein families, LHCI and LHCII, based on their predominant association with the photosystems I (PSI) or 2 (PSII), respectively (Figure 1.2). These are embedded in the thylakoid membrane of the chloroplast and play a vital role as structural scaffolds for the precise orientation of the chlorophyll and carotenoid cofactors (Mussgnug et al., 2007). Besides their function in light capture, these complexes are important for preventing photo-oxidation by means of dissipation of excess light when irradiation surpasses the photosynthetic capacity (Beckmann et al., 2009).

Green microalgae can be found in soil, freshwater and marine environments, in symbiosis with other organisms and also in extreme habitats under high salt concentration or low temperature (Hallmann, 2007).

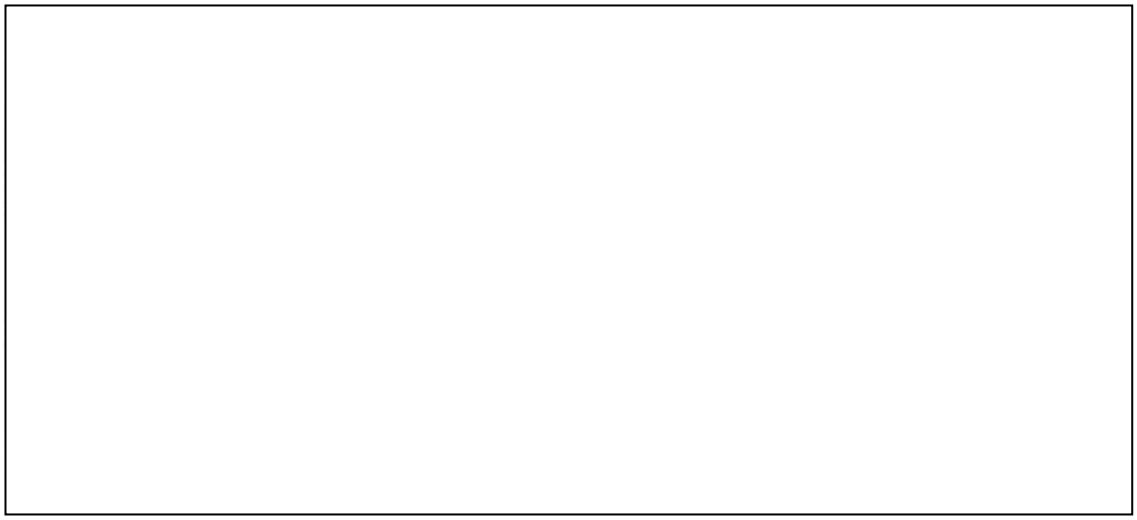

Figure 1.2 A) Schematic representation of the thylakoyd membrane in the chloroplast with all the different components involved in photosynthesis. B) Simplified representation of the structure of a photosystem (Reproduced from Campbell et al., 2008).

Taxonomically, green microalgae branch from the clade *Viridiplantae,* which is further subdivided in two major lineages: *Chlorophyta* and *Streptophyta* (Figure 1.3). The clade *Chlorophyta* comprises most of what has been commonly denominated green microalgae, composed by both green swimming individual cells or colonies (Lewis and McCourt, 2004). Within this clade, the monophyletic group *Chlorophyceae* is the one of major interest in research, since it includes many of the model organisms, such as *Chlamydomonas reinhardtii*, that have been traditionally used to study flagellar motion, photosynthetic mutations and genetic manipulation (Manuell and Mayfield, 2006).

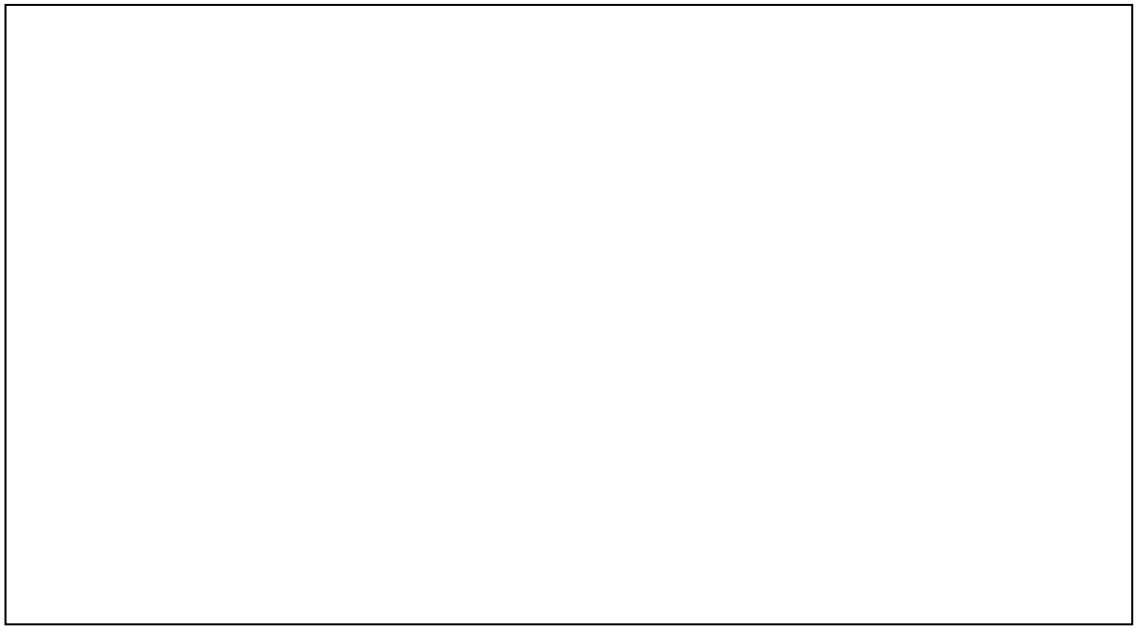

Figure 1.3 Overview phylogeny of the green lineage, starting from a hypothetical ancestral green flagellate (AGF). The *Chlorophyta* includes the majority of described species of green algae, whereas the *Streptophyta* are comprised of the charophytes, a paraphyletic assemblage of freshwater algae, and the land plants (replicated from Leliaert et al. 2012).

1.1.1.1 The microalga *Chlamydomonas reinhardtii*

The green microalga *Chlamydomonas reinhardtii* has been an actively investigated microalga during the past decades (Harris et al., 2009a). Taxonomically, it belongs to the Eukaryote domain (Table 1.1), but like all green algae and plants, it possesses a plastid of prokaryote origin (Dorrell and Howe, 2012; Higgs, 2009; Scharff and Bock, 2014). In addition, chloroplast ribosomes and an RNA polymerase present in the chloroplast resemble bacterial ones, and the majority of chloroplast genes are organised in polycistronic units that resemble bacterial operons (Barkan, 2011).

Table 1.1 Taxonomic classification of *Chlamydomonas reinhardtii*

Domain	*Eukaryota*
Kingdom	*Plantae*
Phylum	*Viridiplantae*
Division	*Chlorophyta*
Class	*Chlorophyceae*
Order	*Volvocales*
Family	*Chlamydomonadaceae*
Genus	*Chlamydomonas*
Species	*Chlamydomonas reinhardtii*

This unicellular organism is an ovoid cell between 10 – 20 μm along its long axis and it possesses multiple mitochondria, two anterior flagella for motility and mating, a large pyrenoid for CO_2 fixation, an eyespot responsible for the swimming orientation with respect to light, and a single chloroplast that contains the photosynthetic apparatus and is the location of critical metabolic pathways (Figure 1.4) (Harris et al., 2009b). Its cell wall is composed mainly of hydroxyproline-rich glycoproteins, with no presence of cellulose (Harris, 2001). The nuclear genome is 100 to 110 million base pairs (bp), comprising 17 genetic linkage groups (chromosomes), with a very high guanosine and cytidine (GC) content of ~ 65 % (Harris, 2001; Mayfield and Kindle, 1990; Merchant et al., 2007).

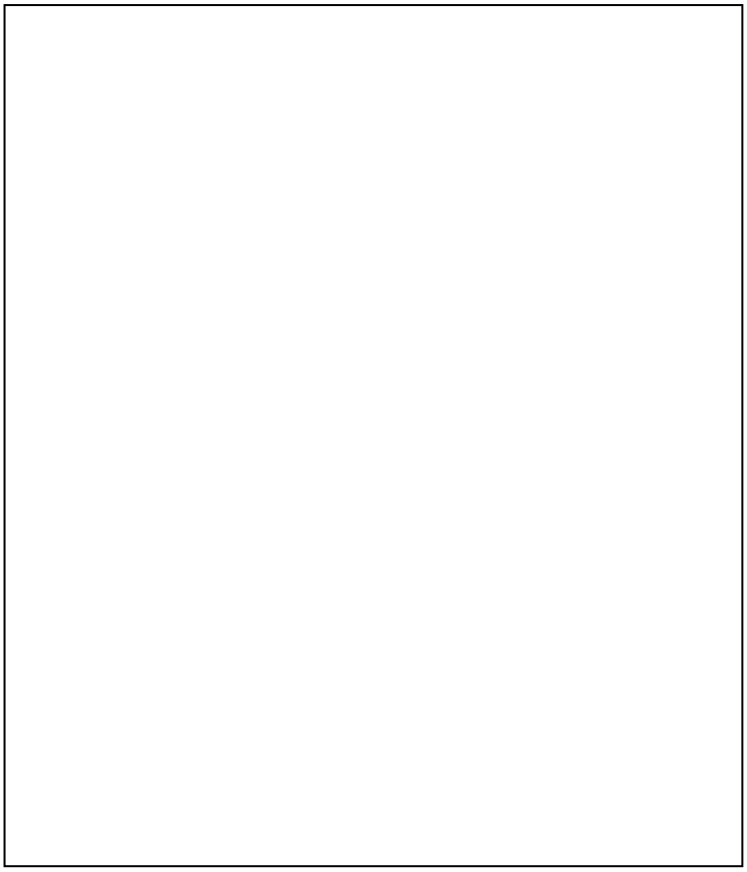

Figure 1.4 *Chlamydomonas reinhardtii* structure (replicated from Merchant *et al*. 2007)

The sequencing of the *C. reinhardtii* genome was completed in 2007 (Merchant et al., 2007) and a flux balance analysis (FBA) to estimate intracellular fluxes of its central and intermediary metabolism under different cultivation conditions was carried out as well (Boyle and Morgan, 2009).

The chloroplast surrounds the nucleus, covering approximately 40 – 60 % of the cell volume. This organelle possesses its own genome (plastome), which is a circular structure of 203 kb with a GC content of 34.6 % and a high proportion of repetitive DNA that accounts for 20 % of the sequence. It encodes 99 genes, including five rRNA genes, 17 ribosomal protein genes, 30 tRNAs specifying all of the amino acids, five genes encoding the catalytic core of a eubacterial-type RNA polymerase and 33 genes encoding proteins associated with photosynthesis (Maul et al., 2002). An important feature is its polyploidy, meaning that approximately 50 – 80 identical copies of the plastome can be found in the chloroplast (Franklin and Mayfield, 2005; Higgs, 2009; Purton, 2007).

C. reinhardtii cells are haploid, existing as two genetically distinctive mating types, (mt+) and (mt-), and these cells can reproduce asexually by binary fission, or can be induced to undergo a sexual cycle. As illustrated in Figure 1.5, nitrogen deprivation triggers pairing of opposite gametes, and this fusion forms a diploid cell (zygospore) with a particularly strong outer wall, in order to offer protection against adverse environmental conditions. Once nitrogen levels are restored, the sexual division process (meiosis) proceeds, forming four haploid cells: two of each mating type (Harris, 2001; Pröschold et al., 2005).

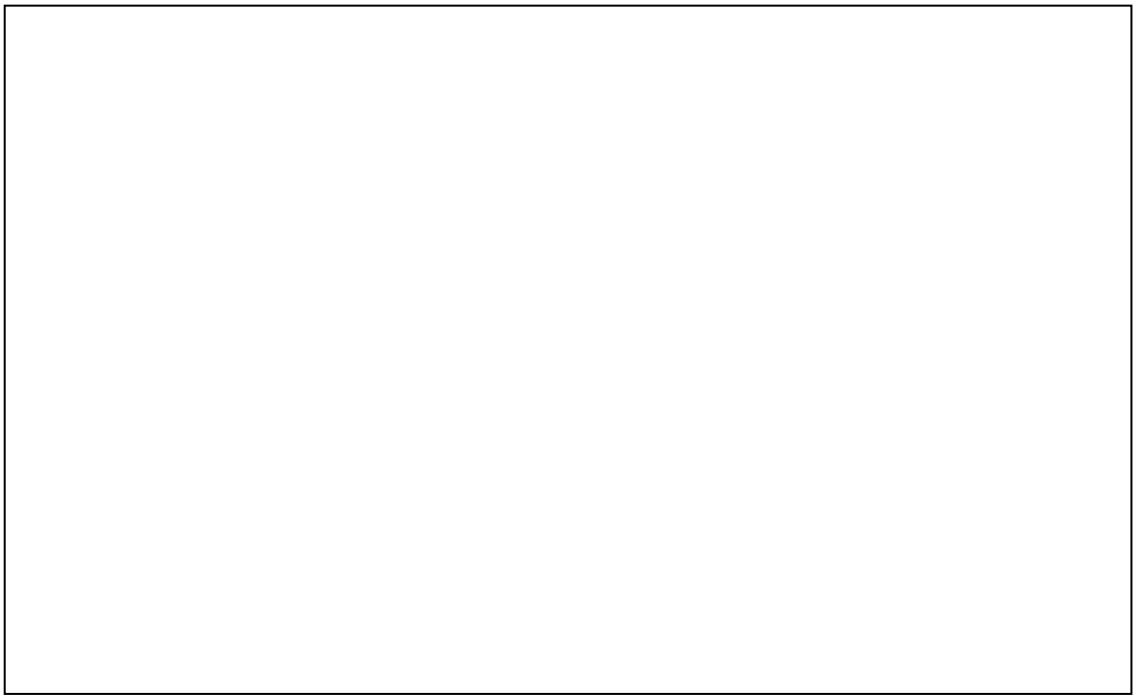

Figure 1.5 *Chlamydomonas* cell cycle, showing both sexual and asexual reproduction (replicated from www.chlamy.org).

1.2 Genetic Manipulation of *Chlamydomonas reinhardtii*

Chlamydomonas reinhardtii remains the model organism for comprehensive genetic engineering studies and the expression host for heterologous genes in microalgae (Rasala et al., 2014; Wijffels et al., 2013). Over the last years, extensive research has been carried out with this alga, establishing robust methods for genetic manipulation of its three genomes: nuclear, chloroplast and mitochondrial. Each genome presents distinctive features and challenges, which will be discussed in the following sections.

1.2.1 Nuclear transformation

The transformation of the nuclear genome in *C. reinhardtii* has been extensively studied during the past two decades and various methods of DNA delivery into the cell have been developed. Transformation methods such as microparticle bombardment (biolistics), vortexing in the presence of plasmid DNA and glass beads, agitation in the presence of DNA and silicon carbide whiskers, electroporation, and *Agrobacterium* infection have all been achieved (Hallmann, 2007; Potvin and Zhang, 2010; Walker et al., 2005). Of all methods, glass bead agitation (Kindle, 1990) remains the preferred one due to the low cost and non-specialist equipment that is required. In this procedure, the abrasive action of the beads forms transient pores in the cell wall/membrane through which the foreign DNA can enter the cell. Higher transformation rates have been demonstrated when using cell wall-less mutants since the lack of a wall facilitates the entry of DNA (Kindle, 1990).

Several factors control the expression of different nuclear genes and these have been exploited in the expression of transgenes. For example, it has been shown that light increases the transcription level of genes that encode the small subunit of ribulose bisphosphate carboxylase and the chlorophyll *a*/*b* binding proteins; deflagellation causes a transient increase in the synthesis of tubulin; copper deprivation induces the synthesis of cytochrome C_6; ammonium deprivation stimulates the synthesis of nitrate reductase; and sulphur limitation induces the production of a periplasmic arylsulfatase (Davies et al., 1992). Making use of a potential reporter function from such genes, a mutant expressing a chimeric sequence encoding the arylsulfatase gene (*ars*) fused to the promoter of the endogenous β2-tubulin gene was developed. It was noted that the transcript accumulation was relatively low in comparison to the endogenous gene, suggesting that other factors may play a role in the level of transcription (Davies et al., 1992). Similar results were obtained by Debuchy et al. (1989) who expressed the *ARG7* gene encoding argininosuccinate lyase in transformed *arg7* cells, finding that although most transformants appear to contain multiple *ARG7* insertions, the level of transcription was low.

The most extensively dominant marker used is encoded by the *ble* gene, which confers resistance to the phleomycin antibiotic family. This gene has several advantages as a selectable marker, such as its small size, its portability as a cassette, it contains no repetitive DNA and the selection method for transformants is straightforward (Lumbreras

et al., 1998; Stevens et al., 1996). Moreover, it appears to be suitable for a range of algal species, particularly those that show inherent resistance to most antibiotics and herbicides (Walker et al., 2005).

Approaches considered for improving transgene expression include the incorporation of *cis*-elements near or within the inserted sequence, in the form of endogenous promoters or endogenous introns. The promoter from the ribulose bisphosphate carboxylase/oxygenase small subunit 2 gene (*RBCS2*) has been used with good success for transgene expression (Nelson et al., 1994; Stevens et al., 1996). It has also been observed that the promoter of the endogenous *HSP70A* works as a transcriptional activator when fused to the promoter of the reporter gene (Schroda et al., 2000). Further studies by Schroda et al. (2002) have identified that this promoter acts by reducing transcriptional silencing, with transgene silencing droping from 80 % to 36 % when the *HSP70A* promoter was present. Other regulatory elements, such as introns, have provided enhancement also. The first intron of *RBCS2* has given good results as an enhancer of transgene expression when inserted within the sequence of the *ble* marker, resulting in higher antibiotic resistance and protein expression (Lumbreras et al., 1998). It is acknowledged that most of the nuclear genes in *C. reinhardtii* need introns to be actively expressed; however, heterologous genes should not contain their own introns as they will most likely not be spliced correctly. Thus, a combination of a heterologous gene with homologous introns appears to be the ideal design (Hallmann, 2007; Specht et al., 2010).

A major difficulty when transforming nuclear DNA is the inability to perform homologous recombination, which leads to transgenes integrating in random locations within the genome. As a result, the isolation of mutants is a long process that comprises a distribution of expression levels. The expression of a foreign gene can be enhanced when selecting or designing genes that have a similar codon bias to the one of endogenous genes, with a GC content comprising 66.3 % of the total. Additionally, the third nucleotide among codons is almost 85 % of the times G or C (Nakamura et al., 2000). This codon usage is likely to have an effect on whether a transgene will or will not be translated efficiently and possibly on any silencing effects observed at transcriptional and post-transcriptional levels (Sharp and Li, 1987; Tuller et al., 2010).

1.2.2 Chloroplast transformation

C. reinhardtii has become a model species for molecular-genetic studies of the chloroplast genome since it is one of the few organisms for which chloroplast transformation is well established (Walker et al., 2005). Furthermore, the chloroplast is the location of some important biosynthetic pathways and where soluble proteins and intrinsic membrane proteins can be stored. Thus, this compartment presents itself as an ideal place for the synthesis and accumulation of high-value recombinant compounds (Purton, 2007).

The most established method for chloroplast transformation is microparticle bombardment (biolistics), but biolistics requires expensive equipment and materials, and agitation with glass beads in the presence of DNA is a more cost-effective alternative (Kindle et al., 1991). This simple method has been further refined and is at present used routinely (Economou et al., 2014). Selection of transformants can be performed either by co-transformation with genes conferring antibiotic resistance or by means of phototrophic rescue and both strategies are widely used (Purton et al., 2013).

The codon bias of the *C. reinhardtii* chloroplast shows a distinctive GC content of 33.72 % and favours A or T in around 80 % for the third position (Nakamura et al., 2000). These features need to be considered for the construction of transgene inserts, since it has been widely demonstrated that using the codon bias of the chloroplast gives a higher expression of the foreign gene (examples of this shown in Table 1.2).

Unlike nuclear transformation, gene insertion in the chloroplast happens via homologous recombination, and thus transformation can be precisely targeted to a specific location within the genome (Figure 1.6). The chloroplast provides transgene containment since chloroplast genome inheritance occurs from the maternal parent (mt+) only, while the chloroplast DNA of the (mt-) parent is destroyed during cell mating (Harris et al., 2009c; Umen and Goodenough, 2001). Moreover, the chloroplast offers a higher level of protein expression, the ability to introduce groups of genes as operons and no gene silencing effects (Purton, 2007; Rasala et al., 2010; Scharff and Bock, 2014; Walker et al., 2005).

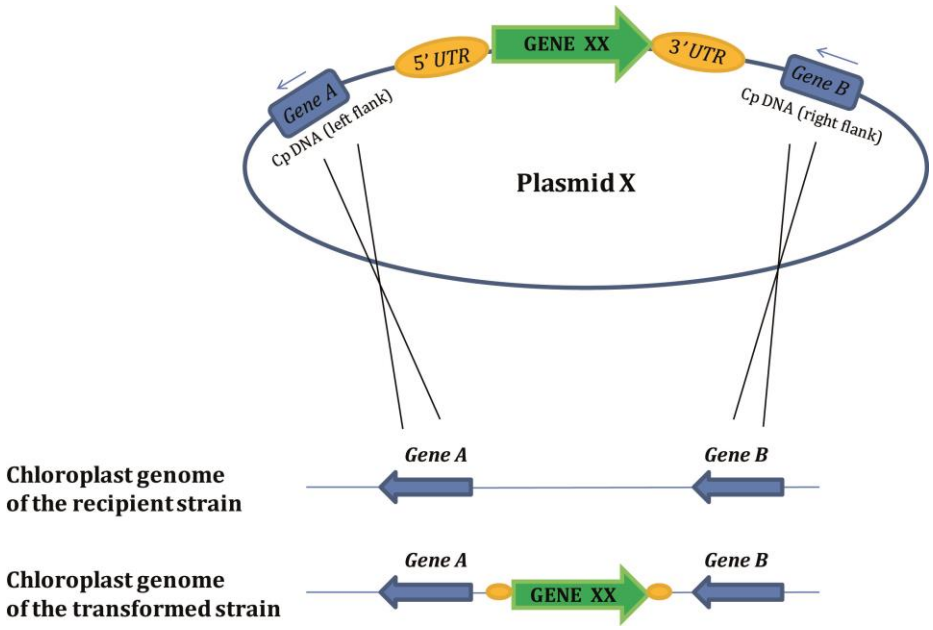

Figure 1.6 Diagram representing homologous recombination in the *C. reinhardtii* chloroplast after transformation. Gene XX contained in plasmid X is recombined in the targeted locus flanked by genes A and B.

In order to allow efficient recombination and make a transformation event stable, foreign DNA requires plenty of homologous sequence flanking it. Conventionally, this flanking sequence corresponds to approximately 1 kb of homology on either side of the insert to be introduced. Nonetheless, it has been observed that with flanking regions of as little as 51 bp upstream and 121 bp downstream of the recombination event for complementation of *psbA*, coding for a subunit of the PSII, the transformation was successful (Dauvillee et al., 2004).

Although the search for more successful promoters and UTRs is still under development, best results to date in terms of recombinant protein concentration have been obtained with the *psbA* regulatory elements, mainly in *psbA*-deficient strains (Rasala et al., 2010; Specht et al., 2010) and with the *psaA* promoter/5' UTR (Michelet et al., 2011).

The interaction of *cis*-acting elements with nuclear-encoded *trans*-acting factors is also an important consideration when maximising the expression of transgenes in the chloroplast. The expression of three different heterologous proteins resulted in low levels of protein production in comparison with the levels achieved by endogenous genes carrying the same leader sequence, despite similar levels of mRNA accumulation (Franklin and Mayfield, 2004). One possible factor that was suggested to play a role is the endogenous UTRs and coding regions that have evolved to form secondary structures enhancing

translational efficiency through interactions with *trans*-acting factors. This suggests that when heterologous coding sequences lacking these structures are used, then interactions are affected, leading to diminished translational levels. This assumption was partially demonstrated by Suay et al. (2005) when studying the effect of a stem-loop structure in the 5' end of the *rbcL* transcript, which is responsible for the folding of a proximal short sequence that provides stability to the transcript. The requirement of this specific structure for stabilisation may suggest the interaction of a *trans*-acting factor that protects transcripts from rapid degradation. A further demonstration of this *cis*-*trans* interaction was observed by Michelet el at. (2011). When a nuclear-encoded factor associated with *psaA* splicing was mutated, accumulation of both the chimeric mRNAs and the recombinant proteins expressed under the control of the promoter/5'UTR of *psaA* were considerably increased, indicating a clear influence of this *trans*-acting element in the expression of chloroplast transgenes.

Nuclear-encoded proteins could also act as light-regulated *trans*-acting factors (Bruick and Mayfield, 1999; Eberhard et al., 2011). This fact was observed in photosynthesis-deficient nuclear mutants, in which specific relationships between nuclear factors and the 5' UTR of chloroplast mRNAs (such as *psbA, psbC, psbD* and *atpA*) were discovered. Many of these nuclear proteins showed increased binding activity to their corresponding chloroplast 5' UTR under illuminated conditions, potentially acting as light-dependent translational activators, offering a regulatory tool to modulate certain chloroplast gene expression.

Five different endogenous promoters/5' UTR and four endogenous 3' UTR were analysed and even though it was not possible to identify novel RNA structures formed in chimeric mRNAs, a distinctive effect of the 5' UTR was discovered. When varying the 5' UTR sequence, increases on the level of transcription (8-fold) and translation (65-fold) of a heterologous *gfp* were detected, whereas no effect originated from the type of 3' UTR used was observed. However, the 3' UTR is required to be present for transcript accumulation (Barnes et al., 2005). Another interesting change observed was the effect of light as a driving force when using different light-regulated 5' UTRs, which appears to cause an effect completely differentiated from the translation efficiency, a phenomenon that was also observed for *psbA* (Eberhard et al., 2002).

It has been demonstrated that gene copy number and transcript abundance have a relatively small effect on the level of protein synthesis for cells cultivated in either mixotrophic or phototrophic conditions (Eberhard et al., 2002). Recently, considering the

low overall rate of mRNA translation obtained for three codon-optimised heterologous proteins in comparison to an endogenous protein, it was suggested that translation may be the core stage limiting the expression of recombinant proteins, and reduced ribosome association could contribute to this decrease (Coragliotti et al., 2011; Specht et al., 2010).

Lastly, only one sequence resembling the activity of an enhancer has been identified in the chloroplast, which is contained in the coding sequence of *rbcL*, approximately 140 bp downstream of the transcription starting site (Klein, 2009). This sequence enhances transcription by approximately 10-fold and it has been noted that without this 'enhancer' element, the *rbcL* promoter is weaker and comparable to the *atpB* promoter.

1.2.3 Mitochondrial transformation

The insertion of foreign DNA into the mitochondria follows the pattern observed in the chloroplast, where the DNA is inserted via homologous recombination (Boynton and Gillham, 1996). Codon optimisation can be taken into account as well, following the base composition of the mitochondrial genome that accounts for 47.5 % GC, with a predominance of 51.35 % for G or C in the third position (Nakamura et al., 2000).

Mitochondrial transformation was first achieved using biolistics, which resulted in the recovery of the respiratory function of a mutant carrying a deletion in the mitochondrial *cob* gene encoding cytochrome *b* (Boynton and Gillham, 1996). Transformants were capable of growing under heterotrophic conditions, but the first colonies appeared on the selective plates only after 4-8 weeks, a slower recovery in comparison to the appearance of chloroplast transformant lines. It is suggested that both the higher number of mitochondria per cell and the lower probability that a single mitochondrion incorporates multiple DNA inserts could contribute to this delay on the appearance of transformants.

Several years later, another attempt with respiration-deficient strains transformed with intact mitochondrial DNA and DNA constructs containing the missing regions, resulted in the generation of transformants within 2-4 weeks (Yamasaki et al., 2005). Homologous recombination occurred in several regions of the mitochondrial genome, but the transformation yield was low. Further studies have been performed in this regard; however, mitochondrial transformation is not a straightforward procedure yet (Cardol and Remacle, 2009).

1.3 Foreign gene expression in the *Chlamydomonas reinhardtii* chloroplast

A major challenge in chloroplast engineering is to produce a desired protein in its active form at high concentration, in order to make a process commercially viable. *C. reinhardtii* can potentially produce recombinant proteins at a lower cost than other systems in a transgene-containment manner, overcoming issues that make the use of higher plants not as straightforward so far and clearly challenging traditional bioprocess platforms (Scharff and Bock, 2014).

As explained in the previous section, genetic manipulation of the chloroplast of *C. reinhardtii* presents itself as a very promising strategy to generate high-value recombinant proteins, and the ongoing advances in this regard will be described in the following sections.

1.3.1 Expression of recombinant proteins

The feasibility of producing recombinant proteins of high value in the *C. reinhardtii* chloroplast has been demonstrated by different groups and offers several benefits. Among these features it is possible to highlight that a) transformation is a straightforward procedure than can produce transformants within a short period of time of about 4-6 weeks; b) this organism has a short generation time of approximately 8 – 12 hours, achieving high cell densities under proper light and aeration; c) it can grow under phototrophic, heterotrophic and mixotrophic conditions; d) there is a variety of well characterised endogenous *cis* elements (promoters and UTRs) to drive expression; e) as there is only one chloroplast per cell, a homogenous expressing culture is obtained; f) it can be grown at different scales in a cost-effective manner; g) it shows an important level of transgene retention, ensuring the containment of a genetically-modified organism; and h) the chloroplast possesses a variety of chaperones and disulfide isomerases that can assist in the folding of complex multicomponent proteins (Cardi et al., 2010; Gong et al., 2011; Potvin and Zhang, 2010; Purton, 2007; Rasala et al., 2010; Tran et al., 2009; Walker et al., 2005). Table 1.2 summarises the main achievements in the expression of recombinant proteins used as reporters or markers in the *C. reinhardtii* chloroplast.

It is worth mentioning the results obtained when expressing luciferase, where a higher level of the recombinant protein was achieved when the luciferase gene was fused to the promoter and UTRs of the endogenous gene *psbA* and was incorporated in a recipient

strain lacking the *psbA* gene (Mayfield and Schultz, 2004). This was further studied by Manuell et al. (2007) and it was concluded that the 5'UTR of the mRNA encoding *psbA* competed with that of the foreign gene to undergo translation initiation. They also noticed that when *psbA* was reinserted elsewhere under the control of the *psbD* promoter/5' UTR photosynthesis was restored without altering the expression level of the foreign protein, obtaining a photosynthetic culture with higher productivity (Rasala et al., 2010). This latter approach of phototrophic recovery is currently used as selection method for transformants. Furthermore, this same approach was used by Muto et al. (2009) with the *rbcL* endogenous gene, obtaining important increases in protein productivity as well.

Despite the successful expression of a few fluorescence-based reporter genes such as green fluorescent protein or luciferase in the chloroplast of *C. reinhardtii*, as observed in Table 1.2, it has not been possible to find a reporter that produces enough fluorescence in order to use it to quantify protein accumulation. The availability of such a reporter would serve as a powerful tool to explore various regulatory sequences and protein accumulation.

Another example of the application of the *C. reinhardtii* chloroplast expression platform is in the field of edible vaccines, especially for disease control in high-density farms. A fusion protein against the foot-and-mouth disease virus (FMDV), the agent of an important disease of livestock, was produced by Sun et al. (2003). This protein reached 3 % of total soluble protein (TSP) and was able to bind to the intestinal membrane GM1-ganglioside receptor, indicating its potential as a mucosal vaccine source. Evidence has been gathered that *C. reinhardtii* delivery of antigens against the bacterial kidney disease by feed or by immersion can induce antibody production in different tissues in juvenile rainbow trout (Siripornadulsil et al., 2007). Further studies were performed with rabbits where transformed *C. reinhardtii* was ingested either as pellets containing freeze-dried algae or as drinking live algae, and in this case only the live organism induced immune response. Current work in the Purton group (P. Rajakumar, personal communication) aims to investigate the production of a vaccine for the poultry pathogen Infectious Bronchitis Virus (IBV) using the antigenic regions of two IBV proteins expressed as a fusion and linked to the protein adjuvant Cholera Toxin B (CTB) with the purpose of using this as an edible vaccine.

Table 1.2 Expression of reporter and marker proteins in the chloroplast of *Chlamydomonas reinhardtii*. Genes with * represent sequences that have been codon-optimised to the codon bias of the chloroplast.

Gene Expressed	Insert Features	Expression detected	Reference
Bacterial neomycin phosphotransferase II	Maize chloroplast promoter *rbcL*	Accumulation of recombinant mRNA, but no protein	Blowers *et al.*, 1989
aadA	Promoter and UTR from endogenous genes	Antibiotic-resistant transformants. Established as a useful reporter and dominant marker	Goldschmidt-Clermont, 1991
Bacterial β-glucuronidase	Endogenous *rbcL, psbA* or *atpA* promoter, 5' and 3' UTRs	Enzymatic activity observed, but low protein concentration	Ishikura *et al.*, 1999
Luciferase	Promoter and 5' UTR of endogenous *atpA*	Luminescence in the presence of substrate coelenterazine and a 38 kDa polypeptide of relatively low concentration	Minko *et al.*, 1999
aphA-6	Promoter and UTR from different endogenous genes fused to a *psbH* gene fragment	Higher expression under *psbA* promoter. *aphA-6* proposed as a new alternative for antibiotic-resistance marker	Bateman & Purton, 2000
**GFP*	5' and 3' UTR of endogenous *rbcL*	80-fold increase in expression compared to non codon-optimised gene, accumulating 0.5 % TSP in its active form, but not enough for *in vivo* detection	Franklin *et al.*, 2002
**Luciferase (luxCt)*	Promoter and 5' UTR of endogenous *atpA*, 3' UTR of *rbcL*	78-kDa fusion protein, i*n vivo* visualisation in the presence of decanal	Mayfield & Schultz, 2004
	Promoter and 5' UTR of *psbA.*	10-fold increase in protein concentration and 9-fold increase in luminescence (~0.1 % TSP)	
**GFP*	5'/3' UTRs from five/four different endogenous genes, respectively	Highest mRNA and protein expression using either the *atpA* or *psbD* 5' UTRs. No effect from varying 3' UTR	Barnes *et al.*, 2005
**Luciferase (lucCP)*	Promoter and 5' UTR of *psbD* and *tufA*; both containing the 3' UTR of *atpB*.	Similar luminescence in presence of substrate luciferin	Matsuo *et al.*, 2006
**Luciferase*	Fused to the endogenous *rbcL* gene, but cleavable *in vivo*	Inserted into an *rbcL*-deficient host: 140-fold increase in activity compared to luciferase expressed alone.	Muto *et al.*, 2009

1.3.2 Expression of human therapeutic proteins

Traditionally, most recombinant proteins of human application have been produced in transgenic mammalian cell cultures, such as different Chinese hamster ovary (CHO) cell lines, but these systems are expensive due to the complications of growing and maintaining sterile cultures, reaching costs in the range of US$75 – US$150/g protein (Franklin and Mayfield, 2005). Factors such as the complexity of the medium, low oxygen and nutrient distribution, toxic metabolite accumulation, pathogen contamination and low resistance to shear stress make this type of cells difficult to handle (Potvin and Zhang, 2010). On the other hand, yeast and bacterial cultures, despite being a cheaper alternative, may present other problems such as the inability to produce a soluble fully biologically active protein due to inappropriate folding and lack/different type of post-translational modifications. Attempts to express therapeutic proteins have been made in some species of higher plants, offering a cheaper successful alternative; however, length of time to produce and grow the transgenic plants and recover the final product from leaves or other tissues may take years and transgene containment is not possible due to gene flow via pollen, which is a major concern with respect to food supply being contaminated by transgenic crops (Fletcher et al., 2007; Franklin and Mayfield, 2005; Hallmann, 2007).

Chloroplasts cannot perform complex post-translational modifications of proteins such as glycosylations. Nevertheless, and as it will be further discussed, the expression of certain non-glycosylated versions of proteins such as antibodies has provided evidence that this feature could have improved biological functionality compared to mis-glycosylated forms. This is due to antibody-dependent cell-mediated cytotoxicity provided by glycosylations, and the observation that glycosylation is not necessarily required for antigen binding activity (Mayfield et al., 2007). Disulfide-bond formation, another important post-translational modification, has been demonstrated for recombinant proteins synthesised in the chloroplast owing to its reducing environment, providing an advantage for *C. reinhardtii* chloroplasts over *E. coli* platforms when used for therapeutic protein production (Cardi et al., 2010; Specht et al., 2010; Tran et al., 2009).

The first approach using microalgae to produce a human therapeutic protein was carried out over a decade ago by Mayfield et al. (2003). This group expressed a large single-chain antibody against the herpes simplex virus, obtaining levels of the recombinant antibody of between 0.5 – 1 % TSP in its fully active form, despite that it did not include the

glycosylations of the natural human antibody. A few years later, a protein concentration comparable to bacterial systems of up to 10 % TSP was achieved for the first time by Manuell et al. (2007), when expressing the mammalian protein bovine mammary-associated serum amyloid (M-SAA), replacing in the host cell the endogenous gene *psbA* with a *psbA-m-saa* construct, a replacement strategy that was previously shown to improve transgene expression (Mayfield and Schultz, 2004). The protein produced, which was largely in soluble form, was capable of activating mucin synthesis in the human gut epithelial cells at comparable level as the human M-SAA. Following these good results, another study carried out by Rasala et al. (2010) tested a set of seven human proteins of potential therapeutic application in order to assess the versatility of *C. reinhardtii* as a useful platform for commercial recombinant protein synthesis. They observed that three proteins accumulated to levels above 1% TSP (3 % maximum) and one accumulated to similar levels when fused to a stable highly-expressed protein. Even though productivity could still be improved, these values can be taken as a good starting point for commercial development, and provide evidence of the potential of *C. reinhardtii* as a valuable platform for recombinant biopharmaceutical production.

Monoclonal antibodies and antigens have also been successfully expressed in the algal chloroplast. A full-length human immunoglobulin monoclonal antibody against anthrax composed of two heavy-chain and two light-chain proteins was produced with a yield of 100 μg protein/g dry biomass (Tran et al., 2009). This recombinant antibody showed almost identical antigen affinity to the antibody expressed in mammalian cells, once again without the presence of the original glycosylations. Moreover, the protein remained soluble avoiding costly stages of denaturation and folding, as usually happens with bacterial systems. In terms of antigens, the antigenic structural protein E2 from the swine fever virus was produced at a concentration of 2 % TSP (He et al., 2007), and it was shown that it could trigger an immune response in mice when provided subcutaneously. In 2008, the first report on the production of a human auto-antigen emerged when the human glutamic acid decarboxylase (hGAD65) associated with type I diabetes was expressed in *C. reinhardtii* chloroplasts with antigenicity and functionality. The yield was moderate (0.3 % TSP), however, codon and regulatory-sequences optimisation were not applied in this case, which gives plenty of room for yield improvement (Wang et al., 2008).

Due to the prokaryotic origin of the chloroplast, and the possibility to express properly folded eukaryotic proteins that are otherwise toxic to eukaryotic organisms, a different

type of proteins, known as immunotoxins, have been considered. These human-made proteins consist of an antibody domain for binding target cells and molecules of a toxin that inhibits the proliferation of the targeted cell. These proteins accumulated in soluble form and proved their activity *in vitro* inducing cellular apoptosis (Tran et al., 2013).

In terms of microalgal vaccines, a heat-stable fusion antigen against *Staphylococcus aureus* was produced. This construct is composed of the D2 fibronectin-binding domain of *S. aureus* fused to the cholera toxin B subunit, a mucosal adjuvant that promotes the proper association of the antigen with its receptors in the gut and improves antigen-specific immune responses. The transgenic line produced the fusion protein at a concentration of 0.7 % TSP (Dreesen et al., 2010). Importantly, they demonstrated the feasibility of using *C. reinhardtii* as an edible vaccine, observing successful antigen binding, which initiated mucosal and systemic immune responses producing the corresponding immunoglobulins, and reducing the bacterial dissemination and infection in mice. Additionally, a transmission blocking vaccine against malaria has recently been successfully expressed. The *Plasmodium falciparum* surface protein Pfs48/45 has proven difficult to express in other expression platforms due to the presence of several disulfide bonds in its structure; however, in the *C. reinhardtii* chloroplast it was found to contain the epitopes necessary for its activity (Jones et al., 2013).

1.3.3 Foreign gene expression as complementation of a metabolic pathway

Genetic recombination aiming at introducing or complementing a metabolic pathway that could change metabolic profiles in chloroplasts is still in its infancy. Most developments in this area have been performed in other organisms, such as tobacco plants metabolically engineered to produce polyhydroxybutyrate (Wang et al., 2009). Su et al. (2005) demonstrated the feasibility to express a prokaryotic cyanobacterial polycistron encoding the photosynthetic heterodimer allophycocyanin in *C. reinhardtii* chloroplast reaching 2-3 % TSP, providing for the first time groundwork for the expression of foreign pathways, but no further advances have been reported thus far.

1.4 Microalgal cultivation

Microalgae can be grown in various conditions depending on the requirements of the particular strain under study. In recent years there has been a huge development in terms of suitable systems for this purpose, particularly concerning light penetration in order to achieve high cell densities. The following sections will present a brief introduction to cultivation systems available and cultivation conditions utilised for the growth of *Chlamydomonas reinhardtii*.

1.4.1 Culture systems

Algae can be grown in open or enclosed systems. Open systems are mainly represented by shallow open ponds, which have been widely used for the production of healthy foods, such as *Spirulina* (Ugwu et al., 2008), and for the production of commercially desirable supplements with various applications, such as the pigment astaxanthin in *Haematococcus pluvialis*. Enclosed systems, known as photobioreactors, have the great advantage of allowing better control of the cultivation parameters, making them more suitable for the production of different compounds, especially due to higher biomass productivity. Additionally, this method of cultivation is more appropriate for sensitive strains that cannot compete easily with other organisms in open systems, and products of higher added-value such as pharmaceuticals and nutraceuticals, can be generated with high standards of process safety and purity (Rosello Sastre et al., 2007). Figure 1.7 shows different configurations and designs of photobioreactors, together with a typical open pond (raceway) system and large scale outdoor ponds for commercial production of algae.

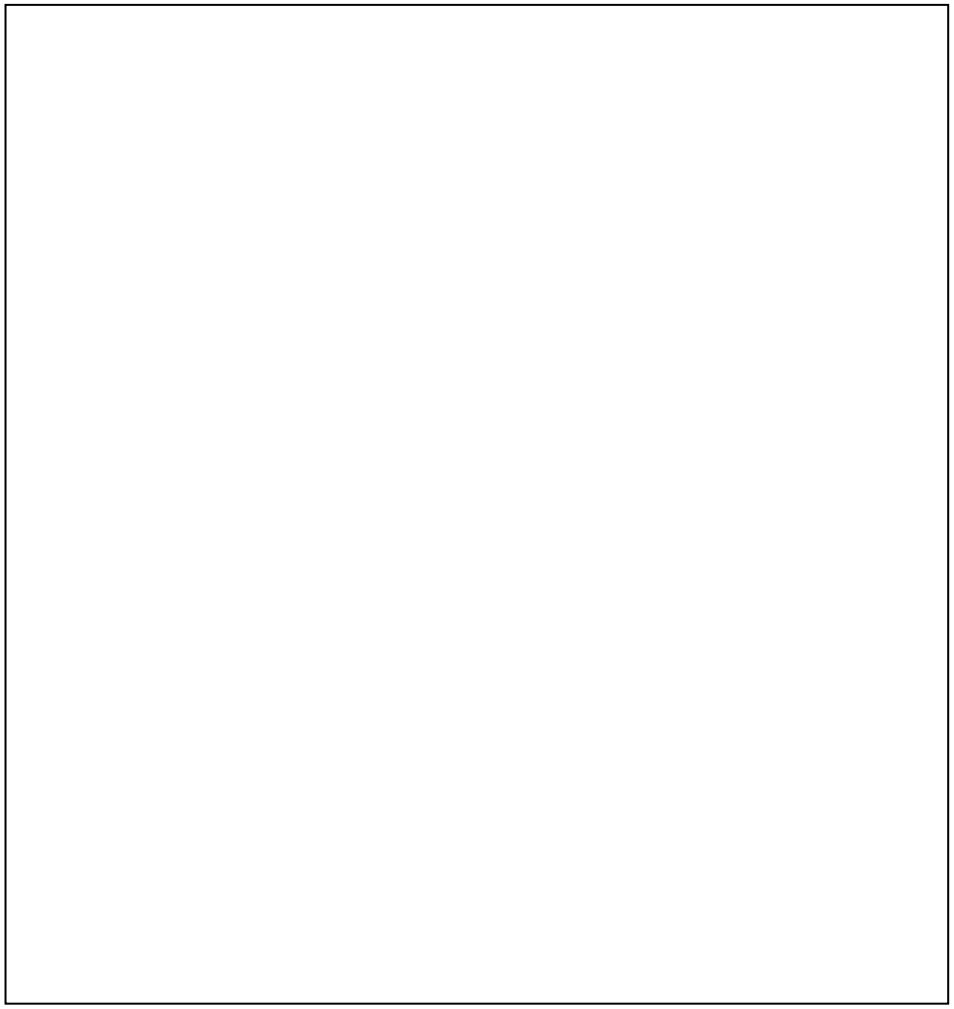

Figure 1.7 Various configurations of photobioreactors (PBR) and open ponds for algal cultivation. First row: large scale production in outdoor ponds; second row: raceway ponds; third row: tubular systems and bags; fourth row: indoor cultivation systems such as flat panels, a conventional photobioreactor and disposable bags (replicated from www.algaeindustrymagazine.com)

Different photobioreactor systems have been designed in order to achieve efficient cultivation, with the main challenge being the difficulty of achieving light penetration that is consistent with the cell density. For high-value products, the use of enclosed systems illuminated with artificial light is commonly considered, since much more control of light intensity, light wavelength, use of light/dark cycles and other variables can be achieved. Light can be supplied by natural or artificial sources, or a combination of both. Generally, laboratory-scale photobioreactors are illuminated with artificial light and can be easily controlled for temperature, whereas most pilot- and large-scale systems are illuminated with solar light (mainly due to high costs) and temperature maintenance requires additional efforts (Ugwu et al., 2008). Table 1.3 summarises the main advantages and disadvantages of various cultivation systems.

Table 1.3 Summary of main advantages and disadvantages of different algae cultivation systems (adapted from Ugwu et al., 2008)

Culture system	Advantages	Disadvantages
Open ponds	Relatively economical, easy to build, manipulate and clean up, good for mass cultivation	Poor control of culture conditions, low productivity, diffusion of CO_2, use of large areas, inefficient stirring, easily contaminated, water evaporation
Flat-panel photobioreactors	Large illumination surface area, suitable for outdoor cultures, good light path, good biomass productivities, relatively cheap, easy to clean up, readily tempered, low O_2 accumulation	Scale-up require many compartments and support materials, difficulty in controlling culture temperature, some degree of wall growth, possibility of hydrodynamic stress to some algal strains
Tubular photobioreactors	Large illumination surface area, suitable for outdoor cultures, good biomass productivities, relatively cheap	Gradients of pH, dissolved O_2 and CO_2 along the tubes, fouling, poor mass transfer, possible photoinhibition, some degree of wall growth, difficult temperature control
Vertical-column photobioreactors	High mass transfer, good mixing, low shear stress, low energy consumption, high potential for scalability, easy to sterilise, readily tempered	Small illumination surface area, sophisticated materials for construction, shear stress to algal cultures under high mixing rates, decrease of illumination surface area upon scale-up
Internally-illuminated photobioreactors	Efficient usage of both natural and artificial light, heat-sterilized under pressure	Outdoor mass cultivation requires further development, capital costs, cleanability, loss of energy in transmission to optical fibers
Plastic bags photobioreactors	Low cost, sterility, scalability	Inadequate mixing, disposal of great amounts of plastic (large scale), fragile

1.4.2 General culture parameters

Many algae species are flexible in terms of temperature conditions, being able to grow in a wide range normally between 15 – 30 °C. However, for *C. reinhardtii* a temperature range of 20 – 25 °C has been traditionally recommended. Regarding pH, this parameter usually fluctuates due to CO_2 intake and O_2 generation, not affecting growth within a certain range proximal to neutral. However, O_2 needs to be controlled in larger scale cultures so that it does not build-up and reach inhibitory levels, which are known to affect negatively photosynthesis in many algal species (Acién Fernández et al., 2013; Wang et al., 2012). CO_2

is usually supplemented in a concentration of 5 % in air and its limitation in phototrophic conditions can generate metabolic changes that result in accumulation of large amounts of starch (Harris, 2001).

Mixing is crucial for aeration, and to avoid sedimentation and shading of cells in the interior of the culture, which interferes with the light penetration and, therefore, light incidence. Cultures should be stirred or shaken constantly for maximum growth yield (Harris et al., 2009a; Wang et al., 2012).

There are three modes of cultivation for *C. reinhardtii* based on the carbon source used for energy and biomass synthesis: phototrophic, heterotrophic and mixotrophic modes. Phototrophic cultivation requires light and an inorganic carbon source in the form of CO_2; heterotrophic cultivation is based in the use of organic carbon sources only; and mixotrophic cultivation benefits from both of the previous modes, metabolising both inorganic and organic carbon sources. As a result of a flux balance analysis (FBA) of *C. reinhardtii* cultivated under different conditions, it was possible to estimate the yields on carbon for biomass production, observing that heterotrophic cultivation has a low yield, while mixotrophic and phototrophic modes are significantly more carbon efficient. These estimates can also be taking into account for the selection of one mode over the other, depending on the type of recombinant product expressed, considering for example whether or not it is growth-associated (Boyle and Morgan, 2009). These yields of biomass production are in agreement with the observations that both phototrophic and mixotrophic modes of cultivation induce faster growth than heterothophic mode (Harris, 2001)

1.4.3 Phototrophic culture

C. reinhardtii can be grown under phototrophic conditions supplemented with inorganic carbon (CO_2) as the carbon source and minimal medium containing mostly salts, nitrogen, phosphorous, potassium and trace elements. Light provides the energy necessary for maintenance and cell growth, which is accumulated in the form of ATP. When irradiation exceeds the photosynthetic capacity of the cell, only a fraction of it is actually absorbed and used for growth and maintenance. The remaining light, which can account for as much as 85 – 90 %, is dissipated as heat or fluorescence, making light absorption an inefficient process (Janssen et al., 2003; Mussgnug et al., 2007). In general terms, light conditions for

phototrophic cultivation of *C. reinhardtii* are in the range of 50 – 100 μmol m^{-2} s^{-1} for low light intensity, and 350 – 1200 μmol m^{-2} s^{-1} for high light intensity (Niyogi, 2009).

In dense cultures, light intensity decreases with the distance from the illuminated surface due to self-shading of the cells and light absorption by intracellular pigments. This fact, together with the existing mixing conditions, creates cycles of light and dark phases, which can be easily observed in an air-lift reactor (Figure 1.8), in which the light seems to form a gradient as it penetrates the reactor (Barbosa et al., 2003).

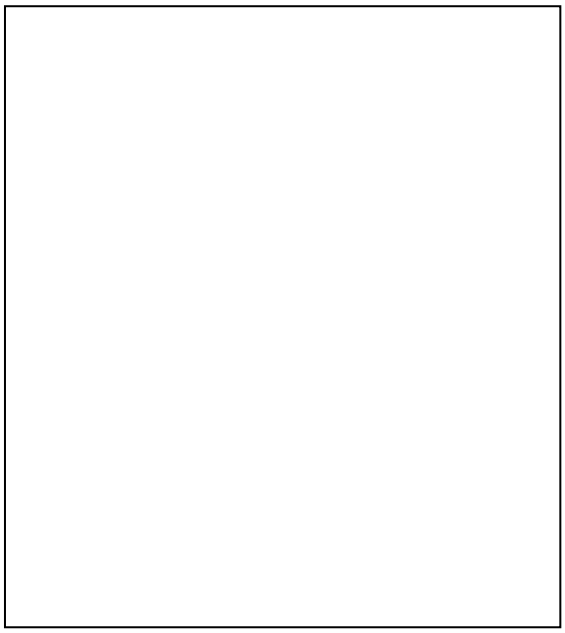

Figure 1.8 Example of an air-lift photobioreactor and the light gradient formed along its radial section (replicated from Barbosa et al., 2003)

In an experiment carried out by Janssen et al. (2000a) , *C. reinhardtii* cells were cultivated in a turbidostat-type reactor (constant turbidity) and exposed to continuous light and defined light/dark cycles with distinct light fractions (fraction of time cells are subjected to light during a light/dark cycle given by biomass density) and different exposure times to darkness, finding that a photon flux density (PFD) higher than 700 μmol m^{-2} s^{-1} caused inhibition of the growth rate. When comparing 24 hours of saturating continuous light against 16/8 hours day/night cycle, the growth rate decreased by only 12 %, even though the light supply was decreased by a third.

Another study conducted by the same group (Janssen et al., 2000b) used air-lift reactors, where gas exchange is discarded as a limiting factor due to efficient mixing, and analysed the effect of photoinhibition given by higher PFDs. It was observed that the specific growth

rate of *C. reinhardtii* under continuous illumination of 1153 μmol m^{-2} s^{-1} was the same as the growth rate determined at 627 μmol m^{-2} s^{-1} (highest non-inhibitory PFD according to the previous study), which agrees with the premise that photosynthetic organisms are more efficient at low photon flux densities. Also, the growth rate observed at this high PFD under continuous illumination and different light/dark cycles gave evidence of the acclimation of the light-absorbing photosystems to diverse light regimes.

1.4.4 Heterotrophic culture

Heterotrophic cultivation offers some advantages in comparison to phototrophic cultivation, comprising exclusion of light limitation, a potential higher cell density and productivity, and lower costs of processing (Chen and Chen, 2006). Moreover, light-induced proteases in the chloroplast are less active potentially diminishing the protein degradation rate under this growth condition (Adam and Clarke, 2002; Nair and Ramaswamy, 2004).

C. reinhardtii is a facultative phototroph and can therefore be grown in the dark supplied with an alternative organic carbon source. However, this organism can only grow heterotrophically when provided with acetate; other intermediates of the tricarboxylic acid cycle cannot sustain heterotrophic growth, nor other carbon sources such as hexoses, pentoses, glycerol, ethanol or organic compounds (Harris et al., 2009d). Acetate can be directly activated to acetyl-CoA in one step mediated by the enzyme acetyl-CoA synthetase, and in this way incorporated into the glyoxylate cycle. This cycle generates one molecule of succinate starting from two molecules of acetate, which is further used in the tricarboxylic acid cycle (TCA) to produce energy (Figure 1.9).

When *C. reinhardtii* was grown in a chemostat in darkness at 35 °C and pH 7.2 using acetate as the sole carbon and energy source (3.4 g L^{-1}), cell densities of around 1.5 g L^{-1} were obtained. Acetate worked as a growth inhibitor at high cell concentrations, most probably due to sodium accumulation (when sodium acetate is supplemented), which has been reported to be inhibitory at concentrations near 7 g L^{-1}; therefore, the use of other acetate substrates, such as ammonium acetate or acetic acid, has been suggested (Chen and Johns, 1996).

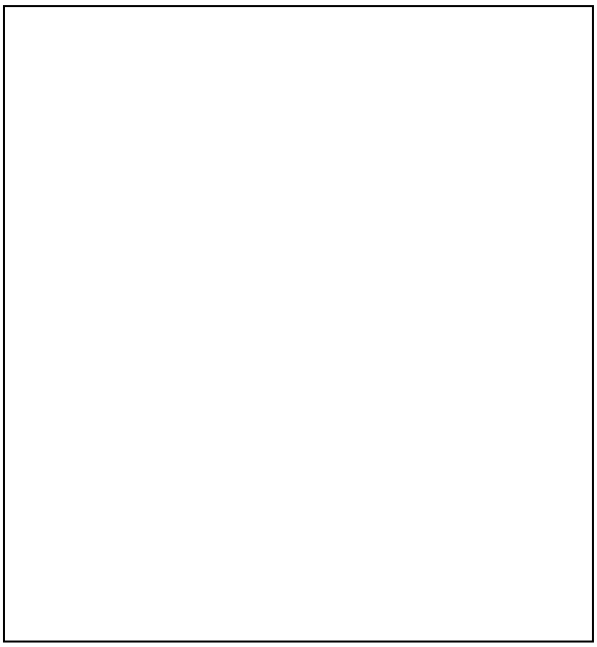

Figure 1.9 Scheme of the glyoxylate cycle in *Chlamydomonas reinhardtii* (replicated from Stern, 2009).

Regarding the nitrogen source, different sources have been evaluated (Zhang et al., 1999) finding that urea gave the best results for maximum cell concentration and specific growth rate, however, *C. reinhardtii* uses preferably inorganic ammonium salts as the nitrogen source (Harris et al., 2009d).

1.4.5 Mixotrophic culture

Mixotrophic cultivation of *C. reinhardtii* using both organic and inorganic carbon sources seems to be the most effective growth strategy, since the effect of light limitation is less pronounced. Moreover, it has been clearly observed that this mode of cultivation gives the highest biomass yield, when appropriate concentrations of acetate are applied (Moon et al., 2013).

Cultures supplemented with acetate and dim light (4 μmol m^{-2} s^{-1}) displayed a plastome content at least twice as high as its counterpart grown under phototrophic conditions (20 μmol m^{-2} s^{-1}), most likely due to a shorter generation time of the cells grown mixotrophically (5 h instead of 12). Nonetheless, this phenotypic change did not give improve results in terms of recombinant protein productivity (Eberhard et al., 2002).

A broader study analysed the effect of CO_2 concentration on photosynthesis efficiency in phototrophic cultures and compared it to a mixotrophic condition (Fischer et al., 2006).

When exposed to a light intensity of 120 μmol m^{-2} s^{-1}, the mixotrophic culture showed higher growth rate, whereas the high-CO_2 phototrophic culture showed the highest oxygen production, surpassing by over 2-fold the level in the other conditions (low-CO_2 phototrophic and mixotrophic). These three modes of cultivation were also exposed to high-intensity light (2500 μmol m^{-2} s^{-1}), where the high-CO_2 culture showed a dramatic decrease and subsequent cell death, while the other cultures were less sensitive showing a much slower decrease on cell density. In order to address how this photo-oxidative stress affects gene expression, DNA microarrays containing different nuclear or plastid genes for all culture modes were evaluated. Fischer and colleagues found that induction of gene expression was higher in both mixotrophic and high-CO_2 cultures. However, only approximately half of the genes were strongly induced under both conditions, suggesting a distinctive effect of the acetate metabolism on the genome expression, which was linked to alternative respiration processes protecting the cells from photo-oxidative stress.

1.5 Limitations when expressing foreign genes

Different limitations need to be addressed and overcome in order to increase cell density and protein productivity in a recombinant algal culture with the ultimate purpose of establishing a commercially efficient process for the production of a recombinant protein. *Chlamydomonas reinhardtii* can be genetically modified in order to alter or introduce variations in its genome, which could, as a result, lead to the generation of advantageous traits for the strain's growth or for its protein production machinery. In a similar manner, the cultivation conditions used for growing *C. reinhardtii* such as media composition, light supply, light intensity and temperature, to name some, can also trigger changes in the cell culture performance, growth rate and protein productivity. Therefore, the use of these two approaches is analysed in the following sections with the objective of selecting genetic modifications and cultivation parameters to be studied that could potentially maximise biomass and/or protein productivity.

1.5.1 Genetic modification approaches

A strategy that has been scarcely studied in algae for improving transgene expression is the incorporation of regulatory sequences in the insert such as operators, in order to generate an inducible expression system that could overcome the disadvantages observed

in constitutively-expressed cassettes, in which the transgene expression can affect the algal metabolism and biomass density (Cardi et al., 2010). Research carried out by Kato et al. (2007) considered the design of a controllable gene expression system composed by either the promoters from 16S rRNA or *rbcL*, containing the *lac* repressor expression cassette. They examined the effect of the position of the operator, and both the repression and induction of transcription with the correspondent repressor and inducer molecules. For the *rbcL* promoter, induction was achieved, but repression was not observed; opposite results were obtained for the 16S rRNA promoter.

As discussed previously for phototrophic cultivation, several strategies have been developed in order to achieve an optimal light exposure, in terms of light intensity, day/night cycle, and light/dark cycles within the light phase, but it will ultimately depend upon the type of photobioreactor available whether these manipulations can be effectively achieved. Conversely, it is possible to engineer certain cell photon-capture features in order to minimise efficiency losses in light absorption. One approach towards this goal has been performed by means of diminishing the light-harvesting antenna size.

A mutant strain of *C. reinhardtii* that had down-regulation of the LHC gene family was produced, exhibiting a decreased level of light-capture complexes and of chlorophyll content through a reduction in the antenna size. This feature additionally conferred a pale green phenotype and, as a result, deeper penetration of the light into the centre of the reactor, while maintaining a good rate of photosynthesis (Mussgnug et al., 2007). It could be observed that light dissipation from the antenna in the transformed strain was significantly reduced and photon capture efficiency was improved. Moreover, they discovered a higher tolerance to high-intensity light exposure (1400 μmol m^{-2} s^{-1}) and, therefore, lower photoinhibition. Given this tolerance, cultures were grown at 1000 μmol m^{-2} s^{-1}, and it was observed that cell growth and replication of the transformed strain was also considerably faster in comparison to the control, providing an additional advantage for the use of this type of engineered strains. A similar approach was subsequently used by Beckmann et al. (2009) to construct a new strain with constitutive repression of the LHC gene family, which showed a reduced concentration of LHCII proteins, a reduction of about 15 % in the antenna size and a pale green phenotype as well. Additionally, they observed increasing photon conversion efficiency as light intensity increased, and higher cell density. This strategy could be utilised in high cell density cultures were cells are forced to acclimate to uneven light intensity distributions, such as the normal light gradients that

occur in the radial dimension of a reactor. Unfortunately, none of these studies evaluated the expression of a heterologous protein in such a mutant.

1.5.1.1 Incorporation of a proteorhodopsin gene

In some microorganisms it is possible to find completely different photoactive proteins that are distinct from the photosystems of algae and plants. These complexes are responsible for light absorption and utilisation, and they present an interesting alternative protein to be co-expressed in the chloroplast of *C. reinhardtii*.

These photoactive proteins are known as microbial rhodopsins and are seven-helix transmembrane proteins that bind covalently to all-*trans*-retinal. Light can induce isomerisation of all-*trans*-retinal to 13-*cis*-retinal (Figure 1.10), resulting in conformational changes of the rhodopsin structure that turn it into either a light-activated ion pump or phototactic/photophobic biosensor. Recent research on marine bacteria and eukaryotes has revealed novel forms of retinal-based phototrophy with wider functions, including light-switched enzymes, light-gated ion channels and light sensors which couple to transducer proteins (Bryant and Frigaard, 2006; Ernst et al., 2014).

Figure 1.10 Proteorhodopsin is activated by photoisomerization of all-*trans* retinal to 13-*cis* retinal at wavelengths of 470 nm. After photoisomerization, the covalently bound retinal spontaneously relaxes to all-*trans* in the dark, providing closure of the ion channel and regeneration of the chromophore (replicated from Wong et al., 2012).

The first evidence of the existence of this type of protein in the *Bacteria* domain was reported 14 years ago (Béjà et al., 2000). These so called proteorhodopsins have the ability to generate a photochemically reactive pigment when linked to all-*trans* retinal. Once expressed in *E. coli* supplemented with retinal, a net outward transport of protons was observed, providing evidence for its suspected function as a light-driven proton pump (Figure 1.11), and the demonstration of its fast photocycle half-time confirmed this function rather than as a sensory rhodopsin.

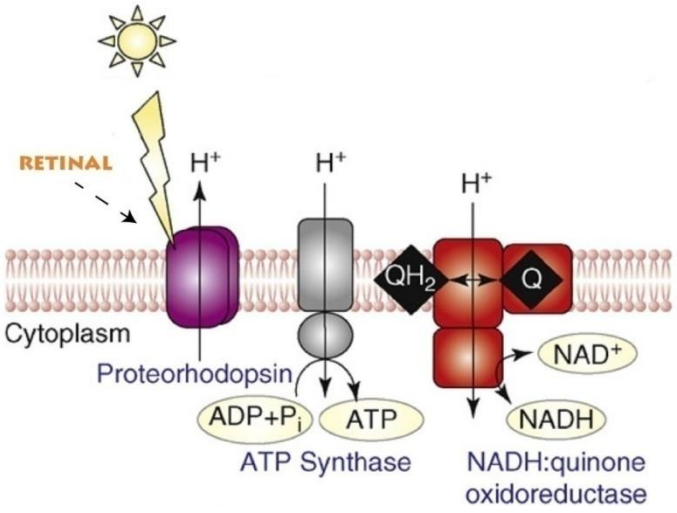

Figure 1.11 Schematic diagram representing the location and function of proteorhodopsin in the cell membrane. When activated by light in the presence of all-*trans*-retinal, it triggers proton pumping outwards, and these protons are reincorporated by means of the ATP synthase, generating in this way ATP (Adapted from Johnson and Schmidt-Dannert, 2008).

From this point onwards, the existence of different types of proteorhodopsins has been reported (Béjà et al., 2001), where energy-generating pigments are spectrally tuned to either shallow or deeper water light fields, evolving into the classification of blue-absorbing proteorhodopsins, BPR, (absorbance maximum of 490 nm) and green-absorbing proteorhodopsins, GPR, (absorbance maximum of 520 nm).

For one class of *Flavobacteria* expressing a recombinant proteorhodopsin, it was observed that light had a positive effect on growth, being primarily stimulated by green rather than blue or red light (Gómez-Consarnau et al., 2007). It was additionally noticed that supplementation with low or intermediate concentrations of organic matter together with light exposure, improved growth and size of the cells. Other studies performed in *E. coli* expressing the proteorhodopsin demonstrated that a) during respiratory challenges, light-powered proton pumping with green illumination could increase the cellular electrochemical potential of protons across the membrane to the extent that it powered cell motility and enhanced cell survival (Walter et al., 2007), and b) ATP synthesis could be augmented when the culture was light-induced due to reincorporation of protons to the cell through the ATP synthase complex, representing a 29 % increase over identical cell preparations without light exposure (Martinez et al., 2007). A study with populations of *Flavobacteria* and bacteria from the SAR11 clade expressing proteorhodopsin was performed, and these cultures were exposed to continuous light, continuous dark and 12/12 hour dark/light cycles. It was found that for both bacteria types the population

showed a higher growth when grown under dark/light cycles (Lami et al., 2009). Regarding proteorhodopsin transcript to gene ratio, they observed an up-regulation of proteorhodopsin expression by continuous light and dark/light cycles, along with a down-regulation by continuous dark, and the differential expression of proteorhodopsin in these two systems could be possibly linked to the physiological status and nutrient availability.

Soon after, evidence was gathered for the presence of green-absorbing proteorhodopsins in a member of the *Vibrio* genus and it was demonstrated that proteorhodopsin phototrophy represents a physiological mechanism that imparted an increased capacity to survive during periods of starvation in seawater (Gómez-Consarnau et al., 2010). This research observed an improved survival during starvation when cells were exposed to light, and improved capacity to recover growth in nutrient-rich environments after starvation when exposed to light. Another group observed that the expression of proteorhodopsin in the bacterium *Shewanella oneidensis* conferred extended viability under nutrient limitation as well, in addition to an increase in electricity generation (Johnson et al., 2010). More recently, some evidence of naturally-occurring proteorhodopsin in eukaryotic organisms has been reported (Slamovits et al., 2011) but its function has not been identified thus far. It has been speculated that this protein could be useful to absorb light in the green spectrum in order to fill the gap in the chlorophyll spectrum (Figure 1.12), expecting that PR could either increase the rate of carbon fixation or the growth rate of photosynthetic organisms by means of the additional energy supply (Walter et al., 2010).

In terms of green light usage, it has been observed that in vertical-column reactors green light was able to penetrate further inside into the reactor, but this could have been detected because the chlorophyll *a* of the green alga cultivated does not absorb light of this wavelength (Janssen et al., 2003). However, this fact demonstrates how this light is unused because no green-absorbing machinery is present in this type of organisms.

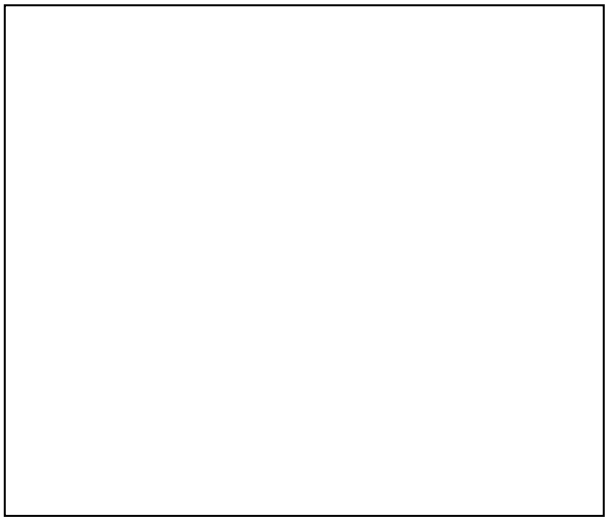

Figure 1.12 Gap filled in the light absorption range by incorporation of proteorhodopsin in *Chlamydomonas reinhardtii* (replicated from Walter *et al*. 2010)

The incorporation of a third photosystem for green light capture and enhanced photophosphorylation is considered as a promising strategy to pursue. It is expected that the expression of this protein in the chloroplast could increase overall energy production and, hence, cell growth. Further details of the protein chosen for this study are detailed in chapter 3.

1.5.2 Cultivation condition approaches

As discussed in previous sections, cultivation parameters can significantly influence the recombinant protein yield, affecting cellular mechanisms, microalgal growth and cell density. In addition to the major effect of light, it has been observed that media can also have a marked influence on cell growth and protein expression (Moon et al., 2013). Moreover, it is widely accepted that cultivation under certain conditions, such as nitrogen deprivation, can trigger specific metabolic pathways conducive to the accumulation of particular metabolites, in this case, accumulation of storage starch and triacylglycerols (TAGs) (Msanne et al., 2012; Yen et al., 2013).

Other parameters such as temperature and pH have not been intensively studied, but can clearly affect cultivation performance. To be best of my knowledge, only one published work studying the temperature effect on cell growth and lipid production in *C. reinhardtii* is available in the literature (James et al., 2013) and it was reported that temperatures between 32 – 35 °C improve cell growth rate, whereas a temperature of 38 °C, or below the traditional 25 °C, have a detrimental effect on cell growth rate and cell density achieved.

No observations were made on the effect of temperature on the expression of a recombinant protein.

Fluorescent proteins have become increasingly important as tools to evaluate gene expression *in vivo*. As mentioned in section 1.3.1, the availability of a fluorescent protein as a detectable marker in the chloroplast of *C. reinhardtii* has proven very challenging, with no well-expressed fluorescent proteins available so far. Such a marker would be of great benefit for studies of different cultivation parameters as well as the effect of various regulatory sequences, in order to identify optimal conditions that maximise protein accumulation.

There are several features of a fluorescent protein that make it eligible for a certain organism/objective. Among these, it is worth mentioning that this protein should not be toxic to the host, it should be expressed efficiently and provide sufficient brightness that can be detected above the auto-fluorescence of the host, and it should be insensitive to environmental changes (Shaner et al., 2005).

Many fluorescent proteins are currently available; however, a novel green fluorescent protein isolated relatively recently from the coral species *Cyphastrea microphthalma* named vivid Verde Fluorescent protein (VFP) has been reported to be at least twice as bright as the enhanced green fluorescent protein (EGFP) (Ilagan et al., 2010). VFP offers a potential improved marker to be tested in *C. reinhardtii*, not only for evaluating gene expression, but also to visualise how different culture parameters affect the culture's growth and recombinant protein expression.

1.6 Motivation and rationale

There is an ever-increasing need for the production of recombinant proteins, especially for human application, using efficient, low-cost hosts. Green microalgae seem to be a promising group of organisms for such biotechnology. The aim of this project was, therefore, to address some of the main factors limiting recombinant protein production in the chloroplast of *Chlamydomonas reinhardtii* in order to obtain a higher recombinant protein level.

The project encompassed two different approaches:

1. Genetic manipulation of the chloroplast of *Chlamydomonas reinhardtii*, in order to generate strains with improved features, in terms of both growth rate and recombinant protein expression.

   Light-capture efficiency was addressed by expressing a gene encoding a proteorhodopsin, and its effect was analysed in terms of improved specific growth rate/cell density and extension of the culture lifespan.

   Gene expression and protein accumulation was addressed by testing different promoters and regulatory sequences. To assess these different regulatory sequences, a gene for the newly reported fluorescent protein VFP was expressed and its expression as a reporter was characterised.

2. Bioprocess optimisation for the expression of a recombinant protein in the chloroplast of *Chlamydomonas reinhardtii*, comprising a study of three different parameters that may affect cell growth and protein productivity of a *C. reinhardtii* culture. This section included the usage of the fluorescent protein in different genetic backgrounds, by which not only protein expression but functionality of the protein produced can be assessed. The parameters chosen for this study were light intensity, media composition and temperature.

By merging both approaches it was expected to establish genetic and bioprocess parameters that lead to an increased recombinant protein productivity, and move towards the overall objective of developing the microalgal chloroplast as an expression system comparable to current bacterial systems.

CHAPTER 2

MATERIALS AND METHODS

2 MATERIALS AND METHODS

2.1 Strains and culture conditions

2.1.1 Escherichia coli

The *Escherichia coli* strain DH5α was used as a host cell for DNA amplification and plasmid construction. This strain shows an F- genotype, which describes a strain that does not contain the fertility factor (F), and therefore is not able to mate by conjugation, acting as a recipient only (www.openwetware.org). Among its features, it includes *lac*ZΔM15 for blue/white colour screening of colonies on plates containing X-gal; *rec*A1, which ensures increased insert stability and prevents unwanted recombination; and *end*A1, which improves the yield and quality of plasmid DNA prepared from minipreps (www.lifetechnologies.com).

This strain was grown in lysogeny broth (LB) at 37 °C and 200 rpm in a shaker incubator (SI60 Incubator, Stuart Scientific). When grown in solid medium, plates with LB medium supplemented with 1.5 % agar were used. When DH5α contained a plasmid carrying the *bla* gene, conferring ampicillin resistance, the medium was supplemented with 100 μg mL^{-1} of the antibiotic. For long term storage, strains of *E. coli* were stored in 25 % glycerol at -80 °C.

2.1.2 Chlamydomonas reinhardtii

Different *Chlamydomonas reinhardtii* strains were used depending on the purpose. The wild-type strain CC-1021 (mt+) was used as a control strain. Expression of *proteorhodopsin* and *vfp* were carried out in the cell wall-deficient strain TN72, which is a *psbH*-deficient strain developed in the Purton group (Ninlayarn, 2012) and originated from the strain CW15.3A (mt+). The recipient strain Bst-same (BST), used for expression of *vfp*, is a cell-walled *psbH*-deficient strain originated from the wild-type strain CC-1021 (O'Connor et al., 1998). The *rbcL*-deficient strains CC-2803 and CC-2653 are both cell-walled strains with defective *rbcL.* The strain CC-2803 was developed by Newman *et al*. (Newman et al., 1991) and features a disrupted *rbcL* with a 0.48 kb insertion from the yeast plasmid YEp24, whereas the strain CC-2653 was shown to contain a point mutation (T**G**G mutated to T**A**G) in the residue 66 near the 5′ end region of the *rbcL* coding sequence, causing an early termination of the RbcL protein synthesis and ultimate absence

of RuBisCo (Spreitzer et al., 1985). All strains were part of the Purton laboratory's stock, except for CC-2653, which was purchased from the Chlamydomonas Resource Center (University of Minnesota, USA).

Apart from CC-1021, all of the previously mentioned algal strains are photosynthesis-deficient; therefore, these were all grown in dim light (~ 5 μmol m^{-2} s^{-1}) using tris-acetate-phosphate (TAP) medium. When photosynthesis was restored through transformation, these were cultivated in mixotrophic mode in 25 mL flasks with TAP medium, and operation conditions were 140 rpm of agitation, 25 °C and continuous light exposure (~ 150 μmol m^{-2} s^{-1}) in an illuminated incubator shaker (Innova 4430 Incubator shaker, New Brunswick Scientific), unless otherwise stated.

When grown on solid medium, nutrient agar plates containing TAP medium supplemented with 2 % bacto agar were used. Plates were incubated at 25 °C and continuous light exposure varied between 30 – 50 μmol m^{-2} s^{-1}. Long term storage was also carried out in plates containing TAP medium supplemented with 2 % bacto agar in dim light (~ 5 μmol m^{-2} s^{-1}) at 20 °C. Plates were streaked every 4 weeks in order to ensure a permanently viable stock.

Starter cultures were made using a loop of healthy *C. reinhardtii* which was inoculated into a 50 mL flask with 25 mL of TAP medium. This culture was grown to mid-exponential phase. Optical density at 750 nm (OD_{750}) was measured at this point in order to inoculate a fresh flask with TAP medium to a final OD_{750}=0.25 (unless otherwise stated). For cultivation in the photobioreactor, a starter culture at the same conditions as above mentioned was established, and this was used to inoculate a 500 mL flask of the corresponding medium to an OD_{750}=0.25 (unless otherwise stated).

Different temperature conditions were used, which correspond to 25 (standard cultivation temperature), 30 and 37 °C. Light intensity was also varied, using either 30, 50 or 150 μmol m^{-2} s^{-1} in shaking incubator and 20, 200 or 800 μmol m^{-2} s^{-1} in the photobioreactor.

2.2 Media composition

Bacterial cultures were grown in LB medium (10 g L^{-1} bacto-tryptone, 5 g L^{-1} yeast extract and 10 g L^{-1} sodium chloride). For solid medium, granulated 1.5 % Difco agar was added.

C. reinhardtii was grown using different media, which include tris-acetate-phosphate (TAP), high salt minimal medium (HSM) and tris-acetate-phosphate medium without acetate, also known as tris-minimal (TP). TP and HSM do not contain any carbon source; therefore, they only allow phototrophic growth. Media compositions are shown in Table 2.1. In the case of TP medium, its preparation follows the same recipe as TAP, but its pH is adjusted with HCl rather than acetic acid. All chemicals used were of analytical grade and distilled water was used in all preparations.

Table 2.1 Media composition for tris-acetate-phosphate (TAP) and high salt minimal medium (HSM) used for *C. reinhardtii* growth (Adapted from Rochaix *et al.*, 1988).

For 1 L	TAP medium	HSM medium
H_2O	975 mL	925 mL
Tris	2.42 g	-
[a] 4 X Beijerinck Salts	25 mL	25 mL
[b] 1M (K)PO_4 pH 7.0	1 mL	-
[c] Trace Elements	1 mL	1 mL
[d] 2x PO_4 for HSM	-	50 mL
Glacial Acetic Acid	~1 mL to pH 7.0	-

[a] 4 X Beijerinck Salts: 0.3 M NH_4Cl, 14 mM g $CaCl_2 \cdot 2\ H_2O$, 16 mM $MgSO_4 \cdot 7\ H_2O$

[b] 1M (K)PO_4 pH 7.0: 1M K_2HPO_4 titrated to pH 7.0 with 1M KH_2PO_4

[c] Trace elements: 180 mM H_3BO_4, 77 mM $ZnSO_4 \cdot 7\ H_2O$, 26 mM $MnCl_2 \cdot 4\ H_2O$, 18 mM $FeSO_4 \cdot 7\ H_2O$, 7 mM $CoCl_2 \cdot 6\ H_2O$, 6 mM $CuSO_4 \cdot 5\ H_2O$, 0.9 mM $(NH_4)_6Mo_7O_{24} \cdot 4\ H_2O$

[d] 2x PO_4 for HSM: 80 mM K_2HPO_4 and 50 mM KH_2PO_4, adjusted to pH 6.9 with KOH

2.3 Cell density and dry biomass measurements

Cell density was determined by measuring absorbance at 750 nm (UV2 UV/Vis Spectrometer, Unicam) where there is no chlorophyll interference. This absorbance represents the optical density (OD) of the culture. Cell count was carried out using a hemocytometer and a bright field microscope at 40 X magnification (CH, Olympus). Due to

cell motility, a volume of 1 mL of algal sample was first treated with 10 µl of tincture of iodine (0.25 g iodine in 100 mL 95 % ethanol), which immobilizes cells.

For determining dry cell biomass, 500 mL cultures were grown in the photobioreactor and 50 mL of culture were harvested at different stages, centrifuged at 4000 x g and the pellet was stored at – 20 °C overnight. This pellet was dried overnight in a pre-weighted tube using a freeze drying system (Freeze Dryer Modulyo, Edwards) and the final weight was recorded once it stabilised. A calibration curve was developed (appendix 2) in order to calculate dry biomass in the different cultivation conditions used.

2.4 Growth rate calculations

Specific growth rate (µ) was calculated as shown in equation 2.1:

$$\mu = (\ln OD_t - \ln OD_0)/t \qquad (2.1)$$

where OD_t and OD_0 represent the optical density at 750 nm of the culture at time t and time zero of the exponential stage. µ is expressed in h^{-1}.

The doubling time (Td) was calculated from equation 2.2:

$$Td = \ln 2/\mu \qquad (2.2)$$

2.5 Molecular Biology

2.5.1 Bacterial plasmid isolation

Low concentration (< 20 µg) plasmid isolation and purification was performed using the commercial GeneJET plasmid miniprep kit (Thermo Scientific) as per manufacturer's instructions. Briefly, 1.5 mL of bacterial culture was harvested and lysed. The lysate was then cleared by centrifugation and applied on a silica column to selectively bind DNA molecules at a high salt concentration. The adsorbed DNA was washed to remove

contaminants, and the pure plasmid DNA was eluted in 20 µL of elution buffer. An estimate concentration of the DNA in each sample was determined measuring the absorbance of the sample at a wavelength of 260 nm (ND-1000 Spectrophotometer, Nanodrop).

For isolation of a larger amount of plasmid (< 100 µg) the commercial QIAfilter Plasmid Midi Kit (Qiagen) was used as per manufacturer's instructions. Briefly, a 4 mL bacterial culture was grown for 8 hours and used to inoculate a fresh 50 mL LB medium flask that was grown overnight. The whole culture volume was lysed and cleared by centrifugation. The cleared lysate was then loaded onto an anion-exchange tip where plasmid DNA selectively binds under appropriate low-salt and pH conditions. RNA, proteins, metabolites, and other low-molecular-weight impurities were removed by a medium-salt wash, and pure plasmid DNA was eluted in high-salt buffer. The DNA was concentrated and desalted by isopropanol precipitation and collected by centrifugation, to then be eluted in 50 µL of elution buffer. These purified plasmids were used for transforming *C. reinhardtii*.

2.5.2 Polymerase chain reaction

DNA amplification was carried out by means of the polymerase chain reaction (PCR). The primers (synthesised by Eurofins) used for each reaction are listed in Appendix 1. All reactions were performed in a final volume of 50 µL, where the reagents listed in Table 2.2 were added. When more than two primers were used, or more DNA volume was added, the according volume difference was subtracted from the distilled water volume. Reactions were run in a TC-3000G thermocycler (Techne) and the following cycle conditions were used: 30 s of initial denaturation at 98 °C, 25 cycles of 10 s denaturation, 30 s of annealing at 3 °C above the annealing temperature (Tm) of the lowest Tm primer, and extension at 72 °C for 15 s per kb for plasmid DNA/30 s per kb for genomic DNA. A final elongation of 5 min at 72 °C was carried out and the cycle was held at 4 °C.

Table 2.2 Reagents and volume added to perform polymerase chain reaction (PCR).

Reagent	Stock concentration	Volume [µl]
DNA	~ 1 µg genomic DNA ~ 20 ng plasmid DNA	2
Phusion HF reaction buffer	5 X	10
Forward primer	100 pmol μL^{-1}	0.5
Reverse primer	100 pmol μL^{-1}	0.5
Nucleotides mix (dNTPs)	100 mM	1
Phusion polymerase	100 U	0.5
Distilled water		35.5
Final Volume		50

2.5.2.1 PCR screening for homoplasmic transformants in TN72/BST transformed with the pASapI vector

Screening for homoplasmic transformants when using the expression vector pASapI for transformation was performed following the strategy displayed in Figure 2.1 (Ninlayarn, 2012) using the primers FLANK1, atpA.R, rbcL.Fn and MluR2.

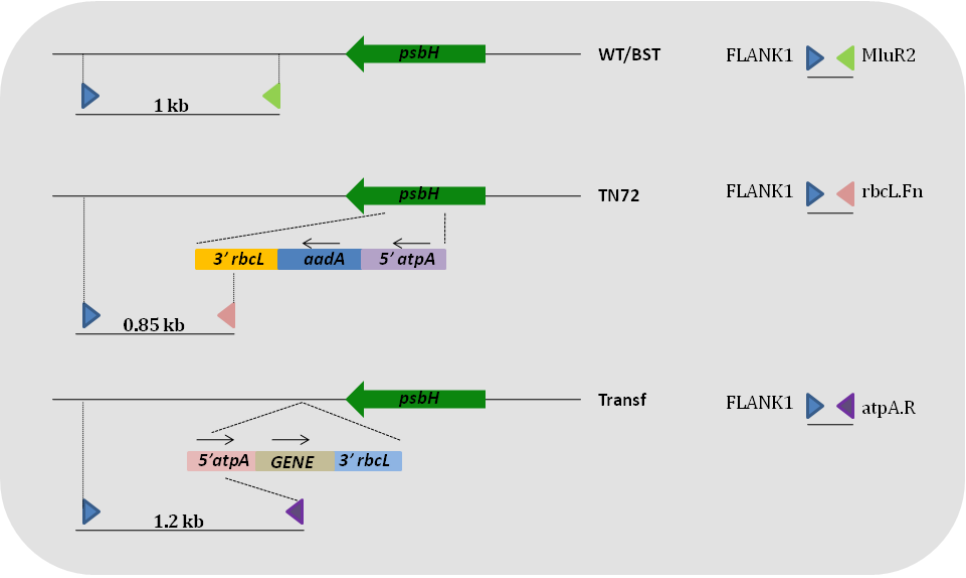

Figure 2.1 Primers used for PCR screening of homoplasmic transformants in TN72/BST hosts.

The wild-type strain CC-1021 and the strain TN72 were used as controls. Expected bands are as follows: wild-type (WT) 1.0 kb; TN72 0.85 kb, positive transformant 1.2 kb. For the case of BST transformants, the TN72 assay was not needed.

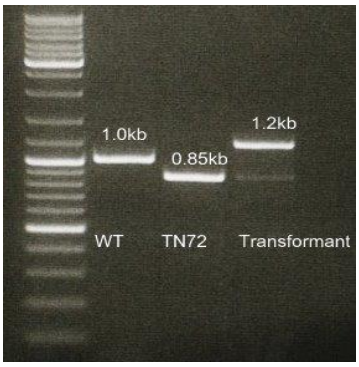

Figure 2.2 PCR screening for TN72 transformants expressing a foreign gene using the pASapI expression vector. Primers used are FLANK1, atpA.R, rbcL.Fn and MluR2. Expected bands are as follows: wild-type (WT) 1.0 kb; TN72 0.85 kb; homoplasmic transformant 1.2 kb.

2.5.3 Restriction endonuclease digestion

DNA samples were digested with the appropriate restriction enzyme (New England Biolabs) as per manufacturer's instructions. The only exceptions to this were the enzymes *SapI* and *SphI*, which were supplied by Fermentas due to improved performance in double digestion.

2.5.4 Agarose gel electrophoresis

Agarose gel electrophoresis was carried out using 1 % agarose gels in 1X TAE buffer (0.04 M Tris, 1 mM sodium EDTA, 17.5 mM glacial acetic acid) supplemented with 0.1 μg mL^{-1} of ethidium bromide. Gels were run in 1X TAE buffer at 90 V (Sigma tanks; Power pac 300, Biorad) and visualized using a 302 nm UV illuminator. Images were printed on black/white thermal paper (UVP Gel Documentation System).

For loading DNA samples into the gel, 6X loading buffer (2.5 % Ficoll 400, 11 mM EDTA, 3.3 mM Tris-HCl, 0.017 % SDS, 0.015 % bromophenol blue) was used to a concentration of 1X. The markers GeneRuler DNA ladder mix and GeneRuler 1 kb DNA ladder (Thermo Scientific) were used at a concentration of 0.5 μg per lane.

2.5.5 DNA fragment extraction from agarose gels

The commercial GeneJET gel extraction kit (Thermo Scientific) was used for recovery of DNA fragments from agarose gels. In short, bands were excised from the agarose gel,

solubilised in binding buffer and purified on a silica-based membrane contained in a spin column, from where the pure DNA fragment was eluted.

2.5.6 Removal of 5' phosphate from DNA using Antarctic phosphatase

In order to prevent re-ligation of the backbone vector after digestion, Antarctic phosphatase (New England Biolabs) was used to remove the 5' phosphate. DNA samples were treated with 2 units of enzyme per ug of DNA and incubated for 30 min at 37 °C. The reaction was inactivated with 20 min incubation at 65 °C.

2.5.7 PCR product purification

PCR fragments were purified using the GeneJET PCR purification kit (Thermo Scientific) as per manufacturer's instructions. In brief, primers, dNTPs, unincorporated nucleotides, enzymes, and salts from PCR and other reaction mixtures were removed using a silica-based membrane in the form of a spin column, and the DNA fragment was then eluted and recovered for further experiments.

2.5.8 DNA Ligation

The purified DNA fragments were ligated using a molar ratio of insert:backbone of 3:1. The ligation was conducted using 1 unit of T4 DNA ligase (New England Biolabs) per 1 µg of DNA, supplemented with 10 mM ATP and T4 DNA ligase buffer to a final volume of 10 µL. The reaction was incubated for 2 h at room temperature.

2.5.9 Cloning PCR products into the pJET vector

Cloning of PCR products for the formation of the psbC.KO plasmid was performed using the commercial vector CloneJET PCR cloning kit (Fermentas) as per manufacturer's instructions. In brief, the pJET 1.2/blunt vector was ligated to the blunt-end PCR fragment by the action of the T4 DNA ligase. This plasmid was used for transformation in DH5α and cells were streaked onto LB plates supplemented with 100 µg mL^{-1} ampicillin. The recircularised vector expresses a lethal restriction enzyme after transformation and is not propagated, ensuring that only recombinant clones containing the insert appear on the transformation plates.

2.5.10 Gibson assembly for the generation of recombinant plasmids

The principle of this method relies on the recombination of DNA fragments sharing terminal sequence overlaps. A 5' exonuclease removes the nucleotides from the 5' ends of adjacent double-stranded DNA fragments, giving the opportunity for complementary single-stranded DNA overhangs to anneal, followed by a seamless repair and sealing performed by a DNA polymerase and DNA ligase.

For the generation of the plasmid P266-rbcL-VFP using the one-step isothermal DNA assembly, the following procedure was carried out:

1) Preparation of the 5X isothermal reaction buffer using the following reagents (volumes in brackets): 1 M DTT (50 µL), 100 mM NAD (50 µL), 1 M Tris-HCl (pH 7.5) (500 µL), 2 M $MgCl_2$ (25 µL). A mass of 0.25 g of PEG-8000 was dissolved in the previous mixture, and the resulting volume was centrifuged briefly and made up to 1 mL with distilled water. This volume was filter-sterilised using a 0.22 µm disposable filter.

2) Preparation of the assembly mastermix: addition of 0.64 µL of T5 exonuclease to 320 µL of the 5X isothermal reaction buffer. Then, to 32.1 µL of the buffer-exonuclease mix, the following reagents (volumes in brackets) were added: phusion polymerase (2 µL), Taq DNA ligase (16 µL), dNTP mix (3.2 µL) and distilled water (66.7 µL), reaching a final volume of 120 µL, which was aliquoted and stored at -20 °C.

3) DNA fragments were added to the assembly mastermix, following equation 2.3 to make up a final volume of 20 µL.

$$pmol \times N \times 660 \frac{pg}{pmol} \times 1 \frac{\mu g}{10^6 pg} = \mu g\ DNA\ fragment \qquad (2.3)$$

where pmol is the recommended amplicon value used in the reaction (0.01375 – 0.025 pmol for 6 kb DNA fragments), N is the size of the DNA fragment in bp, and 330 pg $pmol^{-1}$ is the average molecular weight of a nucleotide. A value of 0.01935 pmol for the backbone fragment, and 0.02275 pmol for the VFP fragment were used, and this mixture was incubated at 50 °C for 60 min.

4) The entire mixture was used for bacterial transformation as detailed in section 2.6.1, and bacteria were streaked onto LB plates supplemented with 100 μg mL^{-1} of ampicillin for transformant selection.

2.5.11 Genomic DNA extraction

Genomic DNA extraction was carried out in the following way: a small loop of actively-growing cells was resuspended in 20 μL of sterile water, 20 μL of absolute ethanol were added to the tube and incubated for a minute at room temperature. Then, 200 μL of a 5 % suspension of Chelex 100 resin (Bio-Rad) were added and the sample was vortexed and heat shocked at 98 °C for 5 minutes. After brief cooling on ice, the tube was centrifuged for 2 minutes at maximum speed and the supernatant was transferred to a fresh tube and kept at – 20°C.

2.5.12 DNA Sequencing

DNA was sent for sequencing at the Wolfson Institute for Biomedical Research (UCL) using a Beckman Coulter CEQ 8000 genetic analysis system. Customised primers were provided at a concentration of 5 pmol μL^{-1}, and DNA was supplied at a concentration of 100 ng μL^{-1} for plasmid DNA, and 1 ng μL^{-1} per 100 bp for PCR fragments.

2.6 Genetic Transformation

2.6.1 Bacterial transformation

Firstly, generation of competent cells was carried out using the strain DH5α from a frozen glycerol stock, which was streaked onto a LB plate and left overnight at 37 °C. A single colony was picked and inoculated into 10 mL of LB and left overnight at 37 °C. A volume of 1 mL of the previous culture was added to 100 mL of fresh LB and incubated for 2.5 h at 37 °C. The culture was cooled on ice for 15 min and centrifuged at 4000 x g for 5 min in 4 tubes. The supernatant was removed from each tube and replaced by 10 mL of cold 50 mM $CaCl_2$. Cells were resuspended and left on ice for 30 min. The tubes were centrifuged using the same conditions, and the supernatant was replaced by 1.5 mL of fresh 50 mM $CaCl_2$. At

this stage the four sterilin tubes were pooled in one single tube and 3.5 mL of sterile 50 % glycerol were added. The resulting suspension was aliquoted and kept at -80 °C.

Transformation was performed in the following way: to a tube containing 100 µL of competent DH5α cells, 1 µL of DNA (concentration 10-20 ng) was added, left on ice for 30 min and then heat shocked at 42 °C for 60 s (Thermomixer comfort, Eppendorf). Once returned to ice, 1 mL of LB was added and the tube was placed in the shaker incubator for 60 min at 37 °C. Volumes of 100, 200 and 800 µL of culture were spread onto solid LB supplemented with 100 µg/mL of corresponding antibiotic and left in a 37 °C incubator overnight for colony growth. Transformant colonies were picked and grown separately in 10 mL of liquid LB with the corresponding antibiotic overnight for further analyses.

2.6.2 Chloroplast transformation of *Chlamydomonas reinhardtii*

2.6.2.1 Transformation method using glass beads

Firstly, a 25 mL starter culture was grown in mixotrophic conditions in TAP medium and this was used as inoculum for a 400 mL culture. Cells were harvested in mid-exponential phase and centrifuged at room temperature at 4000 x g for 5 min and the pellet was resuspended in HSM to a concentration 2 x 10^8 cells mL^{-1}. Then, 300 µL of this cell suspension and 5 µg of plasmid DNA were added into an autoclaved 5 mL test tube containing 0.3 g of 0.4 mm diameter glass beads (BDH). The mixture was vortexed for 15 seconds. Then, 3.5 mL of molten HSM supplemented with 0.5% bacto agar at 42 °C were added to each tube and poured quickly onto 2% bacto agar HSM plates, which were immediately covered with a black cloth to prevent phototactic migration of the cells, and allowed to set for 20 minutes. The plates were incubated under bright light (150 µmol m^{-2} s^{-1}) for 3 – 4 weeks.

When transformant colonies appeared and had reached an appropriate size to be picked (~ 1 mm), they were transferred individually to fresh HSM plates in order to force selection of transformants by phototrophy and to promote homoplasmy of the polyploid chloroplast genome. After three passages in HSM plates, a sample of each colony was collected and its genomic DNA was extracted in order to perform PCR analysis, as detailed in section 2.5.2.1.

2.6.2.2 Transformation method using microparticle bombardment

The transformation yield with glass beads in host strains with intact cell wall can be low; therefore, microparticle bombardment was used as an alternative technique for chloroplast transformation. The principle of this technique relies on the bombardment of a lawn of algal cells streaked on an agar plate with tungsten particles coated with the DNA to be introduced. These particles are accelerated to very high velocity, and thus they can penetrate the cell wall and membranes of the alga and get into the chloroplast, where DNA can integrate by homologous recombination (Kindle et al., 1991).

A 25 mL starter culture was grown in mixotrophic condition in TAP medium and this was used as inoculum for an 800 mL culture. Cells were harvested in mid-exponential phase and centrifuged at room temperature at 4000 x g for 5 min and the pellet was resuspended in HSM to a concentration 2 x 10^8 cells mL^{-1}. In a sterile laminar flow, 0.25 mL of the cell suspension were streaked on TAP plates supplemented with 3 % bacto agar and incubated at 25 °C in dim light (~ 10 µmol m^{-2} s^{-1}) overnight.

DNA is introduced into the chloroplast using microcarriers, which are prepared in the following manner (for 12 bombardments): in a 1.5 mL microfuge tube, 60 mg of tungsten particles were weighed, and 0.5 mL of 70 % ethanol was added. The mixture was vortexed for 180 – 300 s and incubated for 15 min. The mixture was centrifuged for 5 sec and the supernatant was discarded. The following steps were repeated 3 times: addition of 0.5 mL of sterile double de-ionised water, vortexing for 60 s, incubation to leave particles to settle for 60 s, centrifugation of the mixture for 5 s, and supernatant removal. Finally, 100 µL of 50 % sterile glycerol were added.

For coating of the microcarriers with the plasmid DNA, the microcarrier solution was vortexed for 300 s in order to resuspend and disrupt any agglomerated particles (and this was performed continuously throughout the procedure). While vortexing, the following reagents were added in the stated order: 7 µL of the DNA, 50 µL of 2.5 M $CaCl_2$ and 20 µL of 0.1 M spermidine (Sigma-Aldrich). The mixture was vortexed for 120 – 180 s, allowed to settle for 60 s and centrifuged for 2 s. The supernatant was discarded and 140 µL of 70 % ethanol were carefully added without disturbing the pellet. The liquid was removed and 140 µL of 100 % ethanol were added without disturbing the pellet. The liquid was removed and 48 µL of 100 % ethanol were added. The pellet was resuspended by tapping the side of the tube several times and by vortexing at low speed for 2 – 3 s.

In a sterile laminar flow, 6 μL aliquots of microcarriers were placed on the centre of a sterile macrocarrier that was mounted in a macrocarrier holder. These were left to desiccate and then used for bombardment.

The bombardment system used (Biolistic PDS1000/He System, Bio-Rad) is shown in Figure 2.3. To operate this system, it needs to be pressurized using Helium. For *C. reinhardtii*, a burst pressure of 900 – 1100 psi is normally used.

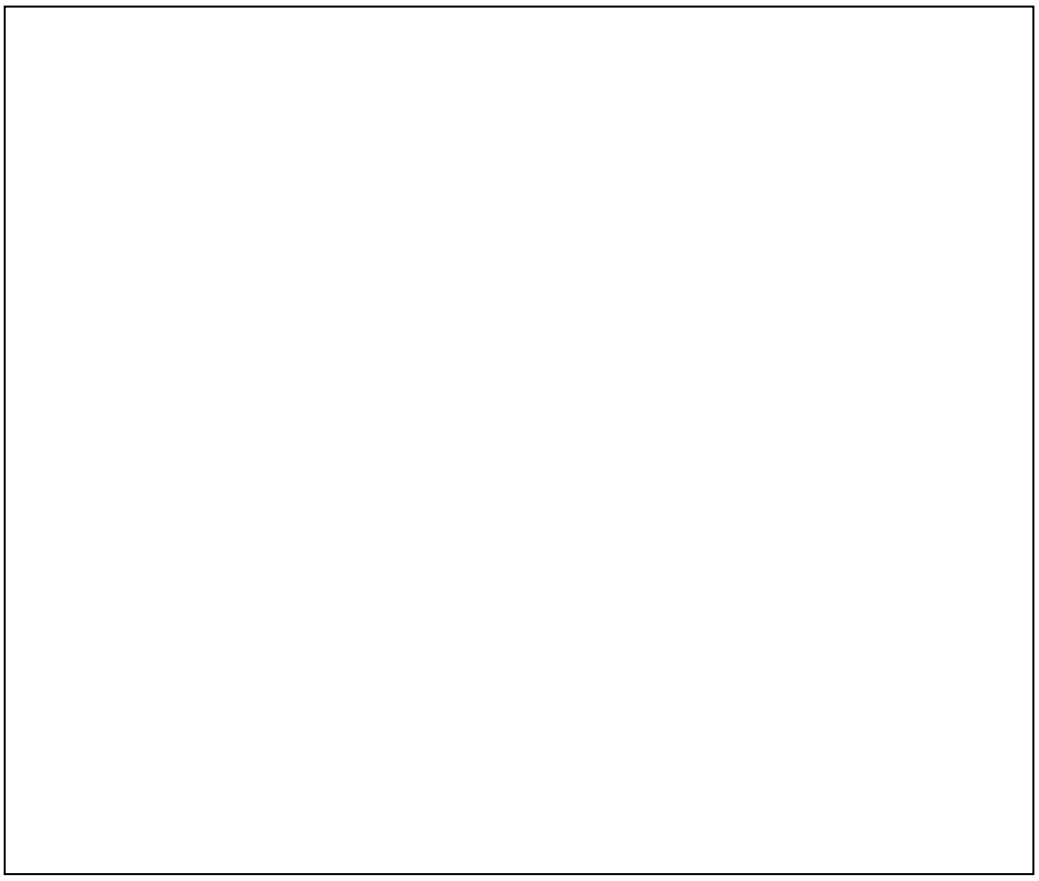

Figure 2.3 Microparticle bombardment equipment. A) Unit components, front view. B) microparticle bombardment device, front view. C) Insertion of macrocarrier into macrocarrier holder with plastic insertion tool. D) Rupture disks. Images taken from www.bio-rad.com.

For assembling the system, a rupture disk was placed in the recess of the rupture disk retaining cap. This cap was screwed onto the gas acceleration tube. A sterile stopping screen was placed on top of the stopping screen support, and the macrocarrier holder with macrocarrier was installed on the top rim of the fixed nest, with the microcarriers facing down towards the stopping screen. The microcarrier launch assembly was located on the second slot from the top in the sample chamber.

A TAP plate with the lawn of *C. reinhardtii* cells was placed on the petri dish holder, and this holder was placed at the 3 different levels inside the chamber and the sample chamber door was closed.

For firing the system, the vacuum pump was turned on, and once the desired vacuum was reached, the vacuum switch was put in the hold position and then fired. After vacuum was released, the sample chamber door was opened and the TAP plate was immediately covered and removed. The assembly was carried out as described previously for each event of transformation and the plates were incubated in bright light at 25 °C for 3 – 4 weeks until transformant colonies were recovered.

When transformant colonies appeared and had an appropriate size to be picked, they were transferred individually to fresh HSM plates in order to force selection of transformants by phototrophy and to promote homoplasmy of the chloroplast DNA. After three passages in HSM plates, a sample of each colony was collected and its genomic DNA was extracted in order to perform PCR analysis, as detailed in section 2.5.2.1 (unless otherwise stated).

2.7 Protein Expression Analyses

2.7.1 Preparation of whole cell extracts for Western blot analysis

Cells were harvested at different stages of cultivation depending on the experiment carried out. A volume that would represent a cell concentration equivalent to an OD_{750}=15 in 1 mL of volume was harvested, in order to normalise loading concentration of cells per well. This volume was transferred to a sterilin tube and centrifuged at 4000 x g for 5 min. The pellet was resuspended in 500 µL mL of solution A (0.8 M Tris-HCl pH 8.3, 0.2 M sorbitol, 1 % β-mercaptoethanol). Samples were used directly for SDS-PAGE or stored at – 20 °C.

Just before running the gel, 50 µL of each sample were mixed with 5.5 µL of 10 % SDS and boiled for 5 min in a block heater at 99 °C (Thermomixer R, Eppendorf). The samples were briefly cooled on ice and centrifuged for 2 min at maximum speed. 30 µL of the supernatant were loaded into a well of the gel (unless otherwise stated). When a positive control was used, this corresponded to a transformant line with a highly expressed HA-

tagged protein that was processed in the same way, but only 10 µL were loaded onto the gel.

2.7.2 Membrane protein extraction

In order to generate an enriched membrane-protein fraction, the Mem-PER Eukaryotic Membrane Protein Extraction Reagent Kit (Thermo Scientific) was used as per manufacturer's instructions, following the mammalian cell protocol. In brief, cells were lysed with a detergent and then a second detergent was added to solubilise the membrane proteins. The cocktail was incubated at 37 °C to separate the hydrophobic proteins from the hydrophilic proteins through phase partitioning.

2.7.3 SDS-polyacrylamide gel electrophoresis

Sodium dodecyl sulfate polyacrylamide gel electrophoresis (SDS-PAGE) was used to separate proteins according to weight. Gels were cast using the mini-PROTEAN Tetra system (Bio-Rad). Each SDS gel encompasses two different gel fractions and it was prepared in the following way:

- 15 % Resolving gel: 2.5 mL of acrylamide/bisacrylamide (40% stock at 37:1 acryl:bis ratio) were mixed with 0.835 mL of 8X resolving gel buffer (3.0 M Tris-HCl pH 8.8), 67 µL of 10% SDS and 3 mL of distilled water. This mixture was left for degassing for 10 min and then 0.25 mL of 10 % ammonium persulphate and 7.5 µL of TEMED were added and the mixture was quickly poured into a gel caster and allowed to polymerise. A thin layer of ethanol was added, causing the top of the resolving gel to form a smooth surface, and once the gel was set the alcohol was washed away.
- 3.75 % Stacking gel: 0.235 mL of of acrylamide/bisacrylamide (40% stock at 37:1 acryl:bis ratio) were mixed with 0.625 mL of 4X stacking gel buffer (0.5 M Tris-HCl pH 6.8), 25 µL of 10 % SDS, 1.5 mL of distilled water, 0.125 mL of 10 % ammonium persulphate and 1.875 µL of TEMED. The gel was poured on top of the resolving gel and a 1 mm thickness well comb was placed to form the wells. After the gel was polymerised, the comb was removed.

Samples were loaded into the gel, and the PageRuler Plus prestained protein ladder (Thermo Scientific) was used as a molecular weight marker. Gels were run in 1X Reservoir

buffer (10X buffer: 0.25 M Tris, 1.92 M glycine, 1 % SDS) at 120 V for 2.5 hours, or until the desired resolution was achieved.

2.7.4 Immunological detection by Western blot analysis

After running SDS-PAGE, the gel was soaked in Towbin buffer (25 mM Tris, 192 mM glycine, 0.1 % SDS, 20 % methanol), together with the Hybond-ECL nitrocellulose membrane (GE Healthcare) and 12 pieces of 3 MM Whatman blotting paper for 30 minutes at room temperature. Proteins from the gel were transferred to the membrane by semi-dry electroblotting (Trans-Blot SD Semi-dry transfer cell, Bio-Rad). The transfer stack was assembled placing 6 sheets of blotting paper above and below the membrane, with the gel placed on top of the membrane. The assembly was rolled out to remove any bubbles and the electroblotting was run at 20V for 1 hour.

The membrane was blocked in 0.5 % low fat milk in TBS-T (20 mM Tris base, 137 mM NaCl, 1 M HCl, 0.1 % Tween-20) at either room temperature for 1 hour or 4 °C overnight. After blocking, it was rinsed 3 times with TBS-T in an orbital shaker (Mini orbital shaker SSM1, Stuart) and incubated in an orbital shaker with the primary antibody in a 1:2000 dilution in 0.5 % milk in TBS-T for 1 hour. Primary antibodies used were anti-HA antibody from rabbit (Sigma), anti-D1 from rabbit (Purton's stock), and anti-rbcL from rabbit (Purton's stock). The membrane was rinsed 4 times with TBS-T and incubated in an orbital shaker with a 1:25000 dilution of the secondary antibody in 0.5 % milk in TBS-T. Secondary antibodies used where anti-rabbit IgG: horseradish peroxidase linked whole antibody (GE Healthcare) for ECL detection, and anti-rabbit IR dye 800 nm fluorophore linked (Li-Cor Biosciences). Again, 3 washes with TBS-T were performed.

In the case of ECL detection, excess TBS-T was removed from the membrane and the latter was incubated for 5 min with SuperSignal West Pico Chemiluminescent substrate (Pierce) as per manufacturer's instructions. Excess substrate was removed and the membrane was sealed in between plastic sheets using a heat sealer and placed in an exposure cassette. The membrane was exposed to Hyperfilm ECL (GE Healthcare) for times ranging from 5 sec to 1 hour depending on the antibody used, and the film was developed using an a Xograph automatic film developer. For infrared detection, the membrane was additionally rinsed twice with TBS buffer to remove any traces of Tween-20, left to dry for 30 min and

scanned using a quantitative fluorescence detection system (Odyssey Infrared Imaging System, Li-Cor Biosciences).

2.7.5 Quantification of recombinant protein

Quantification of HA-tagged proteins was carried out using a commercial HA-tagged protein (human CARHSP1, AbCam) of known concentration. For estimation of band concentration in gels, stocks of 50, 100 and 150 ng per well of standard protein were prepared and loaded. CARHSP1 protein gives a band of approximately 40 kDa.

For calculations to estimate VFP concentration, the size of both CARHSP1 and VFP (27 kDa) were considered, as shown in equation 2.4

$$concentration\ CARHSP1\ band\ [ng] \times \frac{size\ VFP\ [kDa]}{size\ CARHSP1\ [kDa]} = concentration\ VFP\ band\ [ng] \qquad (2.4)$$

This VFP concentration corresponds to 10 µL of sample loaded in the well.

To calculate the protein concentration per volume of culture on each condition, the volume of Solution A and SDS (section 2.7.1) used to prepare samples for Western blot was taking into account, as shown in equation 2.5

$$VFP\ \left[\frac{ng}{\mu L}\right] \times 1.1\ \times \frac{500\ \mu L\ Solution\ A}{X\ \mu L\ culture\ volume} = VFP\ concentration\ in\ culture\ [\frac{ng}{\mu L}] \qquad (2.5)$$

2.8 Fluorescence Measurements

2.8.1 PSII auto-fluorescence measurement

At room temperature, fluorescence in *Chlamydomonas reinhardtii* is mainly emitted by the chlorophylls of the PSII in the chloroplast, as observed in Figure 2.4. In order to assess the phenotype of PSII-mutants in terms of their expected higher autofluorescence, samples from *psbC*/*psbK* knockout transformants were grown in TAP medium and harvested during exponential growth by centrifugation at 4000 x g for 5 min. The pellet was resuspended in HSM, and cell concentration was measured by absorbance at 680 nm. Cells

suspensions were normalised to an optical density of OD_{680}=0.5 and samples were scanned across the range 550 – 800 nm for fluorescence emission at an excitation wavelength of 500 nm.

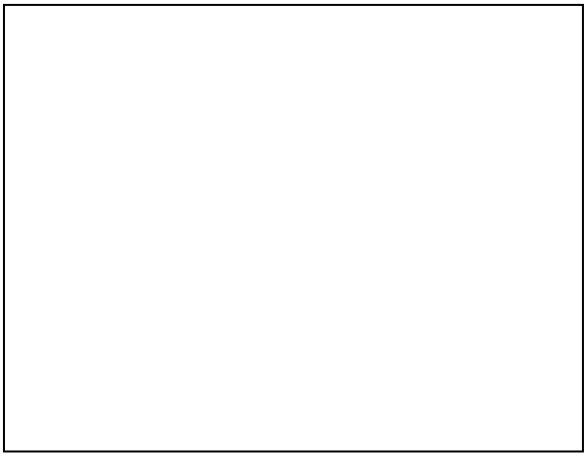

Figure 2.4 Fluorescence emission of *Chlamydomonas reinhardtii* cell suspension measured at room temperature (RT) and 77 K. Arrows indicate the main PSI and PSII emission peaks (replicated from Molecular Genetics of Chlamydomonas, EMBO practical course, 2006).

2.8.2 Confocal Microscopy

A volume of 5 µL of suspension samples of *C. reinhardtii* expressing VFP was mounted on a slide, let to dry for 20 min and examined with a Leica TCS SP5 confocal microscope. VFP was excited by the 488 nm laser line.

2.8.3 Flow cytometry

Flow cytometry was carried out using a Cyan ADP system (Beckman Coulter) fitted with a standard FITC filter and fluorescence was detected in the range 510 – 550 nm. A volume of 1 ml of each sample at an OD_{750} = 0.3 was used for each test. Control strains not expressing VFP grown in the same cultivation conditions as the strains expressing VFP were used for every measurement to account for the auto-fluorescence of each VFP-expressing strain.

The median value obtained for the top 50 % population was used as the parameter for fluorescence. Values above auto-fluorescence (median value of the control strain) were attributed to VFP. The median value of fluorescence obtained for the VFP-expressing strain was compared to the value obtained from its negative control, and this shift was expressed as a percentage of fluorescence. Standard error was calculated for each condition measured (n = 4).

2.9 Cell size measurement

Algal cells growing in different media conditions were evaluated for their average cell size using a particle size analyser (Mastersizer Hydro 2000SM, Malvern Instruments). Cells were harvested in mid-exponential phase and resuspended on its respective media to an OD_{750} = 0.5. A standard solution with particles of 30 nm was used. Data of cell size was obtained from the Mastersizer 2000 software.

CHAPTER 3

EXPRESSION OF AN ADDITIONAL LIGHT-CAPTURE SYSTEM IN THE CHLOROPLAST OF *CHLAMYDOMONAS REINHARDTII*

3 EXPRESSION OF AN ADDITIONAL LIGHT-CAPTURE SYSTEM IN THE CHLOROPLAST OF *CHLAMYDOMONAS REINHARDTII*

Light capture and utilisation in photosynthetic organisms is carried out by the light-harvesting antenna complexes (LHCs) from the two photosystems present in chloroplasts, namely Photosystem I (PSI) and Photosystem II (PSII). Pigments such as chlorophylls and carotenoids are associated with these LHCs and their primary function is to absorb light triggering a series of oxido-reduction reactions that ultimately lead to the generation of O_2, energy-storage molecules in the form of ATP, and reducing power in the form of NADPH. Chlorophylls *a* and *b* are the predominant antenna pigment forms in green tissues and they have distinctive absorption maxima in the blue-violet (wavelengths 400 – 500 nm) and the red (wavelengths 600 - 700 nm) regions of the light spectrum. When observing the chlorophyll a/b absorption spectrum it is undoubtedly noted that light is not efficiently absorbed in the green region (wavelengths 500 – 600 nm) (Figure 3.1). However, in chloroplasts of leaves it has been shown that green light can drive photosynthesis with high efficiency when absorbed (Terashima et al., 2009).

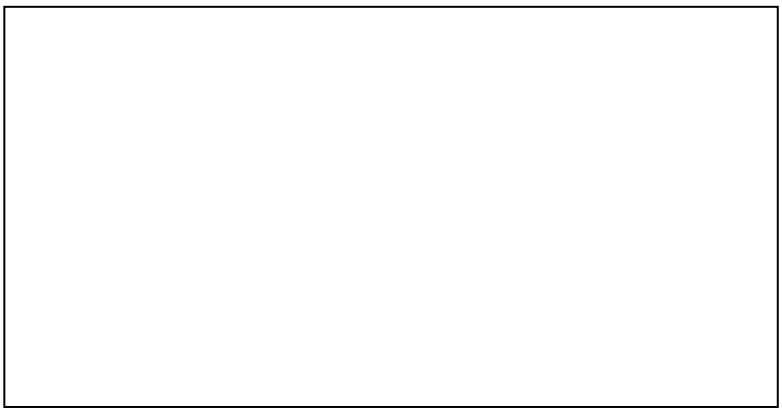

Figure 3.1 Chlorophyll *a*, *b* and carotenoid absorbance spectra (replicated from Baker *et al.* 2012).

As introduced in section 1.5.1, there is a different mechanism for light capture found in nature, which is based on retinal, and this form of phototrophy is widely observed in *Archaea*. Among these rhodopsin-like proteins, proteorhodopsins receive special attention since they have been found to be widely distributed in surface-dwelling prokaryotes (Béjà et al., 2001, 2000; Fuhrman et al., 2008). Proteorhodopsins can be classified into green-absorbing or blue-absorbing proteorhodopsins, depending on the absorption maxima

exhibited, and they have been acknowledged to work as light-driven proton pumps (Béjà et al., 2000). The proton gradient generated transmembrane is efficiently used for ATP production.

With this background on mind, it is hypothesised that the insertion of a green-absorbing photosystem like proteorhodopsin into the thylakoid membrane of a plant or algal chloroplast such as that of *Chlamydomonas reinhardtii* could fill the spectral hole and result in augmented proton pumping leading to a higher degree of photophosphorylation, which could consequently increase the ATP/NADPH ratio (Figure 3.2).

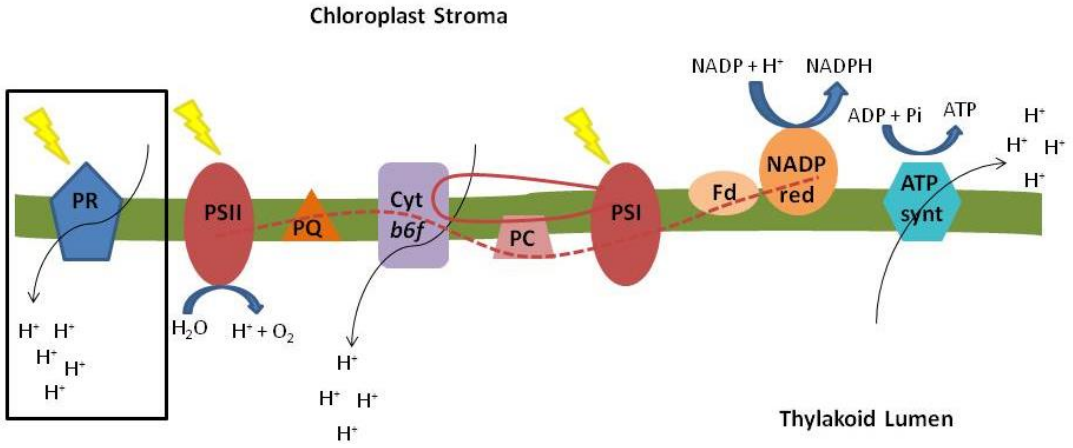

Figure 3.2 Diagram representing the light-depending reactions of photosynthesis occurring in the thylakoid membrane. The red line shows the electron flow for cyclic photophosphorylation, where only ATP is produced, whereas the red dotted line shows the electron flow for non-cyclic photophosphorylation, where ATP and NADPH are produced. Proteorhodopsin incorporation into the membrane (black square) would increase the proton level in the thylakoid lumen, which could translate into higher ATP production.

It is difficult to predict the exact physiological effects of such an increase, although one could speculate that it might obviate the need for cyclic electron flow around PSI, which is an adaptive response where the ratio of ATP/NADPH is increased by down-regulating NADPH synthesis. Cyclic electron flow is activated under a variety of stress conditions including drought or transfer from darkness to light (Johnson, 2005) and might be involved in activating photoprotection mechanisms. In consequence, proteorhodopsin activity might then confer enhanced resistance to those stresses without compromising the supply of NADPH required for carbon fixation and other reductive processes in the chloroplast.

3.1 Expression of proteorhodopsin in the *Chlamydomonas* chloroplast

Proteorhodopsin represents one of the simplest light-utilising systems that can be expressed in the *C. reinhardtii* thylakoid membrane. The proteorhodopsin apoprotein is a single polypeptide with no evident requirements for a set of assembly factors. Moreover, the retinal chromophore is readily available in *C. reinhardtii* since this alga possesses the metabolic machinery to generate all-*trans*-retinal, which occurs naturally in the eyespot and is used to activate the rhodopsin-like photoreceptors (chlamyrhodopsin) in response to phototaxis and photophobia (Deininger et al., 1995).

Additionally, the fact that there is a genetic toolbox available for the insertion of foreign genes into the *C. reinhardtii* chloroplast genome allows expression within the organelle avoiding any difficulties associated with transgene expression in the nucleus and the following import of membrane proteins from the site of synthesis in the cytosol into the chloroplast (Purton, 2007).

The expression of proteorhodopsin was evaluated by introducing a codon-optimised synthetic gene into the chloroplast genome of the *psbH*-deficient strain TN72, and the effect of the transgene's expression and functionality on *C. reinhardtii* was evaluated with and without addition of exogenous retinal.

3.1.1 Selection and design of the proteorhodopsin gene

Several proteorhodopsin variants that have been described in the literature have been successfully expressed in bacteria. The protein chosen for this study, which will be referred as PR, comes from the uncultured marine bacterium EBAC31A08, a member of the *γ-proteobacteria*, which was the first rhodopsin-like protein described in the *Bacteria* domain (Béjà et al., 2000). The *PR* gene encodes a 249-amino acid polypeptide, with a molecular weight of 27 kDa. Its structure consists of seven transmembrane α-helices, and retinal is covalently bonded to a lysine residue in the seventh helix, which is a highly conserved feature among archaeal rhodopsins (Figure 3.3) (Reckel et al., 2011).

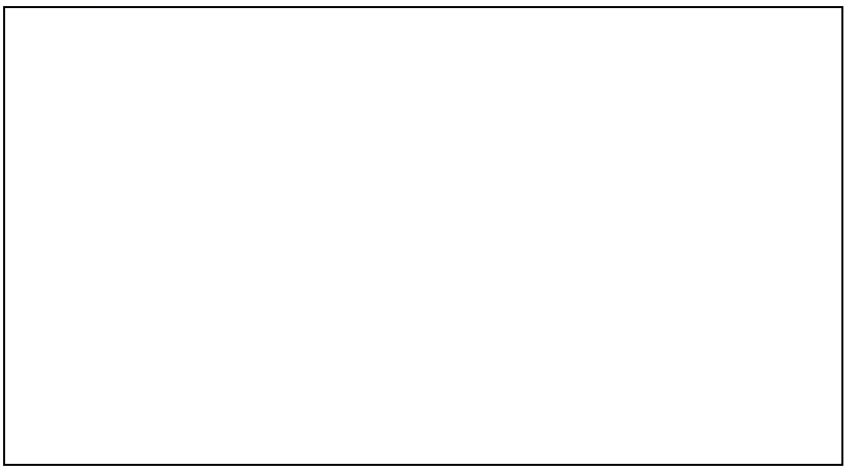

Figure 3.3 a) Crystal structure of proteorhodopsin. Protein chains are coloured from the N-terminus to the C-terminus using a rainbow (spectral) colour gradient. b) Assumed biological molecule (Replicated from Reckel et al., 2011).

The synthesis of this protein in *E. coli* (Béjà et al., 2000) proved its functionality as a light-activated proton pump able to drive ATP synthesis, with a maximum absorbance observed at 520 nm, being classified as a green-absorbing proteorhodopsin. The same PR was expressed in the bacterium *Shewanella oneidensis* strain MR-1 (Johnson et al., 2010), a non-photosynthetic metal-reducing bacterium, and PR provided extended survival in stationary phase.

Additional evidence of the existence of such type of protein in *Bacteria* was found in *Flavobacteria* (Gómez-Consarnau et al., 2007). *Flavobacteria* are the most abundant heterotrophic bacteria in the sea, and it was observed that when supplemented with low or intermediate concentration of organic matter, together with light, an improved growth rate and size of the cells could be detected, and this was particularly enhanced by green light exposure.

These observations form the basis of the hypothesis that introduction of proteorhodopsin into the thylakoid membrane could provide an advantage for microalgal cell growth.

3.1.2 Construction of the plasmid pASapI.PR

A synthesised version of the *PR* gene (GenBank accession number AF279106) was developed taking into account the Kazusa codon usage table for chloroplast genes in *Chlamydomonas reinhardtii*. A codon adaptation index of 0.8 was considered and the stop codon was preceded by a Hemagglutinin (HA) epitope tag for ease of detection using

commercial antibodies. The resulting gene (800 bp) was designed to be easily excised from the Geneart pMK-T plasmid by double digestion with the restriction enzymes *Sap*I and *Sph*I (*PR* sequence in appendix 3).

PR was inserted into the expression vector pASapI (6623 bp) developed in our lab (Economou et al., 2014), which was digested using the same restriction enzymes. This vector contains the promoter and 5' UTR of the *C. reinhardtii atpA* gene, the 3' UTR from *C. reinhardtii rbcL* and a wild-type copy of the *C. reinhardtii psbH* gene within one of the flanking regions of homology (Figure 3.4). *psbH* serves as a selectable marker as it is used to restore phototrophy in the ΔpsbH recipient strain TN72.

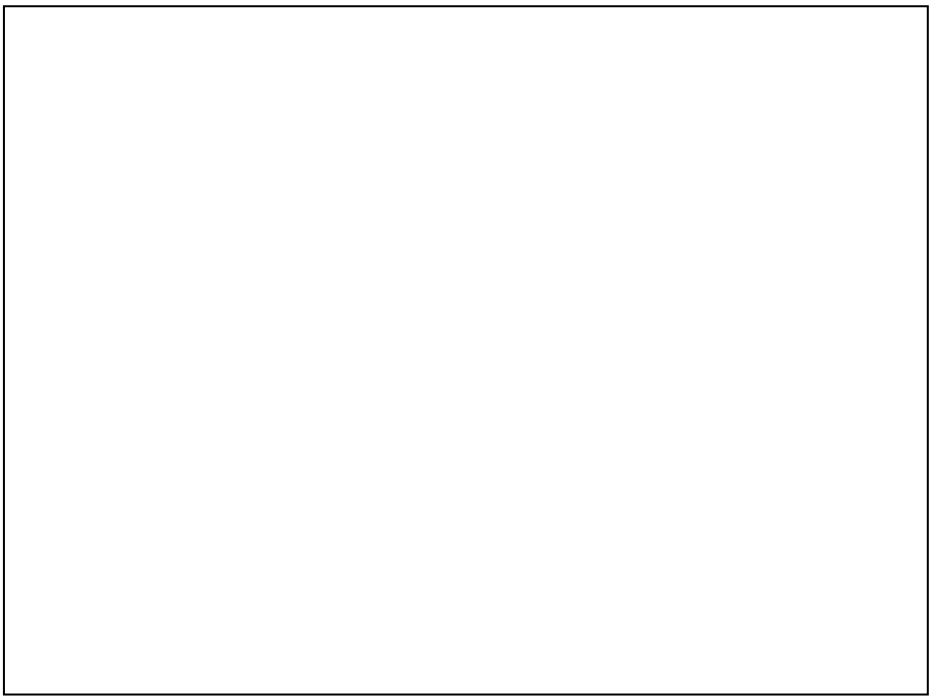

Figure 3.4 Expression vector pASapI developed for transformation of the chloroplast of *Chlamydomonas reinhardtii* by means of phototrophy recovery. Expression is regulated by the promoter and 5' UTR of the *atpA* gene and the 3' UTR from *rbcL.* The gene of interest (goi) is ligated within these regulatory elements. A wild-type copy of the *psbH* gene is used to transform a *psbH*-deficient host (represented by the CC-4388 genome). Successful recombination generates insertion of the gene of interested and restores the native *psbH* (transformed genome) (replicated from Economou et al. 2014).

A ligation of the corresponding fragments (Figure 3.5 A) was carried out, producing the final plasmid pASapI.PR (7366 bp) (Figure 3.5 B), which was further sequenced to corroborate there were no mutations produced in any step. The plasmid was firstly amplified in the *E. coli* strain DH5α and purified for transformation of TN72.

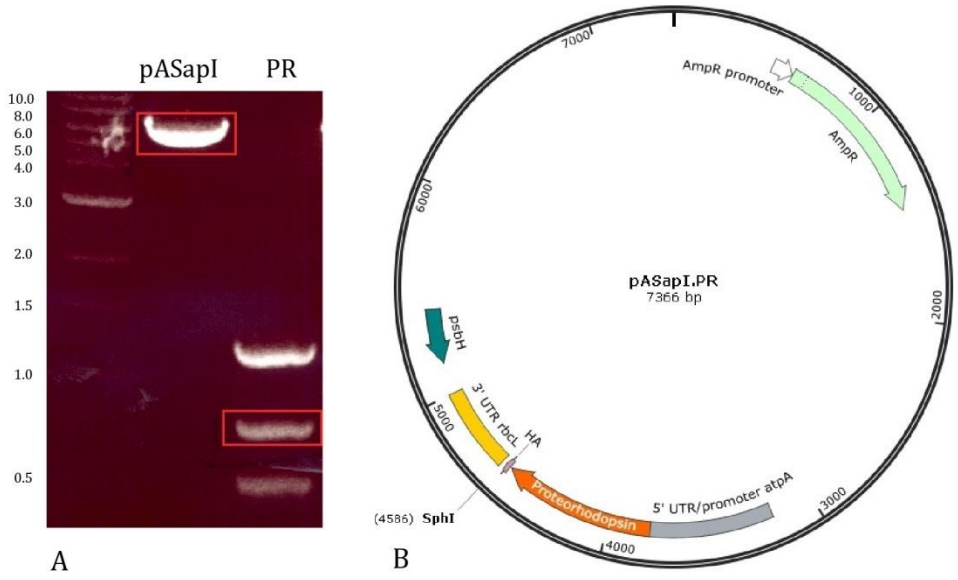

Figure 3.5 A) Gel electrophoresis result for Sap*I*-Sph*I* digested fragments of the pASapI vector and the proteorhodopsin gene. Expected sizes are 6.6 kb and 0.8 kb, respectively. B) Diagram of the pASapI.PR plasmid developed for insertion of the proteorhodopsin gene into the *Chlamydomonas reinhardtii* chloroplast.

3.1.3 Transformation of TN72 with the plasmid pASapI.PR

Insertion of *PR* in TN72 using the pASapI.PR plasmid was performed by vortexing the cells with glass beads in the presence of plasmid DNA as explained in section 2.6.2.1. Figure 3.6 shows the glass tubes used for transformation. Cells that integrate the foreign DNA will restore their photosynthetic activity (Economou et al., 2014). Therefore, high salt minimal (HSM) medium and bright light (100 µmol m^{-2} s^{-1}) were used as driving forces to recover transformant colonies.

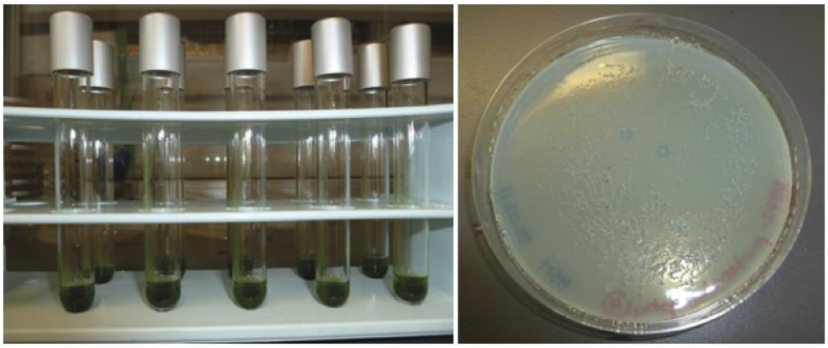

Figure 3.6 Left: glass tubes containing glass beads, plasmid DNA, molten TAP medium supplemented with 0.5 % agar and the algal cell suspension to perform transformation. Right: Plate with minimal medium agar where the volume of one tube is poured and let to settle.

Transformants appeared after 3-4 weeks as single colonies on the surface of the plate, and once these had a size of approximately 1 mm they were picked and streaked onto fresh HSM medium plates (Figure 3.7).

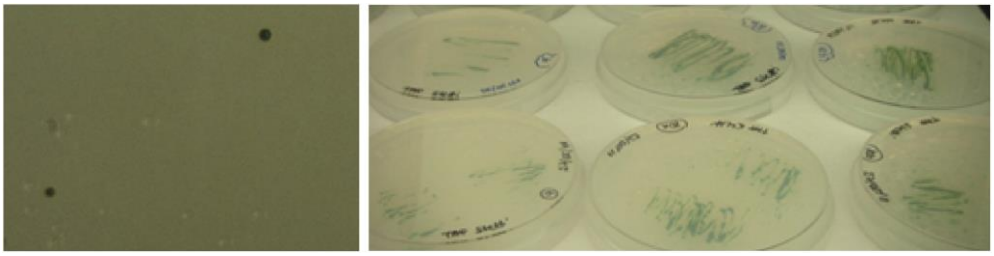

Figure 3.7 Left: first colonies of *C. reinhardtii* transformants in HSM plates, after 4 weeks of transformation. Right: re-streaked colonies in HSM to enhance homoplasmic state of the plastome.

The *Chlamydomonas* chloroplast has a polyploid genome with a copy number of ~80 (Harris et al., 2009a). Heteroplasmy is defined as a condition in which more than one chloroplast genotype prevails in a given organism (Nishimura and Stern, 2010). Initially, chloroplast transformation creates a heteroplasmic state in which only a few genome copies in the chloroplast have acquired the foreign DNA. For stable transformants, it is required to obtain one single genotype (homoplasmy), where all copies have introduced the DNA, and this can be accomplished by restreaking transformant colonies 3 – 4 times in minimal medium with light (Economou et al., 2014).

Proteorhodopsin-containing transformants recovery and confirmation of gene expression

The transformation yield obtained was six colonies from ten plates. Those transformant lines containing the *PR* gene (TN72-PR) were assessed by PCR screening, following the strategy detailed in section 2.5.2.1. Figure 3.8 shows the result of three positive transformants, where it was possible to detect only the 1.2 kb band corresponding to the transformed genome, but not the smaller 0.85 kb band from the original TN72 genome. This indicated that transformants were homoplasmic. The same result was observed for the three remaining lines. Sequencing also indicated that *PR* had been recombined in the expected locus within the chloroplast genome.

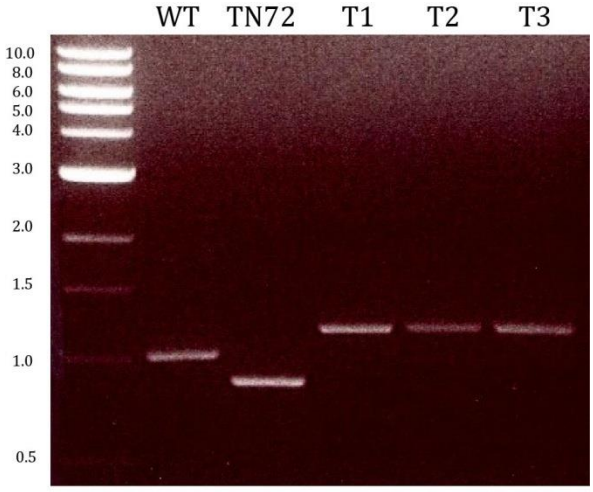

Figure 3.8 PCR screening for TN72 transformants expressing proteorhodopsin (TN72-PR) using FLANK1, atpA.R, rbcL.Fn and MluR2 primers. Bands are as follows: wild-type (WT) 1.0 kb, TN72 host 0.85 kb, TN72-PR transformants (T1, T2, T3) 1.2 kb.

When lines were screened by PCR for the presence of the proteorhodopsin gene using specific primers, a band of the expected size (0.7 kb) was observed for all transformants (Figure 3.9).

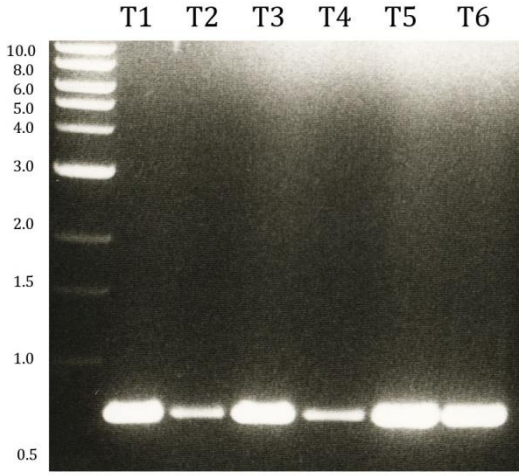

Figure 3.9 PCR analysis for TN72 transformants expressing proteorhodopsin (TN72-PR) using proteorhodopsin primers. Expected band is 0.7 kb for all transformants (T1 – T6).

3.1.4 Proteorhodopsin synthesis in TN72-PR

Proteorhodopsin has a molecular weight of 27 kDa, and the HA tag has an estimated molecular weight of 1.2 kDa; therefore, the HA-tagged PR should give a band of ~ 28 kDa.

In order to assess the accumulation of PR in TN72-PR lines, Western blot analysis was carried out using crude lysate samples from the six transformant lines (Figure 3.10). Cells were harvested in late exponential phase and prepared as detailed in section 2.7.1. Samples (80 µl) were loaded on a 15 % polyacrylamide gel together with a positive control (cell extract containing an HA-tagged protein of 40 kDa) to confirm antibody binding, and a negative control (cell extract from a line transformed with the empty pASapI vector: TNE). Enhanced chemiluminescence (ECL) detection was used to visualise the binding of the anti-HA antibody. As shown in Figure 3.10, a specific band of approximately 23 kDa is seen in all six lines, but is absent in the TNE line and the positive control. The size of the band is smaller than the predicted for the HA-tagged PR (28 kDa); however, this difference in size could be explained by the hydrophobic nature of this membrane-spanning protein which might fail to unfold completely in the presence of sodium dodecyl sulphate (SDS). This has been observed for a number of hydrophobic proteins, and it has been suggested to occur due to altered SDS binding depending upon the tertiary structure of the protein (Rath et al., 2009).

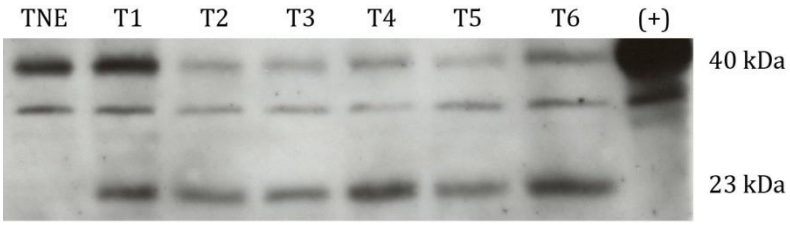

Figure 3.10 Expression of proteorhodopsin in the six transformants obtained is demonstrated by Western blot analysis using anti-HA antibodies (23 kDa band). Cultures were grown in 25 mL TAP medium flasks at 25 °C, 120 rpm and 50 µmol m^{-2} s^{-1}. Lanes are as follows: TN72 transformed with the empty pASapI vector (TNE), TN72-PR transformants (T1-T6), and a highly expressed HA-tagged protein as positive labelling control (+) (40 kDa band). Unspecific band in the middle of the gel serves as a loading control.

In order to confirm location of this protein in the membrane, fractionation of the crude lysate into soluble and membrane fractions was carried out as detailed in section 2.7.2, but the membrane-rich fraction was so dense with chlorophyll and other membrane proteins that PR could not be detected. The fact that proteorhodopsin is a seven-span transmembrane protein increases the difficulty for solubilisation, and the extraction yield depends not only on this but also in the level of protein synthesised by the specific cell type (www.piercenet.com). These two factors could have influenced the lack of detection on PR within the membrane fraction. However, Western blot analysis with anti-HA antibodies on the soluble fraction did not show the presence of PR, reinforcing the assumption that the protein was present in the membrane fraction.

3.1.5 Functionality of proteorhodopsin in TN72-PR

Since there was a clear evidence of the expression of PR in TN72-PR, different tests were performed in order to assess the functionality of this protein.

Retinal is required to activate PR, and it is not clear if PR would be able to access the all-*trans*-retinal present in the eyespot of the cell, although this organelle's structure is closely associated to the thylakoid membrane (Harris et al., 2009b). For this reason, cultures were also grown with added all-*trans*-retinal in the medium. Concentrations used were chosen considering retinal values used for photophobic/phototactic responses studies in carotenoid-deficient strains (Lawson and Satir, 1994; Sineshchekov et al., 1994) and retinal concentrations used when expressing PR in other organisms (Béjà et al., 2000; Johnson et al., 2010).

Proteorhodopsin absorbance at 520 nm

PR is described as having a maximum absorbance at a wavelength of 520 nm. Absorbance at this value (A_{520}) was measured in whole-cell suspensions of two transformants of TN72-PR and in the control strain transformed with the empty pASapI vector (TNE).

Additionally, all-*trans*-retinal at two different concentrations (5 and 10 mM) was added in order to observe if there was any difference in PR activity, and absorbance was measured after 8 hours of addition. Absorbance at 680 nm (A_{680}) was also measured in order to normalise the data to chlorophyll fluorescence (680 nm reflects the chlorophyll absorbance maximum). The ratio of absorbance A_{520}/A_{680} was calculated and results are presented in Table 3.1.

Table 3.1 Absorbance at 520 and 680 nm measured in two TN72 transformants expressing proteorhodopsin (TN72-PR) and in the negative control (TNE) with different concentrations of added all-*trans*-retinal. Cultures were grown in 25 mL TAP medium flasks at 25 °C, 120 rpm and 50 µmol m^{-2} s^{-1}.

Sample	Retinal [mM]	A_{520}	A_{680}	A_{520}/A_{680}
TNE	0	0.690	0.809	0.853
	5	0.642	0.749	0.857
	10	0.537	0.627	0.857
TN72-PR 1	0	0.550	0.665	0.827
	5	0.564	0.668	0.844
	10	0.424	0.508	0.835
TN72-PR 2	0	0.602	0.715	0.842
	5	0.578	0.688	0.840
	10	0.513	0.601	0.854

As can be observed from the A_{520}/A_{680} values, the ratio of absorbance when comparing TN72-PR to its respective negative control remains relatively unchanged regardless of the retinal concentration added.

Growth of TN72-PR and effect of retinal addition

PR is expected to be membrane bound and functional as a proton pump, potentially increasing cell growth rate or culture lifespan. To test this hypothesis, TN72-PR was grown in mixotrophic condition (light intensity of 50 µmol m^{-2} s^{-1}) in acetate-containing medium (TAP) and growth was monitored for a period of 14 days. As shown in Figure 3.11, the growth curves appear unaltered in TN72-PR when compared to the control strain TNE (see specific growth rate data in Table 3.2).

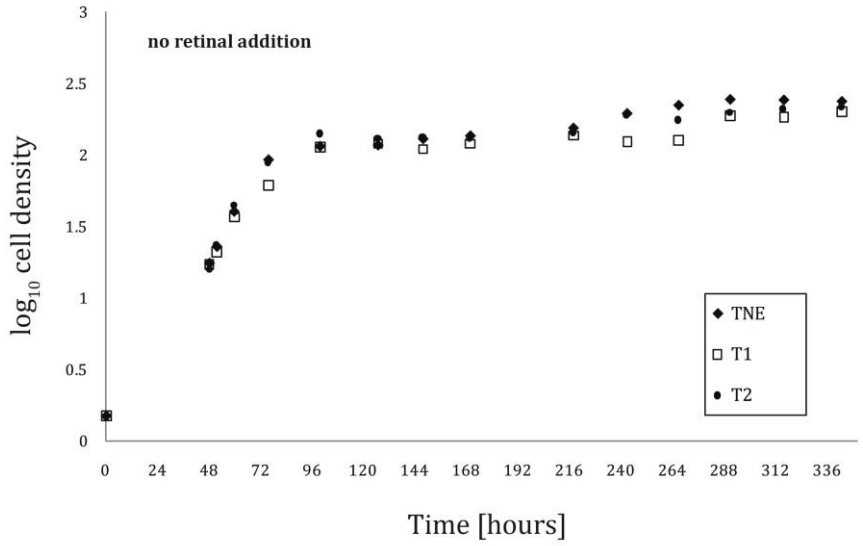

Figure 3.11 Comparison of cell growth of two TN72 transformants expressing proteorhodopsin (T1, T2) and control strain (TNE). Cultures were grown in 25 mL TAP medium flasks at 25 °C, 120 rpm and 50 µmol m^{-2} s^{-1}. Initial cell density was 1.5x10^5 cells mL^{-1}.

From this experiment it can inferred that there is no detectable improvement of cell growth for *C. reinhardtii*; however, it can be also concluded that there is no detrimental effect in specific growth rate due to the expression of this membrane bound protein, which to our understanding is the first attempt to express a membrane protein in the *C. reinhardtii* chloroplast.

All-*trans*-retinal was added at 50 hours of cultivation, when cultures reached a cell density of 2x10^6 cells mL^{-1} and at two different concentrations (5 and 10 mM) to determine if it contributed positively to the activity of PR. Growth was monitored daily for two weeks, and the results are presented in Figure 3.12. It can be observed that the specific growth rate matches the growth rate of the control strain in both cases, indicating that there is no benefit on cell growth in this condition either (see specific growth rate data in Table 3.2).

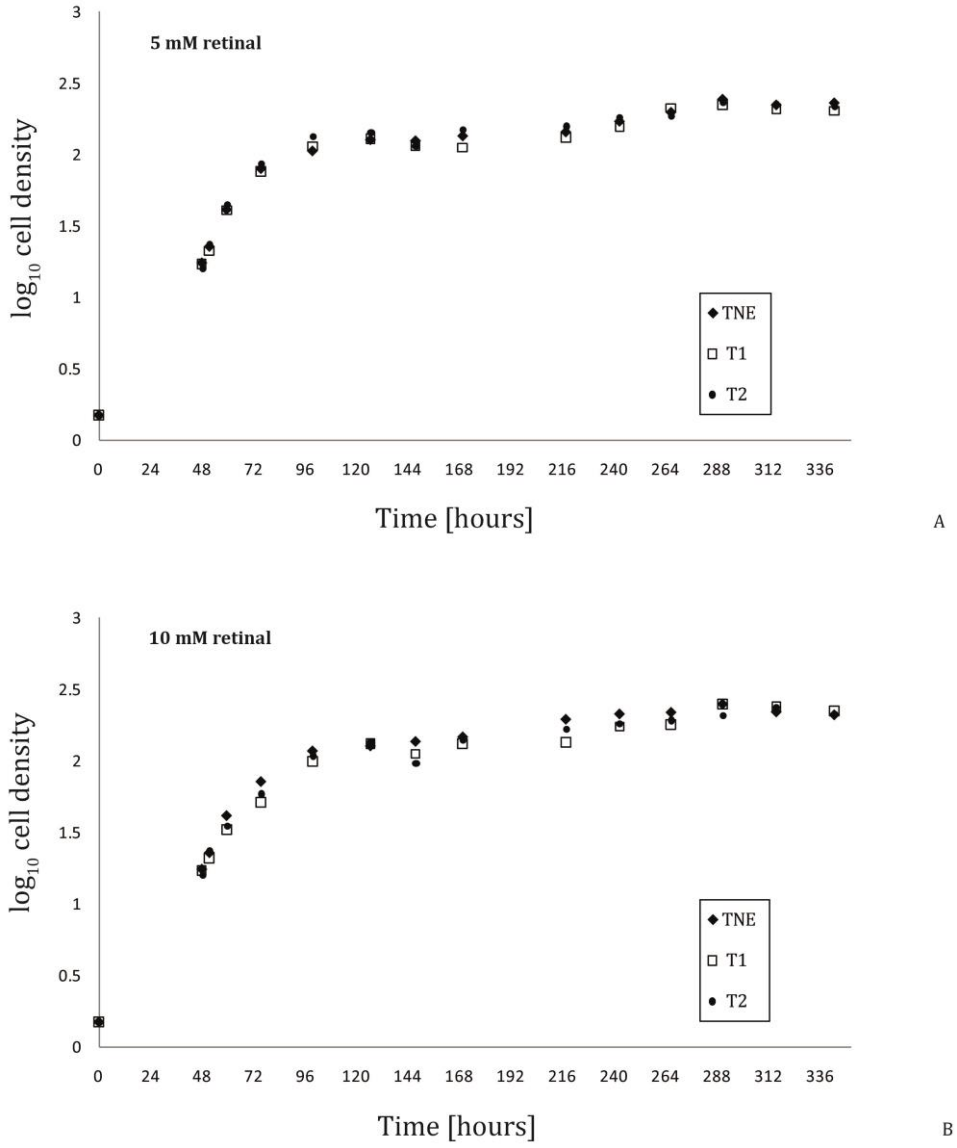

Figure 3.12 Comparison of cell growth of two TN72 transformants expressing proteorhodopsin (T1, T2) and the control strain (TNE) at two different concentrations of added retinal: A) 5 mM added retinal, B) 10 mM added retinal. Cultures were grown in 25 mL TAP medium flasks at 25 °C, 120 rpm and 50 µmol m^{-2} s^{-1}. Initial cell density was 1.5x10^5 cells mL^{-1}. Retinal was added at 50 hours of cultivation.

Table 3.2 presents the values for specific growth rate of the control strain TNE and two transformants of TN72-PR grown with different concentrations of added retinal. Calculations were carried out twice in separate events obtaining matching values of specific growth rate for each condition (standard deviation ≤ 0.003 in all conditions).

Table 3.2 Cell growth rate for cultures of TN72 transformants expressing proteorhodopsin (TN72-PR1 and TN72-PR 2) and the control strain (TNE), with different concentrations of added retinal. Cultures were grown in 25 mL TAP medium flasks at 25 °C, 120 rpm and 50 µmol m^{-2} s^{-1}. Growth rate values are an average of 2 independent experiments.

	Specific growth rate, µ [h^{-1}]								
	TNE			TN72-PR 1			TN72-PR 2		
Retinal [mM]	**0**	**5**	**10**	**0**	**5**	**10**	**0**	**5**	**10**
µ	0.053	0.052	0.050	0.050	0.051	0.047	0.052	0.052	0.049

In order to assess any benefits of proteorhodopsin on the culture lifespan, a set of cultures comprising two TN72-PR strains and TNE with different concentrations of added retinal (0, 5 or 10 mM) were carried out and their cell growth was measured for 45 days, until cell death (Figure 3.13).

In all experiments, the growth pattern and lifespan matched very closely the trend observed for TNE, so it is not possible to attribute to proteorhodopsin a benefit on lifespan under mixotrophic cultivation. It can also be observed that exogenous retinal does not seem to provide any advantages, but rather the opposite, especially at higher retinal concentration (10 mM). In fact, when 20 mM retinal was added, cultures dropped in cell density during the latter (death) phase of the growth curve much quicker, so this condition was not further studied.

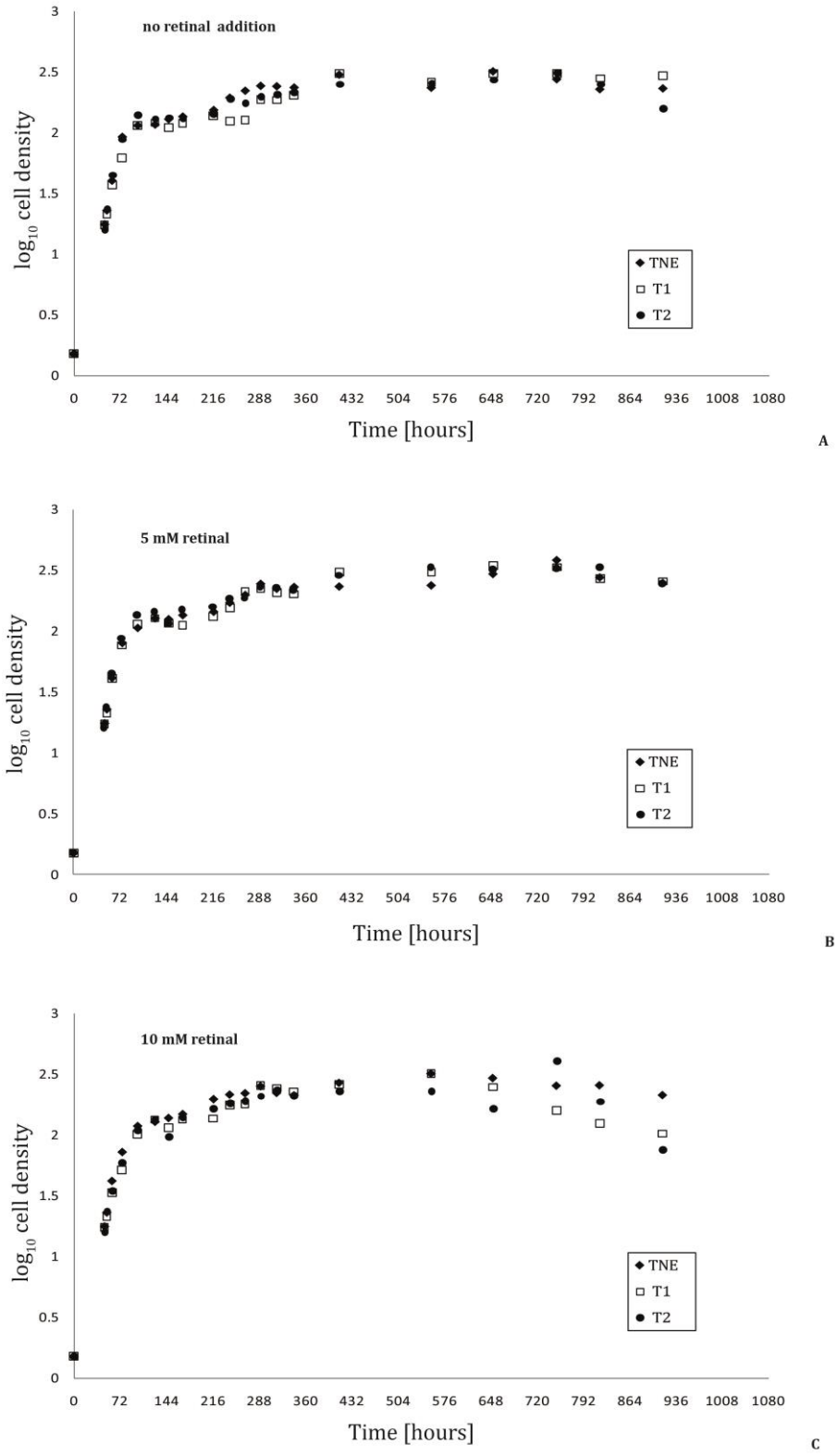

Figure 3.13 Comparison of cell growth of TN72 transformants expressing proteorhodopsin (T1, T2) and the control strain (TNE) with A) no added retinal, B) 5 mM added retinal, and C) 10 mM added retinal, until cell death was reached. Cultures were grown in 25 mL TAP medium flasks at 25 °C, 120 rpm and 50 µmol m^{-2} s^{-1}. Initial cell density was 1.5x10^5 cells mL^{-1}. Retinal was added at 50 hours of cultivation.

Despite the results obtained, TN72-PR and TNE were grown with and without retinal at a larger, well-controlled scale, using a fully automated 1L photobioreactor (Algem®, Algenuity), where cell growth was measured online every 30 minutes by measuring absorbance at 740 nm (A_{740}) for a period of seven days.

When growing TN72-PR against the control strain TNE, the maximum cell density reached was equivalent; however, there was a small difference in growth rate (Figure 3.14). TN72-PR showed a specific growth rate of 0.038 (± 0.006) h^{-1}, against 0.034 (± 0.006) h^{-1} observed in TNE, representing an 11.8 % increase (n=2). Although this is not a major increase, this result was obtained in two independent experiments that provided consistent evidence for an increase in specific growth rate.

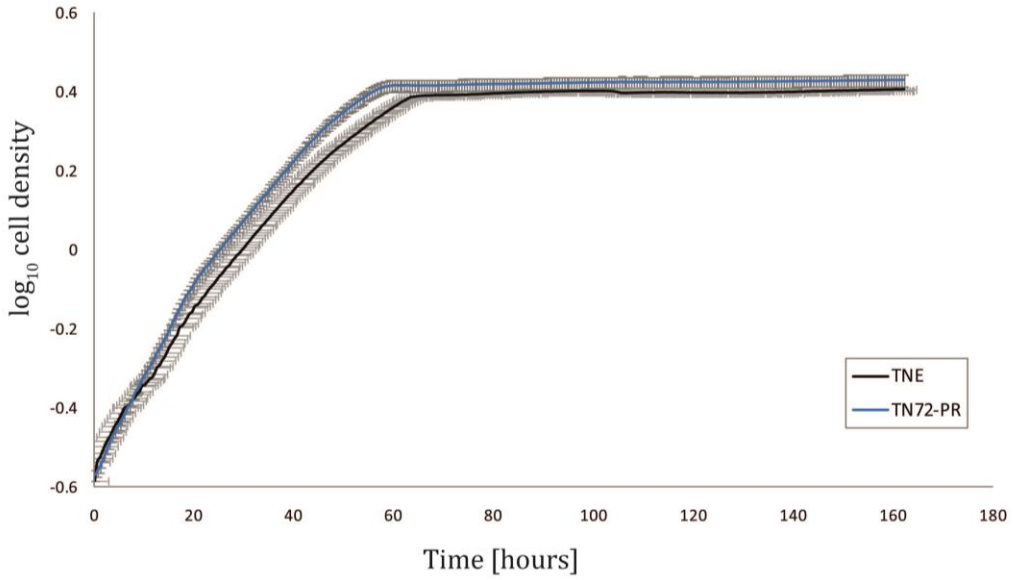

Figure 3.14 Comparison of cell growth of a TN72 transformant expressing proteorhodopsin (TN72-PR) and the control strain (TNE). Cultures were grown in TAP medium in an automated photobioreactor at 25° C, 200 µmol m^{-2} s^{-1} and continuous shaking at 120 rpm. Initial cell density was OD_{740}=0.25. Curves represent the average result of 2 separate experiments, and the grey area represents horizontal error bars for each strain cultivated (n=2).

TN72-PR was then grown under the same cultivation conditions in duplicate, but this time adding all-*trans*-retinal to one of the cultures (Figure 3.15). Retinal was added when cells where in mid-exponential phase (45 h cultivation). Specific growth rate was slightly slower in the culture with retinal addition (decrease of 2 %); once again confirming that exogenous retinal does not provide any benefit.

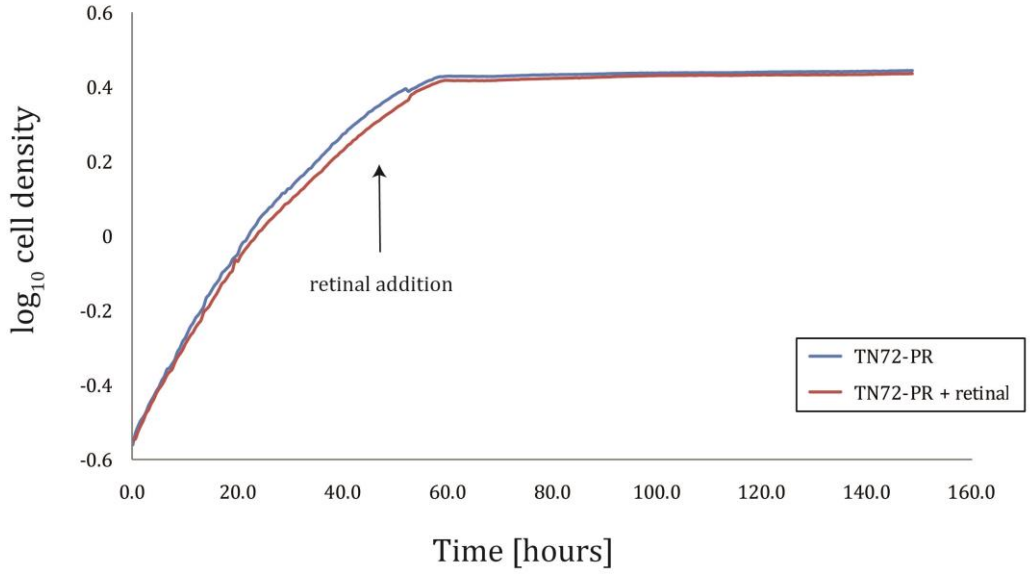

Figure 3.15 Comparison of cell growth of TN72 transformants expressing proteorhodopsin (TN72-PR) with and without retinal addition (10 mM). Cultures were grown in TAP medium in an automated photobioreactor at 25° C, 200 µmol m^{-2} s^{-1} and continuous shaking at 120 rpm. Initial cell density was OD_{740}=0.25. Retinal was added at 45 hours of cultivation.

Growth of TN72-PR in minimal media

In order to assess the potential functionality of proteorhodopsin in more stringent environmental conditions, such as media with no added carbon source, TN72-PR was grown in two different minimal media: tris-acetate-phosphate medium without acetate (TP) and high salt minimal medium (HSM). Cells were grown in phototrophic mode (light intensity of 150 µmol m^{-2} s^{-1}) and growth was monitored for 10 days. As seen in Figure 3.16, there is no detectable difference in growth when growing TN72-PR in minimal media, these cultures performed equally as the control culture TNE.

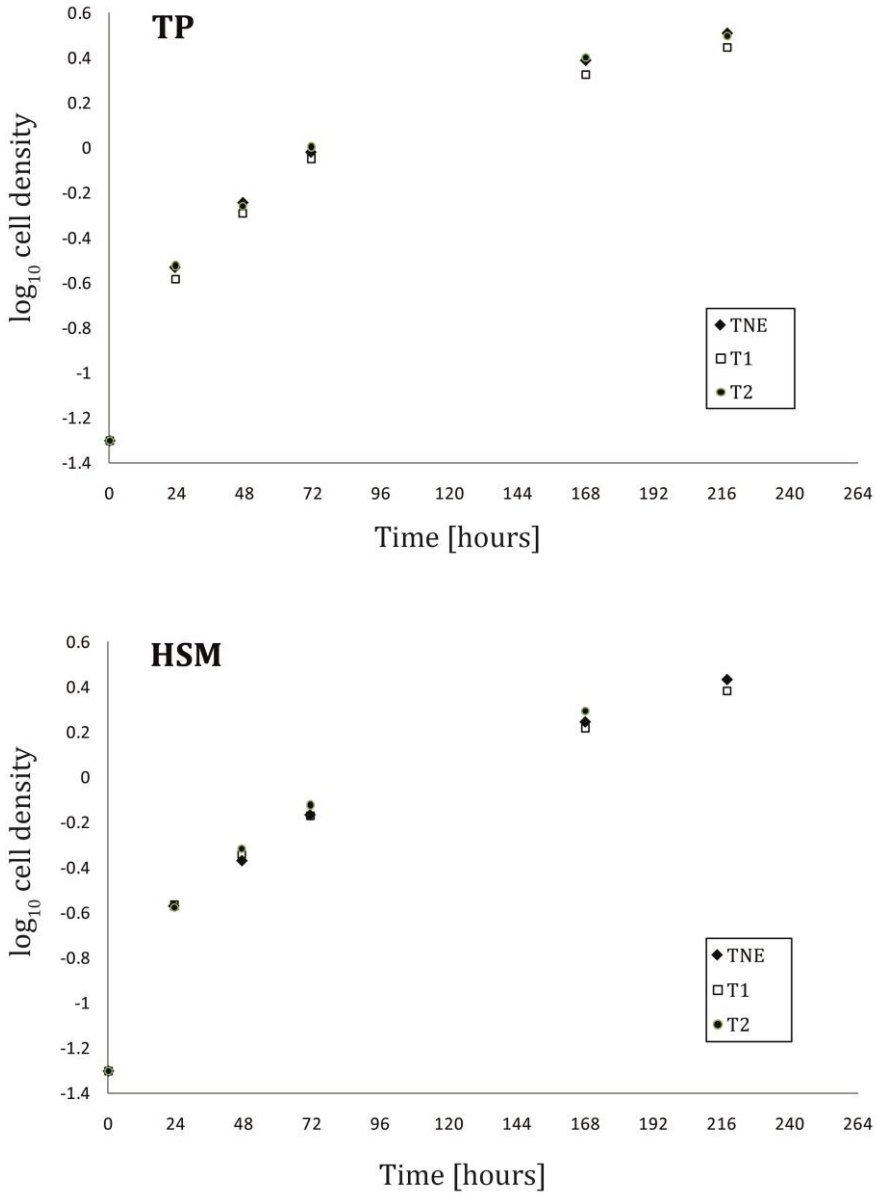

Figure 3.16 Comparison of cell growth of TN72 transformants expressing proteorhodopsin (T1, T2) and the control strain (TNE) in phototrophic conditions in tris-acetate-phosphate medium without acetate (TP) and in high salt minimal medium (HSM). Cultures were carried out in 25 mL shake flasks at 25° C, 150 µmol m^{-2} s^{-1} and continuous shaking at 120 rpm. Initial cell density was OD_{750}=0.25.

TN72-PR was also grown in minimal media (HSM) in the photobioreactor at two different light intensities (200 and 800 µmol m^{-2} s^{-1}) for a period of two weeks. In both conditions tested, there was no detectable improvement on growth or culture lifespan due to the presence of proteorhodopsin (Figure 3.17).

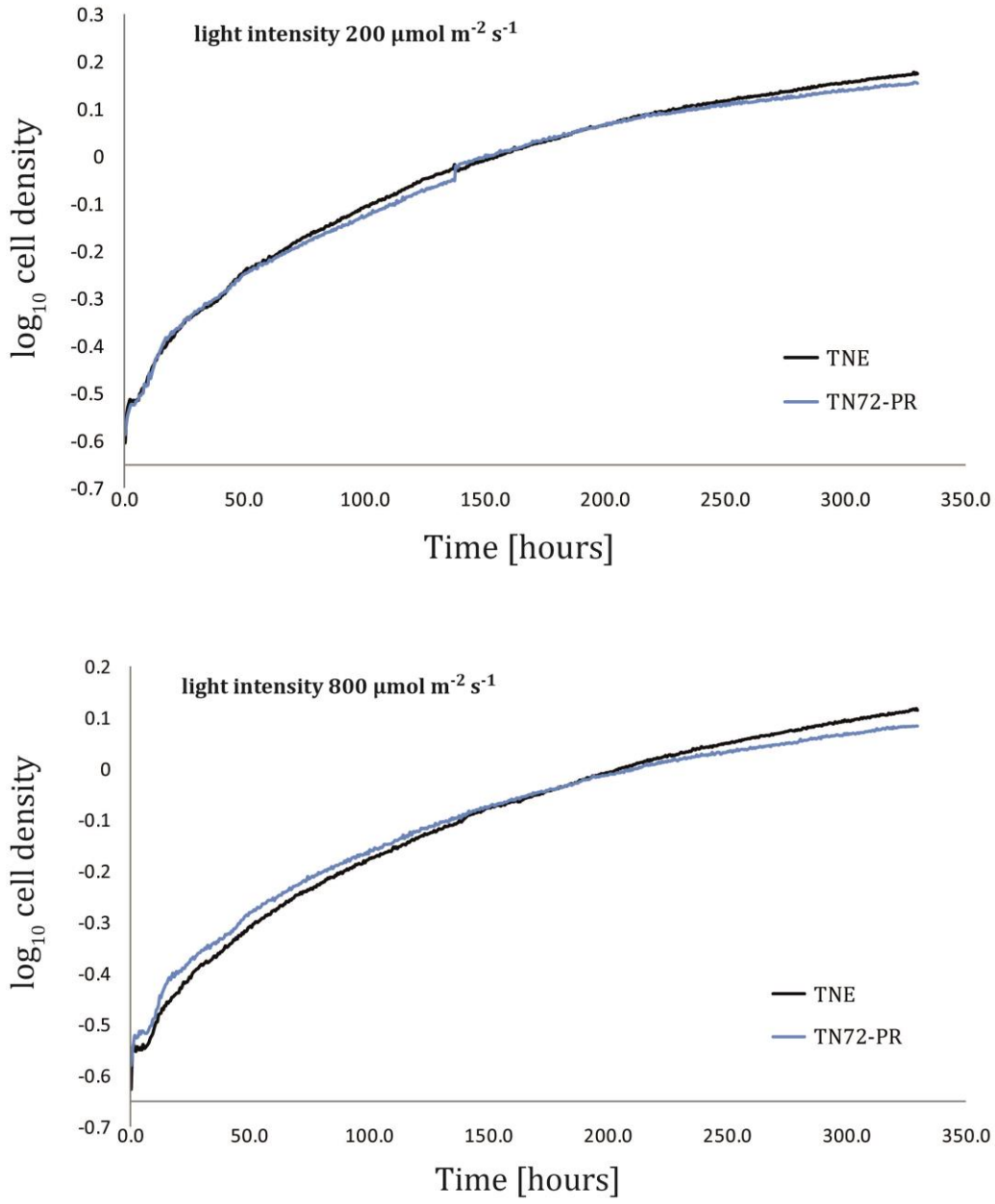

Figure 3.17 Comparison of cell growth of a TN72 transformant expressing proteorhodopsin (TN72-PR) and the control strain (TNE) grown under phototrophic conditions in high salt minimal medium (HSM) at light intensities of 200 and 800 µmol m^{-2} s^{-1}. Cultures were carried out in an automated photobioreactor at 25° C and continuous shaking at 120 rpm. Initial cell density was OD_{740}=0.25.

3.1.6 Conclusion

A synthetic proteorhodopsin gene was successfully designed, cloned into a chloroplast expression vector, and introduced into the chloroplast genome of *Chlamydomonas reinhardtii*, obtaining homoplasmic transformants. The successful expression of the gene, as demonstrated by the accumulation of the PR protein in the transgenic lines, was

confirmed by Western blot. It was not possible to confirm the location of proteorhodopsin since this protein has proven very challenging for detection in the membrane protein-enriched fraction; however, PR was not detected in the soluble fraction which supports the hypothesised location of this protein in the thylakoid membrane.

In order to test PR functionality, cultures of TN72-PR were grown at different scale and conditions with and without exogenous all-*trans*-retinal and it could be concluded that there is no detectable effect of proteorhodopsin at small scale (25 mL flasks). Nevertheless, when growing TN72-PR at a larger and more controlled scale (1L photobioreactor) it was possible to detect an increase in specific growth rate of 11.8 %. This difference in behaviour could be attributed to a better control of the cultivation parameters in an automated reactor, but more importantly to a more standardised measurement of cell density, with no dilutions involved. It can also be noticed that in the photobioreactor light intensity was higher (200 μmol m^{-2} s^{-1}) than in shake flasks (50 μmol m^{-2} s^{-1}), which could have contributed to PR performance. TN72-PR was grown in phototrophic conditions as well in order to assess a potential benefit on the culture lifespan. However, it was not possible to detect any difference in either flask or photobioreactor scale.

No benefit could be attributed to the addition of exogenous retinal at any scale in terms of the variation detected in specific growth rate in some conditions; although, no further studies were carried out in order to identify if this added retinal was actually being taken up and utilised by proteorhodopsin.

The level of PR protein in the transformants was sufficient to make it detectable in crude lysate samples, albeit not being abundant. The thylakoid membrane of the chloroplast, where proteorhodopsin is expected to be embedded, suffers from a high degree of molecular crowding (Goral et al., 2010; Kirchhoff, 2008). This dense protein-packing in the membrane can be observed in the electron microscopy photograph shown in Figure 3.18, and it occurs due to the presence of membrane protein complexes associated with the light-harvesting and light-driven reactions of photosynthesis, such as PSI and PSII , the cytochrome *b6f* complex and the ATP synthase (Olive and Wollman, 1998). These complexes use approximately 80 % of the membrane area and it is speculated that this lack of space could interfere with the stable accumulation and incorporation of proteorhodopsin into the thylakoid membrane. This hypothesis forms the basis of the

following sections, which aimed to eliminate either PSII or PSI in the PR transformant by knocking-out chloroplast genes encoding key subunit of the complexes.

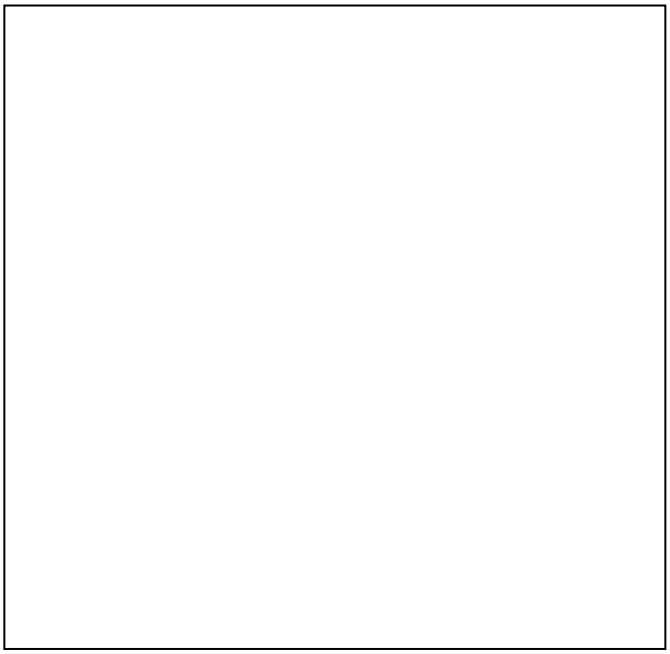

Figure 3.18 Freeze-fractured electron micrograph of isolated thylakoid membranes of *Chlamydomonas reinhardtii*, where a high degree of molecular crowding can be easily observed (replicated from Goodenough and Staehelin, 1971).

3.2 Knockout of the *psbC* gene in transformant TN72-PR

As discussed in the previous section, it is considered that a lack of space in the thylakoid membrane could lead to a lower level of accumulation of proteorhodopsin. This assumption was explored by knocking-out a chloroplast gene encoding a non-essential membrane protein forming part of one of the photosynthetic complexes present in the chloroplast. The knockout strategy involves the design of a construct containing an antibiotic resistance marker flanked by sequences from the target gene to be disrupted. When introduced into the chloroplast, this construct recombines with the target gene, resulting in the insertion of the marker in the gene. The altered gene will produce a non-functional product, if translated at all.

It was decided to create a PR transgenic line that lacked the PSII complex. PSII-deficient mutants of *Chlamydomonas* are not as sensitive to light as PSI-deficient or Cyt. b_6f-deficient mutants since PSII is the main site of photo-oxidative damage (Redding and Peltier, 1998;

Spreitzer and Mets, 1981). This allows for cultivation of PSII mutants in low to moderate light intensity, which is crucial in this case due to the light-dependence of proteorhodopsin for its functionality. The gene chosen for knockout was *psbC*, which encodes the chlorophyll binding polypeptide P6 (also known as protein CP43), a 43 kDa polypeptide forming a core part of the photosystem II complex. It has been reported that mutants lacking PSII activity due to nuclear mutations affecting the expression of *psbC* fail to accumulate wild-type levels of PSII protein complex in the thylakoid membranes (Olive and Wollman, 1998; Rochaix et al., 1989). Additionally, *psbC* was identified to be distant from the locus where proteorhodopsin was inserted (Figure 3.19); therefore, its disruption is expected to produce no interference in the transcription of the *PR* gene.

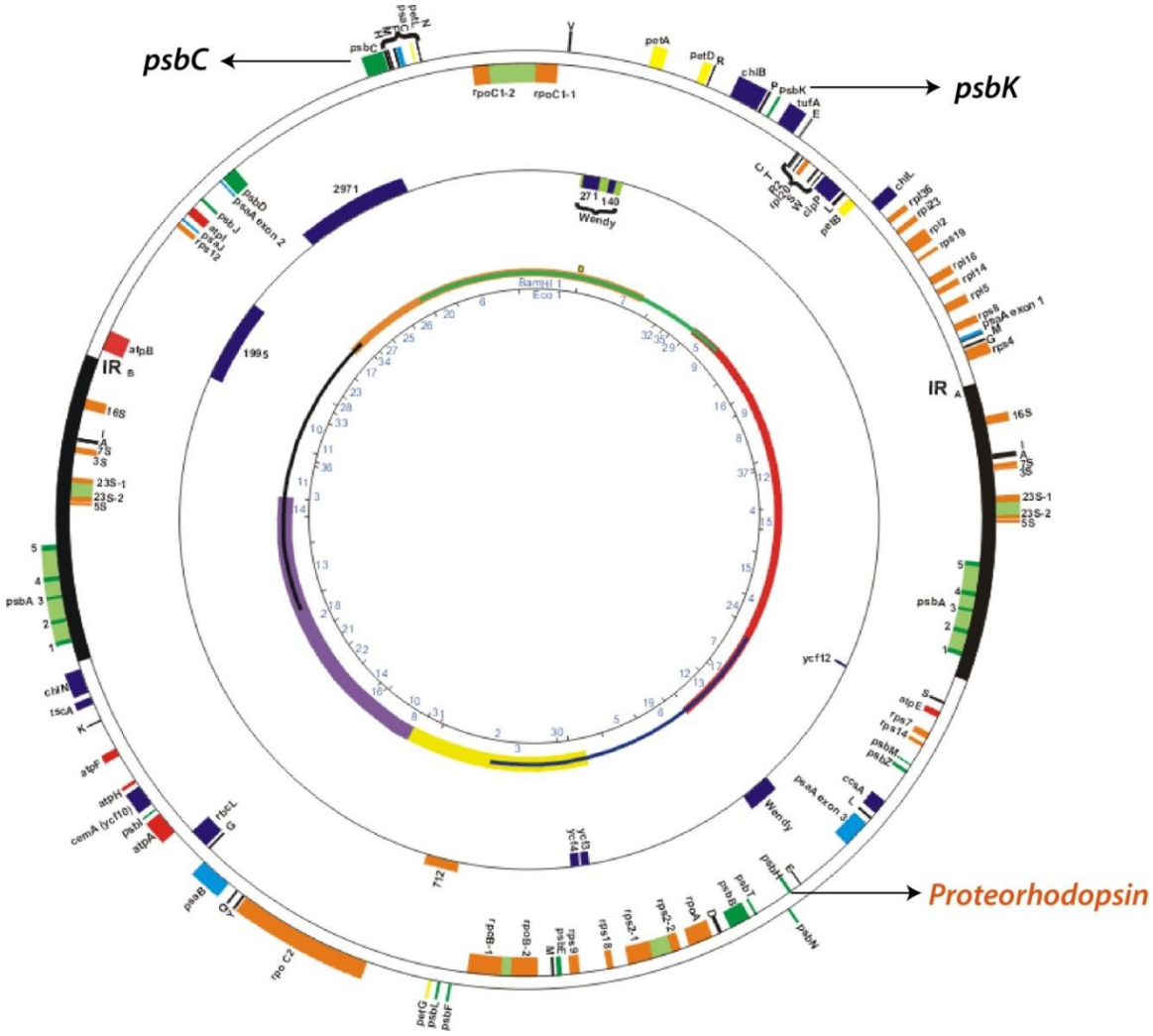

Figure 3.19 Chloroplast genome of *Chlamydomonas reinhardtii*. Arrows show the location of the inserted gene (*Proteorhodopsin*) and of the *psbC* and *psbK* genes, where knockouts were carried out.

3.2.1 Construction of the plasmid psbC.KO

In order to produce a knockout of the native *psbC* gene in TN72-PR, a transformation plasmid was designed comprising the *psbC* gene disrupted with a cassette expressing the aminoglycoside 3' adenyl transferase (*aadA)* gene, conferring resistance to both antibiotics spectinomycin (Sp) and streptomycin (St) (Goldschmidt-Clermont, 1991).

Firstly, *psbC* was amplified from TN72 genomic DNA using appropriate primers (primer sequences in appendix 1) and a product of 1.6 kb was obtained (Figure 3.20 A). This PCR product was inserted into the commercial cloning vector pJET1.2 (2.97 kb) and the new plasmid pJET.psbC was further amplified using the *E. coli* strain DH5α. Colonies were screened in the presence of ampicillin.

A unique restriction site *Msc*I was identified to be present in *psbC* (and absent in pJET1.2) allowing pJET.psbC to be linearised (Figure 3.20 B). The digested plasmid was dephosphorylated on its 5' ends using Antarctic phosphatase to avoid vector self-ligation.

The aadA cassette was excised from the plasmid pUC-atpX-AAD (Goldschmidt-Clermont, 1991), in which the bacterial *aadA* is expressed in a 1.96 kb cassette containing 0.65 kb from the *C. reinhardtii atpA* promoter/5' UTR and 0.45 kb of the *C. reinhardtii rbcL* 3' UTR. This cassette can be conveniently excised using the restriction enzymes *Eco*RV and *Sma*I (Figure 3.20 C).

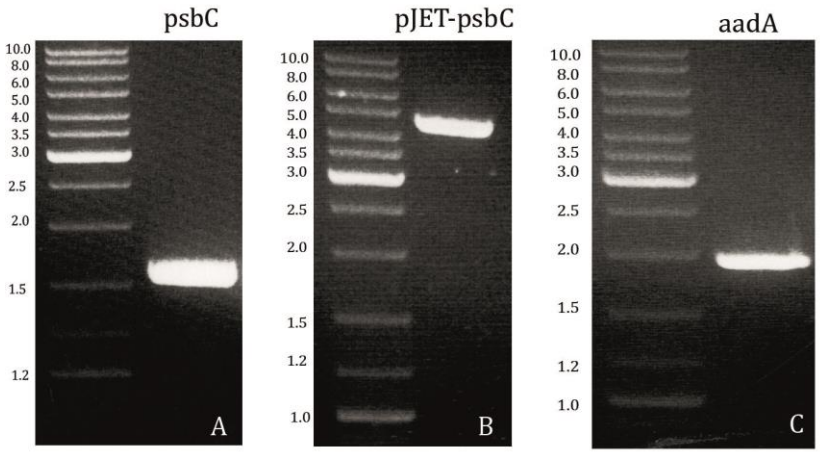

Figure 3.20 A) PCR for the *psbC* gene from TN72, band size 1.6 kb, B) Gel electrophoresis for digested pJET-psbC plasmid using the *Msc*I restriction enzyme, band size 4.6 kb, C) Gel electrophoresis of the digested pUC-atpX-AAD plasmid using the restriction enzymes *Eco*RV and *Sma*I, band size 1.96 kb.

The two fragments – pJET-psbC and the aadA cassette – were ligated to create the plasmid psbC.KO (6558 bp), which was transformed into *E. coli* with selection on both ampicillin and spectinomycin to select for the recombinant plasmid. In order to determine the orientation of *aadA* with respect to *psbC*, several digestions with the restriction enzymes *Eco*RI, *Mfe*I, *Sap*I and *Sph*I were carried out and these results gave the final configuration of the psbC.KO plasmid (Figure 3.21). Sequencing results also confirmed the expected DNA sequence. The plasmid was purified and used for transformation of a TN72-PR transformant line.

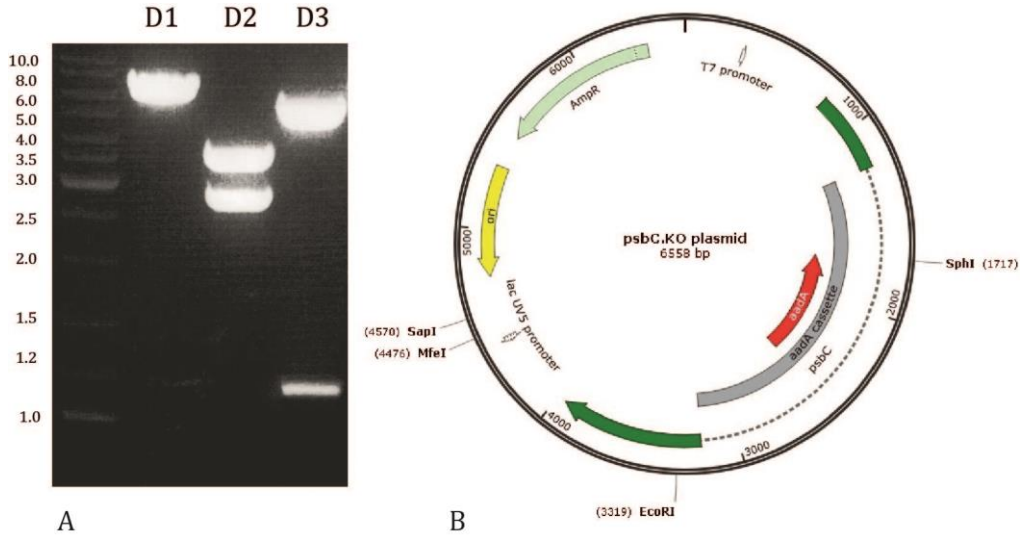

Figure 3.21 A) Digestions of the psbC.KO plasmid with different restriction enzymes to check size and gene orientation: D1, single digestion with *Sph*I (6.55 kb); D2, double digestion with *Sap*I and *Sph*I (2.8 and 3.75 kb); D3, double digestion with *Eco*RI and *Mfe*I (1.1 and 5.55 kb). B) Diagram of the psbC.KO plasmid.

3.2.2 Transformation of TN72-PR with plasmid psbC.KO

The proteorhodopsin-containing *Chlamydomonas reinhardtii* strain TN72-PR was transformed by vortexing in the presence of glass beads and plasmid DNA. The control transformant line TNE lacking *PR* was also transformed in the same manner with the purpose of generating a negative control strain for the *psbC* knockout. The strategic location of the restriction site *Msc*I in the middle of the *psbC* gene, where the aadA cassette was inserted, gives enough flanking sequence at both sides of the *aadA* to be recombined in the TN72-PR chloroplast genome and disrupt the native *psbC*.

The selection method for recovering *psbC* knockout transformants in TN72-PR (TN72-PRΔpsbC) and in TNE (TNEΔpsbC) involved the use of solid TAP medium supplemented

with 100 µg mL^{-1} of spectinomycin in dim light (20 µmol m^{-2} s^{-1}) in a first stage, and bright light (100 µmol m^{-2} s^{-1}) in a second stage.

3.2.3 Recovery of TN72-PR *psbC* knockout transformants and confirmation of gene expression

As *psbC* knockouts were expected to be sensitive to high light, the transformation plates were placed under dim light for the appearance of transformants. However, it seemed that the combination of antibiotic selection and slow growth under dim light was an excessive burden for the recently-transformed cells in order to recover and generate transformants. It was not possible to recover any spectinomycin-resistant colonies from the 35 transformation plates incubated in this condition.

A repeat transformation experiment involved selection under bright light (100 µmol m^{-2} s^{-1}) and this condition gave better results. Transformant colonies appeared after four weeks and the yield of transformation was 32 colonies from 14 plates for TN72-PRΔpsbC, and ten colonies from eight plates for TNEΔpsbC. These were streaked under the same conditions three times to ensure active growth and then placed in the dark before carrying out any further experiments. It was speculated that darkness would increase the chances of obtaining a homoplasmic state of the plastome since these strains would not need *psbC* to be active under this condition.

Growth study using spot tests

PsbC mutants are expected to be dependent on exogenous acetate for growth, show some light-sensitivity and be resistant to both spectinomycin and streptomycin. This phenotype was tested in growth experiments (spot tests) under the following conditions: TAP + light (mixotrophic condition), HSM + light (phototrophic growth), and TAP + light with different concentrations of spectinomycin and streptomycin, as shown in Figure 3.22. TN72, which is PSII-deficient and has the aadA cassette, was used as a control for acetate-dependence and antibiotic resistance, and a wild-type strain was used as control for growth under phototrophic conditions and antibiotic sensitivity.

As observed in the spot tests, the putative transformants grew normally on acetate-containing medium and tolerated very high levels of antibiotic, of up to 1000 µg mL^{-1} of both spectinomycin and streptomycin, and even a mixture of both. This strongly suggests

that they had incorporated the aadA cassette, and were not spontaneous resistance mutants (which would be expected to show resistance to spectinomycin only). However, the strains still managed to grow under phototrophic conditions, which suggested that they still possessed native copies of *psbC*. It is possible, therefore, that the strains were heteroplasmic. For this reason, many transformants were assayed by PCR with different set of primers to determine whether both intact and knockout copies of *psbC* were present in the chloroplast, and to try to identify homoplasmic lines in which all copies of *psbC* had been disrupted.

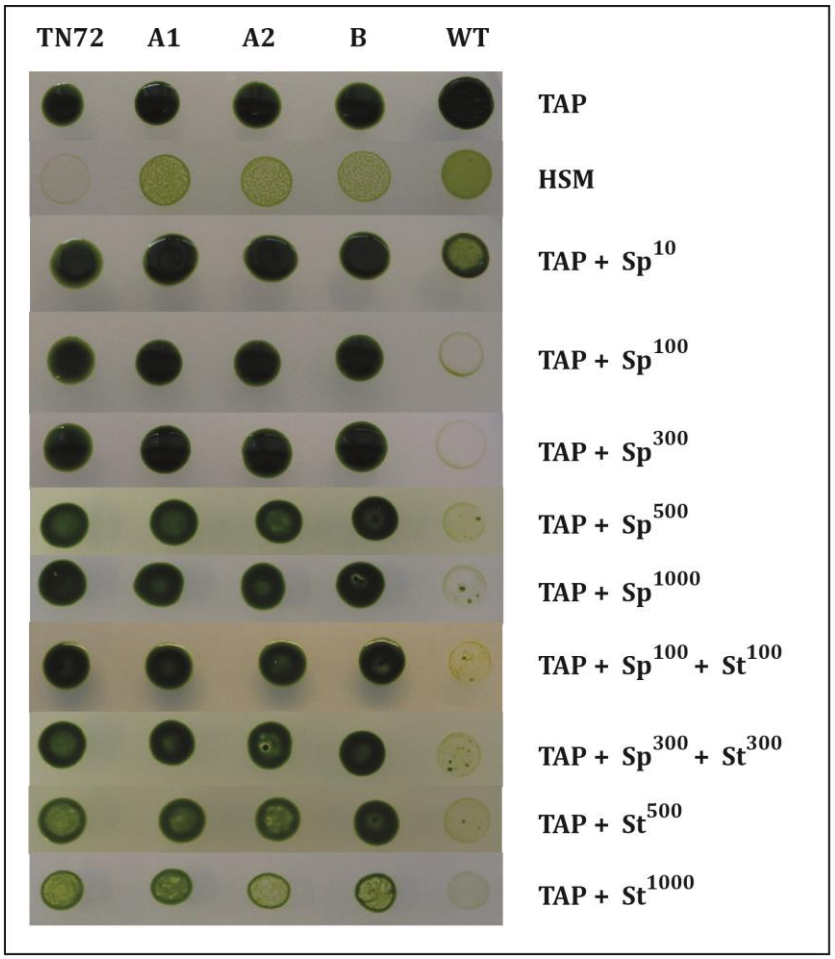

Figure 3.22 Spot tests of TN72 transformants expressing proteorhodopsin in a *psbC*-deficient background (A1 and A2) under different concentrations of spectinomycin (Sp) and streptomycin (St), numbers represent µg mL^{-1}. TN72, which has *psbH* disrupted with the aadA cassette, is used as positive control for acetate dependence and antibiotic resistance; B represents a control strain for the *psbC* knockout (TNE with disrupted *psbC*), and wild-type *C. reinhardtii* (WT) is used as negative control for antibiotic resistance and normal growth in phototrophic conditions.

PSII fluorescence

In addition to the previous experiment, the autofluorescence of PSII in the transformant lines was evaluated. Fluorescence measurement is a widely employed method to assess the functional status of the photosynthetic apparatus. In microalgae such as *C. reinhardtii*, room temperature fluorescence due to chlorophyll *a* is mainly emitted by PSII, and this fluorescence can be detected in the far region of the spectrum (wavelength > 690 nm) (Papageorgiou and Govindjee, 2007). The photons that are re-emitted as fluorescence cannot be used for photosynthesis; therefore, there is an inverse proportionality between photosynthetic activity and fluorescence emission, giving a very distinct profile for PSII mutants.

Cells were harvested during exponential growth phase and excited within the visible region of the spectrum (wavelength = 500 nm) and the emitted fluorescence was detected. This procedure was performed on two putative TN72-PRΔpsbC transformant lines, one putative TNEΔpsbC transformant line, TNE as a negative control, and TN72 (also a PSII mutant) as a positive control, as shown in Figure 3.23. PSII-deficient mutants, including the positive control TN72, showed higher fluorescence than the control strains with intact PSII (TNE and TN72-PR), which gives evidence of the disruption of *psbC*. This same profile has been observed by Dr Joanna Szaub (2013) when analysing PSII mutants (Bst-same strain).

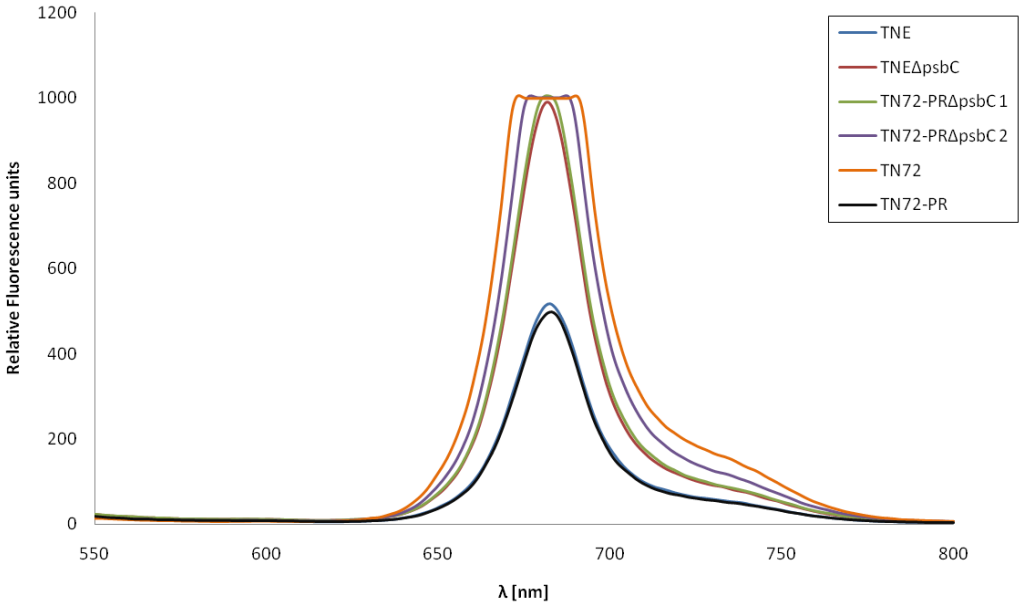

Figure 3.23 PSII fluorescence emitted when cultures were excited at 500 nm at room temperature. A higher peak in fluorescence indicates a lesser degree of photosynthesis, as an indirect measurement of PSII functionality. Cultures were grown in 25 mL TAP medium flasks at 25 °C, 120 rpm and 30 µmol m^{-2} s^{-1}. Samples analysed were TN72, as a positive control for a PSII-deficient strain, TNE as a control for a PSII wild-type strain, two *psbC*-deficient transformants of TN72-PR (TN72-PRΔpsbC 1 and 2) and one *psbC*-deficient transformant in TNE (TNEΔpsbC). All samples were normalised to the same OD_{750}.

PCR screening for homoplasmic transformants

Primers were designed to recognise sequences up- and downstream of *psbC*, and within the aadA cassette (primer sequences in appendix 1) so it was possible to establish clearly if any of the strains generated were homoplasmic. The strategy developed is described in Figure 3.24 A. Primers psbC.F and psbC.R were designed to amplify *psbC* in its wild-type form (1.6 kb) or as a disrupted gene (3.6 kb), whereas primers psbC.F and psbCknock.R would only give a band when the aadA cassette was inserted (1.3 kb). PCR results showed that all the transformants screened possessed either only the native *psbC* gene or were heteroplasmic, despite tolerating high antibiotic concentrations. Figure 3.24 B shows an example of 10 transformants screened where all of them exhibit the native *psbC* band size (1.6 kb), and Figure 3.24 C shows that for the same transformants only three of them (T2, T3 and T5) show the presence of the *aadA* gene in the expected location (1.3 kb band). These results not only confirm heteroplasmy of some transformants but also pose the question as to whether the aadA cassette might have integrated in another location of the genome (or nuclear genome) in some transformant lines.

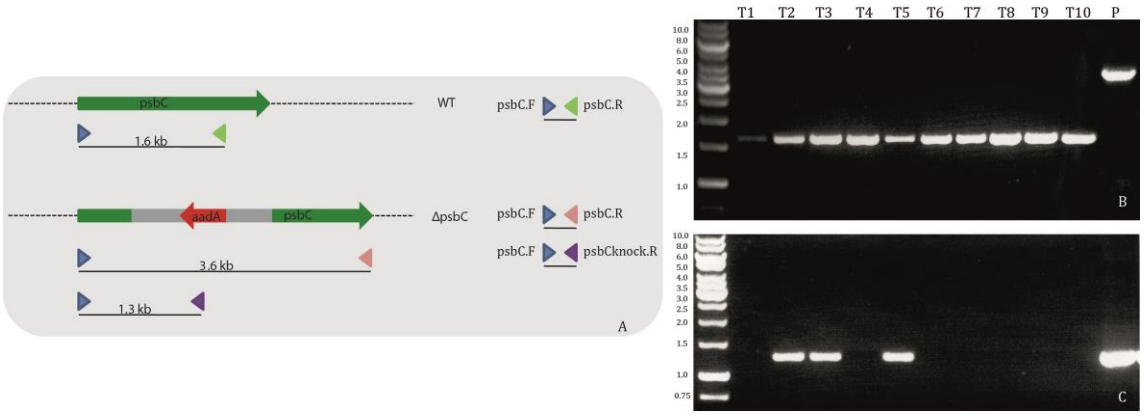

Figure 3.24 A) primers designed for PCR screening of homoplasmic *psbC*-deficient transformants. B) PCR result for 10 transformants (T1-T10) and the psbC.KO plasmid (P) using primers psbC.F and psbC.R. Band size observed is 1.6 kb, which represents the native *psbC* gene. C) PCR result for 10 transformants (T1-T10) and the psbC.KO plasmid (P) using primers psbC.F and psbCknock.R. Band size observed is 1.3 kb, which represents a section of the disrupted *psbC* gene.

A few putative transformants were streaked on TAP medium with reduced nitrogen (TAP 1/10N) and Sp^{100} since a N-limited medium is known to reduce the plastome copy number, a strategy normally used for inducing gametogenesis in *C. reinhardtii* (Remacle et al., 2009). This condition could provide higher chances for the transformants to become homoplasmic under given environmental conditions. However, this approach gave no positive results and all transformants remained apparently heteroplasmic when tested again with the same PCR strategy.

It was a surprise to observe such persistence from these transformants to retain the native *psbC* regardless of the different measures applied. It is known that heteroplasmy will prevail when an essential gene is disrupted in order to ensure survival of the organism (Bock and Knoop, 2012; Goldschmidt-Clermont, 1998). This resistance encouraged us to review the literature for other attempts of knocking-out *psbC* and analyse carefully the chloroplast genome sequence in the genomic regions adjacent to *psbC*.

A study of two *psbC* mutants and the stability of the gene product obtained reported decreased levels of CP43 protein – the protein encoded by *psbC* – due to mutations in the *psbC* sequence (5' UTR and ORF), but when evaluating the *psbC* mRNA it was found to accumulate to similar levels to the wild-type, indicating that these mutations were acting at a post-transcriptional level only (Rochaix et al., 1989). A similar pattern of *psbC* mRNA expression level was observed in a nuclear mutant (Sieburth et al., 1991). Considering

these results, it can be inferred that a lack of CP43 protein is not crucial for *C. reinhardtii* as long as the *psbC* gene is properly transcribed.

When analysing in detail the region surrounding *psbC* in the chloroplast genome, it can be observed that genes encoding essential transfer RNAs (tRNAs) are located downstream of *psbC*. The latter is possibly co-transcribed with one or more of the downstream *tRNA* genes, although rapid processing of the primary transcript results in the mature 2 kb species being the predominant band when Northern blot analysis was carried out using a *psbC* probe (Rochaix et al., 1989). We hypothesised that the insertion of *aadA* prevented synthesis of the primary transcript, and thus the production of the essential tRNAs, and this would lead to an inability to reach the homoplasmic state for a disrupted *psbC* gene. This is in contrast to a knockout of the downstream *psaC* gene, encoding a subunit of PSI, where expression of the *tRNA* genes is not affected and, as a result, homoplasmy can be achieved (Takahashi et al., 1991) (Figure 3.25).

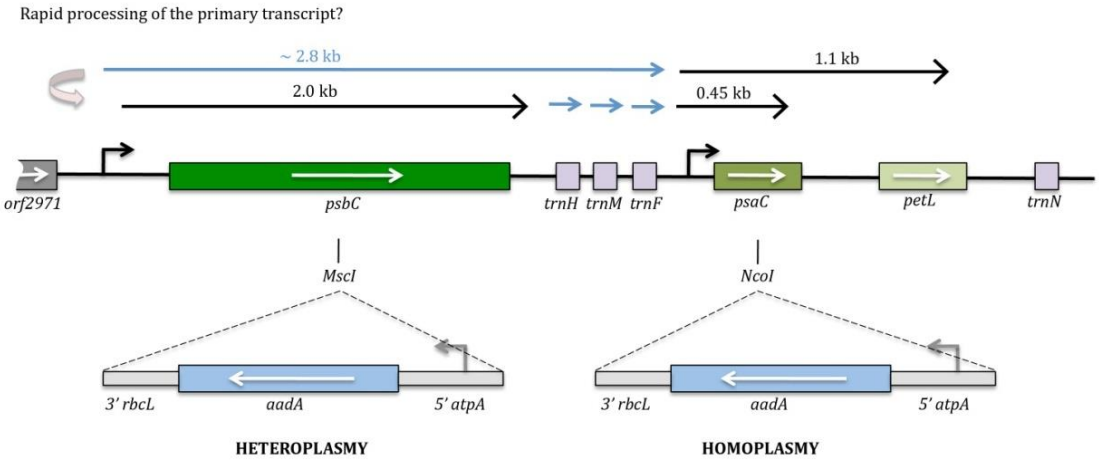

Figure 3.25 Diagram showing the hypothesised manner in which *psbC* is transcribed in *C. reinhardtii*. Transcription of *psbC* mRNA happens somehow overlapped to the transcription of essential tRNA genes, which prevents *psbC* from being fully knocked-out (transformants remain heteroplasmic). In the case of *psaC*, that is situated downstream of these essential genes, a full knock-out of the gene has been reported, with transformants reaching homoplasmy of the disrupted *psaC*.

This *psaC*-deficient strain seemed like an attractive host for our purposes; however, it has been reported that PSI mutants are more light-sensitive than PSII mutants (Takahashi et al., 1994) and need to be grown in dim light or in the dark. Proteorhodopsin is a light-dependent protein, therefore, such a mutant would not benefit our study. A homoplasmic knockout of the PSII *psbK* gene had also been reported in the literature and was shown to tolerate light when supplemented with an exogenous carbon source (Takahashi et al.,

1994), so this knockout was considered as a strategy to develop and will be detailed in section 3.3.

3.2.4 Conclusion

The objective of knocking-out *psbC* in TN72-PR was to create a PSII-deficient mutant, and thus provide more space in the thylakoid membrane for proteorhodopsin to accumulate and perform its function as a proton pump. The high tolerance of the transformants to both antibiotics, as observed in the spot tests, gives evidence for the successful incorporation of the aadA cassette into the chloroplast genome. The results of the PSII fluorescence also indicated that there is an impaired photosynthetic activity in the *psbC* mutants. However, these transformants never reached homoplasmy, as shown by the PCR results, containing both the native and the disrupted versions of *psbC*. Considering these results, it was not possible to draw any conclusions as for a potential decrease in the expression of the P6 polypeptide and subsequent assembly of the PSII complex, and whether this strategy actually released any space for proteorhodopsin.

It was speculated that the presence of essential tRNAs downstream of *psbC* and the apparent co-transcription of these genes would prevent *psbC* from being completely knocked out. Therefore, a different PSII gene (*psbK*) that should not present this issue and that has been already knocked out providing homoplasmic transformants, was chosen for further studies.

3.3 Knockout of the *psbK* gene in TN72-PR

The *psbK* gene was successfully knocked-out by Takahashi et al. (1994). This 136-bp gene encodes a 4 kDa polypeptide (K polypeptide), whose function remains unknown, but presumably has an auxiliary role in PSII function. When *psbK* was disrupted in *C. reinhardtii*, it was observed that the alga was not able to grow under phototrophic conditions and PSII accumulation (observed as accumulation of the D1 protein) was highly reduced.

A transformation plasmid (psbK.KO) containing *psbK* disrupted using the aadA cassette, was kindly provided by Dr. Yuichiro Takahashi (Okayama University, Japan). The plasmid was amplified in *E. coli* strain DH5α and used for transformation of TN72-PR.

3.3.1 Transformation of TN72-PR with plasmid psbK.KO

TN72-PR was transformed by vortexing in the presence of glass beads and plasmid DNA. TNE was also transformed in the same manner with the purpose of generating a control strain for the *psbK* knockout. The selection method for recovering *psbK* knockout transformants in TN72-PR (TN72-PRΔpsbK) and in TNE (TNEΔpsbK) involved the use of solid TAP medium supplemented with 100 μg mL^{-1} of spectinomycin in bright light (100 μmol m^{-2} s^{-1}).

3.3.2 Recovery of TN72-PR *psbK* knockout transformants and confirmation of *aadA* expression

Transformant colonies appeared after four weeks and the yield of transformation was 15 colonies from 42 plates for TN72-PRΔpsbK, and eight colonies from 15 plates for TNEΔpsbK. These were streaked under the same conditions three times to ensure active growth and then placed in the dark before carrying out any further experiments, in order to increase chances of obtaining a homoplasmic state of the plastome.

Growth study using spot tests

With the aim of detecting different phenotypes in the putative transformants, spots tests were carried out in the following conditions: TAP, TAP + Sp^{100}, TAP + St^{100} and HSM, all in light. In this case, a photosynthetic mutant with a disrupted *rbcL* (CC-2653) was used as control for impaired growth in phototrophic conditions, and a strain with wild-type levels of PSII (TNE) was used as control for antibiotic sensitivity and growth in phototrophic conditions (Figure 3.26).

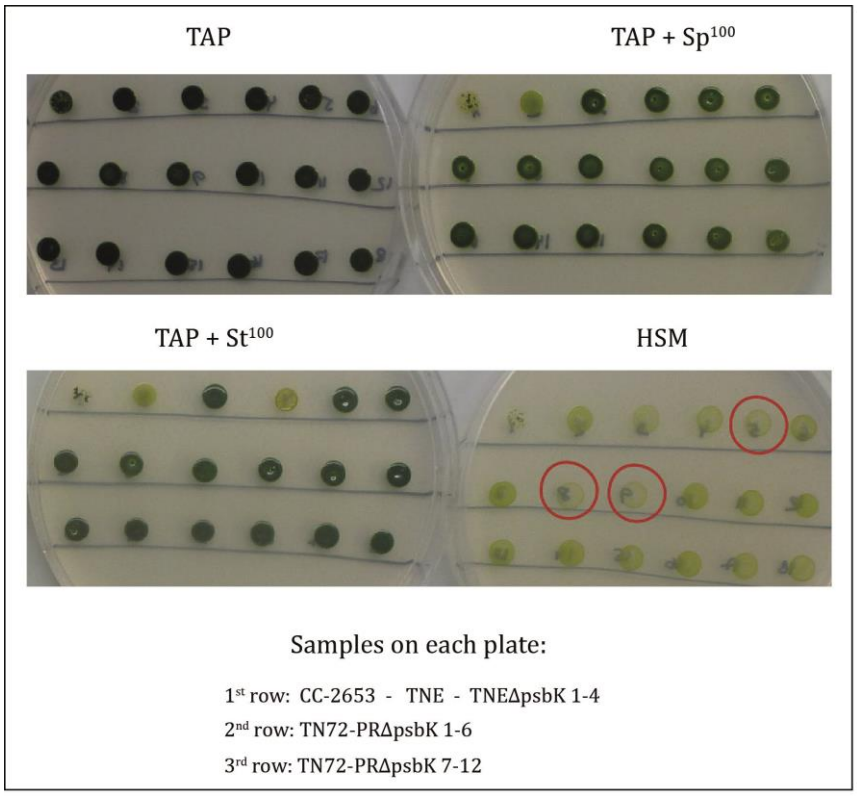

Figure 3.26 Spot tests of TN72 transformants with *psbK* knockout expressing proteorhodopsin, and TNE transformants with *psbK* knockout, grown under different media conditions: tris-acetate-phosphate medium (TAP), TAP with 100 µg mL^{-1} spectinomycin (TAP+Sp^{100}), TAP with 100 µg mL^{-1} streptomycin (TAP+St^{100}), and high salt minimal medium (HSM), all grown at 100 µmol m^{-2} s^{-1} of light intensity. Samples on each plate, from left to right are in 1st row: *rbcL*-deficient strain CC-2653 followed by a wild-type strain (TNE), and 4 putative transformants of TNEΔpsbK (1–4); 2nd and 3rd rows: putative transformants of TN72-PRΔpsbK (1–12).

From the spot tests, three knockout transformants were identified (highlighted in red in Figure 3.26) that exhibited resistance to both antibiotics and showed impaired growth in photosynthetic conditions, two of them in TN72-PR and one in TNE, so these were recovered from the spot test plates and restreaked on TAP + Sp^{100} in dim light for further analyses.

PSII fluorescence

One transformant from TN72-PR and one transformant from TNE were analysed for PSII fluorescence as explained in section 3.2.2. Once again, a distinctive profile was observed for PSII mutants in both the TNE and the TN72-PR lines that have the disrupted *psbK* (Figure 3.27). PSII-deficient mutants evidenced a higher fluorescence, just as observed for the control strain TN72, whereas controls for normal PSII activity (TNE and TN72-PR) showed a lower fluorescence emission.

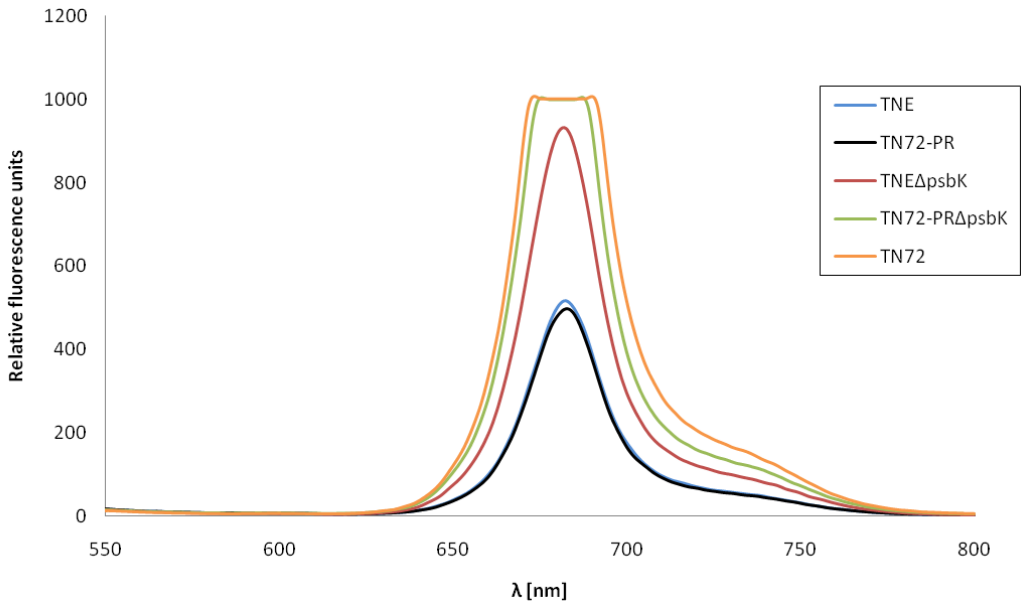

Figure 3.27 PSII fluorescence emitted when cultures were excited at 500 nm at room temperature. A higher peak in fluorescence indicates a lesser degree of photosynthesis, as an indirect measurement of PSII functionality. Cultures were grown in 25 mL TAP medium flasks at 25 °C, 120 rpm and 30 µmol m^{-2} s^{-1}. Samples analysed were TN72, as a positive control for a PSII-deficient strain, TNE as a control for a normal strain, a psbK-deficient transformants of TN72-PR (TN72-PRΔpsbK) and a psbK-deficient transformant in TNE (TNEΔpsbK). All samples were normalised to the same OD_{750}.

PCR screening for homoplasmic transformants

Primers were designed to recognise sequences up- and downstream of *psbK* (primer sequences in appendix 1) so it was possible to determine if the strains generated were homoplasmic for the disrupted *psbK*. The strategy developed is described in Figure 3.28 A. Primers psbK.F and psbK.R were designed to amplify *psbK* in its wild-type form (0.14 kb) or as a disrupted gene (2 kb). A PCR analysis was carried out to the transformant for TN72-PR with increased PSII fluorescence, together with eight additional putative transformants that showed antibiotic resistance in spot tests (Figure 3.28 B), and to the transformant for TNE with increased PSII fluorescence, along with two other putative transformants that showed antibiotic resistance in spot tests (Figure 3.28 C). Results from these indicated that both the transformant in TN72-PR and TNE do indeed contain the disrupted *psbK* gene, and moreover, were homoplasmic (Figure 3.28 B lane T9, and Figure 3.28 C lane T2).

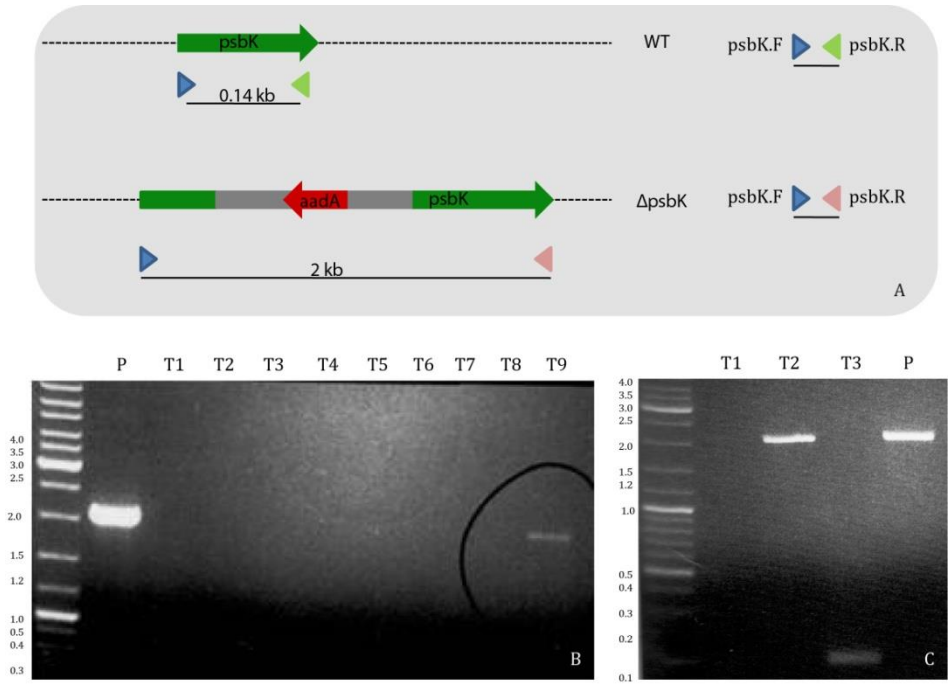

Figure 3.28 A) primers designed for PCR screening of homoplasmic *psbK*-deficient transformants. B) PCR result for the psbK.KO plasmid (P) and nine transformants (T1-T9) of TN72-PRΔpsbK using primers psbK.F and psbK.R. Band size observed is 2 kb, which represents the disrupted *psbK* gene. C) PCR result for three transformants (T1-T3) of TNEΔpsbK and the psbK.KO plasmid (P) using same primers as above. Band sizes observed are 2 kb for the disrupted *psbK* gene, and 0.14 kb for the native *psbK* gene.

In Figure 3.28 B, T1 – T8 exhibited either no band (poor DNA quality for amplification) or the native *psbK* band (0.14 kb). In Figure 3.28 C, it can be clearly observed for T3 the amplification of the native *psbK*, showing an example of an aberrant transformant than showed antibiotic resistance in spot tests but no expression of the *aadA* within the *psbK* sequence.

The fact that some putative transformants showed antibiotic resistance to both Sp and St but no presence of the 2 kb band showing insertion of the aadA cassette in the expected location poses the question as to the aadA cassette might have integrated in the nuclear genome. It is unlikely that antibiotic resistance to both antibiotics occurs as a spontaneous mutation; therefore, we speculate that some cells incorporated the aadA cassette in random locations, as it occurs in nuclear recombination, and in this way exhibited antibiotic resistance. PCR with specific aadA primers was not carried out and these aadA-resistant strains were not further analysed.

PSII complex accumulation

In order to assess that PSII accumulation was actually diminished due to the knockout of a gene involved in its assembly, a Western blot was carried out using antibodies against the D1 protein, one of the core subunits of the PSII complex. Samples were prepared as explained in section 2.7.1. The expected band, with a size of approximately 32 kDa, showed that accumulation of D1 is greatly reduced in the *psbK* mutants, identical to what happens in TN72, the control strain with a *psbH* knockout, which is also incapable of accumulating normal amounts of D1 protein (Figure 3.29).

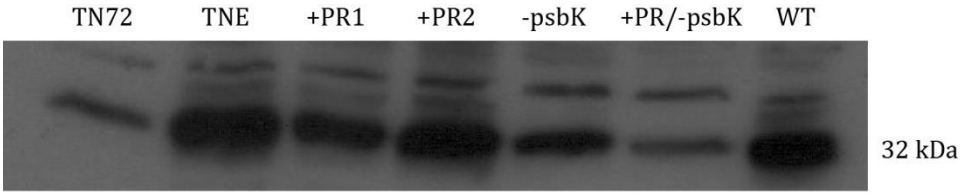

Figure 3.29 Western blot result using anti-D1 antibodies showing decreased expression of D1 protein in PSII-deficient strains (TN72 and –psbK). D1 is represented by the 32 kDa band. Cultures were grown in 25 mL TAP medium flasks at 25 °C, 120 rpm and 30 µmol m^{-2} s^{-1}. Samples are: the *psbH*-disrupted strain TN72, the control strain TNE, two transformants of TN72 containing proteorhodopsin (+PR 1 and 2), a *psbK*-deficient TNE transformant (-psbK), a *psbK*-deficient transformant containing proteorhodopsin (+PR/-psbK), and wild type strain (WT).

3.3.3 Conclusion

The knockout of the *psbK* gene proved to be a successful strategy to generate homoplasmic PSII-deficient strains. Isolation of putative transformants from spot tests resulted useful since the three transformants rescued that exhibited antibiotic resistance and impaired growth in minimal medium were true transformants. Homoplasmy was confirmed by PCR, and Western blot analysis showed that these transformants had reduced accumulation of PSII, in the form of D1 protein. This decrease was also observed by Takahashi et al. (1994).

The next step was to test the hypothesis that this decrease in PSII complex and extra space in the thylakoid membrane would provide any advantage in terms of proteorhodopsin accumulation and functionality.

3.4 Analysis of proteorhodopsin in TN72-PRΔpsbK

3.4.1 Proteorhodopsin levels in TN72-PRΔpsbK

TN72-PRΔpsbK mutants were obtained and successfully checked for homoplasmy of the disrupted *psbK* gene; therefore, the next step was to determine if the steady-state level of proteorhodopsin was affected by the knockout strategy. Western blot analysis of the two TN72-PRΔpsbK lines was carried out using anti-HA antibodies. As before, cells were harvested in late exponential phase and prepared as explained in section 2.7.1. Cell extracts were run on a 15 % SDS polyacrylamide gel, and a positive control (HA-tagged protein) was included for antibody assessment. It could be observed that proteorhodopsin was detectable in both the TN72-PRΔpsbK strains (Figure 3.30). However, there appeared to be no change in the level of proteorhodopsin, which was confirmed in several independent Western blots.

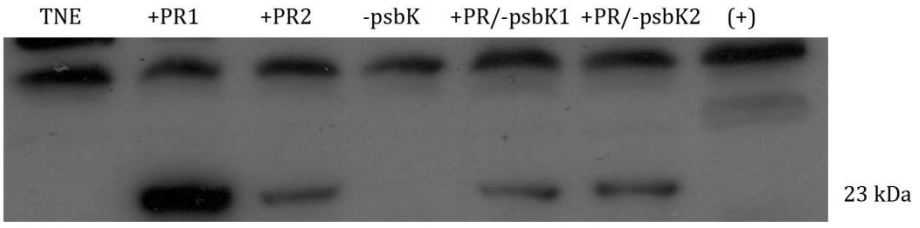

Figure 3.30 Comparison of the expression of proteorhodopsin in TN72 with and without *psbK* knockout, observed by western blot analysis using anti-HA antibodies. Cultures were grown in 25 mL TAP medium flasks at 25 °C, 120 rpm and 30 µmol m^{-2} s^{-1}. Lanes are as follows: the control strain TNE, two transfomants of TN72 containing proteorhodopsin (+PR 1 and 2), a *psbK*-deficient TNE transformant (-psbK), two *psbK*-deficient transformant containing proteorhodopsin (+PR/-psbK 1 and 2), and a highly expressed HA-tagged protein as positive control (+). Unspecific band on the upper section of the gel serves as a loading control.

There seems to be higher protein level for +PR1 (TN72-PR 1) than +PR2 (TN72-PR 2); however, this result is not consistently observed in Western blots carried out, which suggests that this particular protein's level might vary depending upon the specific time (stage in cultivation) in which samples are taken. It is also speculated that this protein might be unstable, which can be somehow expected due to the intrinsic instability and difficulty of detection for membrane proteins (Alguel et al., 2010; Carpenter et al., 2008), specially in this case in which there seems to be a low level of protein being accumulated.

3.4.2 Functionality of proteorhodopsin in TN72-PRΔpsbK

Since it was demonstrated that PR was present in the TN72-PRΔpsbK strain, the functionality of the protein was tested as explained in section 3.1.5.

Proteorhodopsin absorbance at 520 nm

Absorbance at 520 nm was measured in two TN72-PRΔpsbK transformant lines and the control strain TNEΔpsbK in cultures without and with addition of retinal. Absorbance was also measured in the original TN72-PR strains and the TNE control, to be able to compare any potential differences. Again, absorbance at 680 nm was also measured in order to normalise data to chlorophyll fluorescence. Results of these measurements and the ratio A_{520}/A_{680} are shown in Table 3.3.

Once again, there seemed to be no major difference among all lines analysed, and retinal addition did not provide any detectable advantage. The A_{520}/A_{680} results obtained for the two TN72-PRΔpsbK transformant lines matched the values observed for the TN72-PR lines, showing no improvement on this regard. This is in agreement with the equivalent level of proteorhodopsin observed in both transformant lines in Western blots.

Table 3.3 Absorbance at 520 and 680 nm measured in two transformants of TN72 containing proteorhodopsin (TN72-PR 1 and 2) with the negative control (TNE), and in two transformants of TN72 expressing proteorhodopsin in a *psbK*-deficient background (TN72-PRΔpsbK 1 and 2) with the negative control (TNEΔpsbK) with (10 mM) and without added all-*trans*-retinal. Cultures were grown in 25 mL TAP medium flasks at 25 °C, 120 rpm and 30 μmol m^{-2} s^{-1}.

Sample	Retinal [mM]	A_{520}	A_{680}	A_{520}/A_{680}
TNE	**0**	0.676	0.739	0.915
	10	0.671	0.743	0.903
TN72-PR 1	**0**	0.554	0.614	0.902
	10	0.449	0.523	0.859
TN72-PR 2	**0**	0.629	0.684	0.919
	10	0.641	0.704	0.911
TNEΔpsbK	**0**	0.545	0.613	0.889
	10	0.580	0.642	0.903
TN72-PRΔpsbK 1	**0**	0.471	0.522	0.902
	10	0.465	0.514	0.905
TN72-PRΔpsbK 2	**0**	0.428	0.475	0.901
	10	0.392	0.437	0.897

Growth of TN72-PRΔpsbK and effect of retinal addition

The TN72-PR and TN72-PRΔpsbK transformants were grown in mixotrophic mode (light intensity of 50 μmol m^{-2} s^{-1}) and growth was monitored for a period of eight days. From Figure 3.31, it can be observed that the growth rate of the two TN72-PR transformants matched very closely TNE, with similar maximum cell densities, just as observed before. TNEΔpsbK and one of the TN72-PRΔpsbK lines also showed a matching growth profile, demonstrating that when these strains were grown at moderate light intensity with added carbon source, cell growth was equivalent to strains with no mutation of *psbK*.

In contrast, for the second TN72-PRΔpsbK line, a slower growth rate and particularly decreased maximum cell density was observed when compared to all other strains. This fact suggests that a transformation event can actually generate transformant lines with different phenotypes and gene expression levels. This phenomenon has been generally

dismissed, assuming that cell lines generated from a same chloroplast transformation will exhibit the same gene expression and hence, protein accumulation. Although the Western blot result from Figure 3.30 shows the same level of protein accumulation for both TN72-PRΔpsbK lines, it has been widely observed in other Western blots that protein level varies, even when samples were harvested at the same cultivation stage.

This decreased growth of the transformant line 2 might indicate that there could have been other recombination events within the same transformation. DNA insertion in the chloroplast occurs via homologous recombination; therefore, it is easy to track this insertion. However, it is not possible to determine if other events of recombination have occurred in the nuclear genome simultaneously, and this incident could explain different phenotypes due to the mutation of other genes.

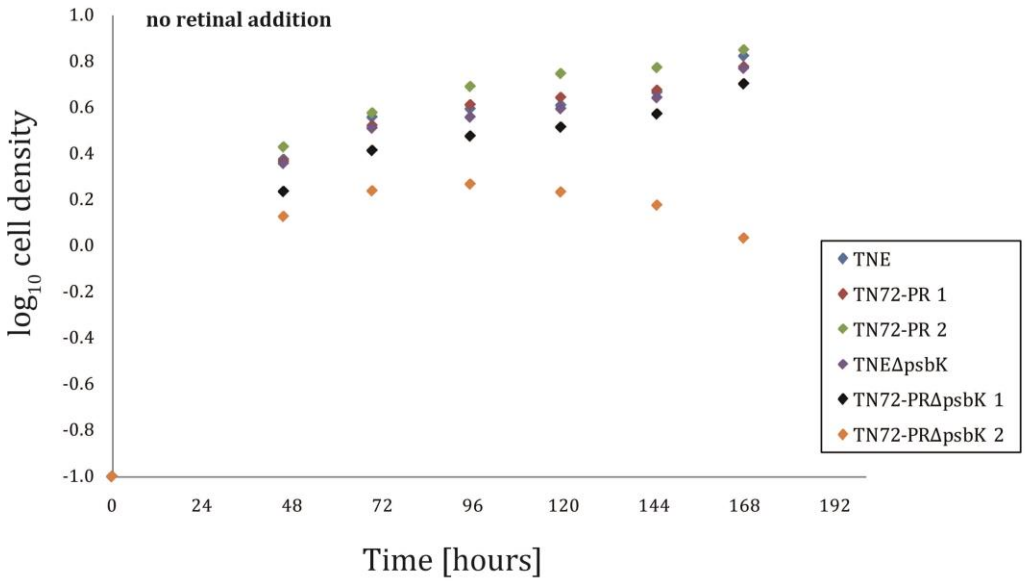

Figure 3.31 Comparison of cell growth of two TN72 transformants expressing proteorhodopsin (TN72-PR 1, 2) with the negative control (TNE) and two TN72 transformants expressing proteorhodopsin in a *psbK*-deficient background (TN72-PRΔpsbK 1 and 2) with the negative control (TNEΔpsbK). Cultures were grown in 25 mL TAP medium flasks at 25 °C, 120 rpm and 50 µmol m^{-2} s^{-1}. Initial cell density was OD_{750}=0.1.

The same set of cultures was run with the addition of 10 mM retinal, in order to determine if there was any difference adding retinal to the cultures in this new genetic background; however, the growth profile obtained was very similar to the one obtained with no retinal addition (Figure 3.32), so once again retinal seemed to provide no detectable benefit. This experiment, with and without retinal addition, was run in two independent events and the same behaviour was observed in all cell lines.

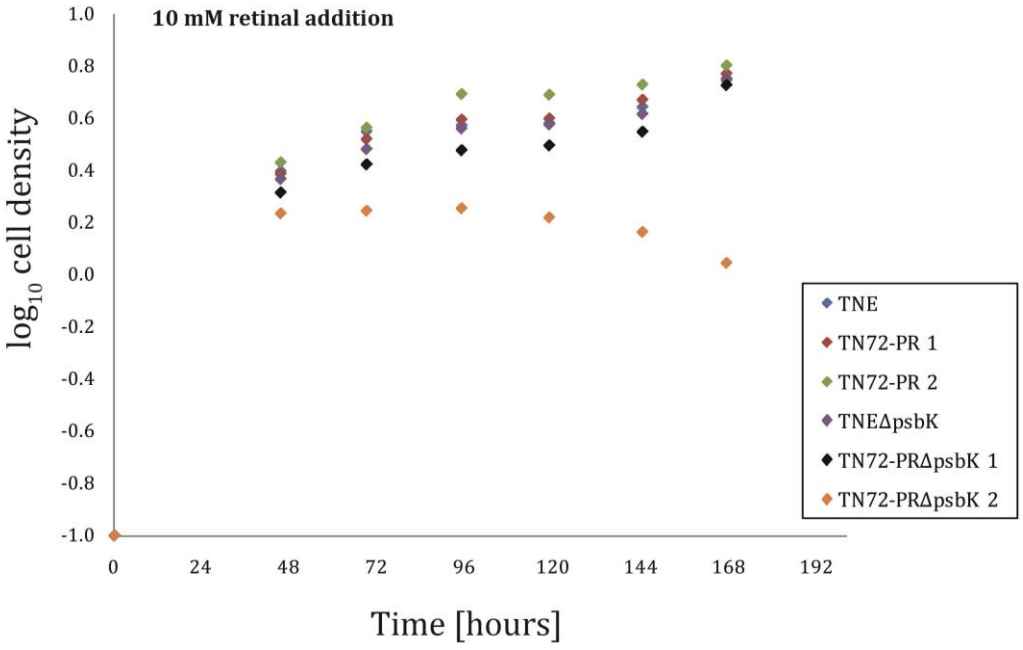

Figure 3.32 Comparison of cell growth of two TN72 transformants expressing proteorhodopsin (TN72-PR 1, 2) with the negative control (TNE) and two TN72 transformants expressing proteorhodopsin in a *psbK*-deficient background (TN72-PRΔpsbK 1 and 2) with the negative control (TNEΔpsbK) with 10 mM retinal addition at 40 hours of cultivation. Cultures were grown in 25 mL TAP medium flasks at 25 °C, 120 rpm and 50 µmol m^{-2} s^{-1}. Initial cell density was OD_{750}=0.1.

The TN72-PRΔpsbK transformant line that showed good growth in flasks (TN72-PRΔpsbK 1) and TNEΔpsbK were grown without retinal in the photobioreactor in TAP medium in dim light (light intensity of 30 µmol m^{-2} s^{-1}), and cell growth (OD_{740}) was measured online every 30 minutes for 7 days (Figure 3.33). The growth profile was almost the same for both strains, which is in agreement with the results observed in flasks. TN72-PRΔpsbK showed a specific growth rate of 0.030 h^{-1}, against 0.031 h^{-1} observed in TNEΔpsbK, which is slightly lower than TN72-PR grown under the same conditions (0.034 h^{-1}).

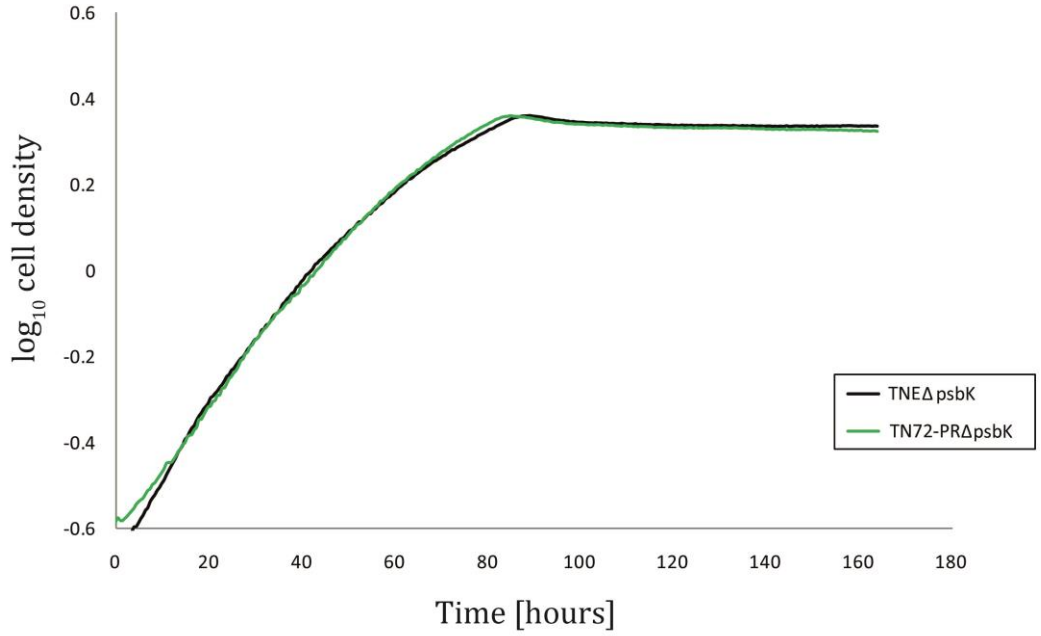

Figure 3.33 Comparison of cell growth of the *psbK*-deficient TN72 transformant expressing proteorhodopsin (TN72-PRΔpsbK) against the negative control (TNEΔpsbK). Cultures were grown in TAP medium in an automated photobioreactor at 25° C, 30 µmol m^{-2} s^{-1} and continuous shaking at 120 rpm. Initial cell density was OD_{740}=0.25.

The main reason for knocking out *psbK* was to test if this strategy would increase the abundance of proteorhodopsin and thus, be able to demonstrate that PR can provide some advantage in terms of cell growth rate. Strains TN72-PR and TN72-PRΔpsbK were grown in the same conditions (light intensity of 30 µmol m^{-2} s^{-1}) in two separate events and in both cases it could be observed that TN72-PR grows slightly faster than TN72-PRΔpsbK (Figure 3.34). Average cell growth rate obtained was 0.033 h^{-1} for TN72-PR against 0.031 h^{-1} for TN72-PRΔpsbK, meaning a 6.5 % higher growth rate in the strain expressing PR without *psbK* knocked-out.

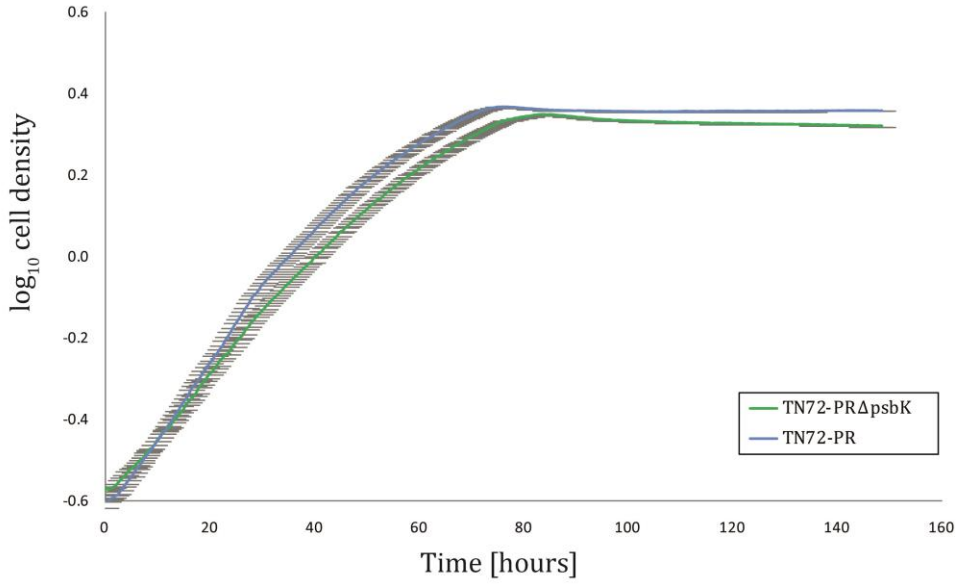

Figure 3.34 Comparison of cell growth of the *psbK*-deficient TN72 transformant expressing proteorhodopsin (TN72-PRΔpsbK) against the TN72 transformant expressing proteorhodopsin (TN72-PR). Cultures were grown in TAP medium in an automated photobioreactor at 25° C, 30 µmol m^{-2} s^{-1} and continuous shaking at 120 rpm. Initial cell density was OD_{740}=0.25. Curves represent the average result of 2 separate experiments, and the grey area represent horizontal error bars for each strain cultivated (n=2).

Since these *psbK* knockout lines were kept in dim light conditions, but it has been reported that they can tolerate high light when an exogenous carbon source is provided (Takahashi et al., 1994), they were also grown at 150 µmol m^{-2} s^{-1} (Figure 3.35).

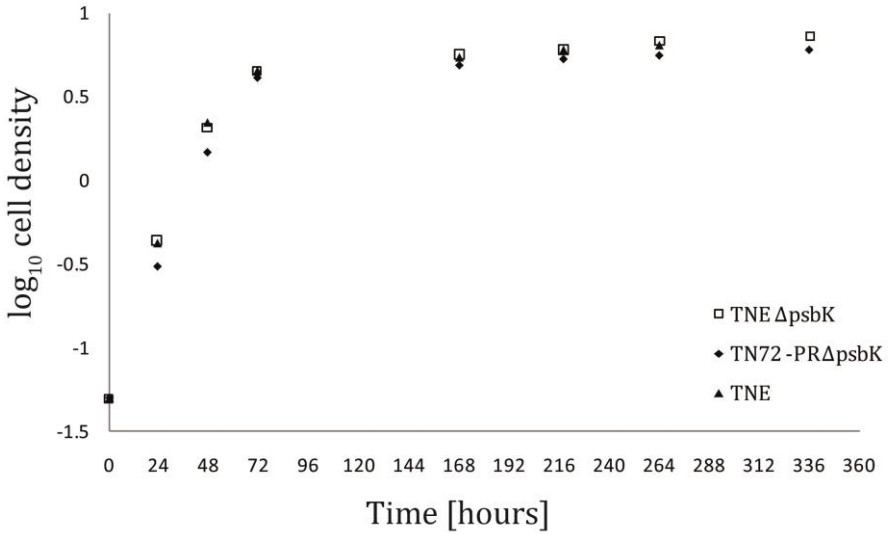

Figure 3.35 Comparison of cell growth of two *psbK* mutants (TN72-PRΔpsbK and TNEΔpsbK) and a strain with the native *psbK* (TNE). Cultures were grown in 25 mL TAP medium flasks at 25 °C, 120 rpm and 150 µmol m^{-2} s^{-1}. Initial cell density was OD_{750}=0.05.

Both TN72-PRΔpsbK and TNEΔpsbK grew well, with very similar specific growth rate and maximum cell density to TNE, so these strains were tested along with TNE and TN72-PR in the photobioreactor at similar light intensity conditions (Figure 3.36). Cell growth was not negatively affected by the higher light intensity, but the opposite, obtaining higher specific growth rates of 0.044 h^{-1} for TN72-PR against 0.046 h^{-1} for TN72-PRΔpsbK. Control strains TNE and TNEΔpsbK showed growth rates of 0.040 and 0.044 h^{-1}, respectively. This experiment gave the first evidence of higher growth rate for TN72-PRΔpsbK over the other cell lines. Nevertheless, this increase reaches a 4.5 % only, which is not a major improvement and does not provide enough evidence of a potential advantage of carrying a disrupted *psbK*.

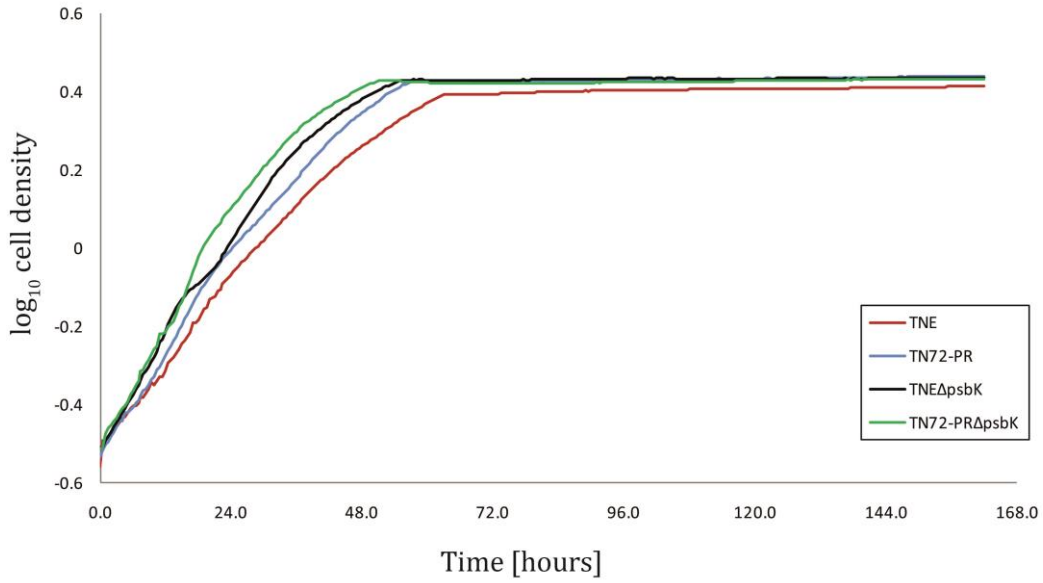

Figure 3.36 Comparison of cell growth of the *psbK*-deficient TN72 transformant expressing proteorhodopsin (TN72-PRΔpsbK) against the TN72 transformant expressing proteorhodopsin (TN72-PR) and controls for both transformant lines without PR. Cultures were grown in TAP medium in an automated photobioreactor at 25° C, 200 µmol m^{-2} s^{-1} and continuous shaking at 120 rpm. Initial cell density was OD_{740}=0.25.

3.4.3 Conclusion

The level of proteorhodopsin in a *psbK*-deficient strain did not exhibit any improvement when compared to the photosynthetic parent strain TN72-PR, despite the evidence of less accumulation of PSII in the thylakoid membrane and, therefore, more membrane space for PR integration.

Experiments to test the functionality of PR in this new background in cultures grown in dim light did not show any benefit in cell growth, especially in the case of one of the transformant lines grown in the small flask cultures, in which PR appeared to have a detrimental effect on growth with respect to all other strains.

It was possible to observe that *psbK* mutants grow normally on bright light when acetate is supplemented, just as reported by Takahashi et al. (1994), so this alleviated the growth rate and cell density imbalance observed at lower light intensity. When growing the different cell lines in the photobioreactor at this higher light intensity, a higher specific growth rate for TN72-PRΔpsbK was measured; however, the increase is quite moderate with respect to TN72-PR, and it does not justify the need for a *psbK*-deficient background. It can also be argued that such a small increase is within the margin of error for a measurement, meaning that this percentage is not statistically significant to be considered as a real increase, even more so considering that for this experiment there are no replicates involved.

Overall, these findings suggest that the presence of proteorhodopsin in a PSII-deficient mutant has no positive contribution to cell growth, and the strategy of reducing PSII levels does not increase PR level. Consequently, limitation on the accumulation of PR is not due to molecular crowding but more likely due to other factors such as instability of the protein, translational/post-translational complications or inefficient integration of the protein into the membrane, such that it is quickly degraded.

3.5 Final remarks

This chapter describes the successful synthesis of a prokaryotic membrane protein in the chloroplast of *C. reinhardtii*. As far as can be found in literature, this is the first report of the synthesis of an integral transmembrane protein in the algal chloroplast. There are only few reports describing the expression of a membrane protein in tobacco chloroplasts, particularly the work of Ahmad and colleagues (Ahmad et al., 2012), who confirmed expression and functionality of a plastid terminal oxidase from *C. reinhardtii*.

Although the accumulation of the 23-kDa PR was clearly demonstrated, the level of protein was low. A knockout strategy was designed in order to lower the protein density in the

thylakoid membrane by reducing the amount of PSII complex and provide more space for proteorhodopsin, and two different PSII genes were disrupted for this purpose. This approach led to the finding that although *psbC* encoded a product that is dispensable, the expression of the gene itself is not, possibly because *psbC* is co-transcribed with essential tRNA genes. As such, stable homoplasmic transformants of a *psbC* knockout could not be recovered. In contrast, homoplasmic *psbK* knockout lines were generated and allowed the testing of the hypothesis that reducing PSII levels would result in increased PR levels.

The functionality of PR was assessed with the main objective of detecting improvement in specific growth rate or culture lifespan, as reported in literature for heterologous expression of PR (Johnson et al., 2010). It was possible to detect a contribution to cell growth for TN72-PR of almost 12 % when growing cells in the photobioreactor; however, this same effect was not observed in shake flasks. This difference in behaviour can be attributed to a better control of the cultivation parameters, particularly light intensity, in the automated photobioreactor and a more standardised measurement of the cell density.

The *psbK* knockout did not contribute to the PR level accumulated, as it was observed in Western blot results. A lesser degree of molecular crowding in the thylakoid membrane due to decreased levels of PSII did not produce the hypothesised result on PR accumulation, and the fact that TN72-PRΔpsbK showed lower specific growth rate and cell density in most conditions studied when compared to TN72-PR made the *psbK* knockout a not helpful strategy for increasing PR level.

In conclusion, the insertion of proteorhodopsin into the chloroplast of TN72 seems to provide a moderate improvement in cell growth under the conditions studied. However, more replicates of this experiment would be advisable in order to have stronger data to support this claim. It is not fully understood if this protein, or a fraction of it, is effectively being embedded into the thylakoid membrane because it was not possible to detect it in membrane-enriched fractions, due to the high concentration on other membrane components. Nevertheless, this protein was not detected in the soluble fraction either, which supports the assumption that proteorhodopsin integrated into the thylakoid membrane.

The addition of exogenous all-*trans* retinal did not provide any advantage, so it is speculated that PR was able to access the endogenous retinal present in *C. reinhardtii*. However, no experiments were carried out to assess if the endogenous retinal was being

utilised by proteorhodopsin, but the fact that a difference in growth rate was observed strongly suggests that proteorhodopsin is active. Another factor that could affect the membrane integration and functionality of PR is the different lipid composition of the thylakoid membrane in comparison to its original location (Opekarová and Tanner, 2003). There is clearly a very different lipid composition in the membrane of Gram (-) bacteria such as the γ-proteobacterium, from where PR was isolated, in comparison to the chloroplast membrane of *C. reinhardtii* and this can definitely pose a challenge to consider.

It is envisaged that PR expression could be enhanced by expressing it under the control of a stronger promoter/5' UTR, such as *psaA*, which as will be shown in the next chapter, provides higher protein accumulation than the *atpA* regulatory elements. An increase in protein accumulation could make it easier for detection of a more pronounced effect on cell growth.

CHAPTER 4

EXPRESSION OF A GREEN FLUORESCENT PROTEIN AS A REPORTER IN THE CHLOROPLAST OF *CHLAMYDOMONAS REINHARDTII*

4 EXPRESSION OF A GREEN FLUORESCENT PROTEIN AS A REPORTER IN THE CHLOROPLAST OF *CHLAMYDOMONAS REINHARDTII*

Reporter genes code for proteins that are mostly used for *in vivo* and *in vitro* applications as indicators of the transcriptional activity in cells, which can be assessed by measuring the reporter mRNA level or the reporter protein itself (Schenborn and Groskreutz, 1999). These reporters have also been used fused to endogenous proteins in order to study protein localisation and protein-protein interactions, and as part of signal transduction events in biosensing systems (Lewis et al., 1998). Ideal reporter genes are not endogenously expressed in the host system, and the reporter product should be easily detectable involving sensitive, quantitative and reproducible methods for its assessment (Lewis et al., 1998; Schenborn and Groskreutz, 1999).

There is a diverse range of fluorescent proteins (FP) that have been used with great success as reporters for the different purposes listed above (Chudakov et al., 2010). Many factors can influence the fluorescence levels provided by a fluorescent protein: these include the background auto-fluorescence in the organism due to the presence of different metabolites and pigments, the FP expression levels, the rate of FP maturation (creation of the chromophore), levels of protein mis-folding, and protein turnover (Rasala et al., 2013).

In addition to the intrinsic features of the particular FP that define its fluorescence, the steady-state level of the FP can be maximised by selecting the appropriate regulatory sequences that will control the expression of the FP gene in the chosen host. These regulatory sequences include the 5' UTR and promoter region, the 3' UTR, and other *cis*- and *trans*-acting elements than can contribute as enhancers or stabilizers.

Different reporters have been expressed in the chloroplast of *Chlamydomonas reinhardtii* with variable degree of success, which include antibiotic-resistance markers and enzymes. However, low levels of protein accumulation have been achieved, making these reporters not suitable for quantitative analyses (Franklin et al., 2002; Mayfield and Schultz, 2004). As displayed in Table 1.2, the search for a suitable FP to study various features of gene

expression and protein accumulation has proven disappointing as well, with low levels of expression and almost non-detectable fluorescence.

This chapter focuses on the expression of a synthetic gene encoding the fluorescent protein Verde Fluorescent Protein (VFP) in different genetic backgrounds, exploring the effect on protein accumulation and functionality of two different promoters/5' UTR (from the endogenous genes *atpA* and *psaA*), the co-expression of a gene for a bacterial chaperone protein (Spy), and the creation of a fusion construct in which VFP is fused to the large subunit of the RuBisCo enzyme. These four approaches aim at increasing the level of protein accumulated in the chloroplast. VFP levels were assessed both by immunodetection and by fluorescence measurements.

4.1 Selection and design of the fluorescent gene

There are plenty of choices of fluorescent proteins nowadays, including numerous variants of the original FPs – green fluorescent protein (GFP) and *Discosoma sp.* red fluorescent protein (DsRed). Variants usually have a few mutations in their protein sequence in order to tune excitation and emission wavelengths, and also aimed at increasing brightness, photostability and maturation temperature (Ilagan et al., 2010; Lippincott-Schwartz and Patterson, 2003).

VFP, which stands for vivid Verde Fluorescent Protein, was discovered in 2010 (Ilagan et al., 2010). This protein was isolated from the coral species *Cyphastrea microphthalma* from warm waters of the Australian Great Barrier Reef (Figure 4.1). The VFP sequence shows a higher sequence identity to DsRed than to GFP, and exhibits maximum excitation and emission peaks at 491 and 503 nm, respectively. Despite sequence similarity to DsRed, VFP spectral properties are more similar to enhanced GFP (EGFP) due to its GFP-like chromophore. This ~ 26 kDa protein was successfully used for *in vivo* labelling when expressed as a fusion construct in zebrafish embryos and its fluorescence could be detected by fluorescence microscopy. Moreover, it was also reported that this protein exhibits at least two-fold higher brightness than EGFP. These promising results encouraged us to investigate whether VFP could be a useful reporter protein in the chloroplast of *Chlamydomonas reinhardtii*.

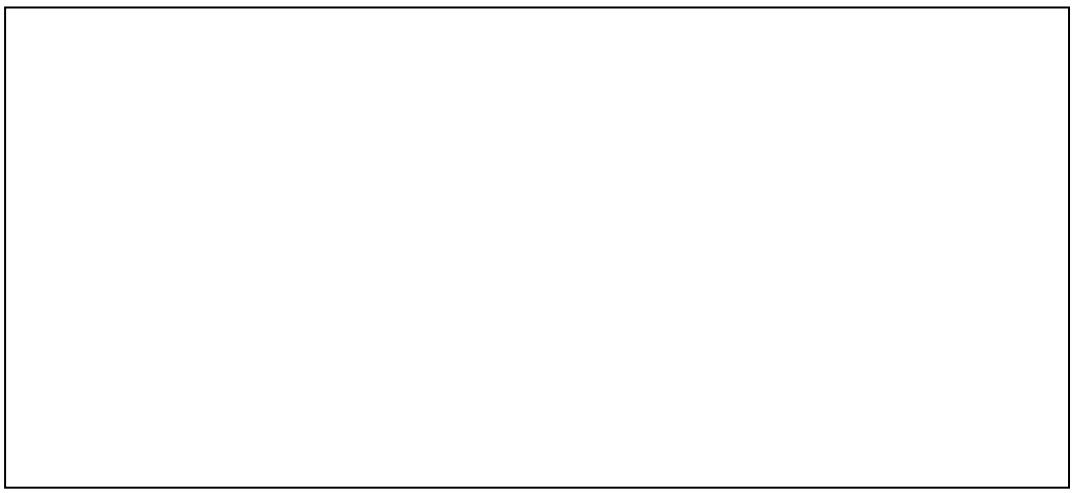

Figure 4.1 A) The coral *Cyphastrea microphthalma*, from where VFP was isolated. B) overlay of the absorption (abs), fluorescence-excitation (ex) and fluorescence-emission (em) spectra of VFP. The samples were excited at 450 nm and the emission spectra were measured from 465 to 650 nm. The fluorescence excitation spectra were obtained from 250 to 515 nm by monitoring the emission at 530 nm. The spectra were normalised at the maximum peak (replicated from Ilagan et al., 2010).

Table 4.1 presents the distinctive features of various fluorescent proteins and relative brightness relative to EGFP, since this is one of the most widely used FP.

Table 4.1 Spectral properties of VFP in comparison to EGFP, Venus and other selected fluorescent proteins (FPs). The excitation and emission wavelengths, the molar extinction coefficients (EC), the relative brightness and the photostability are listed. Photostability was calculated based on 100 % EGFP measured at the same time. ND, not determined (adapted from Ilagan et al., 2010).

Protein	Excitation (nm)	Emission (nm)	EC x 10^{-3} (M^{-1} cm^{-1})	Relative brightness	Photostability (% EGFP)	Reference
VFP	491	503	83.7	84	33	Ilagan et al., 2010
EGFP	488	509	54.4	33	100	Ilagan et al., 2010
Venus	515	527	93.3	70	27	Ilagan et al., 2010
GFP - Anthozoa						
AzamiGreen	492	505	55.0	41	ND	Karasawa et al., 2003
mWasabi	493	509	70.0	56	53	Ai et al., 2008
ZsGreen	493	505	43.0	39	ND	Matz et al., 1999
copGFP	482	502	70.0	42	ND	Shagin et al., 2004
cmFP512	503	512	58.8	39	92	Vogt et al., 2008
aacuGFP2	502	513	93.9	67	ND	Alieva et al., 2008
aeurGFP	504	515	145.7	98	ND	Alieva et al., 2008
eechGFP1	497	510	124.2	93	ND	Alieva et al., 2008
efasGFP	496	507	125.8	101	ND	Alieva et al., 2008
gfasGFP	492	506	102.5	75	ND	Alieva et al., 2008
plamGFP	502	514	98.6	95	ND	Alieva et al., 2008
sarcGFP	483	500	76.7	74	ND	Alieva et al., 2008
GFP – Aequorea derivatives						
Superfolder	485	510	83.3	54	90	Pedelacq et al., 2006
mEmerald	487	509	57.5	39	58	Cubitt et al., 1999
Cyan FPs – Anthozoa						
mTFP1	462	492	64	54	63	Ai et al., 2006
Photoconvertable FPs						
Kaede	508	518	98.8	87	26	Ando et al., 2002
dEos (G)	506	516	84	55	24	Wiedenmann et al., 2004
mEos2 (G)	506	519	56	47	21	McKinney et al., 2009
Photoswitchable FPs						
Dronpa	503	517	95	81	ND	Ando et al., 2004
mKikGR	505	515	49	34	7	Habuchi et al., 2008
cerFP505	494	505	54	30	54	Vogt et al., 2008

4.2 Expression of VFP under the control of the *atpA* promoter/5' UTR

The first approach was to design a synthetic gene encoding VFP and express this in the chloroplast under the control of the *atpA* promoter/5'UTR by using the expression vector pASapI (vector details explained in section 3.1.2).

4.2.1 Construction of the plasmid pASapI.VFP

A synthesised version of *vfp* (GenBank accession number FN597286) was designed taking into account the Kazusa codon usage table for chloroplast genes in *Chlamydomonas reinhardtii*. A codon adaptation index of 0.8 was chosen. The stop codon was preceded by the coding sequence for a Hemagglutinin (HA) epitope tag for ease of detection of VFP using commercial antibodies. The resulting gene (728 bp) was designed to be easily cloned into pASapI by double digestion with the restriction enzymes *Sap*I and *Sph*I (*vfp* sequence in appendix 3).

Insertion of the *vfp* fragment (Figure 4.2 A) into the *Sap*I-*Sph*I digested pASapI vector (Figure 4.2 B) generated the transformation plasmid pASapI.VFP (7294 bp) (Figure 4.2 C), which was further sequenced to corroborate there were no mutations introduced in any step. The plasmid was firstly amplified in the *E. coli* strain DH5α and purified for transformation of TN72.

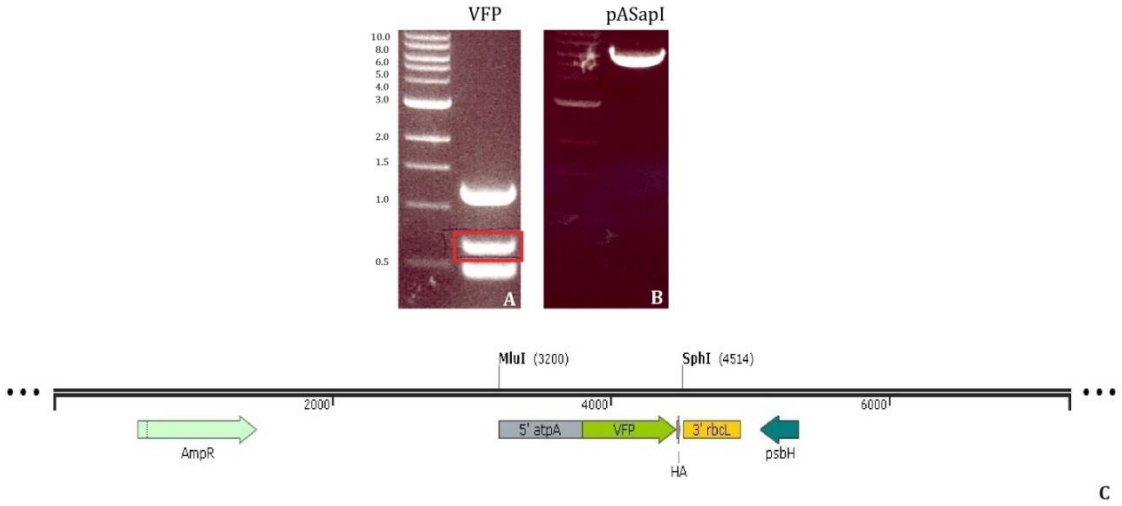

Figure 4.2 A) Gel electrophoresis result for the digested *vfp* with enzymes *Sap*I and *Sph*I. Expected size is 0.72 kb, B) Gel electrophoresis result for the linearised pASapI vector. Expected size is 6.6 kb, C) Diagram of the pASapI.VFP plasmid developed for insertion of *vfp* into the chloroplast of the host strains TN72 and Bst-same.

In case of any detrimental effect of the HA tag on VFP folding and functionality, an alternative version of the plasmid form was created, in which *vfp* did not have the HA tag sequence on its 3' end. For this purpose, *vfp* was amplified by PCR using a forward primer replicating the *Sap*I restriction site (VFP_SapI.F) and a reverse primer that created the stop codon immediately after the coding sequence, followed by a *Sph*I restriction site (VFP_SphI.R) (primer sequences in appendix 1). The resulting fragment (710 bp) was digested with both restriction enzymes and ligated into pASapI forming the plasmid pASapI.VFP.noHA. This plasmid was also sequenced to verify that there were no mutations or mismatches along the generation process.

4.2.2 Transformation of TN72 with plasmids pASapI.VFP and pASapI.VFP.noHA

Transformation of TN72 with the two plasmids was carried out as explained in section 2.6.2.1, using the glass beads vortexing method. Plates were incubated in bright light for 3 – 4 weeks until colonies appeared.

Recovery of *vfp* transformants and confirmation of gene expression

The transformation numbers obtained for the two plasmids are shown in Table 4.2. These transformant lines were assessed by PCR screening, following the strategy detailed in section 2.5.2.1, in which a combination of four primers allows detection of untransformed (0.85 kb band for TN72, 1.0 kb for WT) and successfully transformed (1.2 kb) chloroplast genomes. Figure 4.3 shows the result of this analysis for colonies arising from the pASapI.VFP plasmid, where it was possible to detect the 1.2 kb band for positive transformants in four colonies, and the 1.0 kb band in one, which provides an example of an aberrant transformant where only the *psbH* marker has integrated into the genome. The absence of a 0.85 kb PCR product in any of the transformants indicated that they had reached homoplasmy with no copies of the TN72 genome remaining. Sequencing also confirmed that *vfp* had been recombined in the expected locus without any mutations. In the case of the transformant lines generated using the plasmid containing *vfp* without the HA tag, the same approach was used for screening for gene integration and homoplasmy, and it was confirmed that all four were true transformants.

Table 4.2 Transformation yield for VFP insertion in TN72 using the two different plasmids developed.

Expression vector used	Transformant name	Number of transformation events	Number of colonies recovered
pASapI.VFP	TN72-VFPpA	8	5
pASapI.VFP.noHA	TN72-VFPpAX	7	4

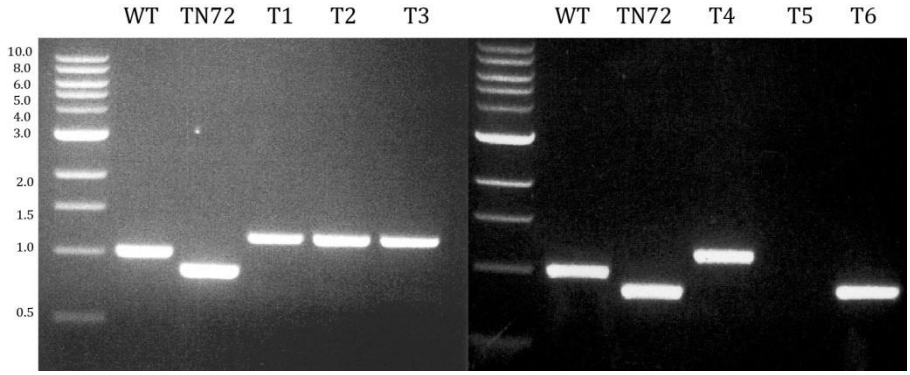

Figure 4.3 PCR analysis of TN72 transformants expressing *vfp* transformed with the pASapI.VFP plasmid (TN72-VFPpA) using FLANK1, atpA.R, rbcL.Fn and MluR2 primers. Bands are as follows: wild-type (WT) 1.0 kb, TN72 and false transformant (T6) 0.85 kb, TN72-VFPpA transformants (T1-T4) 1.2 kb, transformant T5 showed no amplification due to poor DNA quality in this particular PCR.

When the same colonies were screened for *vfp* using specific primers, a positive band of the expected size (0.7 kb) was observed for the same transformants that gave positive results in the previous PCR, including T5 (Figure 4.4).

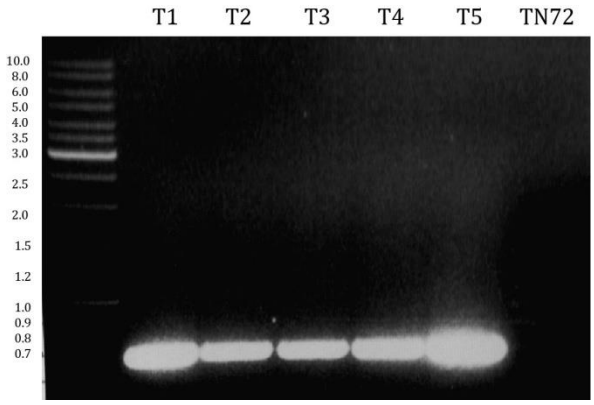

Figure 4.4 PCR analysis of TN72 transformants expressing VFP transformed with the pASapI.VFP plasmid (TN72-VFPpA) using VFP primers. Bands are 0.7 kb for all transformants (T1-T5) and no amplification for TN72.

4.2.3 Growth curve of TN72-VFPpA transformants

In order to verify that there was no detrimental effect on cell growth due to of the expression of VFP, a set of cultures comprising the control strain TNE and two TN72-VFPpA transformants were run in triplicate at 25 °C, 120 rpm and 150 µmol m^{-2} s^{-1} of light intensity. As it can be observed in Figure 4.5, cell growth of the transformant lines matched the growth observed in the control strain, with a specific cell growth rate of 0.064 h^{-1} (standard error = 0.001, n=3).

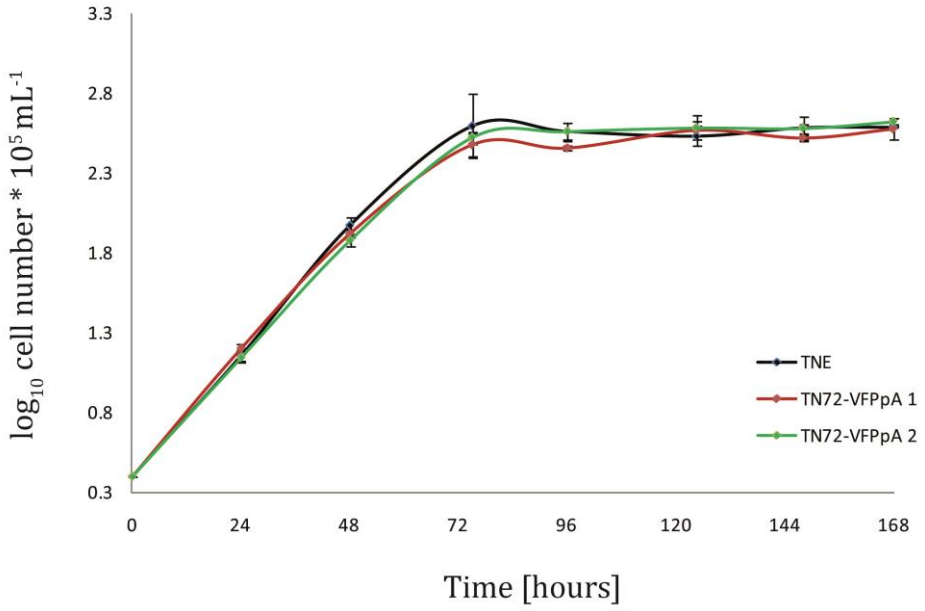

Figure 4.5 Comparison of cell growth of two TN72 transformants expressing VFP (TN72-VFPpA 1 and 2) and the control strain transformed with the empty pASapI vector (TNE). Cultures were grown in 25 mL TAP medium flasks at 25 °C, 120 rpm and 150 µmol m^{-2} s^{-1}. Initial cell density was 1.5x10^5 cells mL^{-1}. Error bars represent the standard error (n=3).

4.2.4 VFP accumulation in TN72

VFP has a molecular weight of ~ 26 kDa, and the HA tag attached to its 3' end has an estimated molecular weight of 1.2 kDa; therefore, the HA-tagged VFP should generate a product of approximately 27 kDa.

In order to assess whether the *vfp* gene is being expressed in the TN72-VFPpA transformants, Western blot analysis was carried out on crude lysate samples from the six putative transformant lines. Cells were harvested during late exponential phase of cultivation and prepared as explained in section 2.7.1. Samples were loaded on a 15 %

polyacrylamide gel together with a negative control (cell extract from a line transformed with the empty pASapI vector: TNE). ECL detection was used to visualise the binding of the HA antibody, and it could be observed that a ~ 25 kDa protein was present in all positive transformants.

In Figure 4.6, T5 represents the transformant line that gave a band showing no insertion of *vfp* in the PCR screening (named T6 in Figure 4.3) and this result once again confirmed that this was not a *vfp* transformant. All other transformant lines showed similar levels of VFP accumulation.

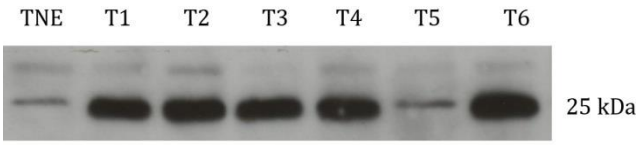

Figure 4.6 Western blot analysis of VFP in transformants generated using the pASapI.VFP plasmid using anti-HA antibodies. Cultures were grown in 25 mL TAP medium flasks at 25 °C, 120 rpm and 150 µmol m^{-2} s^{-1}. Lanes are as follows: TN72 transformed with the empty pASapI vector (TNE), TN72-VFPpA transformants (T1-T4 and T6) showing VFP accumulation, T5 corresponds to the transformant that gave no positive band for *vfp* insertion in the PCR screening.

Fluorescence detection in transformants

The main goal of using a fluorescent protein as a reporter is to be able to use its fluorescence as a facile technique to determine protein accumulation and localisation. Different methods for measuring VFP fluorescence in the *Chlamydomonas* chloroplast were evaluated.

In a first instance, samples from a liquid culture of *C. reinhardtii* in the exponential growth stage were measured for fluorescence using a fluorescence plate reader (Fluostar Optima, BMG Labtech); however, it was not possible to detect any signal. The likely reason behind this was a combination of the low protein concentration present and the very high fluorescence background generated by the chlorophyll. Samples were also measured using a fluorescence spectrometer (LS 55 Fluorescence spectrometer, Perkin Elmer) but again sensitivity of the equipment was not high enough to detect a signal. Finally, samples were tested using flow cytometry (Cyan ADP Analyzer, Beckman Coulter) and this procedure gave measurable results. Hence, fluorescence analyses throughout this research were carried out by means of flow cytometry.

Additionally, transformant lines were observed using confocal microscopy (Leica TCS SP5 confocal microscope) as a means of confirming fluorescence *in vivo*.

Flow cytometry

In order to detect fluorescence in an easy and fast way that could be used for *in situ* monitoring of whole cells at different stages of growth or under different parameters of cultivation, flow cytometry was used as detailed in section 2.8.3.

Fluorescence emission was detected in samples harvested at late-exponential cultivation phase, which corresponds to approximately 75 hours of growth. A shift of the fluorescence peak shown in the histogram correlates with a variation in the median value of fluorescence detected in a VFP-expressing strain in comparison to a control strain without VFP, grown under the same cultivation conditions. The change in fluorescence is expressed as a percentage. Figure 4.7 shows an example of this measurement in which fluorescence was detected for TN72-VFPpA (top right panel) and in the control strain TNE (top left panel), which then produced the overlay of the fluorescence peaks (bottom panel). A shift on this overlay is considered as the fluorescence emitted by VFP.

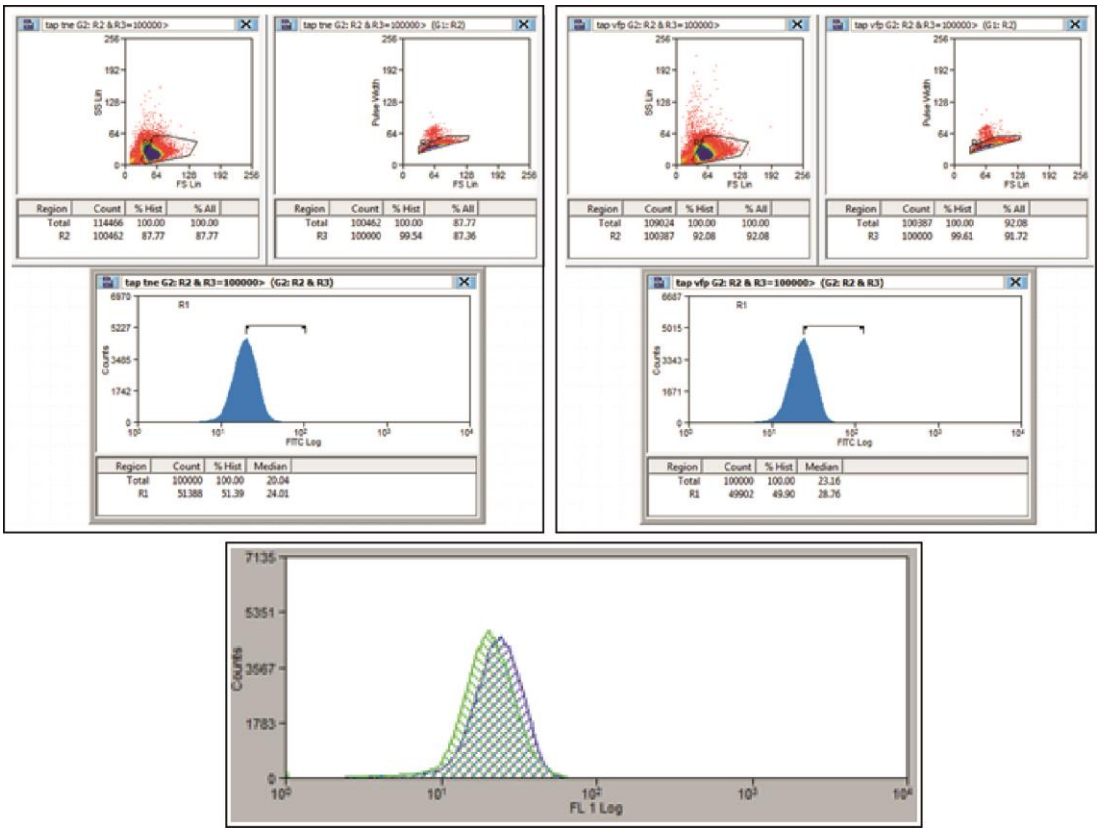

Figure 4.7 Histograms of fluorescence emission at 510-550 nm of a VFP transformant generated using the pASapI.VFP plasmid (top right panel) and TN72 transformed with the empty pASapI vector (TNE) as negative control (top left panel), at the same cultivation conditions (TAP medium, 25 °C, 120 rpm and 150 µmol m^{-2} s^{-1}). In the histograms, fluorescence intensity is plotted on the x axis and cell count plotted on the y axis. The bar on the histograms represents the 50 % of the population. The overlay plot (bottom panel) shows the shift in fluorescence: green curve (negative control), blue curve (VFP transformant).

As observed from this measurement, the population expressing VFP emitted a higher level of fluorescence in the range of 510-550 nm, which comprises the emission range of VFP, than the auto-fluorescence detected in this range in TNE. This measurement was performed in quadruplicate obtaining a 19.17 ± 0.83 % increase in fluorescence, which confirms that VFP is a functional fluorescent protein.

In the case of transformants expressing VFP without the HA tag (TN72-VFPpAX) the median fluorescence value obtained was equivalent to the value obtained for TN72-VFPpA (19.80 % ± 2.37). Consequently, it was possible to verify that the expression of *vfp* with an HA tag sequence fused to its 3' end had no detrimental effect on the functionality (fluorescence) of the protein. The strain TN72-VFPpAX was not used for any further experiments presented in this chapter.

Confocal microscopy

Transformant cells were inspected *in vivo* using a fluorescence microscope, but no fluorescence could be detected. A confocal laser scanning microscope was then used and the results showed that there was a small yet detectable level of fluorescence in TN72-VFPpA transformants (Figure 4.8).

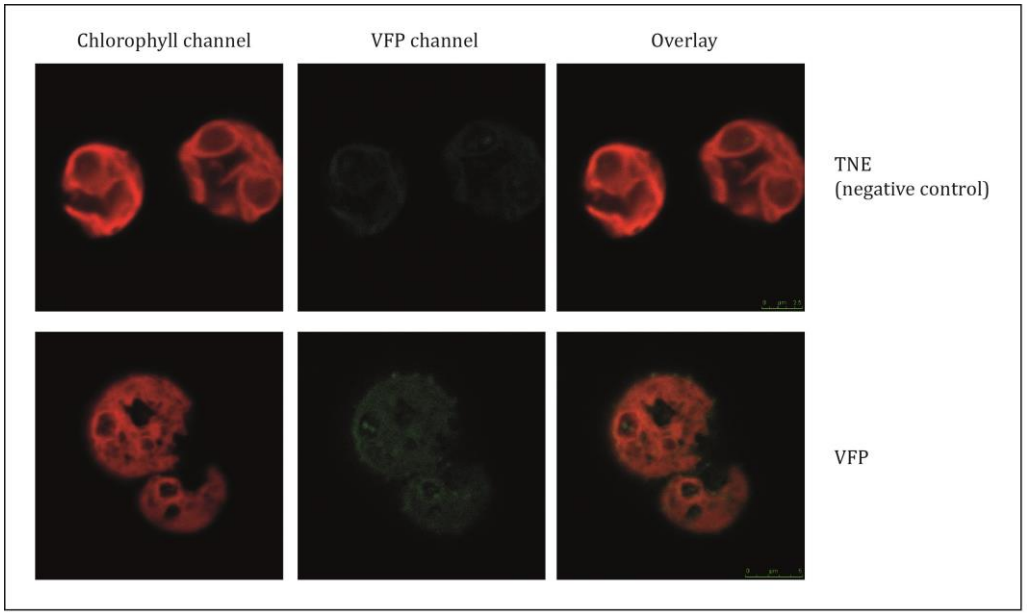

Figure 4.8 Fluorescent image of a VFP transformant generated using the pASapI.VFP plasmid, and TN72 transformed with the empty pASapI vector (TNE) as negative control, collected using a Leica TCS SP5 confocal microscope with objective 100X oil immersion lens. The excitation wavelength was 488 nm emission range, and detection bandwidth was 510 nm.

As observed in Figure 4.8, the VFP fluorescence detected superimposes the auto-fluorescence from the chloroplast due to chlorophyll abundance, showing that VFP is localised in the chloroplast, as expected.

Detection of fluorescence by confocal microscopy proved challenging due to the fragility of TN72 as a cell wall-deficient strain, giving a very short time frame for cells to be inspected. For this reason, it was decided to express *vfp* in a walled strain, and results of this are presented in the following section.

4.2.5 Transformation of Bst-same with pASapI.VFP

It was desirable to express VFP in a different host strain that possesses cell wall, in order to have a more robust strain for imaging purposes. The strain used for this goal is named Bst-same and it is designed to employ the same photosynthesis recovery strategy as TN72 (*psbH*-deficient) for generation of transformants (O'Connor et al., 1998).

Despite being a cell-walled strain, transformation was attempted using the glass beads method which is generally more suitable for cell wall-less strains (Kindle et al., 1991), since transformants can, nevertheless, be recovered at low frequency (S. Purton, personal communication).

Recovery of *vfp* transformants and confirmation of gene expression

A total of six colonies (BST-T1 to BST-T6) were recovered from ten plates. These lines were assessed by PCR screening for those containing *vfp*, following the strategy detailed in section 2.5.2.1. Figure 4.9 shows that there were four positive transformants, where it was possible to detect a 1.2 kb band corresponding to the transformed plastome. The absence of a 1.0 kb PCR product for the untransformed plastome (as seen for both the WT and Bst-same) indicated that the transformants were homoplasmic.

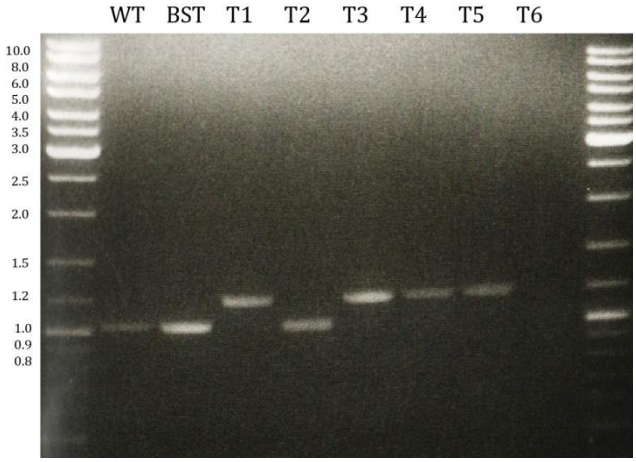

Figure 4.9 PCR analysis for Bst-same transformants expressing VFP transformed with the pASapI.VFP plasmid (BST-VFP) using FLANK1, atpA.R and MluR2 primers. Bands are as follows: wild-type (WT), Bst-same (BST) and failed transformant (T2) 1.0 kb; BST-VFP transformants (T1, T3-T5) 1.2 kb, T6 transformant showed no amplification due to poor DNA quality.

4.2.6 VFP accumulation in Bst-same

A representative transformant line from both the TN72 and Bst-same recipient strains was grown in mixotrophic condition and samples were collected at different time points of the culture lifespan throughout a period of 96 hours. Samples were prepared as explained in section 2.7.1 and loaded on a 15 % polyacrylamide gel together with a positive control (cell extract containing an HA-tagged protein of 40 kDa) to confirm antibody binding. ECL detection was used to visualise the result. Surprisingly, the BST-VFP transformant showed a considerably lower level of protein in comparison to the TN72-VFPpA transformants at the same cultivation stages (Figure 4.10).

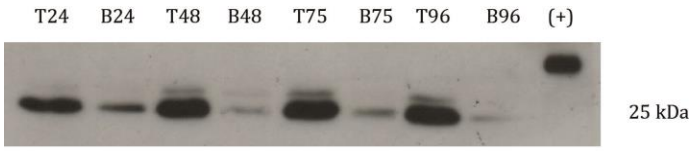

Figure 4.10 VFP accumulation in transformants generated using the pASapI.VFP plasmid in both cell hosts TN72 and Bst-same is demonstrated by Western blot analysis using anti-HA antibodies. Cultures were grown in 25 mL TAP medium flasks at 25 °C, 120 rpm and 150 µmol m^{-2} s^{-1}. Lanes indicate strain and time point as follows: T stands for TN72-VFP and B strands for BST-VFP; numbers stand for the time (in hours) at which the samples were harvested. (+) represents a highly expressed HA-tagged protein as positive labelling control.

Moreover, it was observed that the product generated in the BST-VFP line was less stable, with no detection of any band in samples harvested after 96 hours of cultivation. The reason behind this is most likely to be the presence of random mutations in the nuclear genome of Bst-same that could have accumulated over time, and this might affect chloroplast protein expression, a phenomenon that has been observed and reported in the literature (Bruick and Mayfield, 1999). It is known that many chloroplast genes are regulated in their expression by nuclear factors, including *atpA*, and mutations in such factors could affect *vfp* expression in the Bst-same host (Eberhard et al., 2011). Considering this result and the lack of fluorescence detected with flow cytometry and confocal microscopy, this strain was not studied further.

4.2.7 Conclusion

The expression of *vfp* under the control of the *atpA* promoter and 5' UTR produced homoplasmic transformants in both strains of *C. reinhardtii* transformed; however, VFP levels varied dramatically between the two strains, which were confirmed not only by the

Western blot analysis but also by the lack of fluorescence detected in BST-VFP transformants.

Fluorescence was assessed using flow cytometry, which proved to be a promising alternative for quick and easy fluorescence detection, giving a positive signal without the need to disrupt cells, which can be a key factor for rapid monitoring of fluorescence. Confocal microscopy provided qualitative evidence for fluorescence as well.

Additionally, fluorescence measurements demonstrated that the presence of the HA tag had no detrimental effect on protein stability and functionality; consequently, further studies and generation of new transformant lines in TN72 using other regulatory sequences were carried out using the HA-tagged VFP, as described in the next sections.

4.3 Expression of VFP under the control of the *psaA* promoter/5' UTR

It has been recently shown that higher levels of transgene expression in the *C. reinhardtii* chloroplast can be obtained when using the *psaA* promoter/5'UTR element to drive expression, as opposed to the *atpA* element (Michelet et al., 2011). Consequently, a new expression vector, pSRSapI, was developed in our lab by Dr. Rosie Young. This vector contains the 5' UTR and promoter of the exon 1 from the endogenous *psaA* gene, and a native copy of the *psbH* gene used to restore phototrophy in the Δ*psbH* recipient strain TN72. Similarly to pASapI, this vector can be digested appropriately with the restriction enzymes *Sap*I and *Sph*I for insertion of the foreign gene.

4.3.1 Construction of the plasmid pSRSapI.VFP

The plasmid pSRSapI.VFP was generated in the same manner as pASapI.VFP. Ligation of the *vfp* fragment (Figure 4.11 A) with the *Sap*I-*Sph*I digested pSRSapI vector (Figure 4.11 B) was carried out, generating the transformation plasmid pSRSapI.VFP (6988 bp) (Figure 4.11 C). The *vfp* region was sequenced to confirm there were no mutations introduced in any step. The plasmid was amplified in the *E. coli* strain DH5α and purified for transformation of TN72.

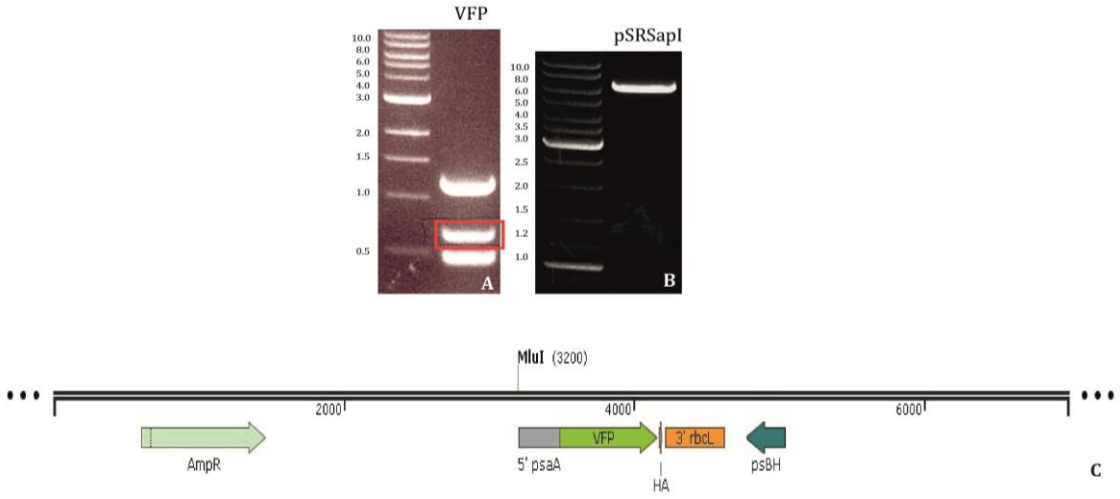

Figure 4.11 A) Gel electrophoresis result for the digested *vfp* fragment with enzymes *Sap*I and *Sph*I. Expected size is 0.72 kb, B) Gel electrophoresis result for the linearised pSRSapI vector. Expected size is 6.2 kb, C) Diagram of the pSRSapI.VFP plasmid developed for insertion of *vfp* into the chloroplast of the host strain TN72.

4.3.2 Transformation of TN72 with plasmid pSRSapI.VFP

Transformation of TN72 with the pSRSapI.VFP plasmid was carried out as described in section 2.6.2.1, using the glass beads vortexing method. Plates were incubated in bright light for 3 – 4 weeks until colonies appeared.

Recovery of *vfp* transformants and confirmation of gene expression

The transformation yield was nine colonies from ten plates. To identify transformants expressing *vfp* (TN72-VFPpS), the same PCR strategy described in section 2.5.2.1 was applied, but using a different primer set (primer sequences in Appendix 1). A band of ~ 1.2 kb was expected for *vfp* transformants, and this was obtained in all transformant lines. Figure 4.12 shows an example of four transformants assessed, in which all of them show the expected band characteristic of homoplasmic strains. Sequencing also confirmed that *vfp* had been recombined in the expected locus within the chloroplast genome.

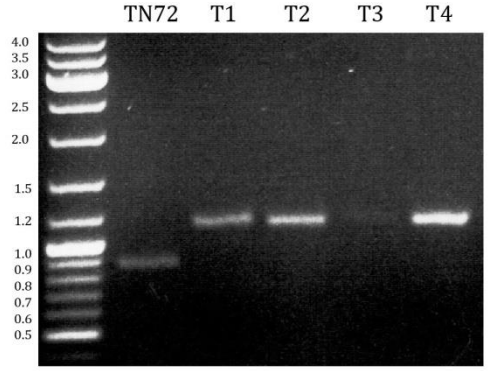

Figure 4.12 PCR analysis for TN72 transformants expressing *vfp* transformed with the pSRSapI.VFP plasmid (TN72-VFPpS) using FLANK1, rbcL.Fn and RY-psaR primers. Bands are as follows: TN72 0.85 kb, TN72-VFPpS transformants (T1, T2 and T4) 1.2 kb, T3 transformant showed weak amplification due to poor DNA quality.

4.3.3 VFP accumulation in TN72

For the assessment of VFP accumulation in TN72-VFPpS transformants, crude cell extracts from two transformants were run alongside that from a TN72-VFPpA transformant line in order to compare protein level between *psaA* and *atpA* elements used to drive expression. Samples were prepared as explained in section 2.7.1 and 10 µl of each were loaded on a 15 % polyacrylamide gel. ECL detection was used to visualise the result. As it can be observed in Figure 4.13, protein accumulation when using the *psaA* promoter and 5' UTR (T1 and T2) is significantly greater than when *vfp* is regulated by the *atpA* regulatory elements (pA). H1 is the control strain transformed with the empty pSRSapI vector.

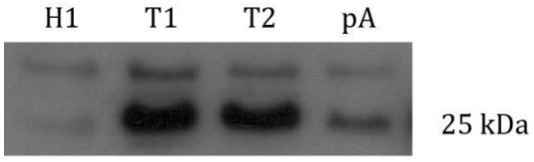

Figure 4.13 Accumulation of VFP in two transformants generated using the pSRSapI.VFP plasmid is demonstrated by Western blot analysis using anti-HA antibodies. Cultures were grown in 25 mL TAP medium flasks at 25 °C, 120 rpm and 150 µmol m^{-2} s^{-1}. Lanes are as follows: TN72 transformed with the empty pSRSapI vector (H1), two TN72 transformants expressing *vfp* driven by the *psaA* regulatory elements (T1, T2), and a TN72 transformant expressing *vfp* driven by the *atpA* regulatory elements (pA).

Both TN72-VFPpS lines showed equivalent amounts of protein accumulation, and it is estimated that this protein level is approximately 10 times higher than the level of protein accumulated in TN72-VFPpA. Improved levels of expression using the *psaA* element have also been observed in our group for other recombinant proteins (Dr Rosie Young, personal

communication), and this result is in agreement with what has been previously observed by Michelet et al. (2011).

Fluorescence detection in transformants

Since confocal microscopy can only be used for qualitative purposes, fluorescence was measured by means of flow cytometry only, and this data was compared to the values obtained for TN72-VFPpA transformants. Figure 4.14 shows the histograms and overlay of fluorescence for TN72-VFPpS (top right panel) compared to its control strain H1 (top left panel). In this case, there was a shift in fluorescence signal of 35.98 ± 0.71 % (n=4) with respect to the negative control, which correlates with the higher level of protein detected in the Western blot. This higher fluorescence signal can be noted in the overlay plot (bottom panel), where it can be observed that the fluorescence peak for TN72-VFPpS (blue curve) has less area overlapped with the fluorescence peak of H1 (green curve).

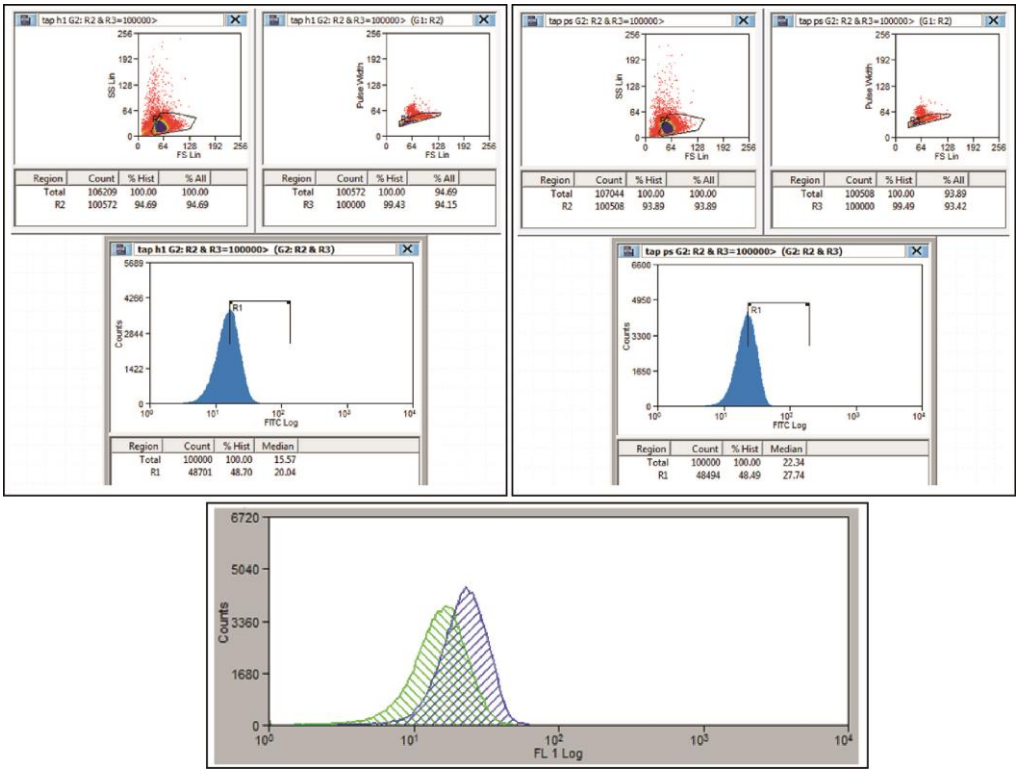

Figure 4.14 Histograms of fluorescence emission at 510-550 nm of a VFP transformant generated using the pSRSapI.VFP plasmid (top right panel) and TN72 transformed with the empty pSRSapI vector (H1) as negative control (top left panel), at the same growth conditions (TAP medium at 25 °C, 120 rpm and 150 µmol m^{-2} s^{-1}). In the histograms, fluorescence intensity is plotted on the x axis and cell count plotted on the y axis. The bar on the histograms represents 50 % of the population. The overlay plot (bottom panel) shows the shift in fluorescence: green curve (negative control), blue curve (VFP transformant).

4.3.4 Conclusion

Expression of VFP under the control of the *psaA* promoter and 5' UTR gave a higher level of protein accumulation, as it was observed by immunodetection. This suggests that *psaA* is a stronger promoter than *atpA* or that translation initiation is more efficient with the *psaA* 5'UTR. This increased level of protein provides a higher signal in fluorescence, as detected by flow cytometry, which makes this strain more suitable than TN72-VFPpA for monitoring recombinant protein expression.

4.4 Expression of VFP co-expressed with a bacterial chaperone

A different strategy to test if the VFP level could be increased was to express *vfp* along with a chaperone protein. Protein levels can be affected by many factors, and when expressing a recombinant protein it is very difficult to envisage whether it will be folded properly, active, stable, or form protein aggregates and be degraded. To overcome most of these issues, the so-called chaperone proteins can be found in most organisms assisting in several ways: supporting the folding of new or denatured proteins; providing folding intermediates so proteins do not aggregate; as mediators for the assembly/disassembly of protein complexes; helping in protein translocation across membranes; and inducing unfoldable proteins into protein degradation (Nordhues et al., 2010). There are five major groups of chaperones (Hsp100, Hsp90, Hsp70, Hsp60, and small Hsps, and their co-chaperones) that are classified based on their molecular mass, and the chloroplast of *C. reinhardtii* contains at least one member from each group (Nordhues et al., 2010). Each of these chaperones seems to have a specific task; therefore, it is unknown if they would provide any support to the stable accumulation of a foreign protein such as VFP.

A bacterial chaperone has been recently described in literature. This chaperone is termed Spy and belongs to a new class of chaperones found in the periplasm of *E. coli* (Quan et al., 2011). This 15.9 kDa protein functions as an ATP-independent folding chaperone that prevents aggregation and helps in refolding unstable proteins, and it is highly induced by the presence of unstable proteins or unfolding environmental conditions. A synthetic gene encoding this protein was co-expressed with *vfp* in order to evaluate if Spy would aid in the folding and accumulation of VFP.

4.4.1 Construction of the plasmid pASapI.VFP.Spy

Previous work performed by Dr. Chloe Economou in the Purton group had generated a codon-optimised version of the Spy chaperone gene that matched the codon bias of the *C. reinhardtii* chloroplast. This gene was expressed in the chloroplast with an HA tag sequence added to the 3' end of the coding region and driven by the *psaA* regulatory elements. Western blot analysis by Dr Economou confirmed protein accumulation, but there was concern that the HA tag might inhibit the function of Spy (C. Economou, pers. comm.). Therefore, it was decided to use the Spy gene without the HA tag sequence and insert this into the pASapI.VFP plasmid upstream of *vfp*, in order to produce the plasmid pASapI.VFP.Spy (8006 bp), as illustrated in Figure 4.15.

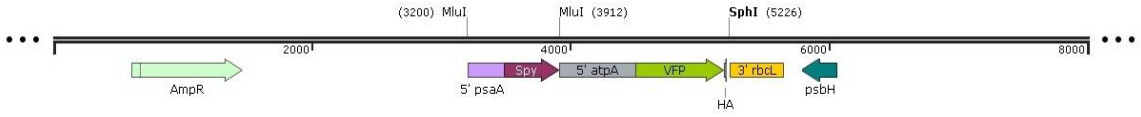

Figure 4.15 Diagram of the pASapI.VFP.Spy plasmid developed for insertion of the Spy chaperone gene co-expressed with *vfp* into the TN72 chloroplast.

4.4.2 Transformation of TN72 with plasmid pASapI.VFP.Spy

Transformation was performed using the glass beads method and transformant colonies were recovered after 3 – 4 weeks. PCR screening performed by Dr Economou confirmed insertion of *Spy* and *vfp* into TN72 and transformant colonies (TN72-VFPSpy) were also successfully checked for homoplasmy.

4.4.3 VFP accumulation in TN72

In order to assess the accumulation of VFP in this new genetic background, a Western blot was carried out alongside the previously developed strains TN72-VFPpA and TN72-VFPpS. Samples were prepared as explained in section 2.7.1 and 10 µL of each sample were loaded per well. As it can be observed in Figure 4.16, VFP level in TN72-VFPSpy is significantly higher than in TN72-VFPpA. This could be due to the activity of the Spy chaperone, since VFP is under the control of the same *atpA* element in both strains; however, it cannot be ruled out that the *psaA* element driving S*py* expression could also be up-regulating the downstream *vfp* gene, since both genes are transcribed in the same

direction (Figure 4.15). Further work is therefore required to test this. For example, a new transformant line could be produced in which the *spy* gene is in the opposite orientation to *vfp*.

However, when comparing the protein level in TN72-VFPSpy to TN72-VFPpS, a higher level is seen in the latter strain, which is attributed to the stronger activity of the promoter and 5' UTR of *psaA*, as observed in Figure 4.13, and suggests that the rate of synthesis rather than stable folding of VFP is the key factor affecting the steady-state level in transformants.

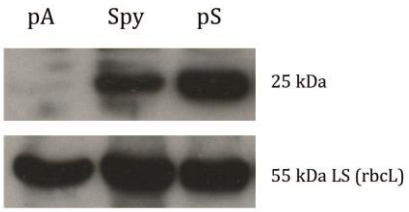

Figure 4.16 Comparison of the expression of VFP in transformants generated by transformation of TN72 with plasmids pASapI.VFP (pA), pASapI.VFP.Spy (Spy) and pSRSapI.VFP (pS) using anti-HA antibodies. Cultures were grown in 25 mL TAP medium flasks at 25 °C, 120 rpm and 150 µmol m^{-2} s^{-1}. The lower lane is the loading control using antibodies against the large subunit of RuBisCo (LS).

Fluorescence detection in transformants

The fluorescence measurement was carried out using TNE as the negative control. Figure 4.17 shows the flow cytometry result for TN72-VFPSpy (top right panel) compared to TNE (top left panel), obtaining a shift in fluorescence of 22.30 ± 2.62 % (n=4). This value is slightly higher than the fluorescence shift detected in the strain TN72-VFPpA without the chaperone (19.17 %), which is in agreement with a higher level of protein accumulated.

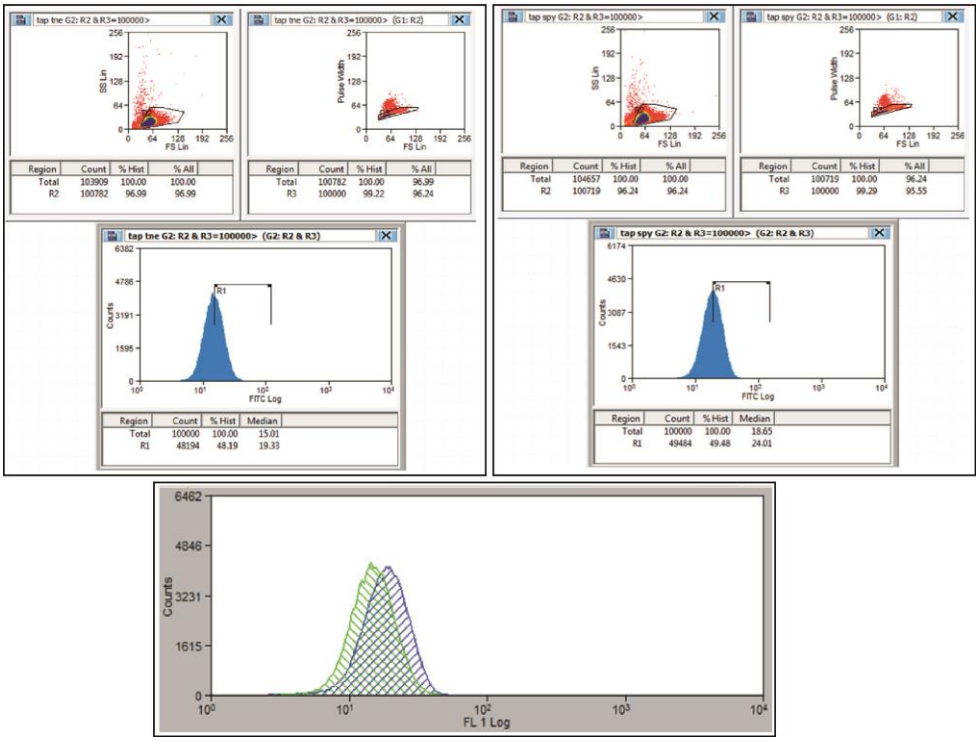

Figure 4.17 Histograms of fluorescence emission at 510-550 nm of a VFP transformant generated using the pASapI.VFP.Spy plasmid (top right panel) and TN72 transformed with the empty pASapI vector (TNE) as negative control (top left panel), at the same growth conditions (TAP medium at 25 °C, 120 rpm and 150 µmol m^{-2} s^{-1}). In the histograms, fluorescence intensity is plotted on the x axis and cell count plotted on the y axis. The bar on the histograms represents 50 % of the population. The overlay plot (bottom) shows the shift in fluorescence: green curve (negative control), blue curve (VFP transformant).

4.4.4 Conclusion

The insertion of the Spy chaperone along with *vfp* produced a positive effect on the accumulation and/or stability of VFP, as can be clearly observed in the Western blot results. However, fluorescence increased only by 16 % in comparison to the fluorescence detected in TN72-VFPpA, which does not correlate proportionally with the protein levels detected in Western blot.

Nevertheless, from these experiments it can be stated that the co-expression of a chaperone such as Spy does provide a positive effect on the level of recombinant protein detected in the chloroplast of *C. reinhardtii*. This result, together with the data reported for this chaperone (Quan et al., 2011), show the potential of this chaperone for the synthesis and accumulation of other recombinant proteins expressed in the chloroplast that might be less stable.

4.5 Expression of a RuBisCo-VFP fusion plasmid in *C. reinhardtii*

The final strategy considered for increasing the level of VFP was to fuse *vfp* to an endogenous gene that is normally expressed to high levels. The ribulose-1,5-bisphosphate carboxylase/oxygenase (RuBisCo) is the key enzyme in CO_2 fixation and the most abundant protein in the chloroplast. It catalyzes the carboxylation of ribulose-1,5-bisphosphate, generating two molecules of 3-phosphoglycerate, which is the first step in the Calvin cycle. RuBisCo is a hexadecamer protein complex composed of eight large subunits (LS) that are encoded in the chloroplast genome (*rbcL*) and eight small subunits (SS) that are encoded by two adjacent genes in the nuclear genome (*RBCS1* and *RBCS2)* (Wostrikoff and Stern, 2009).

Recombinant fusion or chimeric proteins are artificial constructs developed by joining the coding sequences of two or more genes encoding separate proteins that can come from different sources. This approach has been widely used in recent years for the expression of proteins with therapeutic purposes, particularly in monoclonal antibody development (Chen et al., 2013), and also to tag proteins of interest with fluorescent proteins (Snapp, 2005). A fusion protein in normally composed by a first protein sequence without a stop codon, which is linked to a second protein sequence in frame by a linker or spacer sequence, so that both proteins can fold properly as individual entities.

Considering the naturally high protein level of RuBisCo, it was predicted that creating a chimeric construct in which a recombinant protein is fused to the C-terminus of RuBisCo could maximise the steady-state level of the protein. Promising results for this approach have been reported by Muto el al. (2009), who expressed a luciferase fused to the RuBisCo LS. Based on this success, a fusion construct comprising *rbcL* and *vfp* was created by means of Gibson assembly and expressed in an *rbcL*-deficient mutant, as will be detailed in the following section.

4.5.1 Construction of the plasmid P266-rbcL-VFP

In order to create the *rbcL-vfp* fusion sequence, a plasmid (P-266, 6.6 kb) that already contained the *C. reinhardtii rbcL* was used as backbone vector for the generation of the transformation plasmid P266-rbcL-VFP. P-266 was developed in order to introduce the native *rbcL* in *rbcL*-deficient mutants. This plasmid contains a chloroplast DNA fragment of 3.8 kb containing the entire *rbcL* (Newman et al., 1991).

The *vfp* fragment was inserted into P-266 by means of Gibson assembly. This sophisticated technique, also known as one-step isothermal *in vitro* recombination, is widely used in synthetic biology nowadays to create large DNA molecules (Gibson et al., 2009, 2008). The principle of this method relies on the recombination of DNA fragments sharing terminal sequence overlaps as showed in Figure 4.18 (method detailed in section 2.5.10).

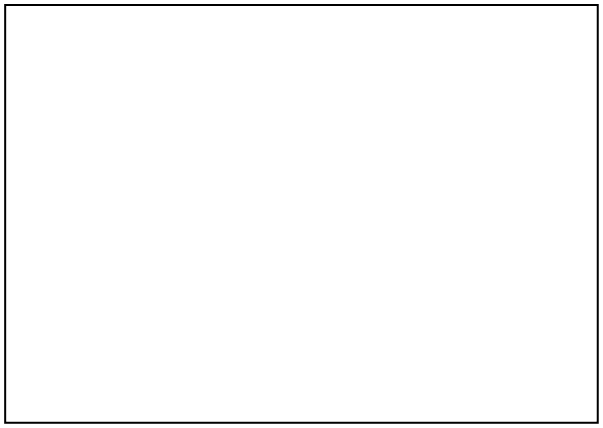

Figure 4.18 One-step isothermal *in vitro* recombination. Two adjacent DNA fragments (magenta and green) sharing terminal sequence overlaps (black) are joined into a covalently sealed molecule in a one-step isothermal reaction (replicated from Gibson et al., 2009).

In order to produce overlapping ends on each piece of DNA to be joined, long-tail primers were designed (Figure 4.19 A and B) (primer sequences in appendix 1). These primers include enough sequence (~ 20 nucleotides) to bind the existing DNA fragment plus an additional DNA sequence that creates the overlap section that will be used to anneal the two DNA fragments. The DNA regions that are part of the existing DNA are represented in Figure 4.19 A: *rbcL* (-TAA) and 3' UTR *rbcL* and in Figure 4.19 B: *vfp* (+TAA) and *vfp*. With this approach the resulting plasmid P266-rbcL-VFP contained *rbcL* without the stop codon, followed downstream by a flexible linker (GC linker), the *vfp* coding sequence, and the 3' UTR from *rbcL* (Figure 4.19 C). The linker is a glycine-serine rich sequence of 14 amino acids codon-optimised to the codon bias of the *C. reinhardtii* chloroplast. This GS-rich amino acid composition enhances the solubility of the linker, providing flexibility between the proteins and promoting their proper folding and functionality (Chen et al., 2013; Snapp, 2005).

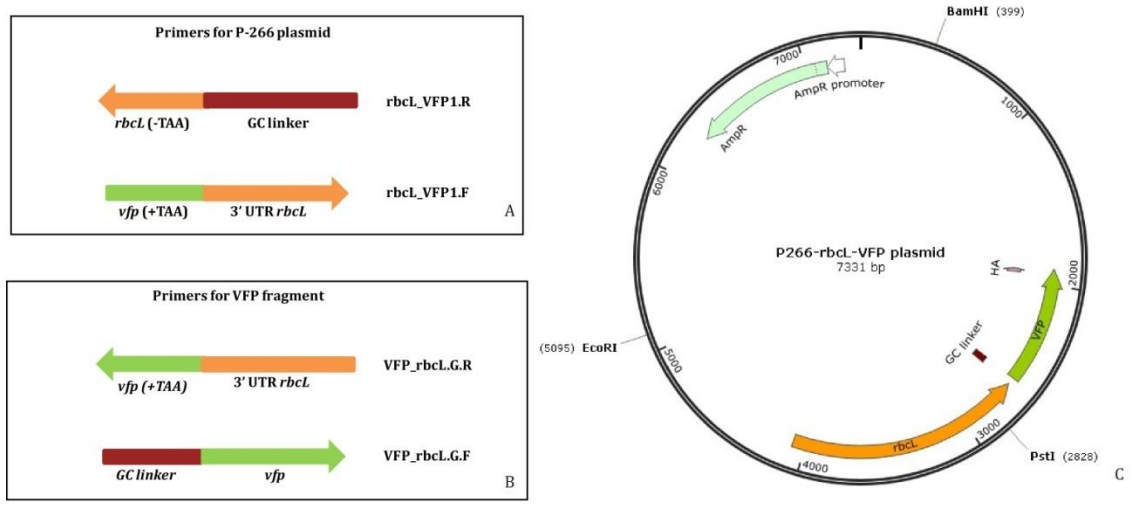

Figure 4.19 A) Long-tail primers designed for amplification of the P-266 plasmid containing the *rbcL* gene in order to generate the overlapping regions for Gibson assembly. B) Long-tail primers designed for amplification of the *vfp* fragment with the overlapping regions for base complemantation. C) Diagram of the P266-rbcL-VFP plasmid developed for insertion of the *rbcL-vfp* fusion into an *rbcL*-deficient strain of *Chlamydomonas reinhardtii*.

Figure 4.20 A shows the amplification of the whole P-266 plasmid using the long-tail primers designed, with a size of approximately 6.6 kb. Similarly, Figure 4.20 B shows the *vfp* fragment amplified from the original pMK plasmid using the long-tail primers, obtaining a DNA band of 0.75 kb. These two fragments were joined as explained in section 2.5.10 to form the 7.3 kb fusion plasmid, which was introduced into *E. coli* strain DH5α. Several colonies were recovered and the plasmid amplified was linearised using *Pst*I *(*Figure 4.20 C) and it can be observed that all of them, apart from transformant T5 (which is the same size as the P-266 plasmid) have the expected size.

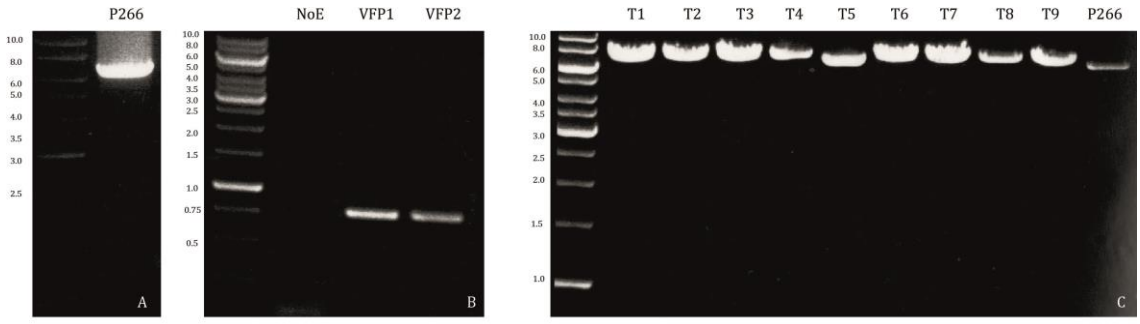

Figure 4.20 A) PCR of the P-266 plasmid using long-tail primers, band size 6.6 kb, B) PCR of *vfp* using long-tail primers, band size 0.75 kb, lanes in gel are negative control without enzyme (NoE) and two dilutions of the pMK plasmid containing *vfp* used as DNA template (VFP1, VFP2), C) Gel electrophoresis of the *Pst*I-digested P266-rbcL-VFP plasmid recovered from *E. coli* transformants. Lanes are: T1-T4 and T6-T9 for positive transformants (band size 7.3 kb), P266 for the original P-266 plasmid (band size 6.6 kb), and T5 for a transformant that exhibits the same band size as P-266.

Finally, sequencing and BLAST analysis of the P266-rbcL-VFP plasmid from three of these transformants confirmed a flawless assembly, and the ExPASy protein analysis platform confirmed that there were no frameshifts between the *rbcL* and *vfp* parts of the fusion.

As explained in section 4.5, RuBisCo comprises eight large subunits and eight small subunits, and each of these large subunits would be fused to a VFP molecule. Figure 4.21 shows a representation made with the PyMOL software of the crystal structure of a section of the expected fusion protein, including one large subunit (green), one small subunit (pink), the flexi-linker (red) and VFP (yellow).

The crystal structure of *C. reinhardtii* RuBisCo was available in the protein structure database (PDB code 1GK8). However, since there is no crystal structure available for VFP, the crystal structure of a green fluorescent protein (PDB code 4DXM) with the highest sequence homology available (80 %) was used for design purposes. The GS-rich linker was built as a mixture of α-helices and parallel β-sheets.

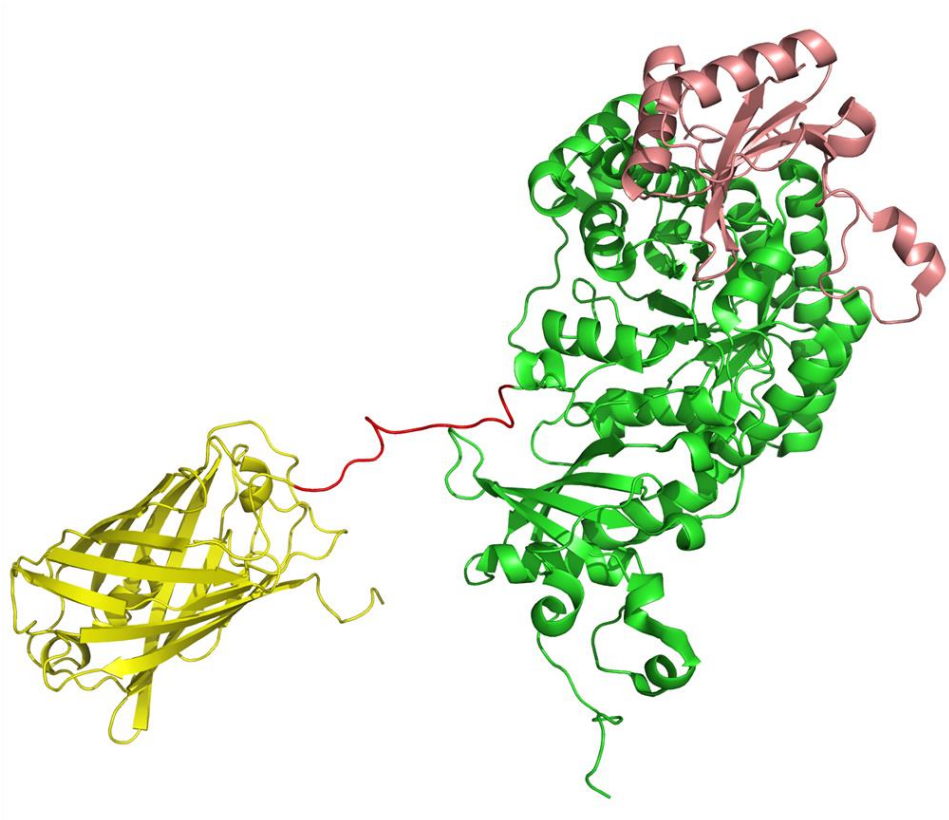

Figure 4.21 Representation of the rbcL-VFP fusion protein based on one unit of RuBisCo shown as the large chain (green) and the small chain (pink). The C-terminus of the large subunit is fused to a GS-rich flexible linker (red), which is then fused to the N-terminus of VFP.

4.5.2 Transformation of an *rbcL*-deficient host with plasmid P266-rbcL-VFP

For expressing the fusion plasmid with no addition of antibiotic markers, it was required to use a RuBisCo mutant strain of *C. reinhardtii* that is unable to grow in phototrophic conditions, in which the defective *rbcL* could be replaced by the chimeric construct, using restored photosynthesis as driving force for selection, as used in the host TN72. Furthermore, such an approach would confirm that the addition of VFP to the LS of RuBisCo did not impair its activity.

The *C. reinhardtii* strain CC-2803 was selected for this purpose since it features a disrupted *rbcL* with a 0.48 kb insertion (Newman et al., 1991). PCR confirmed this insertion and spot tests in TAP and HSM media also demonstrated the inability of this strain to grow in light with no exogenous carbon source. However, several transformation attempts to restore the native *rbcL* using the original P-266 plasmid were unsuccessful, and no transformants with restored photosynthetic activity could be recovered. It was speculated that additional mutations related to photosynthesis had arisen in this mutant strain during its many years maintenance on acetate-containing medium. For this reason, it was decided to search for another *rbcL*-deficient strain since this step was crucial to test that the *rbcL*-mutant strain was able to restore photosynthesis before using it to test the expression of the fusion construct.

The *C. reinhardtii* strain CC-2653 was chosen for further studies and expression of the fusion construct. This strain possesses a point mutation on *rbcL* which stops LS accumulation. It was reported as host for the expression of an alcohol dehydrogenase with a construct containing the native *rbcL*, obtaining transformants expressing the enzyme and with restored photosynthesis (Chen and Melis, 2013).

4.5.2.1 Transformation of CC-2653 with P-266

In order to test that CC-2653 could restore photosynthetic competency by transformation with the P-266 plasmid, transformation was carried out using microparticle bombardment, commonly known as biolistics, due to the presence of cell wall in this strain and the lesser likelihood of obtaining transformants with the glass beads vortexing procedure.

Biolistics was first developed for chloroplast transformation over 25 years ago (Boynton et al., 1988). The procedure was carried out as explained in section 2.6.2.2, and plates were incubated in bright light for 3 – 4 weeks for the appearance of transformant colonies. The yield of transformation obtained was one colony from eight plates.

In parallel, CC-2653 was also transformed using the glass beads vortexing method and surprisingly, transformant colonies were also obtained and in higher amount than with biolistics. The transformation yield in this case was four colonies from 12 plates, and as observed in Figure 4.22, transformant lines (T1 and T2) with restored phototrophy grew normally in minimal medium.

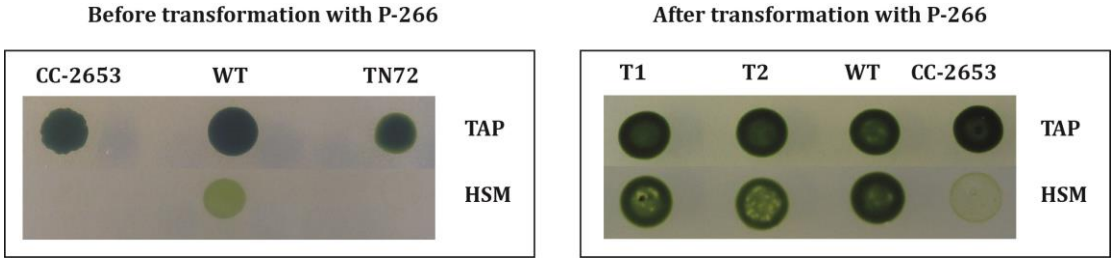

Figure 4.22 Spot tests of the *rbcL*-deficient strain CC-2653 before and after transformation with the P-266 plasmid containing the native *rbcL*. Strains were spotted in tris-acetate-phosphate medium (TAP) and high salt minimal medium (HSM). Control strains used are wild-type *C. reinhardtii* (WT) and TN72 as a non-photosynthetic strain. T1 and T2 are two transformants that integrated the native *rbcL* gene.

Sequencing confirmation of replacement of native *rbcL*

Since the *rbcL* disruption in CC-2653 is a point mutation, the generation of novel PCR products cannot be used for confirmation of transformants. Thus, the *rbcL* region from two transformants was therefore amplified by PCR with appropriate primers (primer sequences in appendix 1) and this DNA fragment was sequenced. Results from sequencing showed that both transformants had the native *rbcL* sequence with the point mutation restored. Figure 4.23 shows the alignment of one of these transformants, where the upper sequence corresponds to the native *rbcL* sequence, which is aligned to the *rbcL* sequence in CC-2653 and in one transformant. It can be clearly observed that the transformant has replaced the adenine by guanine, restoring in this manner the native *rbcL* sequence, which is in agreement with the phenotype observed in the spot tests.

Figure 4.23 Sequence alignment of *rbcL* as native sequence, in the *rbcL*-mutant CC-2653 and in one transformant with restored *rbcL* by transformation with the P-266 plasmid. The highlighted region shows the base replacement.

4.5.2.2 Transformation of CC-2653 with plasmid P266-rbcL-VFP

The fact that the glass beads vortexing method generated more transformants than biolistics for recombination with the P-266 plasmid encouraged its use for transformation of CC-2653 with the P266-rbcL-VFP plasmid. Transformation was performed using the glass beads method as detailed in section 2.6.2.1.

VFP-containing transformants recovery and confirmation of gene expression

The transformation yield obtained was eight colonies from 36 plates. These transformants containing the *rbcL-vfp* fusion (CC-F) were assessed by PCR screening. Two sets of primers were used to analyse the presence of the fusion insert (Figure 4.24).

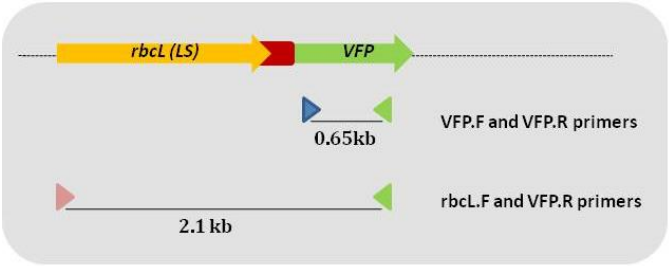

Figure 4.24 Set of primers used for screening of transformants of CC-2653 expressing the P266-rbcL-VFP plasmid.

As can be seen in Figure 4.25, three transformants gave a positive result for the presence of the *vfp* sequence (A) and for the *rbcL-vfp* fusion (B).

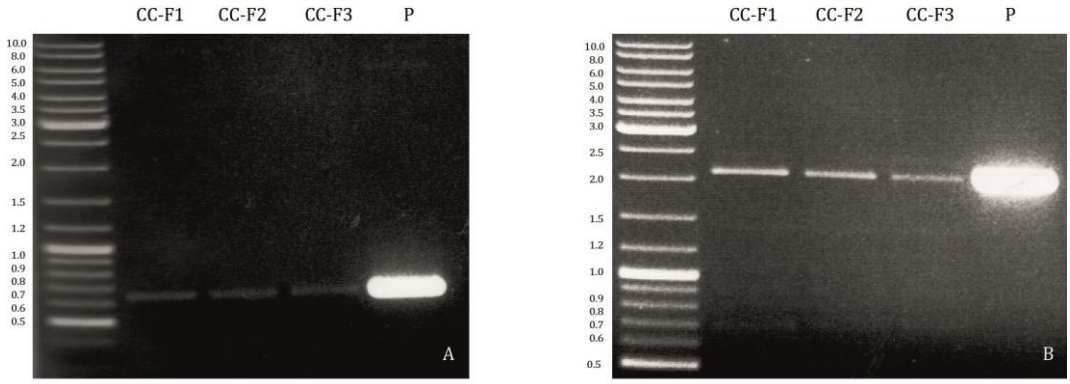

Figure 4.25 PCR analysis for CC-2653 transformed with the p266-rbcL-VFP plasmid (CC-F) using A) VFP primers, band 0.65 kb and B) rbcL.F and VFP.R primers, band 2.1 kb. Lanes in both images are three CC-F transformants (CC-F 1, 2, 3) and the p266-rbcL-VFP plasmid (P) as a control.

4.5.3 VFP accumulation in CC-F transformants

The expected size of the fusion protein is of approximately 83 kDa, comprising the 55 kDa of the LS of RuBisCo, the 1 kDa linker and the 27 kDa VFP. In order to test whether the fusion protein is accumulating in the chloroplast, samples were prepared for Western blot as before, and the membrane was probed with antibodies to the LS. As can be seen in Figure 4.26, the main protein detected shows the approximate size of the native large subunit (55 kDa). This protein is significantly reduced in the CC-2653 mutant as originally reported by Spreitzer et al. (1985), but is restored in both CC-F1 and CC-F2 with no evidence of the large fusion protein. When these same samples were assayed using the anti-HA antibody, there was no detection of any bands.

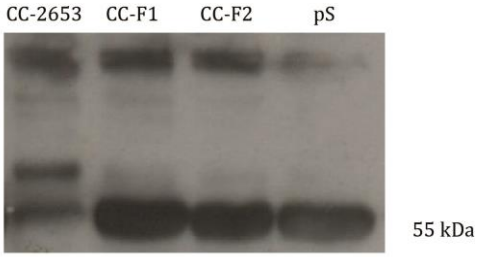

Figure 4.26 Western blot analysis of two transformants generated using the P266-rbcL-VFP plasmid using antibodies against the large subunit of RuBisCo (LS). Cultures were grown in 25 mL TAP medium flasks at 25 °C, 120 rpm and 150 µmol m^{-2} s^{-1}. Lanes are as follows: CC-2653 (empty host, which accumulates only approximately 10 % of the RuBisCo LS), two transformant lines (CC-F1 and 2), and pS (a TN72-VFPpS transformant) as a comparison of a strain with wild-type levels of LS.

A new Western blot analysis was carried out with fresh samples of CC-F transformants, including the other strains expressing *vfp* (TN72-VFPpA, TN72-VFPpS and TN72-VFPSpy), and this time the incubation was performed simultaneously with anti-LS and anti-HA antibodies (Figure 4.27). Once again, it was not possible to detect the expected fusion protein (82 kDa). The large subunit showed the native size in all strains (55 kDa). The 25 kDa band for VFP was observed in the three construct (pA, Spy, pS) but not in CC-F, providing more evidence for the lack of the fusion protein.

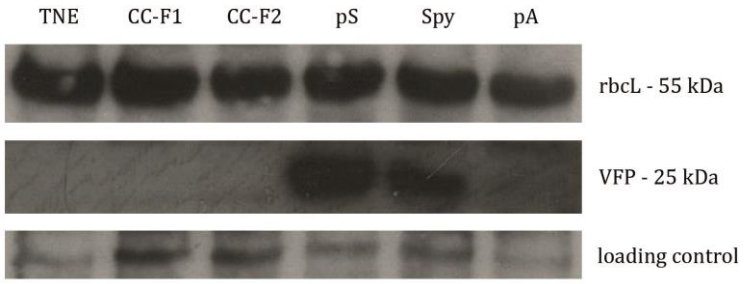

Figure 4.27 Western blot analysis using anti-LS (rbcL) and anti-HA (VFP) antibodies for the different strains expressing VFP. Cultures were grown in 25 mL TAP medium flasks at 25 °C, 120 rpm and 150 µmol m^{-2} s^{-1}. Lanes are as follows: TN72 transformed with the empty pASapI vector (TNE), two transformants of the P266-rbcL-VFP fusion plasmid (CC-F1 and CC-F2), VFP transformants generated using the plasmids pSRSapI.VFP (pS), pASapI.VFP.Spy (Spy) and pASapI.VFP (pA). All strains show approximately wild-type levels of LS, no detection of the fusion construct was observed. An unspecific band was used as loading control.

There are two possible explanations for this, based on the assumption that there could be a structural interference to RuBisCo by the VFP, preventing phototrophy. Firstly, it could be that the only transformants recovered are those in which a point mutation arises within the *rbcL-vfp* sequence during transformation, resulting in termination of translation close to the natural end of LS. However, all attempts to amplify this DNA region from transformants were largely unsuccessful, and it was not possible to produce DNA in sufficient amount for sequencing. A more plausible explanation is that transformation resulted in repair around the *rbcL* lesion in CC-2653 in some copies of the plastome within a cell and integration of the whole rbcL-vfp DNA in other copies, thus creating a heteroplasmic state. This would explain both the restoration of phototrophy and the presence of rbcL-vfp DNA in the initial transformant lines. This heteroplasmy would not have lasted for long under phototrophic selection so eventually these transformants would have lost the few copies containing the *rbcL-vfp* fusion sequence, which would explain why PCR carried out later on for sequencing purposes produced low amounts or no DNA for sequencing. This would also explain why the whole fusion protein could not be observed in Western blots.

Lastly, when samples of CC-F were assessed for fluorescence using flow cytometry no signal of fluorescence was detected.

4.5.4 Conclusion

Gibson assembly allowed the rapid and simple construction of an *rbcL-vfp* gene fusion in an 8 kb expression plasmid. This plasmid was successfully introduced in an *rbcL*-deficient host and it was possible to detect transformants containing the expected insertion in the plastome, and recovery of photosynthetic activity.

However, it was not possible to detect the expected fusion protein; in fact, all transformants were shown to accumulate wild-type levels of the large subunit of RuBisCo at its native size of ~ 55 kDa.

4.6 Concluding remarks

The objective of this research was to generate stable transformant lines of *Chlamydomonas reinhardtii* expressing a FP in the chloroplast that could be easily and quickly detected. Such strain would allow the study of different parameters of cultivation and their effect on recombinant protein accumulation and functionality.

Transformation of the chloroplast genome of *C. reinhardtii* is a reliable and effective method that can generate stable transformants within a few weeks, and the transformants described in this chapter incorporated *vfp* in the targeted locus and reached a homoplasmic state. The selection strategy based on photosynthetic recovery is attractive since it produces transformants that contain only the gene of interest as foreign DNA, without the use of selection markers such as antibiotic-resistance genes than can compromise the use of such lines in commercial applications, especially if it is aimed at producing recombinant proteins for human use.

It was observed that different promoters/5' UTR elements allow different levels of gene expression and protein accumulation, as reported in other studies (Barnes et al., 2005; Franklin and Mayfield, 2004; Michelet et al., 2011). In this case, a higher level of recombinant protein was achieved when the foreign gene was expressed under the

control of the *psaA* elements, instead of the *atpA* elements. It could also be observed that the co-expression of a bacterial chaperone appeared to enhance the protein level, and could therefore be valuable as a stabiliser of recombinant proteins in the algal chloroplast. The last strategy attempted with the aim of increasing recombinant protein expression was the fusion of the VFP to the highly abundant protein RuBisCo; however, it was not possible to detect the fusion construct despite the promising results when screening for positive transformant lines. It is speculated that the fusion of VFP onto the enzyme interfered with its activity and as such, the only transformants recovered were those in which the wild-type rbcL had been restored. Nevertheless, it might be possible to use this strategy for other recombinant proteins, as was demonstrated for luciferase (Muto et al., 2009) and an increase in the linker length might resolve problems of interference.

Flow cytometry has proven its usefulness as a sensitive method to detect fluorescence in whole cells, and showed that VFP fluorescence in a culture of *C. reinhardtii* can be easily measured at different stages of growth and after any perturbation or changes in culture conditions. This provides the opportunity to study protein expression using VFP as a reporter under different culture parameters such as temperature, media composition and lighting, which will be the subject of the following chapter.

CHAPTER 5

STUDY OF DIFFERENT CULTIVATION CONDITIONS FOR OPTIMISING CELL GROWTH AND PROTEIN PRODUCTION

5 STUDY OF DIFFERENT CULTIVATION CONDITIONS FOR OPTIMISING CELL GROWTH AND PROTEIN PRODUCTION

To successfully design and optimise a recombinant protein production system, it is crucial to study and characterise the behaviour of the particular strain under different culture conditions in order to assess its growth rate and protein productivity.

The main reasoning for using a fluorescent protein as the test recombinant protein relies on its suitability as an easily-detectable and quantifiable marker that can be measured *in situ*, avoiding lengthy and laborious procedures to detect protein concentration and functionality. This can be particularly useful when studying various cultivation parameters simultaneously.

The generation of different strains of *Chlamydomonas reinhardtii* that were able to express detectable amounts of the fluorescent protein VFP makes it possible to study the effect of different cultivation parameters such as media composition, light intensity and temperature on protein levels with the aim of determining optimised conditions for VFP expression and accumulation. This research intended to establish cultivation parameters that can be transferred to the expression of other recombinant proteins produced in the chloroplast, in which the final product would be a protein of commercial interest.

5.1 Selection of cultivation parameters

This section introduces the parameters chosen for the evaluation of cell growth and VFP accumulation in the three strains (TN72-VFPpA, TN72-VFPpS and TN72-VFPSpy) described in chapter 3 that showed good fluorescence and protein level. These parameters, which are temperature, media composition (cultivation mode) and light intensity, are evaluated in all three strains in order to study if any of these environmental factors has an effect on the regulatory sequences that each strain possesses.

Temperature and media composition were selected because there are few reports to date on the effect of these two factors on protein expression in microalgae. The temperatures studied were 25, 30 and 37 °C, with 25 °C as the standard condition.

Four different cultivation modes were tested, which involve the use of three different media: tris-acetate-phosphate (TAP), high salt minimal (HSM) and tris-minimal (TP) media. The cultivation modes were: 1) mixotrophic cultivation with TAP medium; 2) heterotrophic cultivation with TAP medium; 3) phototrophic cultivation with TP medium; and 4) phototrophic cultivation with HSM medium.

Light intensity was chosen taking into consideration the vast amount of data demonstrating the importance of this factor not only for cell growth but also for the induction of certain promoters and metabolic processes that can ultimately affect the expression of a recombinant protein (Bruick and Mayfield, 1999; Eberhard et al., 2011, 2002). Light intensity was set at 30 μmol m^{-2} s^{-1} for dim light, and 150 μmol m^{-2} s^{-1} for bright light.

Standard cultivation conditions used as control were mixotrophic cultivation in TAP medium with bright light at 25 °C.

5.2 Cultivation in different modes

As explained before, the different cultivation modes are mixotrophic cultivation (in short, TAP), heterotrophic cultivation (dTAP), phototrophic cultivation using TP medium (TP), and phototrophic cultivation using HSM (HSM).

Cultures of the three different strains, that for ease will be abbreviated as pA (TN72-VFPpA), pS (TN72-VFPpS) and Spy (TN72-VFPSpy), were cultured in these four modes at 25 °C and bright light. Heterotrophic cultures were wrapped in aluminium foil and placed in the same incubator as the other cultures. Cell growth was determined for each condition by measuring OD_{750} every 24 hours. Protein level was assessed by Western blot and an estimation of the recombinant protein level was determined using an HA-tagged standard protein of known concentration. Fluorescence was assessed by flow cytometry.

5.2.1 Growth rate

Cell density was measured as explained in section 2.3 and specific growth rate was calculated as detailed in section 2.4. The three strains expressing VFP (pA, Spy, pS), as well as the control strains TNE (for pA and Spy) and H1 (for pS), had matching growth rate in the standard cultivation condition (data presented in chapter 3). This same behaviour was observed in the other three cultivation modes; therefore, cultures of these five strains were treated as replicates for specific growth rate calculations, and once again it could be confirmed that the expression of the *vfp* gene had no detrimental effect on growth. Figure 5.1 shows the growth results, and as observed from the error bars (n=5), an almost identical growth curve was obtained from all five strains.

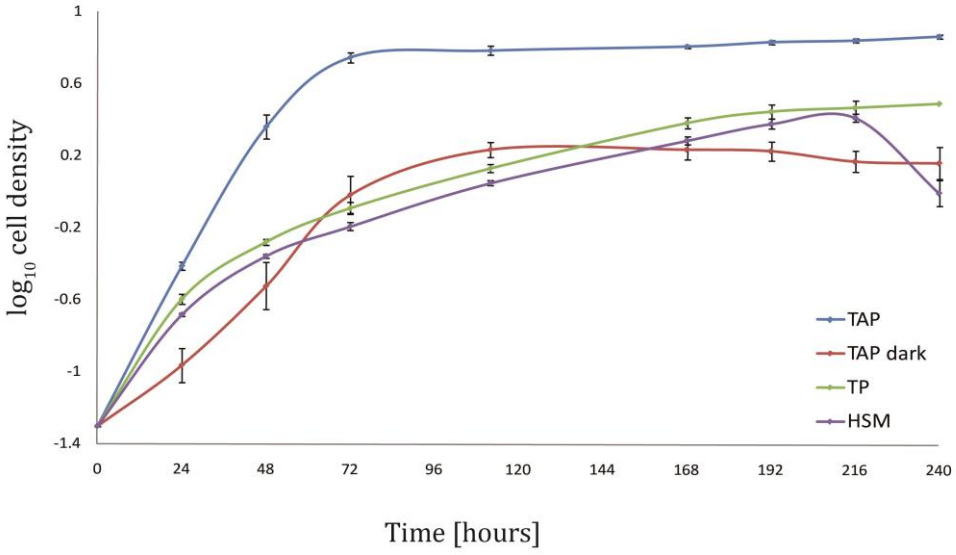

Figure 5.1 Comparison of cell growth of TN72 in different cultivation modes: mixotrophic cultivation in TAP (red), heterotrophic cultivation in TAP (blue), phototrophic cultivation in TP (purple), and phototrophic cultivation in HSM (green). Cultures were carried out in 25 mL shake flasks at 25° C, 150 µmol m^{-2} s^{-1} and 120 rpm. Initial cell density was OD_{750}=0.5. Cultures were run in quintuplicate and error bars represent the standard error (n=5).

Table 5.1 presents the values of specific growth rate, doubling time and maximum cell density (expressed as g L^{-1}) obtained for each condition. As can be observed, there is a notable difference in specific growth rate when growing *C. reinhardtii* in mixotrophic mode in comparison to any other cultivation condition. Maximum cell density achieved varies considerably as well, with up to five-fold difference in dry biomass concentration among the different cultivation modes evaluated. In terms of specific growth rate,

doubling time and dry biomass concentration, mixotrophic cultivation at 25 °C gives the highest values.

Table 5.1 Specific growth rate, doubling time and maximum cell density obtained for VFP-expressing strains under the different cultivation modes studied. Cells were grown in 25 mL flasks at 25 °C and 120 rpm of agitation in different media at 150 µmol m^{-2} s^{-1} of light intensity. Specific growth rate values are presented along with the standard deviation (n=5).

Cultivation mode	Specific growth rate [h^{-1}]	Doubling time [h]	Dry biomass concentration [g L^{-1}]
Mixotrophic (TAP)	0.064 ± 0.001	10.8	1.02
Heterotrophic (dTAP)	0.034 ± 0.001	20.4	0.2
Phototrophic in TP (TP)	0.030 ± 0.0003	23.3	0.33
Phototrophic in HSM (HSM)	0.029 ± 0.001	24.5	0.28

5.2.2 Western blot analysis and recombinant protein quantification

Protein accumulation was assessed by Western blot in order to determine if different cultivation conditions had an effect. Cultures of the pA strain in the four different conditions were set up and samples for Western blot were harvested at different stages of growth. Samples were prepared as explained in section 2.7.1 and loaded on a 15 % polyacrylamide gel. ECL detection was used to visualise the binding of the HA antibody. The result of this is presented in Figure 5.2, and as can be observed, VFP level remained constant throughout the culture growth. The heterotrophic condition gave a higher protein productivity (on a per cell basis), which can be explained by the inactivation of certain light-induced proteases present in the chloroplast (Purton, 2007). This phenomenon was also reported by Chen and Chen (2006).

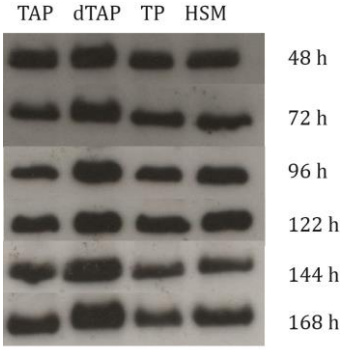

Figure 5.2 VFP accumulation in TN72 transformed with the pASapI.VFP plasmid at different stages of cultivation, indicated on the right side in hours. Cultures were grown in 25 mL shake flasks at 25 °C, 120 rpm and 150 µmol m^{-2} s^{-1} of light intensity in the four different cultivation modes tested: mixotrophic (TAP), heterotrophic (dTAP), phototrophic with TP minimal medium (TP), and phototrophic with HSM medium (HSM). Lanes were loaded with the same concentration of cell lysate. This panel represents the result observed in several western blots.

Taking into account this result and the unchanged level of VFP throughout the culture lifespan, samples of different strains were harvested at late exponential phase only (~ 96 h) for immunodetection, unless otherwise stated. VFP levels were also visualised for the other two strains (Spy and pS) and compared to pA in the four cultivation conditions tested, as observed in Figure 5.3. As it can be seen, the three strains in TAP showed the same VFP level profile presented in chapter 4, where pS exhibits the highest level of VFP, followed closely by Spy, and lastly by pA, with considerably less VFP accumulation. Cultures grown in the heterotrophic condition showed a higher protein accumulation in all strains which again can be explained by inactivation of the light-induced proteases. pS accumulates more protein than the other two strains in phototrophic conditions, which, as reported in chapter 4 in mixotrophic condition, could be accounted by the greater translation efficiency mediated by the *psaA* promoter/5'UTR element (Michelet et al., 2011). This Western blot showed particularly low VFP level for pA and Spy in phototrophic conditions, which, as observed in other Western blots presented in this chapter, is not generally that pronounced.

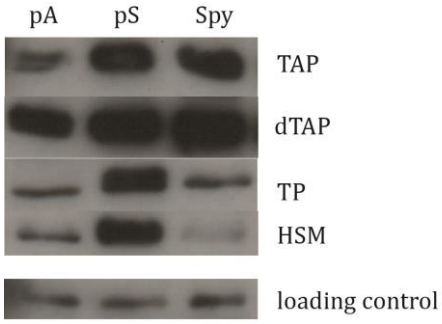

Figure 5.3 VFP accumulation in TN72 transformed with the pASapI.VFP (pA), pSRSapI.VFP (pS) and pASapI.VFP.Spy (Spy) plasmids. Cultures were grown in 25 mL shake flasks at 25 °C, 120 rpm and 150 µmol m^{-2} s^{-1} of light intensity in the four different cultivation modes tested: mixotrophic (TAP), heterotrophic (dTAP), phototrophic with TP medium (TP), and phototrophic with HSM medium (HSM). Samples were harvested during late exponential phase and lanes were loaded with the same amount of cell lysate. An unspecific band serves as loading control.

In order to quantify the VFP accumulation, a commercial HA-tagged protein named CARHSP1 (40 kDa) of known concentration was used, as detailed in section 2.7.5. This protein was loaded at three different concentrations per lane (50, 100 and 150 ng) and the intensity of the band was compared to the intensity of the bands obtained for the VFP cultures grown in different conditions (Figure 5.4).

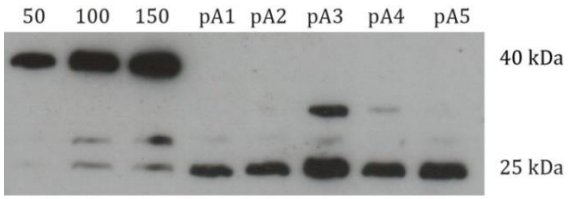

Figure 5.4 Estimation of protein concentration in cultures expressing VFP in TN72 transformed with the pASapI.VFP plasmid, using the standard protein CARHSP1 (40 kDa). Cultures were grown in 25 mL shake flasks at 25 °C, 120 rpm and 150 µmol m^{-2} s^{-1} of light intensity in the four cultivation modes studied. Samples, from left to right, are: CARHSP1 50/100/150 ng per well (50,100,150); two transformants grown in mixotrophic mode (pA1 and pA2); a transformant grown in heterotrophic mode (pA3); a transformant grown in phototrophic mode on TP (pA4); and a transformant grown in phototrophic mode on HSM (pA5). Samples were harvested in late exponential phase and lanes were loaded with the same concentration of cell lysate.

The protein concentration estimated for each cultivation condition is shown in Table 5.2. As observed, mixotrophy gives the highest protein concentration per volume of culture, reaching a concentration of 1.65 mg VFP L^{-1} culture. However, when taking into account the dry biomass produced per volume of culture in each cultivation condition, protein productivity varies and the highest yield is obtained in heterotrophic condition, with 3.3 mg VFP g^{-1} dry biomass.

Table 5.2 Values of protein concentration for VFP expressed in TN72 transformed with the pASapI.VFP plasmid (pA) and of overall VFP productivity in cultures grown in different cultivation modes.

Cultivation Mode	Protein production [mg protein L^{-1}]	Protein productivity [mg protein g^{-1} dry biomass]
Mixotrophic	1.65	1.62
Heterotrophic	0.66	3.30
Phototrophic in TP	0.63	1.91
Phototrophic in HSM	0.56	2.00

5.2.3 Flow cytometry

Fluorescence was assessed for the three strains grown under the four cultivation conditions. For each strain/mode of cultivation a specific control culture was used, involving the strain transformed with the respective empty vector (TNE for pASapI vector, or H1 for pSRSapI vector) and grown in the same cultivation condition. The fluorescence measurement was carried out at two stages of cultivation: late exponential phase (~ 75 h) and late stationary phase (~ 160 h).

The results obtained for the shift in fluorescence relative to the control are presented in Figure 5.5 for the samples taken at exponential phase, and in Figure 5.6 for the samples taken at stationary phase. Values obtained are an average of four independent measurements.

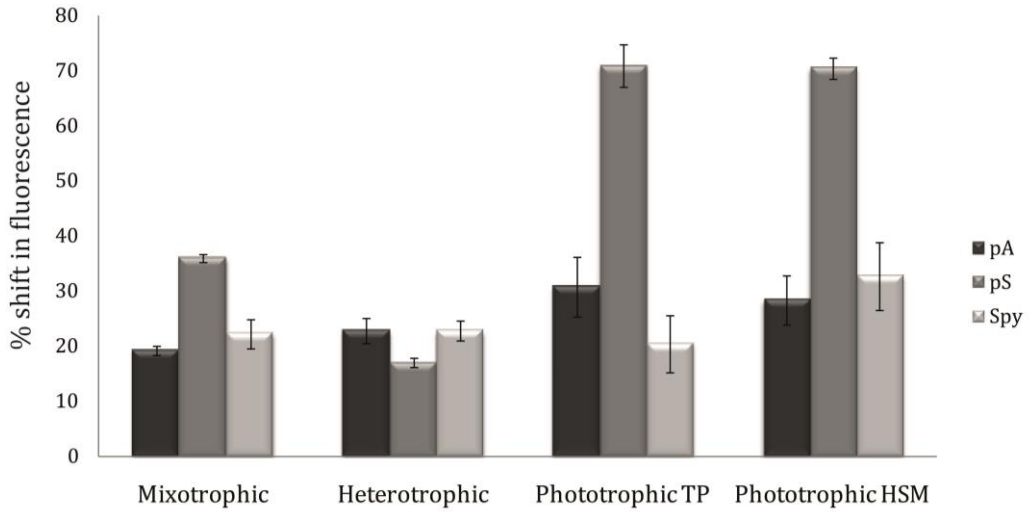

Figure 5.5 Fluorescence emission detected in the three strains developed for expression of VFP grown under four different cultivation conditions. Samples were harvested at late exponential phase of cultivation (75 hours). Values represent the shift in fluorescence in comparison to the respective control strain grown under the same condition. Error bars represent the standard error (n=4).

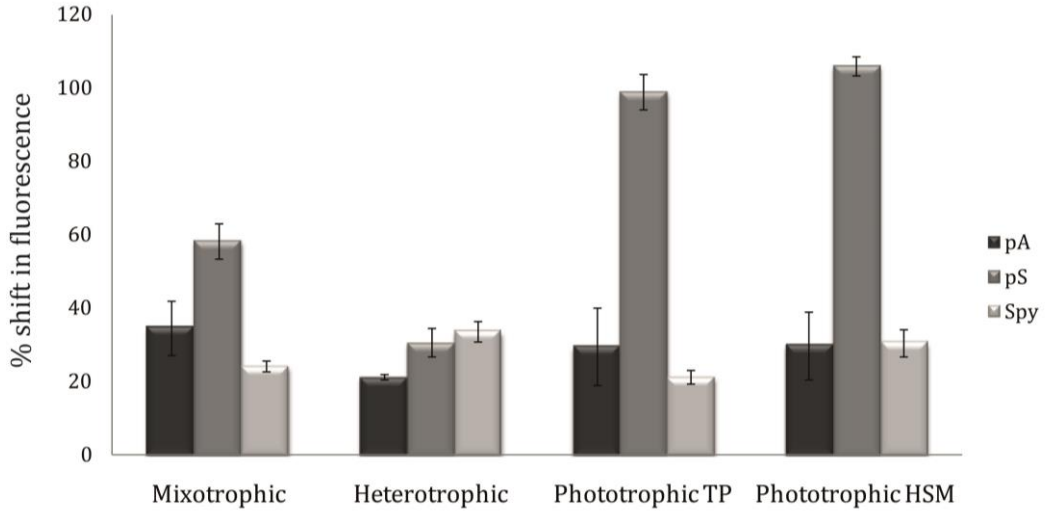

Figure 5.6 Fluorescence emission detected in the three strains developed for expression of VFP grown under four different cultivation conditions. Samples were harvested at late stationary phase of cultivation (160 hours). Values represent the shift in fluorescence in comparison to the respective control strain grown under the same condition. Error bars represent the standard error (n=4).

From the previous sets of graphs it can be inferred that pS gives the highest fluorescence emission in all cultivation conditions studied, with the exception of heterotrophic cultivation. This result is in agreement with the Western blot results presented in section 4.3.3, which showed that VFP has a higher expression level under the control of the *psaA* promoter. Additionally, it can be noted that the presence of light in the cultivation mode has a positive effect on the fluorescence emission, particularly in the case of phototrophic cultivation. This effect is more pronounced for the strain pS. It is not clear how a lower

protein level for pS in phototrophic condition can generate a higher level of fluorescence emitted, as opposed to the heterotrophic conditions that shows higher protein accumulation (as seen in Western blot results in Figure 5.3) but lower fluorescence. It is speculated that a better folding and post-translational creation of active chromophore could be involved in this increased fluorescence.

Fluorescence was also measured in the strain TN72-VFPpAX, which is the strain that was generated without the HA tag fused to *vfp* (refer to section 4.2.1). This strain was grown in the four cultivation conditions, and values of fluorescence matching the values obtained for the pA strain were detected. This confirmed that in all conditions studied VFP gives the same fluorescence regardless of the presence of the HA tag. The strain TN72-VFPpAX was not used for any further experiments.

5.2.4 Cell size measurement

The average cell size was evaluated in the pS transformant line at exponential stage and late stationary stage of cultivation when grown in different cultivation modes. This measurement was carried out since flow cytometry results suggested a different physiology of the samples tested. As observed in Figure 5.7, cells in earlier stage of cultivation have a very similar average size of approximately 6 μm, irrespective of the cultivation mode. This cell size distribution changes over time, as seen in Figure 5.8, where it can be observed that cells enlarged and the cultivation condition has a more pronounced effect. Cells grown in heterotrophic mode have the smallest increase in size; reaching an average size of almost 7 μm, while cells grown with light exhibit a slightly larger size of approximately 8 μm. These results reflect the higher availability of energy in cultivation conditions with light, which results not only in faster specific growth rate and higher cell density, but also larger cells.

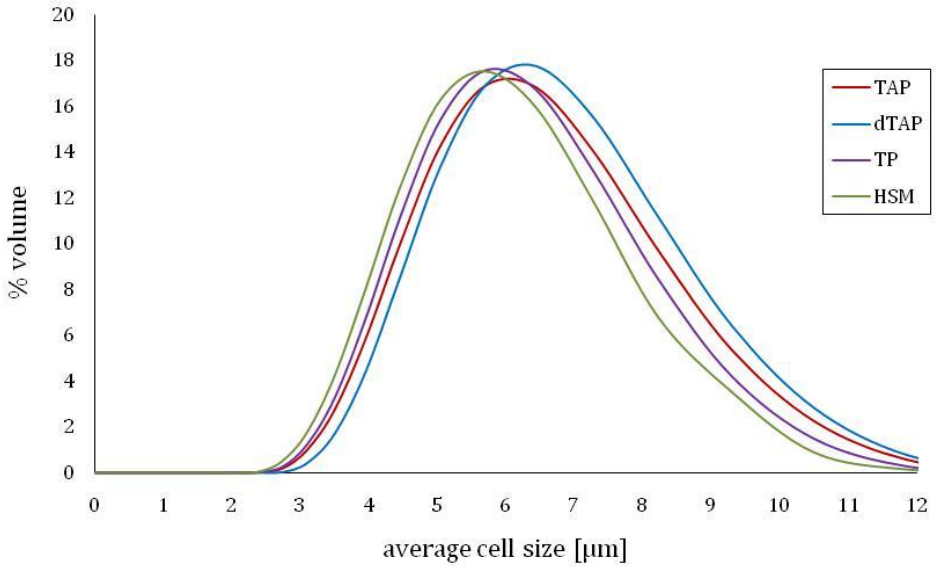

Figure 5.7 Average cell size distribution for cultures of *C. reinhardtii* grown in different cultivation modes. Samples were harvested at late exponential phase of cultivation (75 hours).

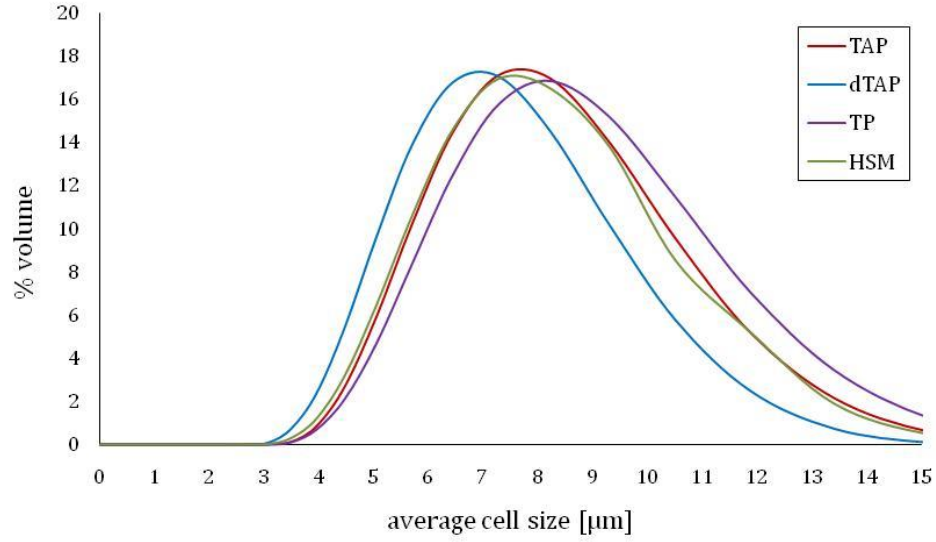

Figure 5.8 Average cell size distribution for cultures of *C. reinhardtii* grown in different cultivation modes. Samples were harvested at late stationary phase of cultivation (150 hours).

5.2.5 Conclusion

Growth rate and cell density were evaluated in the three strains developed that showed VFP accumulation and fluorescence under four different cultivation conditions. It could be observed that all strains (controls included) had matching values of specific growth rate

and maximum cell density for the same cultivation condition. The mixotrophic cultivation provided the highest value for biomass productivity, reaching 1.02 g biomass L^{-1} of culture.

In terms of protein accumulation, the heterotrophic condition gave the highest VFP level for all three strains which, as discussed previously, can be attributed to a lesser activity of light-induced proteases (Ramundo et al., 2014). This result was observed in Western blots and quantified using a standard protein of known concentration, obtaining a value of 3.3 mg protein g^{-1} dry biomass. However, biomass productivity is 5-fold lower in this condition, which indicates the need to produce more volume in order to achieve a good productivity. It was observed that the pS strain has higher level of VFP accumulation in all conditions tested, which provides more evidence of the stronger activity of the *psaA* promoter/5' UTR element and a protein accumulation that was around 10-fold higher than in pA.

Finally, fluorescence was detected in all strains and cultivation conditions analysed. It could be observed that fluorescence increased slightly over time, maintaining the trend in terms of the most fluorescent strain/condition. The pS strain gave the highest values of fluorescence, which correlates with higher levels of protein accumulation. For the other two strains pA and Spy, there was no major difference in fluorescence at the different cultivation conditions, and protein accumulation remained similar as well.

5.3 Cultivation at different temperatures

Two temperatures above the standard temperature of 25 °C were studied, prompted by growth test ('spot tests') showing that *Chlamydomonas* could grow faster at a higher temperature. Protein accumulation and fluorescence were measured in all four cultivation modes at 30 and 37 °C, and compared to the values obtained at 25 °C. Also, VFP was reported to mature at 37 °C (Ilagan et al., 2010), so it was desirable to assess if this higher temperature gives higher fluorescence due to more suitable conditions for the conformation of the chromophore.

5.3.1 Growth rate

Cultures of the three strains were grown under the four cultivation modes at 25, 30 and 37 °C, and cell density was monitored daily in order to calculate specific growth rate in each condition. These cultures were grown at a lower light intensity (30 μmol m^{-2} s^{-1}) due to the difficulty of changing temperature in incubators with higher light intensity. For this reason, specific growth rates of cultures at 25 °C presented in Table 5.3 are slower than the values reported in Table 5.1, which will be discussed in the corresponding section analysing the effect of light intensity (section 5.4.1).

Table 5.3 Specific growth rate obtained for VFP expressing strains grown at three different temperatures (25, 30 and 37 °C) in the different cultivation modes studied. Cells were grown in 25 mL flasks at 120 rpm of agitation and in different media and low light intensity (30 μmol m^{-2} s^{-1}). Specific growth rate values are an average of two independent experiments.

Cultivation mode	Specific growth rate [h^{-1}]		
	25 °C	**30 °C**	**37 °C**
Mixotrophic (TAP)	0.044	0.044	0.038
Heterotrophic (dTAP)	0.036	0.035	0.035
Phototrophic in TP (TP)	0.023	0.028	0.020
Phototrophic in HSM (HSM)	0.023	0.029	0.020

From this data it can be concluded that an increase of temperature to 30 °C provides a moderate benefit in terms of growth rate in phototrophic cultivation, but no improvement was detected in either mixotrophic or heterotrophic condition. Maximum cell density achieved remained the same as in cultures grown at 25 °C. Cultivation at 37 °C proved to be of no benefit, since both specific growth rate and, to a greater extent, maximum cell density dropped by a 70 % in mixotrophic condition.

It can be noted that specific growth rate in the heterotrophic mode remains the same, regardless of the temperature used. However, it is not clear how temperature and heterotrophy could benefit from each other. Maximum cell density was the same also, but its maximum value at all temperature values studied is very low (four-fold lower than the maximum cell density in mixotrophic condition at 25 °C); therefore, the heterotrophic

condition does not compete with the mixotrophic mode in terms of biomass produced per volume of culture.

5.3.2 Western blot analysis

The protein level was evaluated at all three temperatures and at all cultivation conditions for strain pA. Samples were harvested at late exponential phase and prepared as explained in section 2.7.1. Western blot analysis was carried out using anti-HA antibodies and the result can be observed in Figure 5.9. For hetero- and phototrophic conditions, the protein level accumulated (on a per cell basis) remained the same despite the temperature used for growth. Yet, for mixotrophic cultivation it was possible to observe an increase in protein accumulation as temperature increased.

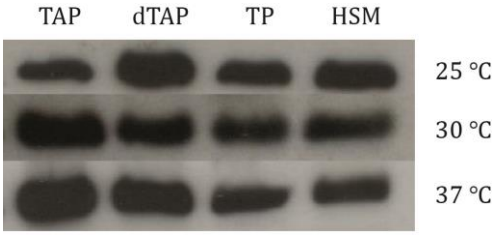

Figure 5.9 VFP accumulation in TN72 transformed with the pASapI.VFP plasmid (pA). Cultures were grown in 25 mL shake flasks at 25, 30 and 37 °C, 120 rpm and 30 µmol m^{-2} s^{-1} of light intensity in the four different cultivation modes tested: mixotrophic (TAP), heterotrophic (dTAP), phototrophic with TP minimal medium (TP), and phototrophic with HSM medium (HSM). Samples were harvested in late exponential phase and wells were loaded with the same concentration of cell lysate.

5.3.3 Flow cytometry

Fluorescence was measured in all strains grown in the four cultivation conditions at the three temperature values studied. Once again fluorescence was analysed in samples taken at late exponential (Figure 5.10) and late-stationary (Figure 5.11) stages of cultivation.

As observed in Figure 5.10, in all four cultivation conditions pS grown at 37 °C provided the highest value of fluorescence. This might indicate that the *psaA* promoter/5' UTR element, in addition to being light-inducible, could also be temperature-induced, showing increased expression at higher temperature. This phenomenon has been observed for other promoters in *Chlamydomonas*, such as the HSP70 promoter (Schroda et al., 2000); however, this protein is associated with the heat shock response. In strains pA and Spy, there were no major changes in the fluorescence emitted under the different cultivation

modes. The temperature value of 30 °C seems to be a peculiar condition for fluorescence emission, because it does not follow the trend that might be predicted between 25 to 37 °C. In many cases fluorescence emitted dropped slightly at this temperature and then increased at 37 °C. The reason behind this phenomenon is unknown and was not addressed further.

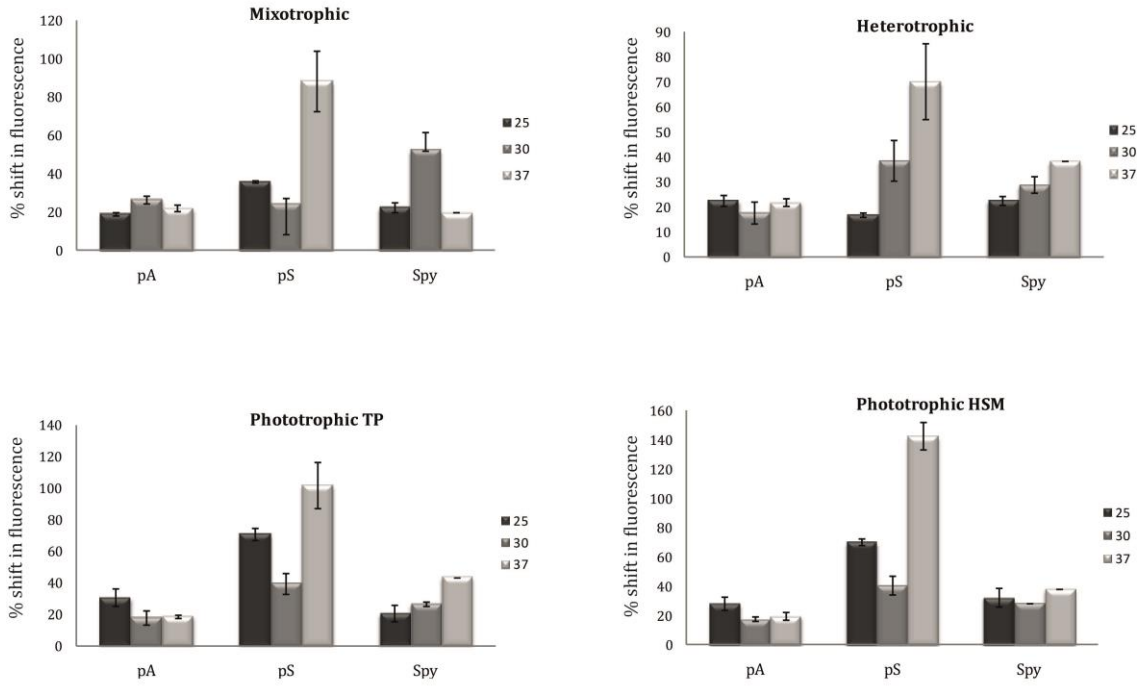

Figure 5.10 Fluorescence emission detected in the three strains developed for expression of VFP grown under four different cultivation modes at the three different temperatures studied. Samples were harvested at late exponential phase of cultivation (75 hours). Values represent the shift in fluorescence in comparison to the respective control strain grown under the same condition. Error bars represent the standard error (n=2).

The fluorescence emitted by the same set of cultures and conditions in late stationary phase, as shown in Figure 5.11, showed an even higher increase of up to five fold in fluorescence for pS at 37 °C, with the exception of the heterotrophic condition. For the remaining cultures, they seemed to handle better lower temperature, which was observed not only due to higher fluorescence at 25 °C for pA, but also considering the values of cell density. The same odd effect on fluorescence at 30 °C observed in exponential phase was observed in stationary phase, with reduced fluorescence in most conditions.

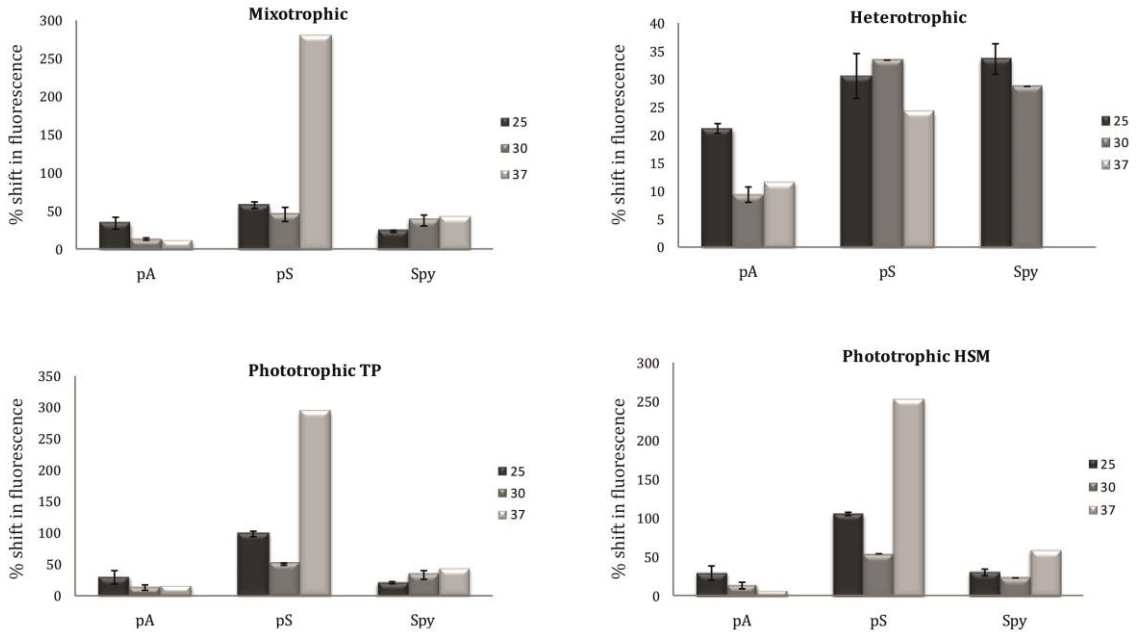

Figure 5.11 Fluorescence emission detected in the three strains developed for expression of VFP grown under four different cultivation modes at the three different temperatures studied. Samples were harvested at late stationary phase of cultivation (160 hours). Values represent the shift in fluorescence in comparison to the respective control strain grown under the same condition. Error bars represent the standard error (n=2). Bars missing mean that the culture was not viable at that time point.

5.3.4 Conclusion

Three temperature conditions were studied in terms of specific growth rate, cell density reached and protein accumulation. An increase from 25 to 30 °C showed no change in growth rate and cell density, except from the cultivation in phototrophic conditions, with an increase in specific growth rate of approximately 26 %. The protein level, as observed in Western blot, increased 3-4 folds in mixotrophic cultivation, and no improvement or decline was detected in the other cultivation conditions. The fluorescence measured remained unaltered at this temperature condition, with the exception of the strain pS. This result suggests that activity of the *psaA* promoter/5' UTR element is heat-sensitive. The lack of a Western blot analysis for this strain makes it impossible to correlate this result to a higher level of protein, but considering the increase in protein level detected for the pA strain, it is speculated that the same trend would be observed for pS.

In the case of a further increase to 37 °C, a decrease in both specific growth rate and maximum cell density was observed for most cultivation conditions. Protein accumulation only increased significantly under the mixotrophic condition, approximately a 5-fold increase when compared to protein levels detected at 25 °C. In the case of fluorescence, a

further increase was detected for the pS strain, particularly in cultivation conditions with light, which provides evidence of the heat and light induction of the *psaA* promoter/5' UTR element.

With this data it can be concluded that the best condition for accumulation of biomass and recombinant protein is mixotrophic cultivation at 30 °C using the 5' and UTR elements of *psaA* to control gene expression. Fluorescence values at this temperature, which represent the functionality of the protein, were either slightly lower or equivalent to the values obtained at both 25 and 37 °C, but this is a very protein-dependent measurement and would not necessarily account for the functionality of other proteins.

Regarding proper maturation of the chromophore of VFP, it is believed that this was not an issue because strains pA and Spy did not show consistently higher fluorescence values at 37 °C. Higher values of fluorescence at 37 °C for the pS strain are attributed to an effect of the *psaA* element activity rather than being a more suitable condition for the chromophore formation and, hence, protein stability.

5.4 Cultivation using different light conditions

As explained in the previous section, two different light intensities were used due to the light incubators available and this allowed for comparison of specific growth rate, cell density and protein accumulation. Additionally, due to higher protein accumulation in heterotrophic condition, a two-mode cultivation comprising a first stage of mixotrophic growth followed by heterotrophic cultivation was performed in order to assess protein accumulation in this regime.

5.4.1 Cultivation using different light intensities

The light intensities used were 150 μmol m^{-2} s^{-1} for bright light, and 30 μmol m^{-2} s^{-1} for dim light. Specific growth rate and maximum cell density were determined in both conditions for the four different cultivation modes used and results of these are presented in Table 5.4. It can be clearly noted that the light intensity has an effect on specific growth rate, with a 45 % increase in maximum growth rate for the mixotrophic condition, and a 30 % increase in the case of phototrophic condition using higher light intensity. Moreover,

maximum cell density also varies and with higher light intensity it is possible to reach twice as much biomass than with lower light intensity. This difference in biomass achieved is even more pronounced in phototrophic cultivation, where light and CO_2 are the only sources of energy available. It is noteworthy mentioning that the bright light condition used in these experiments is by no means a strong light condition that could harm cells or provoke photoinhibition (Janssen et al., 2000b).

Table 5.4 Specific growth rate and maximum cell density obtained for VFP expressing strains under the different cultivation modes studied using two different light intensities: 150 µmol m^{-2} s^{-1} for bright light, and 30 µmol m^{-2} s^{-1} for dim light. Cells were grown in 25 mL flasks at 25 °C and 120 rpm of agitation.

	Specific growth rate [h^{-1}]		Dry biomass concentration [g L^{-1}]	
Cultivation mode	**Bright light**	**Dim light**	**Bright light**	**Dim light**
Mixotrophic (TAP)	0.064	0.044	1.02	0.53
Heterotrophic (dTAP)	0.034	0.036	0.2	0.19
Phototrophic in TP (TP)	0.030	0.023	0.33	0.13
Phototrophic in HSM (HSM)	0.029	0.023	0.28	0.11

Western blot analysis

Protein accumulation was analysed by Western blot, and samples were prepared as explained in section 2.7.1. These were loaded on a 15 % polyacrylamide gel and ECL detection was used to visualise the binding of the HA antibody. The result can be observed in Figure 5.12, where there is no difference detected in protein level between the VFP level of cells grown in dim light (DL) against cells grown in bright light (BL), concluding that the effect of light is limited to growth. In the case of the *psaA* promoter/5' UTR, whose results presented previously accounted for it as a light-induced promoter, it was a matter of the presence of light and not the intensity of it that triggered its activity.

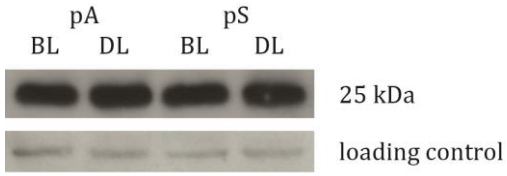

Figure 5.12 Accumulation of VFP in TN72 transformed with the pASapI.VFP (pA) and pSRSapI (pS) plasmids. Cultures were grown in 25 mL shake flasks at 25 °C, 120 rpm and different light intensities of 150 µmol m^{-2} s^{-1} (BL) and 30 µmol m^{-2} s^{-1} (DL). Lower band is an unspecific band serving as loading control.

5.4.2 Cultivation using mixed cultivation mode

As explained in previous section, it was observed that the VFP level obtained increased in heterotrophic conditions; however, cell density and specific growth rate were diminished. Taking these facts into consideration, it was decided to explore the accumulation of VFP by growing cells in a two-step cultivation strategy, involving a first stage in the mixotrophic condition, in order to achieve a higher cell density, followed by a second stage of heterotrophic growth during the stationary phase, with the aim of achieving higher protein accumulation.

Cultures were grown in duplicate for 96 hours in mixotrophic mode, and at this stage they reached an OD_{750}=6.4, which is three times higher than the OD achieved at this same stage under heterotrophic condition. At this point, one of the duplicates was wrapped in aluminium foil and from this point onwards, samples were taken periodically for Western blot analysis.

Western blot analysis

Strains that showed higher VFP accumulation (Spy and pS) were used for this experiment. Samples were harvested 40 hours after the light condition was changed and prepared as explained in section 2.7.1. ECL detection was used to visualise the binding of the HA and the rbcL (LS) antibodies. Figure 5.13 shows the VFP level accumulated by strains Spy and pS that were either left in mixotrophic cultivation during stationary phase (Spy/L and pS/L) or switched to heterotrophic mode at the stationary phase (Spy/D and pS/D). Anti-rbcL antibody was used as a loading control. It can be observed that the protein level was very similar between light and dark stationary phase for pS, whereas for Spy there seems to be an increase in protein accumulation when the culture is shifted to heterotrophic mode, which was observed previously in section 5.2.2.

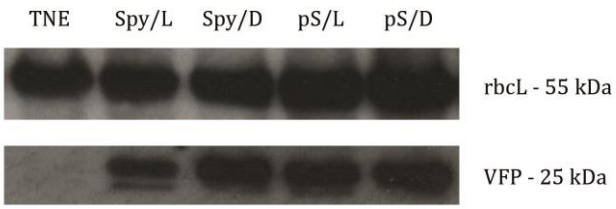

Figure 5.13 VFP accumulation in TN72 transformed with the pASapI.VFP.Spy (Spy) and pSRSapI (pS) plasmids. Cultures were grown in 25 mL shake flasks at 25 °C, 120 rpm and 150 µmol m^{-2} s^{-1} for 96 hours, and then either kept in mixotrophic mode (/L) or changed to heterotrophic mode (/D) for the next 40 hours, when cells were collected. The rbcL LS band serves as loading control.

Cultivation of each strain was carried out in the same conditions, but this time samples were harvested at different stages of cultivation to better assess the effect of light on VFP accumulation. Both Western blots were visualised using anti-HA antibodies and an unspecific band was used as a loading control. Figure 5.14 shows VFP accumulation at three different time points (128, 168 and 216 hours of cultivation) for the Spy strain. The first lane (96/L) represents VFP level at 96 hours of cultivation, stage in which one of the duplicate cultures was switched to heterotrophic condition. Cultures kept in mixotrophic condition (L) and cultures shifted to heterotrophic mode (D) exhibited a similar VFP level (25 kDa band), and cells harvested at 128 hours seem to have an equivalent amount of VFP. However, when taking into account the unspecific band detected for the two latter samples (168 and 216 hours), it seems that samples L had less amount of protein loaded per well. With this result, it is not possible to conclude a beneficial effect of darkness on protein synthesis or accumulation.

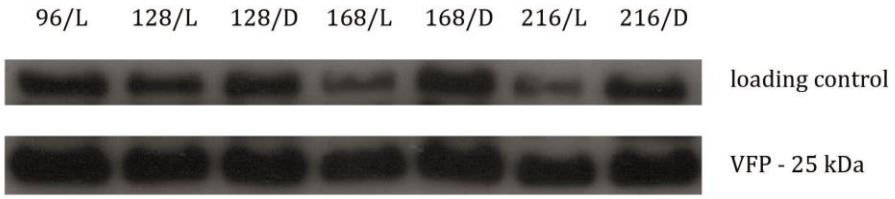

Figure 5.14 VFP accumulation in TN72 transformed with the pASapI.VFP.Spy (Spy) plasmid. Cultures were grown in 25 mL shake flasks at 25 °C, 120 rpm and 150 µmol m^{-2} s^{-1} for 96 hours, and then one duplicate was kept in mixotrophic mode (/L) and the other changed to heterotrophic mode (/D). Numbers represent time of the cultivation (hours) at which the cells were collected. Unspecific band serves as loading control.

Figure 5.15 shows VFP accumulation in pS and it can be observed that VFP accumulates the same level of protein throughout the culture lifespan and regardless of the cultivation mode, similar to what was observed in Figure 5.3 when comparing VFP accumulation in different cultivation modes. In this case, again samples L seem to have less protein loaded

per well (as observed in the loading control band), which would indicate that there is no benefit of shifting cultivation mode in stationary phase for protein accumulation.

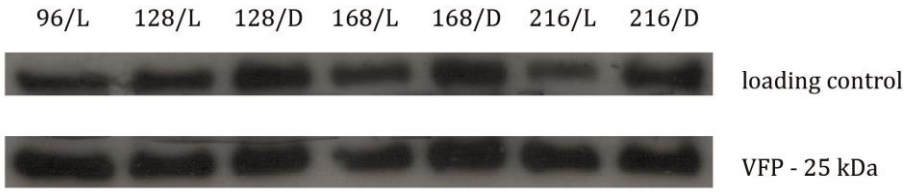

Figure 5.15 VFP accumulation in TN72 transformed with the pASapI.VFPpS (pS) plasmid. Cultures were grown in 25 mL shake flasks at 25 °C, 120 rpm and 150 µmol m^{-2} s^{-1} for 96 hours, and then one duplicate was kept in mixotrophic mode (/L) and the other changed to heterotrophic mode (/D). Numbers represent time of the cultivation (hours) at which the cells were harvested. Unspecific band serves as loading control.

5.4.3 Conclusion

By testing two different light intensities, it has been possible to observe that this parameter has an important effect on cell growth and cell density. When cultures were grown in bright light (150 µmol m^{-2} s^{-1}), a higher specific growth rate and cell density were achieved, and this was observed not only for phototrophic mode but for mixotrophic growth as well. Protein accumulation, however, remained unaltered.

When testing a two-stage cultivation mode, it was not possible to observe an increase in protein accumulation when cultures were switched to heterotrophic conditions in stationary phase. It is speculated that changing to heterotrophic cultivation half-way through the growth does not provide such a pronounced positive effect on protein level as when cultures are grown in heterotrophic mode from the beginning.

5.5 Improved cultivation conditions for the growth of a strain producing a therapeutic protein

As it has been detailed in this chapter, different cultivation parameters have been varied and studied with the aim of increasing recombinant protein levels in the chloroplast. The use of a fluorescent protein as a reporter has been successfully applied to detect changes in both protein accumulation and functionality under different cultivation conditions. With

all this data gathered, it has been possible to conclude that the highest VFP level was obtained in mixotrophic cultivation with bright light at 30 °C.

The major objective of determining optimised cultivation conditions for protein accumulation is to be able to replicate them when expressing heterologous proteins that can be of commercial interest. For this reason, we tested the best cultivation conditions that were established in this research for the cultivation of a strain of *C. reinhardtii* expressing an antibacterial agent (endolysin) of commercial interest in the chloroplast. The bacteriophage endolysin Cpl-1 (39 kDa) kills specifically *Streptococcus pneumoniae*, the most common cause of pneumonia worldwide, and transformant lines (TN72-Cpl1) developed by Dr Henry Taunt (2013) have been produced synthesising protein levels reaching 9 % TSP. Cpl-1 is expressed in TN72 under the control of the *psaA* regulatory elements, in the same manner as *vfp*.

TN72-Cpl1 was grown at the four different cultivation modes in bright light at 25 °C (TAP represents the standard condition normally used) and at 30 °C (optimised conditions), and samples were harvested for Western blot analysis. Samples were prepared as explained in section 2.7.1, and 10 µL were loaded per well. Since this protein accumulates to a higher level than VFP, it was possible to use a quantitative detection system based on infrared imaging (Odyssey infrared imaging system, Li-Cor); therefore, immunological detection was carried out as detailed in section 2.7.3, but the secondary antibody used was an anti-rabbit IRDye antibody. TNE was used as negative control and results of this can be observed in Figure 5.16.

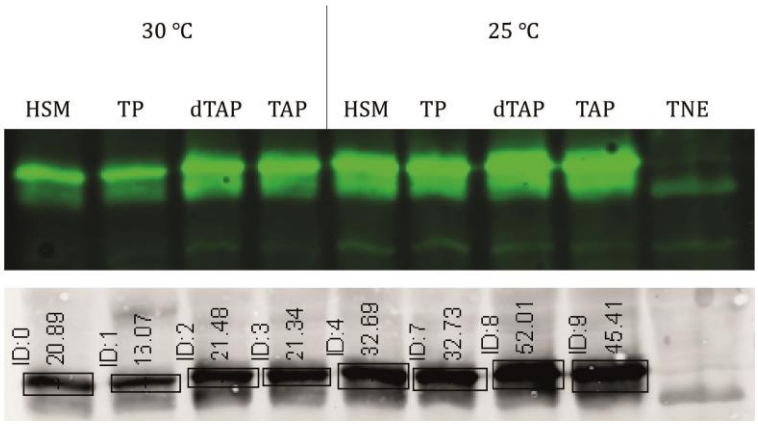

Figure 5.16 Accumulation of Cpl-1 endolysin in TN72 expressing the endolysin gene (TN72-Cpl1) grown in the four different cultivation modes. Cultures were grown in 25 mL shake flasks at 25 and 30 °C, 120 rpm and 150 µmol m^{-2} s^{-1}. Unspecific band serves as loading control. Bottom gel shows the quantification values according to band intensity.

The upper image (green) shows the protein accumulation in all conditions studied, and it can be seen that this particular protein accumulates to a higher extend at 25 °C, for all cultivation modes studied. The lower image (grey) shows the same result but with quantification of the band intensity which allows for a more precise comparison of protein levels. With this values, it can be concluded that at 25 °C Cpl-1 is accumulated in greater amount in heterotrophic condition, which is followed by the mixotrophic mode, and lastly, in equal measure, by both phototrophic conditions. At 30 °C the same trend is observed; however, protein levels are lower in all conditions. This particular protein has the highest yield in mixotrophic cultivation at 25 °C, not at 30 °C as it was expected.

This case study shows that the optimised cultivation conditions determined for VFP cannot be extrapolated directly to the expression and accumulation of other proteins. In the case of Cpl-1, it was expected that a higher level of protein would be achieved at higher temperature since this protein has been routinely produced in *E. coli* (Loeffler and Fischetti, 2003), however, this was not observed. Similar results were obtained by Dr Rosie Young (unpublished data, Purton group), where TN72-Cpl1 was grown at 25 °C and 35 °C, and again there was more protein detected at 25°C. It is speculated that some temperature-induced proteases could be targeting this protein. The fact that this decrease was not observed for VFP could account for its stability as a protein.

5.6 Concluding remarks

This chapter shows the use of a well-expressed fluorescent protein in the chloroplast of *C. reinhardtii* as a reporter to study different cultivation conditions and their effect in protein accumulation and functionality. This approach merges both cell engineering and bioprocess optimisation of a strain of algae widely used in research and has the potential to be applied to other recombinant proteins expressed in *C. reinhardtii* that can be fused to a fluorescent protein.

The study of different cultivation conditions allowed determining the impact of different parameters such as cultivation mode, temperature and light intensity on cell growth, cell density and very importantly protein expression. It could be observed that a much higher cell density – three-fold increase – can be achieved using mixotrophic growth, in comparison to the phototrophic and heterotrophic conditions, a phenomenon that has

been previously estimated (Boyle and Morgan, 2009). On the other hand, protein expression appears to be favoured under heterotrophic mode in TAP medium, suggesting changes in the metabolic pathways in the chloroplast and use of the carbon source in greater proportion for protein synthesis. The mixotrophic condition produced less protein per g of biomass (1.62 mg VFP g^{-1} dry biomass), than the phototrophic growth (~ 2 mg VFP g^{-1} dry biomass), and this result is in agreement with observations from Eberhard et al. (2002), who noted that in mixotrophic growth cells have an increased plastome content than at phototrophic conditions, but there is no detection of a higher level of protein.

Temperature increase had a positive effect on protein accumulation only in mixotrophic cultivation; however, specific growth rate and cell density diminished dramatically, and this decrease could not be compensated by the increase in protein level.

Light intensity had a positive effect on specific cell growth and cell density achieved in all cultivation conditions studied, and this is explained by a higher rate of photosynthesis when light is widely available at non-inhibitory levels. However, there was no obvious effect detected on protein level.

Gathering these results it was possible to establish improved conditions for the production of a protein such as VFP in the chloroplast, by utilising mixotrophic cultivation with bright light at 30 °C. Nevertheless, when testing these conditions for the accumulation of a heterologous protein of commercial relevance and use for human therapeutic applications, as it is the case of the Cpl-1 endolysin, it was not possible to observe the same results in terms of higher protein level as observed for VFP. This fact highlights the issue that has been previously observed in recombinant protein expression where the transcription and translation level can vary widely between proteins, regardless of the regulatory elements involved (Rasala et al., 2010). Also, other factors such as the mRNA secondary structure or the need for *cis*- or *trans*-acting factors can have a remarkable effect on protein accumulation (Coragliotti et al., 2011; Specht et al., 2010; Suay et al., 2005).

CHAPTER 6

GENERAL DISCUSSION AND FUTURE WORK

6 GENERAL DISCUSSION AND FUTURE WORK

6.1 Proteorhodopsin expression and its effect on *C. reinhardtii*

The expression of an additional light-capture system, such as proteorhodopsin (PR), in the chloroplast of *Chlamydomonas reinhardtii* was proposed as a strategy to potentially increase cell growth rate or culture lifespan. A codon-optimised version of PR was inserted in a neutral location within the chloroplast genome, and protein accumulation was detected in all transformant lines generated. It was not possible to determine location of this membrane protein within the chloroplast with precision (thylakoid membrane, inner chloroplast membrane or both), due to a very low protein concentration within the membrane protein-enriched fraction. However, PR was not detected in the soluble fraction, which suggests that this protein was being integrated into the chloroplast membranes. Future work for assessing PR location could include the isolation of thylakoid membranes from the rest of the membranes, and then solubilise membrane proteins according to its hydrophobicity using suitable detergents, as it has been carried out for other membrane proteins that accumulate to very low levels (Lehner et al., 2003). With such sequential enrichment, it is envisaged that PR would be in a higher concentration that could make it detectable.

As for the functionality of this protein, cultures of TN72-PR were grown under different cultivation conditions, including the addition of exogenous all-*trans*-retinal, which is required for activation of PR. Mixotrophic growth in a 1L photobioreactor provided an increase in specific growth rate of 12 % in comparison to a control strain without PR. Cultures were also grown in phototrophic conditions; however, no improvement of cell growth was detected in this case. As for the addition of all-*trans*-retinal to the cultures, there was no detectable difference in specific growth rate in cultures grown with or without exogenous retinal; consequently, it is believed that proteorhodopsin was able to use the endogenous retinal that is required for the eyespot of the chloroplast.

A knockout of two different PSII genes was carried out in TN72-PR in order to alleviate possible molecular crowding within the thylakoid membrane (Goral et al., 2010; Kirchhoff, 2008). The hypothesis presented in chapter 3 proposed that this decrease in protein load in the membrane could enhance the accumulation of PR. Knockout of the *psbC* gene proved

unsuccessful for the generation of homoplasmic PSII-deficient transformants since it became apparent that *psbC* was probably co-transcribed with essential tRNA genes. By contrast, the knockout of *psbK* produced stable homoplasmic mutants, which resulted in decreased levels of D1 protein, and thus decreased steady-state level of the PSII complex. The PR protein level and functionality was determined in this new background, but as a result there was no increase in protein accumulation or specific growth rate. Considering these results, it is concluded that PR accumulation is not limited by space in the thylakoid membrane, but rather other factors such as translation rate and a potential difficulty in the integration of this protein into the membrane, possibly influenced by a different membrane lipid profile (Opekarová and Tanner, 2003). This suggests that it could be interesting to evaluate the lipid profile of the organism from where proteorhodopsin originated, in this case the marine bacterium EBAC31A08, and compare it to the profile of the thylakoid membrane of *C. reinhardtii*.

It is important to note that unless there is a detectable increase in PR level and expected functionality, this PSII knockout strategy is creating a less fit strain that can introduce other effects on cell robustness or growth. However, this approach was carried out as a proof of concept for the hypothesis of molecular crowding and its effect on the insertion of an additional membrane protein.

There are a few considerations that could be easily addressed in the future in order to investigate further what are the limiting steps that could be preventing PR from accumulating to higher levels. The codon optimisation carried out for gene synthesis in this work is based on a codon optimisation index, which considers each codon's frequency according to its respective usage in highly expressed genes from the host genome (Sharp and Li, 1987). However, it has been observed that odd codon pairing (codon context biases) and the subsequent generation of secondary structures in the mRNA can have an important effect as modulators of the translation efficiency, particularly on the elongation rate (Boycheva et al., 2003; Tats et al., 2008). A sequence optimiser programme called Codon Usage Optimiser (CUO) has been developed recently by Kong Khai Jien in the Purton lab (unpublished data), which takes into consideration the codon bias and codon pairing for the chloroplast (http://www.ucl.ac.uk/algae/Genetic_engineering_tools). Such a tool can be of great help in designing synthetic genes with a higher likelihood of being translated more efficiently.

In addition, the use of a stronger promoter/5' UTR element such as that from *psaA*, as demonstrated in chapter 4, can definitely induce a higher level of protein, and it is envisaged that higher protein accumulation could result in a clear phenotypic effect. The co-expression of the chaperone, as observed for VFP in chapter 4, could also improve protein folding and stability, which is a factor that was not addressed in this study but might also be affecting PR levels. A relatively simple experiment can be carried out for this purpose in the future using chloramphenicol, a strong inhibitor of protein synthesis, as it has been efficiently illustrated by Chen and Deutscher (2010). By adding this to a culture of TN72-PR and sampling over a time period, it would be possible to assess the steady-state level of already-synthesised protein over a certain period of time and determine its half-life.

In terms of assessing functionality of this protein in *C. reinhardtii*, it is suggested to test TN72-PR growth in green light only, which is the wavelength that activates PR, and this experiment could shed more light on the functionality of PR within the thylakoid membrane. A proton motive force is defined as the electrochemical potential of protons across the membrane, and it has been demonstrated by Béjà et al. (2000) that a light-driven proton pump such as PR can utilise this potential for ATP production. This potential could be detected by measuring pH differences in a cell suspension grown in light, or alternatively, by assessing cell motility due to use of ATP for flagellar activity, as evaluated by Walter et al. (2007) when expressing proteorhodopsin in *E. coli.*

6.2 VFP expression and its use as a reporter for protein accumulation in *C. reinhardtii*

The need for a suitable reporter protein in the chloroplast of *C. reinhardtii* encouraged us to investigate the expression and accumulation of a novel fluorescent protein (VFP), which was reported to have better properties than other FPs (Ilagan et al., 2010). To study accumulation of this protein, we explored the effect of different regulatory elements (from the endogenous genes *atpA* and *psaA*), the co-expression of a bacterial chaperone upstream of VFP, and the fusion of VFP to the large subunit of the highly abundant RuBisCo. Our findings highlighted a stronger activity of the promoter/5' UTR element of *psaA* in comparison to *atpA*, with VFP levels increasing approximately 10 fold, as observed in Western blots. The co-expression of the *Spy* chaperone apparently contributed

positively to VFP levels, but in order to be certain of its effect, VFP expression should be assessed in a vector in which the promoter driving *Spy* expression is the same as the one driving the expression of *vfp*, or alternatively, the *Spy* gene should be placed in the opposite orientation to *vfp*. The outcome of these two variations would provide a more accurate conclusion regarding the VFP level in order to verify that this protein's increase is not occurring due to an up-regulating effect of the *psaA* element expressing *Spy*.

With the final approach of generating a fusion construct, it was possible to select transformants with restored phototrophy and show the presence of the DNA fusion in the transgenic lines; however, there was no evidence for the production of the 83 kDa fusion protein. It was speculated that the *rbcL*-deficient host did incorporate some copies of the fusion construct, but these were eventually lost, as shown by PCR screening, possibly due to selective pressure towards the repair of the *rbcL* lesion over insertion of the whole fusion construct. The search for new *rbcL*-deficient strains in culture collections that carry other type of mutations, as opposed to a point mutation, might be of help for expression of the *rbcL-vfp* fusion plasmid. The construction of this plasmid by Gibson assembly proved successful and it is envisaged that finding a more suitable host for transformation could lead to the predicted accumulation of higher levels or recombinant protein, as observed by Muto el al. (2009).

Fluorescence can be a very useful tool for rapid monitoring of protein levels and its variation under different cultivation conditions. However, FP levels need to be moderately high in order to have a quantifiable system in which comparison among conditions is easily measurable. Low levels of fluorescence can be very challenging in terms of detection and reproducibility, especially in organisms with such a strong auto-fluorescence as microalgae. This research tested different techniques for detecting fluorescence and flow cytometry was found to be sensitive and reproducible. In addition, it was an easy and quick measurement to perform. However, this detection system is not necessarily available in many laboratories and efforts towards achieving higher FP expression need to be performed in order to not rely on such a sensitive method.

As mentioned in chapter 4, there is a variety of FPs available and the choice of a specific FP depends on many aspects of the protein itself and the host. Rasala et al. (2013) expressed in the nuclear genome of *C. reinhardtii* a set of six FPs that span the visual spectrum, and this study concluded that FPs with longer emission wavelengths (> 500 nm) provided the highest signals. Interestingly, the green fluorescent protein tested (which absorbs light in

the green region of the spectrum just like VFP) was shown to be the least fluorescent. Moreover, it was observed that the highest auto-fluorescence is displayed with green excitation/emission filters suggesting that FPs such as tdTomato (exc 554/em 590), mCherry (exc 554/em 590) or orange FPs are much more suitable candidates as reporter protein for an organism such as *C. reinhardtii*. This recent work gives the first evidence of a parameter to consider when choosing a FP for *C. reinhardtii*, and it should be definitely included in future work exploring new fluorescent proteins as reporters.

6.3 VFP accumulation for assessment of different cultivation parameters

VFP was detectable by Western blot analysis using anti-HA antibodies, and its fluorescence was efficiently measured using flow cytometry; therefore, we used it as a reporter protein to study different parameters of cultivation and their effect on protein productivity. Four different cultivation modes were studied, including mixotrophic, heterotrophic and phototrophic cultivation, and it could be observed that mixotrophic mode gives the highest specific growth rate (0.064 h^{-1}) and maximum cell density (1.02 g biomass L^{-1} culture), which is in agreement with what has been observed by Moon et al. (2013) for biomass yield. In terms of protein accumulation, the heterotrophic condition provided the highest protein concentration, of 3.3 mg protein g^{-1} dry biomass, which is twice as much protein as is produced in the mixotrophic condition. This difference could account for a decreased activity of light-induced proteases under heterotrophic cultivation, which would reduce protein turnover and hence increase accumulation. Additionally, it could be argued that the slower growth rate and lower cell density achieved in heterotrophic condition leads to a higher degree of protein synthesis, since the carbon source is still being used, as observed by the growth progression detected in this culture.

Fluorescence emission appeared to be higher for the strain with the highest protein accumulation (TN72-VFPpS), which gives an expected correlation of protein level and functionality. There is a particularly higher level of fluorescence detected in TN72-pS strains grown under phototrophic cultivation, but the cause of this increase in fluorescence is not understood. Cells seemed to be smaller when grown in phototrophic mode, as observed by microscopy, and for this reason their size in different cultivation conditions was more accurately assessed by cell size measurement. However, there was

no significant variation that could help explain if cell size and physiology had something to do with the difference in the fluorescence detected.

Three different temperatures (25, 30 and 37 °C) were studied, and an increase in temperature to 30 °C resulted in a similar specific growth rate and cell density as at 25 °C, and higher protein accumulation under mixotrophic cultivation. A further step in temperature increase to 37 °C showed an additional increase in protein level, although at this temperature specific growth rate and cell density were severely affected, and the increase in protein accumulation does not compensate for this biomass decrease. A similar negative effect on cell growth was observed by James et al. (2013) at 38 °C; however, they reported an increase in biomass accumulation at 32 °C. The fluorescence measurement gave a more pronounced increase for the strain TN72-VFPpS in all cultivation conditions studied, which again accounts for a stronger activity of the *psaA* regulatory elements and a presumably higher protein level.

Finally, two different light intensities were tested, one condition considered as dim light (30 μmol m^{-2} s^{-1}) and the other one considered as bright light (150 μmol m^{-2} s^{-1})), although the higher light level is not sufficiently bright to cause photoinhibition (Niyogi, 2009). It was observed that the bright light induced faster specific growth rate and higher maximum cell density. However, protein productivity on a per cell basis was the same, which showed that this additional energy from light is being used mainly for cell growth. Additionally, a two-step cultivation mode was tested, in which cells were grown to late exponential phase in mixotrophic conditions favouring biomass accumulation, and then switched to heterotrophy during stationary phase, with the aim that this condition would boost protein accumulation. However, there was no detectable change in protein accumulation and apparently a change in cultivation mode when cells had already reached stationary phase did not lead to an increase in protein level. It is important to notice that when switching cultivation mode, cultures were deprived of light but there was no medium replacement. Acetate was possibly almost depleted and there was no carbon source left for increasing protein production, therefore, any remaining acetate could have been used for maintenance rather that protein synthesis, especially for proteins that are not crucial for cell survival.

With the information gathered analysing these different cultivation parameters and their effect on growth and protein productivity, improved conditions for VFP accumulation were determined as mixotrophic cultivation in bright light at 30 °C, considering the

protein productivity per volume of culture. In order to explore if these conditions could be applied for increasing level of a protein of therapeutic application and commercial interest such as the Cpl-1 endolysin, the strain TN72-Cpl1 , in which Cpl-1 is expressed under the control of the *psaA* regulatory elements, was grown under the improved conditions. Unfortunately, protein levels were not influenced in the same way as for VFP, and these cultivation conditions did not improve protein accumulation. This result was not completely unexpected since Dr Rosie Young from the Purton lab has observed different trends for the accumulation of a variety of proteins when growing cultures at 30 and 35 °C (unpublished data). Her data has shown that for some proteins the accumulation level is not increased at higher temperature despite being driven by the same regulatory elements. This phenomenon has also been observed by Rasala et al. (2010) when expressing a set of seven proteins of commercial relevance that exhibited varied synthesis profiles. This variable accumulation can be attributed to transcriptional/translational obstacles as discussed in section 1.2.2; however, one can speculate that in this case it has more to do with the protein sequence itself and the translation rate since the same regulatory elements have been used, or may be due to poor stability of the final product.

This work presented a study of three cultivation parameters, and the combination of these showed interesting effects on protein production and biomass accumulation. Future efforts should continue in this direction because here it has been demonstrated that the combination of genetic manipulation and bioprocess conditions can contribute simultaneously towards the same goal, and both approaches can provide increased protein productivity. There are plenty of other factors, particularly cultivation conditions, which have not been investigated thoroughly, such as the effect of pH, media composition and presence of toxic compounds, to name some, and it is envisaged that each of these could have an effect on protein accumulation. Design of Experiments (DoE) softwares such as Design-Expert are valuable tools used for planning, analysing and interpreting data in order to evaluate the effect of different parameters simultaneously. Using such software allows for a better coverage of the factors (parameters) and their associated levels (numeric range covered by a specific parameter), known as the Experimental Space, which provides higher efficiency for the optimisation process. Future work should incorporate this tool in order to establish optimal conditions for the production of specific proteins, and this could certainly lead to higher yields of biomass and protein that can make microalgae comparable to conventional systems.

6.4 Final remarks

The research covered in this thesis has presented two different approaches with the aim of developing a more robust, fast-growing and protein-productive microalgal platform using the model alga *Chlamydomonas reinhardtii.* The availability of such a host could contribute to the production of heterologous proteins of high value in microalgae in order to make it commercially feasible and to compete with existing expression platforms. Microalgae present several advantages in terms of manipulation, ease of cultivation, downstream processing, and even public perception; therefore it is truly an opportunity that should be further exploited and investigated.

The combination of approaches such as genetic manipulation, in order to generate a certain phenotype or specific advantageous traits originally inexistent in an organism, together with improvement of the cultivation conditions, by means of a thorough evaluation of the environmental factors affecting the organism's growth, can contribute enormously to the generation of more productive hosts. These improved hosts and conditions can make the difference for microalgal cultures, positioning these organisms as a competitive commercial platform for recombinant protein production.

REFERENCES

REFERENCES

Acién Fernández, F.G., Fernández Sevilla, J.M., Molina Grima, E., 2013. Photobioreactors for the production of microalgae. Rev. Environ. Sci. Biotechnol. 12, 131–151. doi:10.1007/s11157-012-9307-6

Adam, Z., Clarke, A.K., 2002. Cutting edge of chloroplast proteolysis. Trends Plant Sci. 7, 451–456. doi:10.1016/S1360-1385(02)02326-9

Ahmad, N., Michoux, F., Nixon, P.J., 2012. Investigating the Production of Foreign Membrane Proteins in Tobacco Chloroplasts: Expression of an Algal Plastid Terminal Oxidase. PLoS ONE 7, e41722. doi:10.1371/journal.pone.0041722

Alguel, Y., Leung, J., Singh, S., Rana, R., Civiero, L., Alves, C., Byrne, B., 2010. New tools for membrane protein research. Curr. Protein Pept. Sci. 11, 156–165.

Barbosa, M.J., Janssen, M., Ham, N., Tramper, J., Wijffels, R.H., 2003. Microalgae cultivation in air-lift reactors: modeling biomass yield and growth rate as a function of mixing frequency. Biotechnol. Bioeng. 82, 170–179. doi:10.1002/bit.10563

Barkan, A., 2011. Expression of Plastid Genes: Organelle-Specific Elaborations on a Prokaryotic Scaffold. Plant Physiol. 155, 1520–1532. doi:10.1104/pp.110.171231

Barnes, D., Franklin, S., Schultz, J., Henry, R., Brown, E., Coragliotti, A., Mayfield, S.P., 2005. Contribution of 5'- and 3'-untranslated regions of plastid mRNAs to the expression of Chlamydomonas reinhardtii chloroplast genes. Mol. Genet. Genomics MGG 274, 625–636. doi:10.1007/s00438-005-0055-y

Beckmann, J., Lehr, F., Finazzi, G., Hankamer, B., Posten, C., Wobbe, L., Kruse, O., 2009. Improvement of light to biomass conversion by de-regulation of light-harvesting protein translation in Chlamydomonas reinhardtii. J. Biotechnol. 142, 70–77. doi:10.1016/j.jbiotec.2009.02.015

Béjà, O., Aravind, L., Koonin, E.V., Suzuki, M.T., Hadd, A., Nguyen, L.P., Jovanovich, S.B., Gates, C.M., Feldman, R.A., Spudich, J.L., Spudich, E.N., DeLong, E.F., 2000. Bacterial Rhodopsin: Evidence for a New Type of Phototrophy in the Sea. Science 289, 1902–1906. doi:10.1126/science.289.5486.1902

Béjà, O., Spudich, E.N., Spudich, J.L., Leclerc, M., DeLong, E.F., 2001. Proteorhodopsin phototrophy in the ocean. Nature 411, 786–789. doi:10.1038/35081051

Bock, R., Knoop, V., 2012. Genomics of Chloroplasts and Mitochondria. Springer.

Borowitzka, M.A., 2013. High-value products from microalgae—their development and commercialisation. J. Appl. Phycol. 25, 743–756. doi:10.1007/s10811-013-9983-9

Boycheva, S., Chkodrov, G., Ivanov, I., 2003. Codon pairs in the genome of Escherichia coli. Bioinformatics 19, 987–998. doi:10.1093/bioinformatics/btg082

Boyle, N.R., Morgan, J.A., 2009. Flux balance analysis of primary metabolism in Chlamydomonas reinhardtii. BMC Syst. Biol. 3, 4. doi:10.1186/1752-0509-3-4

Boynton, J.E., Gillham, N.W., 1996. Genetics and transformation of mitochondria in the green alga Chlamydomonas. Methods Enzymol. 264, 279–296.

Boynton, J.E., Gillham, N.W., Harris, E.H., Hosler, J.P., Johnson, A.M., Jones, A.R., Randolph-Anderson, B.L., Robertson, D., Klein, T.M., Shark, K.B., 1988. Chloroplast transformation in Chlamydomonas with high velocity microprojectiles. Science 240, 1534–1538.

Bruick, R.K., Mayfield, S.P., 1999. Light-activated translation of chloroplast mRNAs. Trends Plant Sci. 4, 190–195. doi:10.1016/S1360-1385(99)01402-8

Bryant, D.A., Frigaard, N.-U., 2006. Prokaryotic photosynthesis and phototrophy illuminated. Trends Microbiol. 14, 488–496. doi:10.1016/j.tim.2006.09.001

Campbell, N.A., Reece, J.B., Urry, L.A., Cain, M.L., Wasserman, S.A., Minorsky, P.V., Jackson, R.B., 2008. Biology, 8th Edition, 8 edition. ed. Pearson Benjamin Cummings, San Francisco.

Cardi, T., Lenzi, P., Maliga, P., 2010. Chloroplasts as expression platforms for plant-produced vaccines. Expert Rev. Vaccines 9, 893–911. doi:10.1586/erv.10.78

Cardol, P., Remacle, C., 2009. Chapter 12 - The Mitochondrial Genome, in: Harris, E.H., Stern, D.B., Witman, G.B. (Eds.), The Chlamydomonas Sourcebook (Second Edition). Academic Press, London, pp. 445–467.

Carpenter, E.P., Beis, K., Cameron, A.D., Iwata, S., 2008. Overcoming the challenges of membrane protein crystallography. Curr. Opin. Struct. Biol. 18, 581–586. doi:10.1016/j.sbi.2008.07.001

Chen, C., Deutscher, M.P., 2010. RNase R is a highly unstable protein regulated by growth phase and stress. RNA 16, 667–672. doi:10.1261/rna.1981010

Chen, F., Johns, M.R., 1996. Heterotrophic growth of Chlamydomonas reinhardtii on acetate in chemostat culture. Process Biochem. 31, 601–604. doi:10.1016/S0032-9592(96)00006-4

Chen, G.-Q., Chen, F., 2006. Growing phototrophic cells without light. Biotechnol. Lett. 28, 607–616. doi:10.1007/s10529-006-0025-4

Chen, H.-C., Melis, A., 2013. Marker-free genetic engineering of the chloroplast in the green microalga Chlamydomonas reinhardtii. Plant Biotechnol. J. 11, 818–828. doi:10.1111/pbi.12073

Chen, X., Zaro, J.L., Shen, W.-C., 2013. Fusion protein linkers: Property, design and functionality. Adv. Drug Deliv. Rev., 2013 65, 1357–1369. doi:10.1016/j.addr.2012.09.039

Chudakov, D.M., Matz, M.V., Lukyanov, S., Lukyanov, K.A., 2010. Fluorescent Proteins and Their Applications in Imaging Living Cells and Tissues. Physiol. Rev. 90, 1103–1163. doi:10.1152/physrev.00038.2009

Coragliotti, A.T., Beligni, M.V., Franklin, S.E., Mayfield, S.P., 2011. Molecular factors affecting the accumulation of recombinant proteins in the Chlamydomonas reinhardtii chloroplast. Mol. Biotechnol. 48, 60–75. doi:10.1007/s12033-010-9348-4

Dauvillee, D., Hilbig, L., Preiss, S., Johanningmeier, U., 2004. Minimal Extent of Sequence Homology Required for Homologous Recombination at the psbA Locus in Chlamydomonas reinhardtii Chloroplasts using PCR-generated DNA Fragments. Photosynth. Res. 79, 219–224. doi:10.1023/B:PRES.0000015384.24958.a9

Davies, J.P., Weeks, D.P., Grossman, A.R., 1992. Expression of the arylsulfatase gene from the beta 2-tubulin promoter in Chlamydomonas reinhardtii. Nucleic Acids Res. 20, 2959–2965.

Debuchy, R., Purton, S., Rochaix, J.D., 1989. The argininosuccinate lyase gene of Chlamydomonas reinhardtii: an important tool for nuclear transformation and for correlating the genetic and molecular maps of the ARG7 locus. EMBO J. 8, 2803–2809.

Deininger, W., Kröger, P., Hegemann, U., Lottspeich, F., Hegemann, P., 1995. Chlamyrhodopsin represents a new type of sensory photoreceptor. EMBO J. 14, 5849–5858.

Dorrell, R.G., Howe, C.J., 2012. What makes a chloroplast? Reconstructing the establishment of photosynthetic symbioses. J. Cell Sci. 125, 1865–1875. doi:10.1242/jcs.102285

Dreesen, I.A.J., Charpin-El Hamri, G., Fussenegger, M., 2010. Heat-stable oral alga-based vaccine protects mice from Staphylococcus aureus infection. J. Biotechnol. 145, 273–280. doi:10.1016/j.jbiotec.2009.12.006

Eberhard, S., Drapier, D., Wollman, F.-A., 2002. Searching limiting steps in the expression of chloroplast-encoded proteins: relations between gene copy number, transcription, transcript abundance and translation rate in the chloroplast of Chlamydomonas reinhardtii. Plant J. Cell Mol. Biol. 31, 149–160.

Eberhard, S., Loiselay, C., Drapier, D., Bujaldon, S., Girard-Bascou, J., Kuras, R., Choquet, Y., Wollman, F.-A., 2011. Dual functions of the nucleus-encoded factor TDA1 in

trapping and translation activation of atpA transcripts in Chlamydomonas reinhardtii chloroplasts. Plant J. Cell Mol. Biol. 67, 1055–1066. doi:10.1111/j.1365-313X.2011.04657.x

Economou, C., Wannathong, T., Szaub, J., Purton, S., 2014. A simple, low-cost method for chloroplast transformation of the green alga Chlamydomonas reinhardtii. Methods Mol. Biol. 1132, 401–411. doi:10.1007/978-1-62703-995-6_27

Ernst, O.P., Lodowski, D.T., Elstner, M., Hegemann, P., Brown, L.S., Kandori, H., 2014. Microbial and Animal Rhodopsins: Structures, Functions, and Molecular Mechanisms. Chem. Rev. 114, 126–163. doi:10.1021/cr4003769

Fischer, B.B., Wiesendanger, M., Eggen, R.I.L., 2006. Growth condition-dependent sensitivity, photodamage and stress response of Chlamydomonas reinhardtii exposed to high light conditions. Plant Cell Physiol. 47, 1135–1145. doi:10.1093/pcp/pcj085

Fletcher, S.P., Muto, M., Mayfield, S.P., 2007. Optimization of recombinant protein expression in the chloroplasts of green algae.

Franklin, S.E., Mayfield, S.P., 2004. Prospects for molecular farming in the green alga Chlamydomonas reinhardtii. Curr. Opin. Plant Biol. 7, 159–165. doi:10.1016/j.pbi.2004.01.012

Franklin, S.E., Mayfield, S.P., 2005. Recent developments in the production of human therapeutic proteins in eukaryotic algae. Expert Opin. Biol. Ther. 5, 225–235. doi:10.1517/14712598.5.2.225

Franklin, S., Ngo, B., Efuet, E., Mayfield, S.P., 2002. Development of a GFP reporter gene for Chlamydomonas reinhardtii chloroplast. Plant J. Cell Mol. Biol. 30, 733–744.

Fuhrman, J.A., Schwalbach, M.S., Stingl, U., 2008. Proteorhodopsins: an array of physiological roles? Nat. Rev. Microbiol. 6, 488–494. doi:10.1038/nrmicro1893

Gibson, D.G., Benders, G.A., Andrews-Pfannkoch, C., Denisova, E.A., Baden-Tillson, H., Zaveri, J., Stockwell, T.B., Brownley, A., Thomas, D.W., Algire, M.A., Merryman, C., Young, L., Noskov, V.N., Glass, J.I., Venter, J.C., Hutchison, C.A., Smith, H.O., 2008. Complete Chemical Synthesis, Assembly, and Cloning of a Mycoplasma genitalium Genome. Science 319, 1215–1220. doi:10.1126/science.1151721

Gibson, D.G., Young, L., Chuang, R.-Y., Venter, J.C., Hutchison, C.A., Smith, H.O., 2009. Enzymatic assembly of DNA molecules up to several hundred kilobases. Nat. Methods 6, 343–345. doi:10.1038/nmeth.1318

Goldschmidt-Clermont, M., 1991. Transgenic expression of aminoglycoside adenine transferase in the chloroplast: a selectable marker of site-directed transformation of chlamydomonas. Nucleic Acids Res. 19, 4083–4089.

Goldschmidt-Clermont, M., 1998. Chloroplast Transformation and Reverse Genetics, in: Rochaix, J.-D., Goldschmidt-Clermont, M., Merchant, S. (Eds.), The Molecular Biology of Chloroplasts and Mitochondria in Chlamydomonas, Advances in Photosynthesis and Respiration. Springer Netherlands, pp. 139–149.

Gómez-Consarnau, L., Akram, N., Lindell, K., Pedersen, A., Neutze, R., Milton, D.L., González, J.M., Pinhassi, J., 2010. Proteorhodopsin Phototrophy Promotes Survival of Marine Bacteria during Starvation. PLoS Biol 8, e1000358. doi:10.1371/journal.pbio.1000358

Gómez-Consarnau, L., González, J.M., Coll-Lladó, M., Gourdon, P., Pascher, T., Neutze, R., Pedrós-Alió, C., Pinhassi, J., 2007. Light stimulates growth of proteorhodopsin-containing marine Flavobacteria. Nature 445, 210–213. doi:10.1038/nature05381

Gong, Y., Hu, H., Gao, Y., Xu, X., Gao, H., 2011. Microalgae as platforms for production of recombinant proteins and valuable compounds: progress and prospects. J. Ind. Microbiol. Biotechnol. 38, 1879–1890. doi:10.1007/s10295-011-1032-6

Goodenough, U.W., Staehelin, L.A., 1971. Structural differentiation of stacked and unstacked chloroplast membranes. J. Cell Biol. 48, 594–619.

Goral, T.K., Johnson, M.P., Brain, A.P.R., Kirchhoff, H., Ruban, A.V., Mullineaux, C.W., 2010. Visualizing the mobility and distribution of chlorophyll proteins in higher plant thylakoid membranes: effects of photoinhibition and protein phosphorylation. Plant J. Cell Mol. Biol. 62, 948–959. doi:10.1111/j.0960-7412.2010.04207.x

Hallmann, A., 2007. Algal transgenics and biotechnology. Transgenic Plant J. 1, 81-98.

Harris, E.H., 2001. *Chlamydomonas* as a model organism. Annu. Rev. Plant Physiol. Plant Mol. Biol. 52, 363–406. doi:10.1146/annurev.arplant.52.1.363

Harris, E.H., Stern, D.B., Witman, G.B. (Eds.), 2009a. Chapter 8 - Chlamydomonas in the Laboratory, in: The Chlamydomonas Sourcebook (Second Edition). Academic Press, London, pp. 241–302.

Harris, E.H., Stern, D.B., Witman, G.B. (Eds.), 2009b. Chapter 2 - Cell Architecture, in: The Chlamydomonas Sourcebook (Second Edition). Academic Press, London, pp. 25–64.

Harris, E.H., Stern, D.B., Witman, G.B. (Eds.), 2009c. Chapter 7 - Organelle Heredity, in: The Chlamydomonas Sourcebook (Second Edition). Academic Press, London, pp. 211–240.

Harris, E.H., Stern, D.B., Witman, G.B. (Eds.), 2009d. Chapter 6 - The Life of an Acetate Flagellate, in: The Chlamydomonas Sourcebook (Second Edition). Academic Press, London, pp. 159–210.

He, D.-M., Qian, K.-X., Shen, G.-F., Zhang, Z.-F., Li, Y.-N., Su, Z.-L., Shao, H.-B., 2007. Recombination and expression of classical swine fever virus (CSFV) structural protein E2 gene in Chlamydomonas reinhardtii chroloplasts. Colloids Surf. B Biointerfaces 55, 26–30. doi:10.1016/j.colsurfb.2006.10.042

Higgs, D.C., 2009. Chapter 24 - The Chloroplast Genome, in: Harris, E.H., Stern, D.B., Witman, G.B. (Eds.), The Chlamydomonas Sourcebook (Second Edition). Academic Press, London, pp. 871–891.

Ilagan, R.P., Rhoades, E., Gruber, D.F., Kao, H.-T., Pieribone, V.A., Regan, L., 2010. A new bright green-emitting fluorescent protein--engineered monomeric and dimeric forms. FEBS J. 277, 1967–1978. doi:10.1111/j.1742-4658.2010.07618.x

James, G.O., Hocart, C.H., Hillier, W., Price, G.D., Djordjevic, M.A., 2013. Temperature modulation of fatty acid profiles for biofuel production in nitrogen deprived Chlamydomonas reinhardtii. Bioresour. Technol. 127, 441–447. doi:10.1016/j.biortech.2012.09.090

Janssen, M., de Winter, M., Tramper, J., Mur, L.R., Snel, J., Wijffels, R.H., 2000a. Efficiency of light utilization of Chlamydomonas reinhardtii under medium-duration light/dark cycles. J. Biotechnol. 78, 123–137.

Janssen, M., Bresser, L. de, Baijens, T., Tramper, J., Mur, L.R., Snel, J.F.H., Wijffels, R.H., 2000b. Scale-up aspects of photobioreactors: effects of mixing-induced light/dark cycles. J. Appl. Phycol. 12, 225–237. doi:10.1023/A:1008151526680

Janssen, M., Tramper, J., Mur, L.R., Wijffels, R.H., 2003. Enclosed outdoor photobioreactors: light regime, photosynthetic efficiency, scale-up, and future prospects. Biotechnol. Bioeng. 81, 193–210. doi:10.1002/bit.10468

Johnson, E.T., Baron, D.B., Naranjo, B., Bond, D.R., Schmidt-Dannert, C., Gralnick, J.A., 2010. Enhancement of Survival and Electricity Production in an Engineered Bacterium by Light-Driven Proton Pumping. Appl. Environ. Microbiol. 76, 4123–4129. doi:10.1128/AEM.02425-09

Johnson, E.T., Schmidt-Dannert, C., 2008. Light-energy conversion in engineered microorganisms. Trends Biotechnol. 26, 682–689. doi:10.1016/j.tibtech.2008.09.002

Johnson, G.N., 2005. Cyclic electron transport in C3 plants: fact or artefact? J. Exp. Bot. 56, 407–416. doi:10.1093/jxb/eri106

Jones, C.S., Luong, T., Hannon, M., Tran, M., Gregory, J.A., Shen, Z., Briggs, S.P., Mayfield, S.P., 2013. Heterologous expression of the C-terminal antigenic domain of the malaria

vaccine candidate Pfs48/45 in the green algae Chlamydomonas reinhardtii. Appl. Microbiol. Biotechnol. 97, 1987–1995. doi:10.1007/s00253-012-4071-7

Kato, K., Marui, T., Kasai, S., Shinmyo, A., 2007. Artificial control of transgene expression in Chlamydomonas reinhardtii chloroplast using the lac regulation system from Escherichia coli. J. Biosci. Bioeng. 104, 207–213. doi:10.1263/jbb.104.207

Kindle, K.L., 1990. High-frequency nuclear transformation of Chlamydomonas reinhardtii. Proc. Natl. Acad. Sci. 87, 1228–1232. doi:10.1073/pnas.87.3.1228

Kindle, K.L., Richards, K.L., Stern, D.B., 1991. Engineering the chloroplast genome: techniques and capabilities for chloroplast transformation in Chlamydomonas reinhardtii. Proc. Natl. Acad. Sci. U. S. A. 88, 1721–1725.

Kirchhoff, H., 2008. Molecular crowding and order in photosynthetic membranes. Trends Plant Sci. 13, 201–207. doi:10.1016/j.tplants.2008.03.001

Klein, U., 2009. Chapter 25 - Chloroplast Transcription, in: Harris, E.H., Stern, D.B., Witman, G.B. (Eds.), The Chlamydomonas Sourcebook (Second Edition). Academic Press, London, pp. 893–913.

Lami, R., Cottrell, M.T., Campbell, B.J., Kirchman, D.L., 2009. Light-dependent growth and proteorhodopsin expression by Flavobacteria and SAR11 in experiments with Delaware coastal waters. Environ. Microbiol. 11, 3201–3209. doi:10.1111/j.1462-2920.2009.02028.x

Lawson, M.A., Satir, P., 1994. Characterization of the eyespot regions of "blind" Chlamydomonas mutants after restoration of photophobic responses. J. Eukaryot. Microbiol. 41, 593–601.

Lehner, I., Niehof, M., Borlak, J., 2003. An optimized method for the isolation and identification of membrane proteins. Electrophoresis 24, 1795–1808. doi:10.1002/elps.200305387

Leite, G.B., Abdelaziz, A.E.M., Hallenbeck, P.C., 2013. Algal biofuels: Challenges and opportunities. Bioresour. Technol., Special Issue: IBS 2012 & Special Issue: IFIBiop 145, 134–141. doi:10.1016/j.biortech.2013.02.007

Leliaert, F., Smith, D.R., Moreau, H., Herron, M.D., Verbruggen, H., Delwiche, C.F., De Clerck, O., 2012. Phylogeny and Molecular Evolution of the Green Algae. Crit. Rev. Plant Sci. 31, 1–46. doi:10.1080/07352689.2011.615705

Lewis, J.C., Feltus, A., Ensor, C.M., Ramanathan, S., Daunert, and S., 1998. Peer Reviewed: Applications of Reporter Genes. Anal. Chem. 70, 579A–585A. doi:10.1021/ac9819638

Lewis, L.A., McCourt, R.M., 2004. Green algae and the origin of land plants. Am. J. Bot. 91, 1535–1556. doi:10.3732/ajb.91.10.1535

Lippincott-Schwartz, J., Patterson, G.H., 2003. Development and use of fluorescent protein markers in living cells. Science 300, 87–91. doi:10.1126/science.1082520

Loeffler, J.M., Fischetti, V.A., 2003. Synergistic Lethal Effect of a Combination of Phage Lytic Enzymes with Different Activities on Penicillin-Sensitive and -Resistant Streptococcus pneumoniae Strains. Antimicrob. Agents Chemother. 47, 375–377. doi:10.1128/AAC.47.1.375-377.2003

Lumbreras, V., Stevens, D.R., Purton, S., 1998. Efficient foreign gene expression in Chlamydomonas reinhardtii mediated by an endogenous intron. Plant J. 14, 441–447. doi:10.1046/j.1365-313X.1998.00145.x

Ma, J.K.-C., Drake, P.M.W., Christou, P., 2003. The production of recombinant pharmaceutical proteins in plants. Nat. Rev. Genet. 4, 794–805. doi:10.1038/nrg1177

Maliga, P., Bock, R., 2011. Plastid Biotechnology: Food, Fuel, and Medicine for the 21st Century. Plant Physiol. 155, 1501–1510. doi:10.1104/pp.110.170969

Manuell, A.L., Beligni, M.V., Elder, J.H., Siefker, D.T., Tran, M., Weber, A., McDonald, T.L., Mayfield, S.P., 2007. Robust expression of a bioactive mammalian protein in

Chlamydomonas chloroplast. Plant Biotechnol. J. 5, 402–412. doi:10.1111/j.1467-7652.2007.00249.x

Manuell, A.L., Mayfield, S.P., 2006. A bright future for Chlamydomonas. Genome Biol. 7, 327. doi:10.1186/gb-2006-7-9-327

Martinez, A., Bradley, A.S., Waldbauer, J.R., Summons, R.E., DeLong, E.F., 2007. Proteorhodopsin photosystem gene expression enables photophosphorylation in a heterologous host. Proc. Natl. Acad. Sci. U. S. A. 104, 5590–5595. doi:10.1073/pnas.0611470104

Maul, J.E., Lilly, J.W., Cui, L., dePamphilis, C.W., Miller, W., Harris, E.H., Stern, D.B., 2002. The Chlamydomonas reinhardtii plastid chromosome: islands of genes in a sea of repeats. Plant Cell 14, 2659–2679.

Mayfield, S.P., Franklin, S.E., Lerner, R.A., 2003. Expression and assembly of a fully active antibody in algae. Proc. Natl. Acad. Sci. U. S. A. 100, 438–442. doi:10.1073/pnas.0237108100

Mayfield, S.P., Kindle, K.L., 1990. Stable nuclear transformation of Chlamydomonas reinhardtii by using a C. reinhardtii gene as the selectable marker. Proc. Natl. Acad. Sci. U. S. A. 87, 2087–2091.

Mayfield, S.P., Manuell, A.L., Chen, S., Wu, J., Tran, M., Siefker, D., Muto, M., Marin-Navarro, J., 2007. Chlamydomonas reinhardtii chloroplasts as protein factories. Curr. Opin. Biotechnol. 18, 126–133. doi:10.1016/j.copbio.2007.02.001

Mayfield, S.P., Schultz, J., 2004. Development of a luciferase reporter gene, luxCt, for Chlamydomonas reinhardtii chloroplast. Plant J. Cell Mol. Biol. 37, 449–458.

Merchant, S.S., Prochnik, S.E., Vallon, O., Harris, E.H., Karpowicz, S.J., Witman, G.B., Terry, A., Salamov, A., Fritz-Laylin, L.K., Maréchal-Drouard, L., Marshall, W.F., Qu, L.-H., Nelson, D.R., Sanderfoot, A.A., Spalding, M.H., Kapitonov, V.V., Ren, Q., Ferris, P., Lindquist, E., Shapiro, H., Lucas, S.M., Grimwood, J., Schmutz, J., Grigoriev, I.V., Rokhsar, D.S., Grossman, A.R., Cardol, P., Cerutti, H., Chanfreau, G., Chen, C.-L., Cognat, V., Croft, M.T., Dent, R., Dutcher, S., Fernández, E., Fukuzawa, H., González-Ballester, D., González-Halphen, D., Hallmann, A., Hanikenne, M., Hippler, M., Inwood, W., Jabbari, K., Kalanon, M., Kuras, R., Lefebvre, P.A., Lemaire, S.D., Lobanov, A.V., Lohr, M., Manuell, A., Meier, I., Mets, L., Mittag, M., Mittelmeier, T., Moroney, J.V., Moseley, J., Napoli, C., Nedelcu, A.M., Niyogi, K., Novoselov, S.V., Paulsen, I.T., Pazour, G., Purton, S., Ral, J.-P., Riaño-Pachón, D.M., Riekhof, W., Rymarquis, L., Schroda, M., Stern, D., Umen, J., Willows, R., Wilson, N., Zimmer, S.L., Allmer, J., Balk, J., Bisova, K., Chen, C.-J., Elias, M., Gendler, K., Hauser, C., Lamb, M.R., Ledford, H., Long, J.C., Minagawa, J., Page, M.D., Pan, J., Pootakham, W., Roje, S., Rose, A., Stahlberg, E., Terauchi, A.M., Yang, P., Ball, S., Bowler, C., Dieckmann, C.L., Gladyshev, V.N., Green, P., Jorgensen, R., Mayfield, S., Mueller-Roeber, B., Rajamani, S., Sayre, R.T., Brokstein, P., Dubchak, I., Goodstein, D., Hornick, L., Huang, Y.W., Jhaveri, J., Luo, Y., Martínez, D., Ngau, W.C.A., Otillar, B., Poliakov, A., Porter, A., Szajkowski, L., Werner, G., Zhou, K., 2007. The Chlamydomonas genome reveals the evolution of key animal and plant functions. Science 318, 245–251. doi:10.1126/science.1143609

Michelet, L., Lefebvre-Legendre, L., Burr, S.E., Rochaix, J.-D., Goldschmidt-Clermont, M., 2011. Enhanced chloroplast transgene expression in a nuclear mutant of Chlamydomonas. Plant Biotechnol. J. 9, 565–574. doi:10.1111/j.1467-7652.2010.00564.x

Molecular Genetics of Chlamydomonas, Laboratory protocols. EMBO practical course, Geneva, 2006.

Moon, M., Kim, C.W., Park, W.-K., Yoo, G., Choi, Y.-E., Yang, J.-W., 2013. Mixotrophic growth with acetate or volatile fatty acids maximizes growth and lipid production in Chlamydomonas reinhardtii. Algal Res. 2, 352–357. doi:10.1016/j.algal.2013.09.003

Msanne, J., Xu, D., Konda, A.R., Casas-Mollano, J.A., Awada, T., Cahoon, E.B., Cerutti, H., 2012. Metabolic and gene expression changes triggered by nitrogen deprivation in the photoautotrophically grown microalgae Chlamydomonas reinhardtii and Coccomyxa sp. C-169. Phytochemistry 75, 50–59. doi:10.1016/j.phytochem.2011.12.007

Mussgnug, J.H., Thomas-Hall, S., Rupprecht, J., Foo, A., Klassen, V., McDowall, A., Schenk, P.M., Kruse, O., Hankamer, B., 2007. Engineering photosynthetic light capture: impacts on improved solar energy to biomass conversion. Plant Biotechnol. J. 5, 802–814. doi:10.1111/j.1467-7652.2007.00285.x

Muto, M., Henry, R.E., Mayfield, S.P., 2009. Accumulation and processing of a recombinant protein designed as a cleavable fusion to the endogenous Rubisco LSU protein in Chlamydomonas chloroplast. BMC Biotechnol. 9. doi:10.1186/1472-6750-9-26

Nair, J.S., Ramaswamy, N.K., 2004. Chloroplast Proteases. Biol. Plant. 48, 321–326. doi:10.1023/B:BIOP.0000041081.00086.85

Nakamura, Y., Gojobori, T., Ikemura, T., 2000. Codon usage tabulated from international DNA sequence databases: status for the year 2000. Nucleic Acids Res. 28, 292.

Nelson, J.A., Savereide, P.B., Lefebvre, P.A., 1994. The CRY1 gene in Chlamydomonas reinhardtii: structure and use as a dominant selectable marker for nuclear transformation. Mol. Cell. Biol. 14, 4011–4019.

Newman, S.M., Gillham, N.W., Harris, E.H., Johnson, A.M., Boynton, J.E., 1991. Targeted disruption of chloroplast genes in Chlamydomonas reinhardtii. Mol. Gen. Genet. MGG 230, 65–74. doi:10.1007/BF00290652

Nishimura, Y., Stern, D.B., 2010. Differential replication of two chloroplast genome forms in heteroplasmic Chlamydomonas reinhardtii gametes contributes to alternative inheritance patterns. Genetics 185, 1167–1181. doi:10.1534/genetics.110.118265

Niyogi, K.K., 2009. Chapter 23 - Photoprotection and High Light Responses, in: Harris, E.H., Stern, D.B., Witman, G.B. (Eds.), The Chlamydomonas Sourcebook (Second Edition). Academic Press, London, pp. 847–870.

Nordhues, A., Miller, S.M., Mühlhaus, T., Schroda, M., 2010. New insights into the roles of molecular chaperones in Chlamydomonas and Volvox. Int. Rev. Cell Mol. Biol. 285, 75–113. doi:10.1016/B978-0-12-381047-2.00002-5

O'Connor, H.E., Ruffle, S.V., Cain, A.J., Deak, Z., Vass, I., Nugent, J.H.A., Purton, S., 1998. The 9-kDa phosphoprotein of photosystem: II. Generation and characterisation of Chlamydomonas mutants lacking PSII-H and a site-directed mutant lacking the phosphorylation site. Biochim. Biophys. Acta BBA - Bioenerg. 1364, 63–72. doi:10.1016/S0005-2728(98)00013-9

Olive, J., Wollman, F.-A., 1998. Supramolecular Organization of the Chloroplast and of the Thylakoid Membranes, in: Rochaix, J.-D., Goldschmidt-Clermont, M., Merchant, S. (Eds.), The Molecular Biology of Chloroplasts and Mitochondria in Chlamydomonas, Advances in Photosynthesis and Respiration. Springer Netherlands, pp. 233–254.

Opekarová, M., Tanner, W., 2003. Specific lipid requirements of membrane proteins—a putative bottleneck in heterologous expression. Biochim. Biophys. Acta BBA - Biomembr., Overexpression of Integral Membrane Proteins 1610, 11–22. doi:10.1016/S0005-2736(02)00708-3

Papageorgiou, G.C., Govindjee, 2007. Chlorophyll a Fluorescence: A Signature of Photosynthesis. Springer.

Potvin, G., Zhang, Z., 2010. Strategies for high-level recombinant protein expression in transgenic microalgae: a review. Biotechnol. Adv. 28, 910–918. doi:10.1016/j.biotechadv.2010.08.006

Pröschold, T., Harris, E.H., Coleman, A.W., 2005. Portrait of a species: Chlamydonomas reinhardtii. Genetics 170, 1601–1610. doi:10.1534/genetics.105.044503

Purton, S., 2007. Tools and techniques for chloroplast transformation of Chlamydomonas. Adv. Exp. Med. Biol. 616, 34–45. doi:10.1007/978-0-387-75532-8_4

Purton, S., Szaub, J.B., Wannathong, T., Young, R., Economou, C.K., 2013. Genetic engineering of algal chloroplasts: Progress and prospects. Russ. J. Plant Physiol. 60, 491–499. doi:10.1134/S1021443713040146

Quan, S., Koldewey, P., Tapley, T., Kirsch, N., Ruane, K.M., Pfizenmaier, J., Shi, R., Hofmann, S., Foit, L., Ren, G., Jakob, U., Xu, Z., Cygler, M., Bardwell, J.C.A., 2011. Genetic selection designed to stabilize proteins uncovers a chaperone called Spy. Nat. Struct. Mol. Biol. 18, 262–269. doi:10.1038/nsmb.2016

Ramundo, S., Casero, D., Mühlhaus, T., Hemme, D., Sommer, F., Crèvecoeur, M., Rahire, M., Schroda, M., Rusch, J., Goodenough, U., Pellegrini, M., Perez-Perez, M.E., Crespo, J.L., Schaad, O., Civic, N., Rochaix, J.D., 2014. Conditional Depletion of the Chlamydomonas Chloroplast ClpP Protease Activates Nuclear Genes Involved in Autophagy and Plastid Protein Quality Control. Plant Cell Online 26, 2201–2222. doi:10.1105/tpc.114.124842

Rasala, B.A., Barrera, D.J., Ng, J., Plucinak, T.M., Rosenberg, J.N., Weeks, D.P., Oyler, G.A., Peterson, T.C., Haerizadeh, F., Mayfield, S.P., 2013. Expanding the spectral palette of fluorescent proteins for the green microalga Chlamydomonas reinhardtii. Plant J. Cell Mol. Biol. 74, 545–556. doi:10.1111/tpj.12165

Rasala, B.A., Chao, S.-S., Pier, M., Barrera, D.J., Mayfield, S.P., 2014. Enhanced Genetic Tools for Engineering Multigene Traits into Green Algae. PLoS ONE 9, e94028. doi:10.1371/journal.pone.0094028

Rasala, B.A., Mayfield, S.P., 2011. The microalga Chlamydomonas reinhardtii as a platform for the production of human protein therapeutics. Bioeng. Bugs 2, 50–54. doi:10.4161/bbug.2.1.13423

Rasala, B.A., Muto, M., Lee, P.A., Jager, M., Cardoso, R.M.F., Behnke, C.A., Kirk, P., Hokanson, C.A., Crea, R., Mendez, M., Mayfield, S.P., 2010. Production of therapeutic proteins in algae, analysis of expression of seven human proteins in the chloroplast of Chlamydomonas reinhardtii. Plant Biotechnol. J. 8, 719–733. doi:10.1111/j.1467-7652.2010.00503.x

Rath, A., Glibowicka, M., Nadeau, V.G., Chen, G., Deber, C.M., 2009. Detergent binding explains anomalous SDS-PAGE migration of membrane proteins. Proc. Natl. Acad. Sci. 106, 1760–1765. doi:10.1073/pnas.0813167106

Reckel, S., Gottstein, D., Stehle, J., Löhr, F., Verhoefen, M.-K., Takeda, M., Silvers, R., Kainosho, M., Glaubitz, C., Wachtveitl, J., Bernhard, F., Schwalbe, H., Güntert, P., Dötsch, V., 2011. Solution NMR Structure of Proteorhodopsin. Angew. Chem. Int. Ed. 50, 11942–11946. doi:10.1002/anie.201105648

Redding, K., Peltier, G., 1998. Reexamining the Validity of the Z-Scheme: Is Photosystem I Required for Oxygenic Photosynthesis in Chlamydomonas?, in: Rochaix, J.-D., Goldschmidt-Clermont, M., Merchant, S. (Eds.), The Molecular Biology of Chloroplasts and Mitochondria in Chlamydomonas, Advances in Photosynthesis and Respiration. Springer Netherlands, pp. 349–362.

Remacle, C., Cline, S., Boutaffala, L., Gabilly, S., Larosa, V., Barbieri, M.R., Coosemans, N., Hamel, P.P., 2009. The ARG9 Gene Encodes the Plastid-Resident N-Acetyl Ornithine Aminotransferase in the Green Alga Chlamydomonas reinhardtii. Eukaryot. Cell 8, 1460–1463. doi:10.1128/EC.00108-09

Rochaix, J.D., Kuchka, M., Mayfield, S., Schirmer-Rahire, M., Girard-Bascou, J., Bennoun, P., 1989. Nuclear and chloroplast mutations affect the synthesis or stability of the chloroplast psbC gene product in Chlamydomonas reinhardtii. EMBO J. 8, 1013–1021.

Rochaix, J.D., Mayfield, S., Goldschmidt-Clermont, M. & Erickson, J.M., 1988. Molecular biology of Chlamydomonas, in: Plant molecular biology: a practical approach. IRL Press, Oxford, pp. 253-275.

Rosello Sastre, R., Csögör, Z., Perner-Nochta, I., Fleck-Schneider, P., Posten, C., 2007. Scale-down of microalgae cultivations in tubular photo-bioreactors--a conceptual approach. J. Biotechnol. 132, 127–133. doi:10.1016/j.jbiotec.2007.04.022

Russell, D.G., 2001. Mycobacterium tuberculosis: here today, and here tomorrow. Nat. Rev. Mol. Cell Biol. 2, 569–586. doi:10.1038/35085034

Scharff, L.B., Bock, R., 2014. Synthetic biology in plastids. Plant J. 78, 783–798. doi:10.1111/tpj.12356

Schenborn, E., Groskreutz, D., 1999. Reporter gene vectors and assays. Mol. Biotechnol. 13, 29–44. doi:10.1385/MB:13:1:29

Schroda, M., Beck, C.F., Vallon, O., 2002. Sequence elements within an HSP70 promoter counteract transcriptional transgene silencing in Chlamydomonas. Plant J. Cell Mol. Biol. 31, 445–455.

Schroda, M., Blöcker, D., Beck, C.F., 2000. The HSP70A promoter as a tool for the improved expression of transgenes in Chlamydomonas. Plant J. Cell Mol. Biol. 21, 121–131.

Shaner, N.C., Steinbach, P.A., Tsien, R.Y., 2005. A guide to choosing fluorescent proteins. Nat. Methods 2, 905–909. doi:10.1038/nmeth819

Sharp, P.M., Li, W.H., 1987. The codon Adaptation Index--a measure of directional synonymous codon usage bias, and its potential applications. Nucleic Acids Res. 15, 1281–1295.

Sieburth, L., Berry-Lowe, S., Schmidt, G., 1991. Chloroplast RNA Stability in Chlamydomonas: Rapid Degradation of psbB and psbC Transcripts in Two Nuclear Mutants. Plant Cell 3, 175–189.

Sineshchekov, O.A., Govorunova, E.G., Der, A., Keszthelyi, L., Nultsch, W., 1994. Photoinduced electric currents in carotenoid-deficient Chlamydomonas mutants reconstituted with retinal and its analogs. Biophys. J. 66, 2073–2084.

Siripornadulsil, S., Dabrowski, K., Sayre, R., 2007. Microalgal Vaccines, in: León, R., Galván, A., Fernández, E. (Eds.), Transgenic Microalgae as Green Cell Factories, Advances in Experimental Medicine and Biology. Springer New York, pp. 122–128.

Slamovits, C.H., Okamoto, N., Burri, L., James, E.R., Keeling, P.J., 2011. A bacterial proteorhodopsin proton pump in marine eukaryotes. Nat. Commun. 2, 183. doi:10.1038/ncomms1188

Snapp, E., 2005. Design and Use of Fluorescent Fusion Proteins in Cell Biology. Curr. Protoc. Cell Biol. Chapter Unit–21.4. doi:10.1002/0471143030.cb2104s27

Specht, E., Miyake-Stoner, S., Mayfield, S., 2010. Micro-algae come of age as a platform for recombinant protein production. Biotechnol. Lett. 32, 1373–1383. doi:10.1007/s10529-010-0326-5

Spolaore, P., Joannis-Cassan, C., Duran, E., Isambert, A., 2006. Commercial applications of microalgae. J. Biosci. Bioeng. 101, 87–96. doi:10.1263/jbb.101.87

Spreitzer, R.J., Goldschmidt-Clermont, M., Rahire, M., Rochaix, J.-D., 1985. Nonsense mutations in the Chlamydomonas chloroplast gene that codes for the large subunit of ribulosebisphosphate carboxylase/oxygenase. Proc. Natl. Acad. Sci. U. S. A. 82, 5460–5464.

Spreitzer, R.J., Mets, L., 1981. Photosynthesis-deficient Mutants of Chlamydomonas reinhardii with Associated Light-sensitive Phenotypes 1. Plant Physiol. 67, 565–569.

Stern, D., 2009. The Chlamydomonas Sourcebook: Organellar and Metabolic Processes. Second edition. Academic Press.

Stevens, D.R., Purton, S., Rochaix, J.-D., 1996. The bacterial phleomycin resistance geneble as a dominant selectable marker inChlamydomonas. Mol. Gen. Genet. MGG 251, 23–30. doi:10.1007/BF02174340

Su, Z.-L., Qian, K.-X., Tan, C.-P., Meng, C.-X., Qin, S., 2005. Recombination and heterologous expression of allophycocyanin gene in the chloroplast of Chlamydomonas reinhardtii. Acta Biochim. Biophys. Sin. 37, 709–712.

Suay, L., Salvador, M.L., Abesha, E., Klein, U., 2005. Specific roles of 5? RNA secondary structures in stabilizing transcripts in chloroplasts. Nucleic Acids Res. 33, 4754–4761. doi:10.1093/nar/gki760

Sun, M., Qian, K., Su, N., Chang, H., Liu, J., Shen, G., 2003. Foot-and-mouth disease virus VP1 protein fused with cholera toxin B subunit expressed in Chlamydomonas reinhardtii chloroplast. Biotechnol. Lett. 25, 1087–1092. doi:10.1023/A:1024140114505

Szaub, J., 2012. PhD thesis: Genetic engineering of green microalgae for the production of biofuel and high value products.

Takahashi, Y., Goldschmidt-Clermont, M., Soen, S.Y., Franzén, L.G., Rochaix, J.D., 1991. Directed chloroplast transformation in Chlamydomonas reinhardtii: insertional inactivation of the psaC gene encoding the iron sulfur protein destabilizes photosystem I. EMBO J. 10, 2033–2040.

Takahashi, Y., Matsumoto, H., Goldschmidt-Clermont, M., Rochaix, J.-D., 1994. Directed disruption of the Chlamydomonas chloroplast psbK gene destabilizes the photosystem II reaction center complex. Plant Mol. Biol. 24, 779–788. doi:10.1007/BF00029859

Tats, A., Tenson, T., Remm, M., 2008. Preferred and avoided codon pairs in three domains of life. BMC Genomics 9, 463. doi:10.1186/1471-2164-9-463

Taunt, H.N., 2013. PhD thesis: The synthesis of novel antibacterial proteins in the Chlamydomonas reinhardtii chloroplast.

Terashima, I., Fujita, T., Inoue, T., Chow, W.S., Oguchi, R., 2009. Green Light Drives Leaf Photosynthesis More Efficiently than Red Light in Strong White Light: Revisiting the Enigmatic Question of Why Leaves are Green. Plant Cell Physiol. 50, 684–697. doi:10.1093/pcp/pcp034

Tran, M., Van, C., Barrera, D.J., Pettersson, P.L., Peinado, C.D., Bui, J., Mayfield, S.P., 2013. Production of unique immunotoxin cancer therapeutics in algal chloroplasts. Proc. Natl. Acad. Sci. 110, E15–E22. doi:10.1073/pnas.1214638110

Tran, M., Zhou, B., Pettersson, P.L., Gonzalez, M.J., Mayfield, S.P., 2009. Synthesis and assembly of a full-length human monoclonal antibody in algal chloroplasts. Biotechnol. Bioeng. 104, 663–673. doi:10.1002/bit.22446

Tuller, T., Waldman, Y.Y., Kupiec, M., Ruppin, E., 2010. Translation efficiency is determined by both codon bias and folding energy. Proc. Natl. Acad. Sci. 107, 3645–3650. doi:10.1073/pnas.0909910107

Ugwu, C.U., Aoyagi, H., Uchiyama, H., 2008. Photobioreactors for mass cultivation of algae. Bioresour. Technol. 99, 4021–4028. doi:10.1016/j.biortech.2007.01.046

Umen, J.G., Goodenough, U.W., 2001. Chloroplast DNA methylation and inheritance in Chlamydomonas. Genes Dev. 15, 2585–2597. doi:10.1101/gad.906701

Walker, T.L., Purton, S., Becker, D.K., Collet, C., 2005. Microalgae as bioreactors. Plant Cell Rep. 24, 629–641. doi:10.1007/s00299-005-0004-6

Walter, J.M., Greenfield, D., Bustamante, C., Liphardt, J., 2007. Light-powering Escherichia coli with proteorhodopsin. Proc. Natl. Acad. Sci. 104, 2408–2412. doi:10.1073/pnas.0611035104

Walter, J.M., Greenfield, D., Liphardt, J., 2010. Potential of light-harvesting proton pumps for bioenergy applications. Curr. Opin. Biotechnol. 21, 265–270. doi:10.1016/j.copbio.2010.03.007

Wang, B., Lan, C.Q., Horsman, M., 2012. Closed photobioreactors for production of microalgal biomasses. Biotechnol. Adv., Biorefining: Thermochemical and Enzymatic Biomass Conversion International Conference on Biomass and Energy Technologies 30, 904–912. doi:10.1016/j.biotechadv.2012.01.019

Wang, H.-H., Yin, W.-B., Hu, Z.-M., 2009. Advances in chloroplast engineering. J. Genet. Genomics Yi Chuan Xue Bao 36, 387–398. doi:10.1016/S1673-8527(08)60128-9

Wang, X., Brandsma, M., Tremblay, R., Maxwell, D., Jevnikar, A.M., Huner, N., Ma, S., 2008. A novel expression platform for the production of diabetes-associated autoantigen human glutamic acid decarboxylase (hGAD65). BMC Biotechnol. 8, 87. doi:10.1186/1472-6750-8-87

Wijffels, R.H., Kruse, O., Hellingwerf, K.J., 2013. Potential of industrial biotechnology with cyanobacteria and eukaryotic microalgae. Curr. Opin. Biotechnol., 24, 405–413. doi:10.1016/j.copbio.2013.04.004

Wong, J., Abilez, O.J., Kuhl, E., 2012. Computational optogenetics: A novel continuum framework for the photoelectrochemistry of living systems. J. Mech. Phys. Solids 60, 1158–1178. doi:10.1016/j.jmps.2012.02.004

Wostrikoff, K., Stern, D.B., 2009. Chapter 9 - Rubisco, in: Harris, E.H., Stern, D.B., Witman, G.B. (Eds.), The Chlamydomonas Sourcebook (Second Edition). Academic Press, London, pp. 303–332.

Xu, J., Dolan, M.C., Medrano, G., Cramer, C.L., Weathers, P.J., 2012. Green factory: plants as bioproduction platforms for recombinant proteins. Biotechnol. Adv. 30, 1171–1184. doi:10.1016/j.biotechadv.2011.08.020

Yamasaki, T., Kurokawa, S., Watanabe, K.I., Ikuta, K., Ohama, T., 2005. Shared molecular characteristics of successfully transformed mitochondrial genomes in Chlamydomonas reinhardtii. Plant Mol. Biol. 58, 515–527. doi:10.1007/s11103-005-7081-3

Yen, H.-W., Hu, I.-C., Chen, C.-Y., Ho, S.-H., Lee, D.-J., Chang, J.-S., 2013. Microalgae-based biorefinery – From biofuels to natural products. Bioresour. Technol., Biorefineries 135, 166–174. doi:10.1016/j.biortech.2012.10.099

Zhang, X.-W., Chen, F., Johns, M.R., 1999. Kinetic models for heterotrophic growth of Chlamydomonas reinhardtii in batch and fed-batch cultures. Process Biochem. 35, 385–389. doi:10.1016/S0032-9592(99)00082-5

ONLINE REFERENCES

http://www.algaeindustrymagazine.com/scalable-algae-microfarms-part-5 Last accessed 19 November 2014.

http://www.bio-rad.com/en-es/product/pds-1000-he-hepta-systems Last accessed 01 December 2014.

http://cfb.unh.edu/phycokey/phycokey.htm. Baker, A.L. et al. 2012. Phycokey, an image based key to Algae (PS Protista), Cyanobacteria, and other aquatic objects. University of New Hampshire Center for Freshwater Biology. Last accessed 02 May 2014.

http://www.chlamy.org Last accessed 22 August 2014.

http://www.lifetechnologies.com/uk/en/home/life-science/cloning/competent-cells-for-transformation/chemically-competent/dh5alpha-genotypes.html Last accessed 01 September 2014.

http://openwetware.org/wiki/E._coli_genotypes Last accessed 01 September 2014.

http://www.piercenet.com/previews/2013-articles/efficient-mammalian-membrane-protein-extraction/ Last accessed 22 August 2014.

http://www.sbs.utexas.edu/utex/ Last accessed 07 August 2014.

APPENDICES

APPENDIX 1: Primer sequences

Name	Sequence (5'->3')	Annealing Temperature [°C]	GC content [%]
FLANK1	gtcattgcgaaaatactggtgc (22)	58.4	45.5
atpA.R	acgtccacaggcgtcgtaagc (21)	63.7	61.9
rbcL.Fn	cggatgtaactcaatcggtag (21)	57.9	48
MluR2	gatgacgtttctatgagttggg (22)	58.4	45.5
RY-psaR	catggatttctccttataataac (23)	53.5	30
VFP.F	cagacatgcgtattaaattacg (22)	54.7	36.4
VFP.R	taacattgaacaacgagcagc (21)	55.9	42.9
VFP_SapI.F	agaggctcttcgatgaacgttattaaacc (29)	63.9	41.4
VFP_SphI.R	agaggcatgcttattatttagcttgagatggtaac (35)	66.0	37.1
rbcL_VFP1.F	ccatacgatgttccagactacgcttaatttttatttttcatgatgtttatg (51)	69.4	31.4
rbcL_VFP1.R	cgaggaaccaccaccacctccacctgatgagccaccaccaccaagtttgtcaatagtatcaaattcg (67)	> 75	50.7
VFP_rbcL.G.F	ggtggtggtggctcatcaggtggaggtggtggtggttcctcgatgaacgttattaaaccagacatgc (67)	> 75	53.7
VFP_rbcL.G.R	cataaacatcatgaaaaataaaaattaagcgtagtctggaacatcgtatgg (51)	69.4	31.4

rbcL.F	ttccacaaacagaaactaaagc (22)	54.7	36.4
rbcL.R	gtttgtcaatagtatcaaattcg (23)	53.5	30.4
P266.rbcL.R	aagtaaaaacacataactccacg (23)	55.3	34.8
PRD.F	taggttctgttattgctttacc (22)	54.7	36.4
PRD.R	ttgaactttcttttactgctacg (23)	55.3	34.8
psbC.F	gatttttgttgttaaaggtttcacc (25)	56.4	32
psbC.R	cattttccgtgtcagatgagc (21)	57.9	47.6
psbCknock.R	taattcgttcagcttgtaaatgg (23)	55.3	34.8
psbK.F	aactttagcactggtacttgc (21)	55.9	42.9
psbK.R	ttaacggaaactaacagctgc (21)	55.9	42.9

APPENDIX 2: Relationship between dry biomass concentration and optical density (OD_{740})

The standard curve represents the mathematical relationship between dry biomass concentration and optical density measured at 740 nm. Dry biomass concentration was determined by lyophilising samples until weight stabilised. Linear regression does not give a very good correlation ($R^2 < 0.90$), due to the accuracy of the measurements and inherent error weighting mass values in the magnitude of mg.

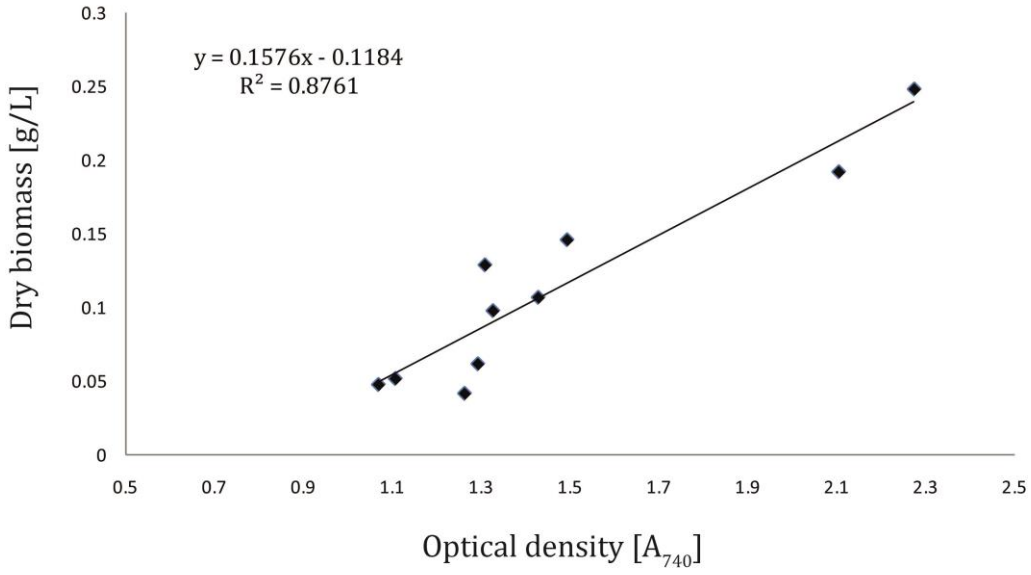

APPENDIX 3: Gene sequences

PROTEORHODOPSIN

5' – **gctcttca**ATGaaattattattaattttaggttctgttattgctttaccaacatttgctgcaggtggtggtgatttagatgcttca
gattacacaggtgtatcattctggttagttacagctgcattattagcttcaacagttttcttcttcgttgaacgtgatcgtgtttcagcaa
aatggaaaacaagtttaacagtttcaggtttagtaacaggtattgctttctggcactacatgtatatgcgtggtgtatggattgaaac
aggtgattctccaacagttttccgttacattgattggttattaactgttccattattaatttgtgaattctacttaattttagctgctgctac
aaacgttgctggttcattattcaaaaaattattagtaggttcattagtaatgttagttttcggttatatgggtgaagcaggtattatggc
agcttggcctgcattcattattggttgtttagcatgggtatacatgatttacgaattatgggcaggtgaaggtaaatcagcatgtaac
actgcaagtcctgcagtacaaagtgcatacaacacaatgatgtacattattattttcggttgggcaatttacccagtaggttacttcac
tggttacttaatgggagatggtggttctgcacttaacttaaaccttatttacaaccttgcagacttcgtaaacaaaattttattcggtct
tattatttggaacgtagcagtaaaagaaagttcaaacgcaggtagttaccttacgacgtacctgactacgcaTAATAA**gcatg**
c – 3'

gctcttc	*Sap*I restriction site
gcatgc	*Sph*I restriction site
tacccatacgatgttccagactacgct	HA tag sequence

VFP

5’ – **gctcttct**ATGaacgttattaaaccagacatgcgtattaaattacgtatggaaggtgctgtaaacggtcacaaattcgttatt
ttaggtgacggtaacggtaaaccatacgaaggtacacaaacaattgacgttacagttaaagaaggtggtccattaccattcgcttac
gacattttaacatcagctttccaatacggtaaccgtgttttcacaaaatacccagatgacattgctgactacttcaaacaatcattccc
agttggttactcatgggaacgttcaatgacatacgaagatggtggtatttgtacagtttcatcagacattaaaatggaaggtaactca
ttcatttatgaaattcgtttccacggtttaaacttcccatcagatggtccagttatgcaaaaaaaaacagttaaatgggaaccatcaa
cagaaaaaatgtacgttcgtgatggtgttttaaaaggtgacgttaacatgacattattattagaaggtggtggtcactaccgttgtga
cttcaaatcaacatacaaagctaaacgtgctgttcaattaccagactaccactacattgaccaccgtattgaaattttatcacacgac
aaagactacaacaaagttaaattatgtgaaaacgctgctgctcgttgttcaatgttaccatctcaagctaaaggttcatacccatacg
atgttccagactacgctTAATAA**gcatgc** – 3’

gctcttc	*Sap*I restriction site
gcatgc	*Sph*I restriction site
tacccttacgacgtacctgactacgca	HA tag sequence

rbcL-VFP fusion

5' – **ATG**gttccacaaacagaaactaaagcaggtgctggattcaaagccggtgtaaaagactaccgtttaacatactacacacct
gattacgtagtaagagatactgatattttagctgcattccgtatgactccacaactaggtgttccacctgaagaatgtggtgctgctgt
agctgctgaatcttcaacaggtacatggactacagtatggactgacggtttaacaagtcttgaccgttacaaaggtcgttgttacgat
atcgaaccagttccgggtgaagacaaccaatacattgcttacgtagcttacccaatcgacttattcgaagaaggttcagtaactaac
atgttcacttctattgtaggtaacgtattcggtttcaaagctttacgtgctctacgtcttgaagaccttcgtattccacctgcttacgtta
aaacattcgtaggtcctccacacggtattcaggtagaacgtgacaaattaaacaaatatggtcgtggtcttttaggttgtacaatcaa
acctaaattaggtctttcagctaaaaactacggtcgtgcagtttatgaatgtttacgtggtggtcttgactttactaaagacgacgaa
aacgtaaactcacaaccattcatgcgttggcgtgaccgtttccttttcgttgctgaagctatttacaaagctcaagcagaaacaggtg
aagttaaaggtcactacttaaacgctactgctggtacttgtgaagaaatgatgaaacgtgcagtatgtgctaaagaattaggtgtac
ctattattatgcacgactacttaacaggtggtttcacagctaacacttcattagctatctactgtcgtgacaacggtcttcttctacaca
tccaccgtgctatgcacgcggttattgaccgtcaacgtaaccacggtattcacttccgtgttcttgctaaagctcttcgtatgtctggtg
gtgaccaccttcactctggtactgttgtaggtaaactagaaggtgaacgtgaagttactctaggtttcgtagacttaatgcgtgatga
ctacgttgaaaaagaccgtagccgtggtatttacttcactcaagactggtgttcaatgccaggtgttatgccagttgcttcaggcggt
attcacgtatggcacatgccagctttagttgaaatcttcggtgatgacgcatgtcttcagttcggtggtggtactctaggtcacccttg
gggtaacgctccaggtgctgcagctaaccgtgtagctcttgaagcttgtactcaagctcgtaacgaaggtcgtgaccttgctcgtga
aggtggcgacgtaattcgttcagcttgtaaatggtctccagaacttgctgctgcatgtgaagtttggaaagaaattaaattcgaattt
gatactattgacaaacttGGTGGTGGTGGCTCATCAGGTGGAGGTGGTGGTGGTTCCTCG**ATG**aacgtta
ttaaaccagacatgcgtattaaattacgtatggaaggtgctgtaaacggtcacaaattcgttattttaggtgacggtaacggtaaac
catacgaaggtacacaaacaattgacgttacagttaaagaaggtggtccattaccattcgcttacgacattttaacatcagctttcca
atacggtaaccgtgttttcacaaaatacccagatgacattgctgactacttcaaacaatcattcccagttggttactcatgggaacgtt
caatgacatacgaagatggtggtatttgtacagtttcatcagacattaaaatggaaggtaactcattcatttatgaaattcgtttccac
ggtttaaacttcccatcagatggtccagttatgcaaaaaaaaacagttaaatgggaaccatcaacagaaaaaatgtacgttcgtga
tggtgttttaaaaggtgacgttaacatgacattattattagaaggtggtggtcactaccgttgtgacttcaaatcaacatacaaagct
aaacgtgctgttcaattaccagactaccactacattgaccaccgtattgaaattttatcacacgacaaagactacaacaaagttaaa

ttatgtgaaaacgctgctgctcgttgttcaatgttaccatctcaagctaaaggttcatacccatacgatgttccagactacgct**TAA**

– 3’

1 – 1425 rbcL

1426 – 1467 GS linker

1468 – 2178 VFP

APPENDIX 4: List of conferences attended and posters presented

10th European Symposium on Biochemical Engineering Sciences and 6th International Forum on Industrial Bioprocesses (France) 09/2014
Talk - Recombinant protein expression in the chloroplast of the green microalga *Chlamydomonas reinhardtii*: a case study using a novel green fluorescent protein as a reporter

16th European Congress on Biotechnology (UK) 07/2014
Talk - Recombinant protein expression in the chloroplast of the green microalga *Chlamydomonas reinhardtii*: a case study using a novel green fluorescent protein as a reporter

Alg' n' Chem Conference (France) 04/2014
Poster - Recombinant protein expression in the chloroplast of the green microalga *Chlamydomonas reinhardtii*: a case study using a novel green fluorescent protein as a reporter

Young Algaeneers Symposium (France) 04/2014
Poster - Recombinant protein expression in the chloroplast of the green microalga *Chlamydomonas reinhardtii*: a case study using a novel green fluorescent protein as a reporter

3rd International Symposium on Chloroplast Genomics and Genetic Engineering (USA) 05/2013
Poster - Expression of a novel fluorescent protein in the *Chlamydomonas reinhardtii* chloroplast: a new marker for recombinant protein production.

9th European Congress of Chemical Engineering and 2nd European Congress of Applied Biotechnology (The Netherlands) 04/2013
Talk - Recombinant protein expression in the chloroplast of the green microalga *Chlamydomonas reinhardtii*: a case study using a novel green fluorescent protein as a reporter.

Plastid Preview (UK) 09/2012
Talk - Expression of a novel fluorescent protein (VFP) in the *Chlamydomonas reinhardtii* chloroplast: a new marker for recombinant protein production in microalgae

8th Asia-Pacific Conference on Algal Biotechnology and 1st International Conference on Coastal Biotechnology (Australia) 07/2012
Poster - Expression of a novel fluorescent protein (VFP) in the *Chlamydomonas reinhardtii* chloroplast: a new marker for recombinant protein production in microalgae.

Young Algaeneers Symposium (The Netherlands) 06/2012
Talk - Exploring the potential for therapeutic protein production in algae

15th International Conference on the Cell and Molecular Biology of *Chlamydomonas* (Germany) 06/2012
Poster - Expression of a novel fluorescent protein (VFP) in the *Chlamydomonas reinhardtii* chloroplast: a new marker for recombinant protein production in microalgae.

Expression of a novel fluorescent protein (VFP) in the Chlamydomonas reinhardtii chloroplast: a new marker for recombinant protein production in microalgae

Stephanie Braun Galleani [a], Frank Baganz [a], Saul Purton [b]
[a] Department of Biochemical Engineering, University College London, UK
[b] Institute of Structural and Molecular Biology, University College London, UK

The chloroplast of Chlamydomonasreinhardtiiis an attractive platform for recombinant protein production since foreign DNA can be precisely targeted to a specific locus and relatively high levels of expression can be obtained without gene silencing issues[1,2]. Additionally, C. reinhardtiican be grown to high density under strictly controlled fermentation conditions similar to other established microbial platforms[3]. Several human therapeutic proteins have been successfully produced in the algal chloroplast, showing appropriate folding and biological activity[4]. The availability of a stable fluorescent reporter would be of value in identifying optimal culture conditions to maximise the expression of such recombinant proteins. We are exploring the suitability of Verde fluorescent protein (VFP) as a novel reporter since it has been shown to possess high fluorescence and good stability[5].

Transformation of the C. reinhardtii chloroplast with the VFP gene using two different strains: TN72 (psbH-deficient, no cell wall) and Bst-same (psbH-deficient, walled)

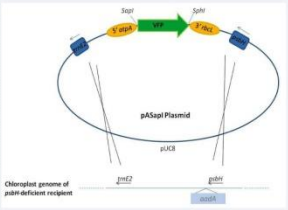

A: Chloroplast transformation strategy. Black crosses show homologous recombination between chloroplast sequences.

A codon-optimised version of the VFP gene including an HA epitope sequence was synthesized and inserted in our expression vector pASapI. Chloroplast transformation was achieved by vortexing plasmid DNA with two different ΔpsbH photosynthetic mutants, TN72 and Bst-same. The pASapI plasmid (Fig. A) carries a functional copy of psbH, so selection was carried out by phototrophic rescue on minimal medium. Cells that incorporated psbH should also contain the VFP gene. This can be checked by PCR (Fig. B & C)

Homoplasmy of the chloroplast genome

Untransformed TN72 :

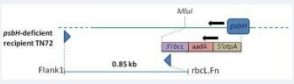

Wild-type Chlamy CC-1021 (and Bst-same):

Transformed cells give the following:

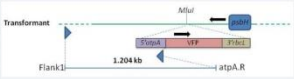

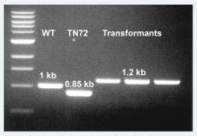

B: PCR with the primers Flank1, rbcL.Fn, atpA.R and MluR2 to show the insertion of the VFP gene in the TN72 strain.

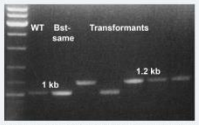

C: PCR with the primers Flank1, rbcL.Fn, atpA.R and MluR2 to show the insertion of the VFP gene in the Bst-same strain.

Protein expression

VFP expression was analysed at different stages of cultivation for both transformed strains by immunological detection using α-HA antibody. Fig. D shows the results obtained for T (TN72 transformant) and B (Bst-same transformant) at different harvesting times.

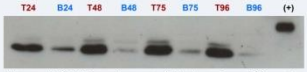

D: Western blot result for VFP transformants in both strains at different times of cultivation (in hours).

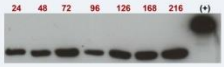

E: Western blot result for VFP transformants in TN72 at different times of cultivation.

VFP expression is much higher in TN72 than Bst-same and the protein remains stable and expressed throughout the culture life span (Fig. E), indicating that VFP has potential as a fluorescent marker.

VFP Fluorescence in vivo

VFP has maximum excitation and emission peaks at 491 and 503 nm respectively. In vivo fluorescence was readily observed by means of confocal microscopy (Fig. F), in collaboration with Queen Mary's University, which showed detectable fluorescence in TN72 transformants. However, low fluorescence was detected for Bst-same transformants, as expected from the previous protein expression results.

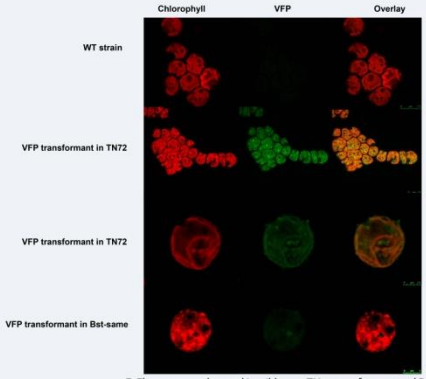

F: Fluorescence observed in wild-type, TN72 transformant and Bst-same transformant strains by confocal microscopy.

TN72 transformants growth curve

A growth curve was produced with two transformants of TN72 (genetically identical) compared to the TN72 host transformed with the empty pASapI plasmid, under mixotrophic conditions (TAP medium, light intensity 100 µmol m^{-2} s^{-1}, 25°C, 130 rpm). As observed in Fig. G, there is no detrimental effect on growth for the transformants.

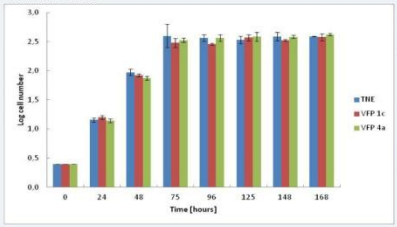

G: Growth curve for TN72 transformants and TN72 transformed with the empty plasmid as negative control.

On average,

Doubling time: 11 h
Growth rate: 0,063 h^{-1}

Conclusions and ongoing work

Transformants in the TN72 host express detectable amounts of fluorescent protein; thus, its use as a tool to detect a desired recombinant protein fused to it seems feasible. Further work aims at developing new strains of Chlamydomonaswith VFP fused to a highly abundance endogenous protein, such as the large subunit (RbcL) of RuBisCo, to observe if this fusion enhances fluorescence. Current work aims at constructing a rbcL-VFP plasmid to be inserted in a ΔrbcL mutant strain of Chlamy.

Since the Bst-same transformants show different expression levels for an identical chloroplast construct, this suggests that the nuclear background of the two strains is influencing VFP levels. This is currently being investigated by genetic analysis. Furthermore, a high level of VFP expression in a cell-walled strain is desirable for studies of cell performance and fragility in a pilot-scale photobioreactor.

References
[1] Franklin et al. (2004) Curr Opin Plant Biol 7:159-165.
[2] Purton (2006) In: Transgenic microalgae as green cell factories.
[3] Walker et al. (2005) Plant Cell Rep 24: 629 -641.
[4] Manuell et al. (2007) Plant Biotech J 5: 402 -412.
[5] Ilagan et al. (2010) FEBS J 277: 1967 -1978.

Attendance at this conference is sponsored by:
Society for General Microbiology www.sgm.ac.uk
UCL Graduate School & Department of Biochemical Engineering
Algae@UCL
SEB Society for Experimental Biology
This research is funded by Becas Chile - CONICYT
CONICYT BECAS CHILE

Expression of a novel fluorescent protein in the Chlamydomonas reinhardtii chloroplast: a new marker for recombinant protein production

Stephanie Braun Galleani [a], Frank Baganz [a], Saul Purton [b]
[a] Department of Biochemical Engineering, University College London, UK. Email: stephanie.braun.10@ucl.ac.uk
[b] Institute of Structural and Molecular Biology, University College London, UK

Unicellular algae such as Chlamydomonas reinhardtii are attracting increasing interest as low cost, GRAS platforms for the synthesis of high-value heterologous proteins. Foreign genes introduced into its chloroplast genome can be targeted to a precise locus and expressed at high level without suffering gene silencing issues [1,2]. Additionally, C. reinhardtii can be grown to high density under strictly controlled fermentation conditions similar to other established microbial platforms [3].

Several human therapeutic proteins have been successfully produced in the algal chloroplast, showing appropriate folding and biological activity [4]. The availability of a stable fluorescent reporter would be of value in identifying optimal culture conditions to maximise the expression of such recombinant proteins. We are exploring the suitability of Verde fluorescent protein (VFP) as a novel reporter since it has been shown to possess high fluorescence and good stability [5].

Transformation Strategy

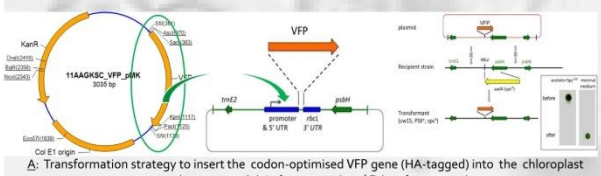

A: Transformation strategy to insert the codon-optimised VFP gene (HA-tagged) into the chloroplast expression vectors A (atpA promoter) and B (psaA promoter).

Protein expression and growth in different conditions

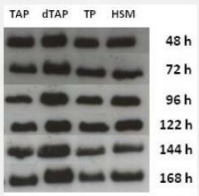

Transformants show constant expression of VFP throughout the culture lifespan (B) for each media tested.

Using a HA -tagged standard protein :
TAP ☒ 30 ng/1 x10⁶ cells
TAP dark ☒ 45 ng/1 x10⁶ cells
TP ☒ 30 ng/1 x10⁶ cells
HSM ☒ 30 ng/1 x10⁶ cells

B: Western blot result for VFP transformant expressed under the atpA promoter, grown in different conditions. TAP: TAP medium in light; dTAP: TAP medium in dark; TP: TAP medium without acetate (in light); HSM: high salt medium (in light).

Fluorescence analysis

Flow cytometry analysis

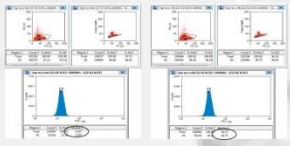

Table 1: Results of flow cytometry and fluorescence emitted (as %) by the different constructs.

Shift on median fluorescence intensity [%]					
Vector A atpA promoter		Vector A atpA promoter/no HA tag		Vector B psaA promoter	
75 h	170 h	75 h	170 h	75 h	170 h
18,9	38,5	19,8	47,8	41,9	62,8
16,9	11,5	17,6	18,1	15,5	19,8
24,2	27,4	43,9	30,4	78,2	84,8
19,8	15,6	33,7	24,4	78,2	91,6

Confocal Microscopy

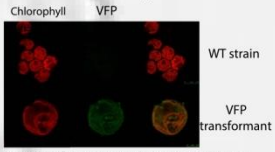

D: In vivo fluorescence observed in wild-type and VFP transformant strains.

The fluorescence intensity at 500 nm was evaluated in different strains (vector A, vector A without HA tag, vector B), and then compared to the negative control (no VFP) (Table 1). This test was carried out in all media considered at two stages of cultivation.

☒ psaA-regulated VFP provides a higher shift in fluorescence in all conditions.
☒ the presence of the HA tag seems to have a slightly positive effect on fluorescence.

Specific growth rate [h⁻¹]	Doubling time [h]
0,064	10,8
0,033	21,4
0,030	23,3
0,028	24,5

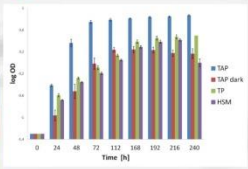

E: Specific growth rate and doubling time of VFP transformant grown in different media at 25 ° C and 150 µmol m⁻² s⁻¹ of light intensity.

In summary, taking into account protein expression (B), specific growth rate (E) and maximum cell density in each condition:

TAP ☒ 9,8 µg protein L -1 h-1
TAP dark ☒ 5,9 µg protein L -1 h-1
TP ☒ 2,9 µg protein L -1 h-1
HSM ☒ 2,6 µg protein L -1 h-1

Co-expression of VFP and the bacterial chaperone Spy

A general chaperone of E. coli (Spy) has been described to increase the steady-state levels of different recombinant proteins[6]. Spy has been co-expressed with VFP to evaluate its effect on expression (F).

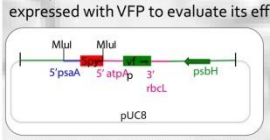

F: Expression vector containing Spy upstream of VFP. C.reinhardtii was transformed as above.

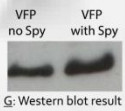

G: Western blot result

Table 2: Flow cytometry results for VFP + Spy construct

Shift on median fluorescence intensity [%]	
75 h	170 h
17,7	49,1
21,8	26,5
28,7	28,8
23,4	15,6

The western blot result (G) suggests an almost identical level of VFP expression. When analysing fluorescence by flow cytometry (Table 2) and comparing it to the fluorescence of VFP in vector A (Table 1), there is a slight increase particularly in cells grown in TAP (dark).

Concluding Remarks and Future Work

It is possible to express a functional fluorescent protein such as VFP in the C. reinhardtii chloroplast and use it to study different genetic variations and culture conditions. The psaA promoter induces higher protein expression, and hence, higher fluorescence emission. The HA tag has no detrimental effect on protein functionality, but somehow the opposite. The co-expression of a Spy chaperone does not improve significantly the VFP protein expression. And in terms of media effect, TAP + light is the best condition observed in terms of growth rate, maximum cell density and overall protein expression.

A new construct in which VFP will be fused to a highly abundant endogenous protein, such as the large subunit (RbcL) of RuBisCo, will be developed to study if this fusion enhances fluorescence.

References
[1] Franklin et al. (2004) Curr Opin Plant Biol 7:159-165.
[2] Purton (2006) In: Transgenic microalgae as green cell factories.
[3] Walker et al. (2005) Plant Cell Rep 24: 629 -641.
[4] Manuell et al. (2007) Plant Biotech J 5: 402 -412.
[5] Ilagan et al. (2010) FEBS J 277: 1967 -1978.
[6] Quan et al. (2011) Nat Struct Mol Biol 18: 262-269

Attendance at this conference is sponsored by:
FEMS
SEB Society for Experimental Biology
UCL Graduate School & Department of Biochemical Engineering
This research is funded by Becas Chile - CONICYT
CONICYT BECAS CHILE

Algae@UCL

Recombinant protein expression in the chloroplast of the green microalga *Chlamydomonas reinhardtii*: a case study using a novel green fluorescent protein as a reporter

Stephanie Braun Galleani [a], Frank Baganz [a], Saul Purton [b]
[a] Department of Biochemical Engineering, University College London, UK. Email: stephanie.braun.10@ucl.ac.uk
[b] Institute of Structural and Molecular Biology, University College London, UK

Unicellular algae such as *Chlamydomonas reinhardtii* (CR) are attracting increasing interest as low cost, GRAS platforms for the synthesis of high -value heterologous proteins. Foreign genes introduced into its chloroplast genome can be targeted to a precise locus and expressed at high level without suffering gene silencing issues [1,2]. Additionally, CR can be grown under strictly controlled fermentation conditions similar to other established microbial platforms [3].

Fluorescent proteins provide a simple tool for monitoring synthesis of recombinant proteins *in vivo*. The availability of such a reporter would be of value in identifying optimal culture conditions to maximise protein expression. We are exploring the suitability of Verde fluorescent protein (VFP) as a novel reporter since it has been shown to possess high fluorescence and good stability [4]. In this study, *VFP* has been expressed in different genetic backgrounds: *atpA* and *psaA* gene promoters, co-expressed with a bacterial chaperone[5] and as a fusion to a highly abundant endogenous protein (RbcL). Additionally, the effect of 4 different culture modalities has been assessed.

Transformation Strategy

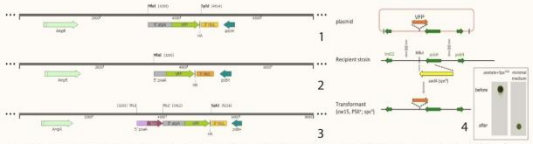

A: Transformation strategy to insert the codon-optimised VFP gene (HA-tagged) into the chloroplast of CR using three different expression cassettes (1,2,3). Recovery of transformants is performed by recovering phototrophic activity (4).

Fluorescence analysis

Flow cytometry analysis

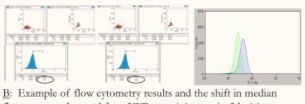

B: Example of flow cytometry results and the shift in median fluorescence observed for a VFP-containing strain (blue) in comparison to the negative control strain (green).

Confocal Microscopy

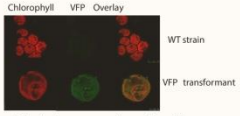

C: In vivo fluorescence observed in wild-type and VFP transformant strains.

The fluorescence intensity (500 nm) of a fixed number of cells was evaluated in the different constructs in all media conditions. The relative fluorescence obtained was then compared to its negative control (no VFP) and a shift in fluorescence was observed.

- VFP is produced as a functional fluorescent protein and its fluorescence can be detected in all constructs.
- Construct 2 provides the highest shift in fluorescence among the 3 constructs tested for all media conditions. This is in agreement with the protein expression results. Constructs 1 and 3 shows similar fluorescence in all conditions.
- The fluorescence intensity emitted seems to vary among media, being the phototrophic conditions (HSM and TP media) the ones that provide higher fluorescence (shifts of 30 – 120 % in comparison to 10 -50 % observed in TAP/dTAP), despite lower protein expression observed in G, H. The reason behind this feature is not fully understood.

VFP as a fusion protein

VFP was fused to the rbcLgene, which encodes for the large subunit of RuBisCo, highly expressed in CR. The expression cassette (D) was produced by Gibson assembly.

D: Vector developed for expression of a rbcL-VFP fusion protein

This vector was used to transform a ΔrbcL mutant (CC-2653) and transformant colonies were obtained thanks to its restored phototrophic activity. Evidence of transgene insertion was observed by PCR; however, transformants only exhibit the native rbcL protein when probed with anti-rbcL antibodies (E). No fusion protein was detected with anti-HA antibodies either (data not shown).

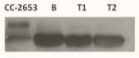

E: RbcL protein expression in the mutant host (CC-2653), a blank tranfsormant with the native rbcL(B) and 2 transformants of the rbcL-VFP fusion. (T1,T2). All the bands exhibit same protein size of ≈55 kDa.

Growth and protein expression in different media conditions

Media	Specific growth rate [h⁻¹]
TAP	0,044
dTAP	0,036
TP	0,023
HSM	0,023

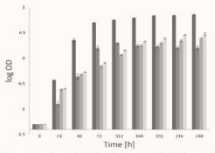

F: Specific growth rate of VFP transformant grown in different media at 25 °C. In legend: TAP: tri-acetate-phosphate medium in light; dTAP: TAP medium in dark; TP: TAP medium without acetate; HSM: high salt medium.

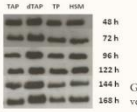

Transformant in vector 1 shows **constant expression** of VFP throughout the culture lifespan for each media tested.

G: Western blot result for VFP transformant expressed under vector 1, grown in different media conditions.

A standard HA-tagged protein was used for estimating protein concentration. Taking into account specific growth rate (F), maximum cell density and protein expression (G) in each condition:

TAP ≈ 9,8 µg protein L⁻¹ h⁻¹
TAP dark ≈ 5,9 µg protein L⁻¹ h⁻¹
TP ≈ 2,9 µg protein L⁻¹ h⁻¹
HSM ≈ 2,6 µg protein L⁻¹ h⁻¹

Growth and protein expression in different temperature conditions

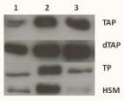

When comparing VFP expression among the different constructs used, there is a clear **increase in expression due to the *psaA* promoter**.

H: Comparison of VFP expression under the control of the 3 different expression vectors in different media.

	Specific growth rate [h⁻¹]		
Media	25 °C	30 °C	37 °C
TAP	0,044	0,048	0,038
dTAP	0,036	0,039	0,035
TP	0,023	0,026	0,020
HSM	0,023	0,026	0,020

Different temperatures were also tested (30 and 37 °C). Specific growth rate and protein expression were determined, showing an **increase in growth rate at 30 °C** in all media conditions.

I: Specific growth rate in different media and temperatures. .

With increased temperature, VFP expression **increased only in TAP** .

However, maximum cell density at 37 °C is 60% lower, which suggests that **30 °C and TAP is the best condition achieved.**

J: Comparison of VFP (construct 1) expression in 3 different cultivation temperatures for all media tested .

Concluding Remarks and Future Work

It is possible to express a functional fluorescent protein such as VFP in the *C. reinhardtii* chloroplast and use it to study different genetic variations and culture conditions. The *psaA* promoter induces higher protein expression, and hence, higher fluorescence emission. The co -expression of a Spy chaperone does improve significantly the VFP protein expression as well. Regarding the effect of cultivation conditions, 30 °C and mixotrophic modality is the best condition observed in terms of growth rate, maximum cell density and overall protein expression. Further studies are being carried out at 30 °C with transformants expressing a recombinant protein of pharmaceutical interest to validate the results presented here.

References
[1] Franklin *et al.* (2004) Curr Opin Plant Biol 7:159165.
[2] Purton (2006) In: Transgenic microalgae as green cell factories.
[3] Walker *et al.* (2005) Plant Cell Rep 24: 629 -641.
[4] Ilagan *et al.* (2010) FEBS J 277: 1967 -1978.
[5] Quan *et al.* (2011) Nat Struct Mol Biol 18: 262269

Attendance at this conference is sponsored by:
This research is funded by Becas Chile - CONICYT